Analysis of Deformation and Tearing of Uniformly Blast-Loaded Circular and Square Plates; Rectangular beams and T-Beams.

MULUH ESAU TICHA

University of Cape Town

Department of Mechanical Engineering

Rondebosch, Cape Town

7700, South Africa.

Analysis of Deformation and Tearing of Uniformly Blast-Loaded Circular and Square Plates; Rectangular beams and T-beams.

MULUH ESAU TICHA

OCTOBER 2002.

Thesis submitted in fulfillment of the requirement for Master of Science in Applied Science in Mechanical Engineering.

Declaration

I, MULUH ESAU TICHA, declare that this thesis is essentially my own work. It is being submitted for the degree of Master of Applied Science in Engineering at the University of Cape Town and it has not been submitted in this or in a similar form for a degree at any other university.

Signed by candidate

MULUH ESAU TICHA

October 2002.

Abstract

This investigation examines the failure of circular and square mild steel plates, aluminium rectangular beams and T-beams subjected to impulsive loads.

The objective of this investigation is to numerically determine the dynamic response of circular and square plates, rectangular beams and T-beams clamped and built-in (integral) at the boundary subjected to uniform blast loading; use material properties that include and exclude temperature dependency to model the plates and beams response and failure and finally to compare the numerical results with experimental results.

The numerical analysis was carried out using the general-purpose finite element code; ABAQUS / Explicit which incorporates non-linear geometry, material effects such as strain rate sensitivity and temperature effects. The circular plates are modelled by exploiting axisymmetry, using axisymmetric four noded elements (CAX4R) with reduced integration and hourglass control to prevent the occurrence of zero energy modes in bending. The square plates, rectangular beams and T-beams are modelled by exploiting symmetry and asymmetry using eight noded brick (C3D8R) reduced integration with hourglass control continuum elements and only a quarter of the plates and beams are modelled. The impulsive blast load, generated by the use of a plastic sheet explosive in the experiments, was simulated in the finite element model by the application of an uniform rectangular pressure pulse on the plates and beams. The clamped and built-in (integral) boundary conditions are modelled with rigid continuum elements.

Mid-point displacement, permanent deformed shape and rupture of the plates and beams are compared to experimental data. The three failure modes: mode I (large inelastic deformation), mode II (tensile failure in outer fibres, at or over the support and mode III (transverse shear failure at the support) observed in the experiments are investigated and results compared with experimental results. Numerical investigation predicts modes II and III failures at impulses lower than those of the experiments. Deflection and tearing is observed to be dependent on the amount of impulse on the plates and beams. It was also observed that tearing occurs in plates and beams with integral boundary at an impulse lower than that for clamped plates and beams. Mesh sensitivity on circular plates was investigated by Wiehahm, Nurick and Böwlse [8] and it

was observed that a coarse mesh gave results that correlated favourably with the experiments than a fine mesh.

Using temperature dependent material properties to show failure occurring as a result of a thermo-mechanical instability and localised shear banding; failure modes II and III were determined. Tearing was observed to occur in localised areas where severe element elongations due to very high strain and high temperatures have taken place.

Results obtained from the approach using material properties that include temperature dependent material properties to model the plates and beams response to uniform blast loads are encouraging.

Table of contents

List of Tables

List of Figures

NOTATIONS

A_o	Area of plate or beam exposed to pressure loading
I	Impulse applied to the plates and beams
t_b	Duration the pressure is applied
W_f	Maximum permanent transverse displacement
H_m	Thickness of plastic membrane
H	Beam depth
V_o	Uniformly distributed impulsive velocity
D, q	Material constants
σ_o	Material static yield stress
R_m	Radius of the plastic membrane
R_o	Radius of loaded area of plate
R	Radius of plate
t	Plate thickness
L_b	Beam half span
B	Width of beam
δ_f	Deflection
Γ	Loading parameter
ξ_o	Geometry parameter
n	Strain rate enhancement
β	Aspect ratio
λ	Dimensionless initial kinetic energy
M_o	Static fully plastic bending moment
Φc	Dimensionless impulse (damage number for circular plates)
Φ_q	Dimensionless impulse (damage number for square plates)
μ	Mass per unit length
Δt	Time step
σ_o^1	Dynamic yield stress

σ_{nom}	Nominal stress
σ_{true}	True stress
ε_{nom}	Nominal strain
ε_{Ln}^{pl}	Logarithmic plastic strain
E	Young's Modulus
υ	Poisson's ratio
τ	Material temperature
σ_{y_o}	Static yield stress at the reference temperature of the tensile test
$\dot{\varepsilon}$	Strain rate
$\dot{\varepsilon}_o$ and η	Material constants
ϖ	Damage parameter
$\Delta \bar{\varepsilon}^{pl}$	Increment of the equivalent plastic strain
$\bar{\varepsilon}_f^{pl}$	Strain at failure
c(T)	Specific heat
$\hat{\theta}$	Non-dimensional temperature
θ	Current temperature
θ_{melt}	Melting temperature
$\theta_{transition}$	Transition temperature defined as the one at or below which there is no temperature dependence on the expression of the yield stress.
A^1, b, S, M	Material parameters measured at or below the transient temperature.
L^{el}	Length of an element

Acknowledgement

The author wishes to thank

His supervisor Professor G.N. Nurick for his valued advise, guidance and support throughout this study.

Mr. V. H. Balden for his assistance in ABAQUS.

The Centre for Research in Computational and Applied Mechanics(CERECAM) and the Department of Mechanical Engineering University of Cape Town for their financial and material support.

1.0 Introduction

In recent years, explosive loads have received considerable attention through different events; intentional or accidental. The results of explosions and collisions are typical events involving impact and are a daily occurrence. Some of these events often result in serious tragedies and loss of life. The dynamic deformation behaviour of structures has become increasingly important in many applications related to the design of armour or system spacecraft, high speed transportation vehicles and high speed machinery. By studying the behaviour of plates and beams subjected to impulsive loading, a better understanding can be gained and this will help as a guide to the development of rational design procedures for a safer world.

A numerical investigation on the deformation and failure of plates and beams is presented and numerical results obtained are compared to the experiments in this study. The response and failure of circular and square steel plates, aluminium rectangular beams and T-beams is presented. Because of steel's superior mechanical properties such as high strength and aluminium alloy having superior mechanical properties such as high strength/weight ratio, good corrosion resistance, excellent weldability and deformability, the metals are considered for use in many applications where the structural components are subjected to dynamic loading. In order to optimise these metals deformation and fracture performance under high loading rates, it is necessary to understand the dynamic deformation mechanisms, temperature effects and the effect of strain rate.

The investigation into the failure of plates and beams subjected to blast loading conditions has been studied for some years as reported by Nurick and Martin [1, 2]. The first found mention of different failure modes was by Menkes and Opat [3] on fully clamped metal beams loaded impulsively. Menkes and Opat [3] classified the failure modes as:

Mode I Large inelastic deformation (a)

Mode II Tearing (tensile failure) in the outer fibers at or over the support (b)

Mode III Transverse shear failure at the supports (c).

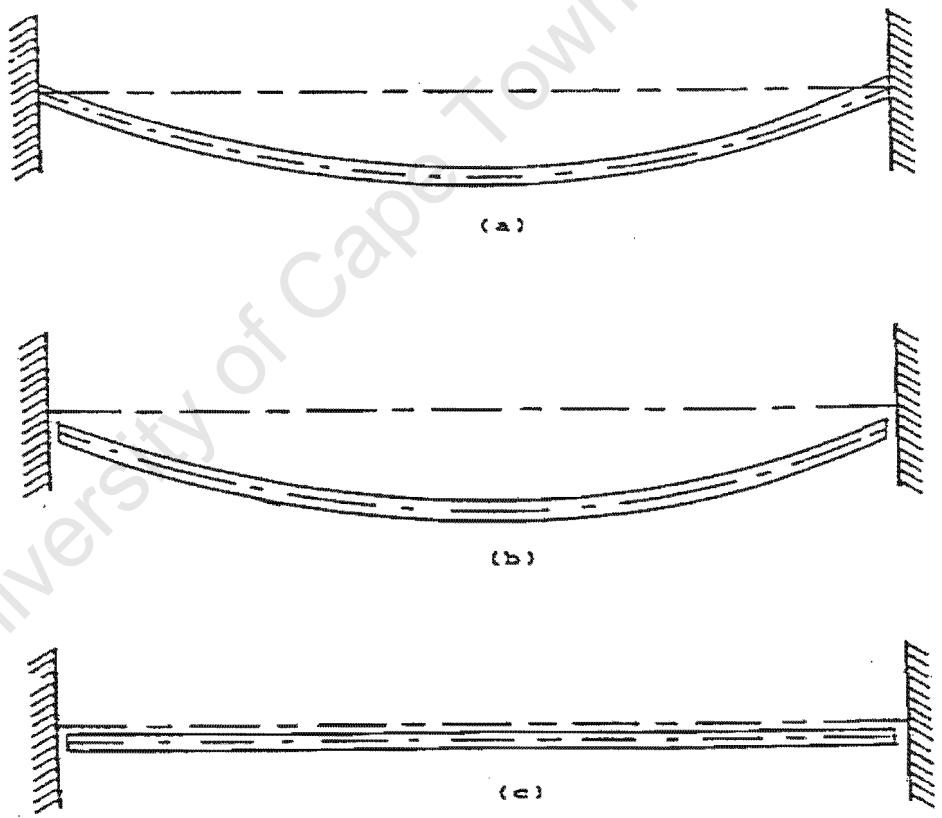

Figure 1.0 : Permanent profile of impulsively loaded plates showing the three failure modes [3].

In this study, clamped and integral boundary conditions are applied at the boundaries of impulsively loaded plates and beams. Failure modes observed are compared with experimental results. Using material properties that include temperature dependency; failure modes II and III are determined. The effect of boundary conditions on the failure of plates and beams is also investigated. The effect of temperature is not pronounced in mode I failure (see sections 5.1.1, 5.2.1, 5.3.1 and 5.4.1 of this investigation).

The response of structural components subjected to blast loads results in deformation strain rates in the range of 10^2 to 10^4 per second. The high strain rate deformation results in rise in temperature of the material. Using material properties that depend on temperature, the failure of the material may be determined. This approach is used in this study to determine the failure of plates and beams mentioned herein. Guedes, Gordo, Teixeira [4], Ji-lin Yu [5], Lee, Sue and Lin [6], Gimpe, Heyer and Dahl [7], Wiehahn, Nurick and Bowles [8] reported on experimental and numerical investigations on the failure of blast loaded plates and beams using material properties that include and exclude temperature dependency.

Considerable success has been achieved in modelling of impulsively loaded plates and beams using finite element models [8, 9, 10, 11]. Mode I failure has been predicted with reasonable accuracy. Modes II and III have been modelled with less degree of accuracy achieved despite the many criteria such as damage models, rupture strain and equivalent plastic strain used.

2.0 LITERATURE REVIEW

The response of thin plates and beams clamped or built-in at the outer edges subjected to uniform or localised blast loading conditions has been studied for a number of years. Several attempts have been made in the past to theoretically and experimentally predict the mid-point deflection, deflection-thickness ratio for plates subjected to impulsive loading as reported by Nurick and Martin [1, 2]. Extensive experimental studies have been carried out to understand the large permanent ductile deformation and rupture of beams, plates and shells. Nurick and Martin [1, 2] present an overview of the theoretical and experimental results from which it is evident that most of the investigations deal with a plate that is loaded uniformly over the entire plate area. Jones [12] reported that it was during the First World War that the first theoretical studies into the influence of dynamic loads on the behaviour of thin disks or circular plates were conducted. There have been several experimental studies to measure large deformations of plates subjected to blast and impact as reported by Nurick and Martin [2]. The early reports were mainly concerned with structures subjected to underwater explosive charge. Taylor [13] describes experiments of large steel plates subjected to underwater explosive blasts fired at various distances from a position normal to the plate through its mid-point. Further studies referred to such as Olson, Fagnan and Nurick [14], Nurick, Olson and Fagnan [15] showed that the focus of such studies has been on circular plates, circular plates with singular stiffeners, square plates, square plates with singular stiffener and rectangular plates with two stiffeners. The recorded response of these structural elements have been compared with the responses predicted analytically and numerically.

In this study; the modelling of circular plates was done using axisymmetric simulation, (2-dimensional) approach where only the plate radius and thickness are modelled along the 1(R) and 2(Z) axes respectively. A quarter of the square plates, rectangular beams and T-beams were modelled along the 1(X), 2(Y) and 3(Z) axes, (3-dimensional). Rigid elements were used to clamp the plates and beams at the top and bottom. For built-in plates and beams, boundary elements of unloaded areas were encastre and symmetry conditions applied to areas that were not clamped or encastre (figure 4.2 to 4.7). Using

ABAQUS / Explicit code, the impulse was simulated as a rectangular pressure pulse and applied to the plates and beams. In chapter five, mid-point deflection (mode I failure) obtained from simulations is compared with that of experiment. A comparison of mid-point deflection of models that include and exclude temperature dependent material properties, clamped and built-in boundaries is also made. Mode II failure is obtained using temperature and logarithmic strain. A comparison of models clamped and built-in at the boundaries is made in this failure mode. Mode III failure is obtained using temperature and equivalent plastic strain and a comparison between a clamped and built-in boundary models drawn.

2.1 Blast Load

There are two different methods of modelling a blast wave using the finite element code ABAQUS / Explicit. The first method involves modelling the blast wave as an applied pressure over a given area for a given time. The second involves modelling the explosive using the Jones-Wilkins-Lee (JWL) equation of state (EOS). The first method is used in this investigation. Two types of loading conditions are applicable to blast loaded structures. The first method is an uniform loading condition (where an uniform load is applied to the structure) and the second method is a localised loading condition (where a central load is applied to the structure). An uniform loading condition is used in this study.

In the experiment, the load is applied by the detonation of an explosive. An explosive is defined as a substance containing a large amount of stored energy that can be released suddenly, thereby converting the substance into compressed gases or swarm of fragments that expand with great force or velocity. Other definitions are: substance or device capable of producing a volume of rapidly expanding gas that exerts sudden pressure on its surroundings. The three main types of explosives as reported by Martin, Reza, Larry and Anderson [16] are: chemical (include black powder, nitroglycerin, dynamite and trinitrotoluene (TNT)), mechanical (over loading a container with compressed air) and nuclear (restricted to military use) explosives. Chemical explosive, which is gaseous, is considered in this study.

The detonation of an explosive generates the violent expansion of hot gases originating a pressure wave, moving outward at high velocity from its source. The blast wave interacts with any structure in its path by imposing impulsive or dynamic blast loads causing the structure to deform or tear. The front of the shock wave at the point of observation gives a sharp pressure rise, followed by an exponential decay to ambient pressure and a negative phase in which the pressure is less than ambient pressure. The actual explosive pressure-time loading is a complex decaying pressure oscillation shown in figure 2.1.

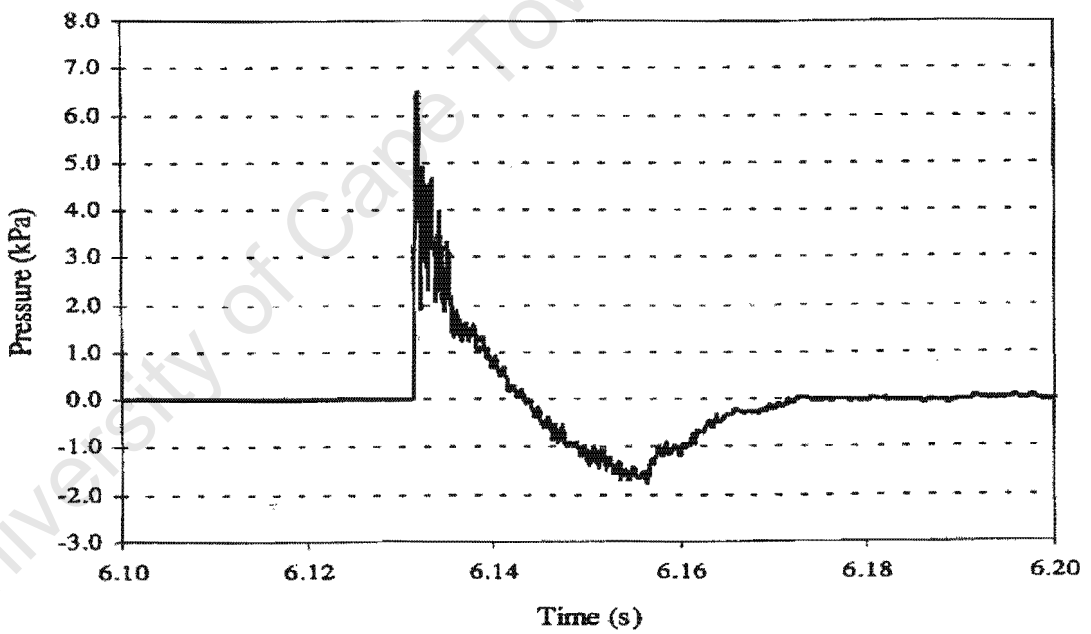

Figure 2.1 : Actual pressure as a function of time for blast loads [11].

For practical reasons, simplification of the explosion pressure-time loading before applying in any structural analysis is necessary as shown in figure 2.2 with a smoothed pressure-time history for a typical blast wave. The peak over-pressure is larger than the peak under-pressure so that the negative phase of the blast can be ignored.

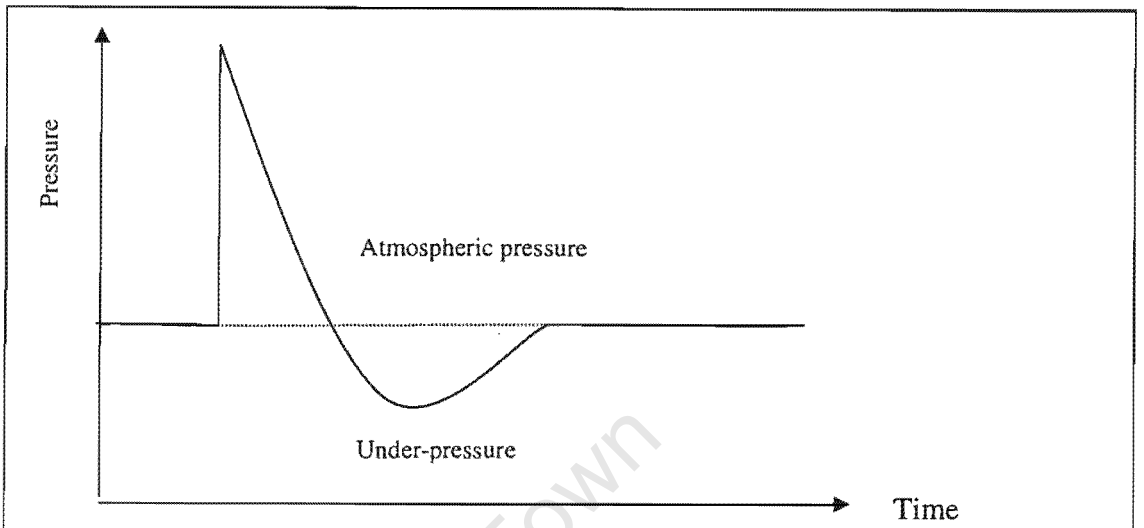

Figure 2.2 : Simplified pressure as a function of time for blast loads.

Several definitions have been given for impulsive loading. Shen and Jones [17] characterised impulsive loading as a pressure pulse having a finite impulse with an infinitely large magnitude and an infinitesimally short duration. The Steel Construction Institute [18] classified blast loads as impulsive if the duration of the load is significantly less than the natural period of the structure and the structure has less time to fully respond to the load; and as quasi-static if the duration of the load is much longer than the natural period of the structure. Loading in the transition region between these two is called dynamic.

The Steel Construction Institute [18] observed that for impulsive loading, that is, external pressure loading of peak intensities of several Megapascals in magnitude over durations of microseconds, maintaining the exact peak load value and the exact load duration is not crucial. It is, however, important to represent the impulse accurately. Some "ideal" pressure-time impulsive loading histories found in the literature, The Steel Construction Institute [18] are shown in figure 2.3.

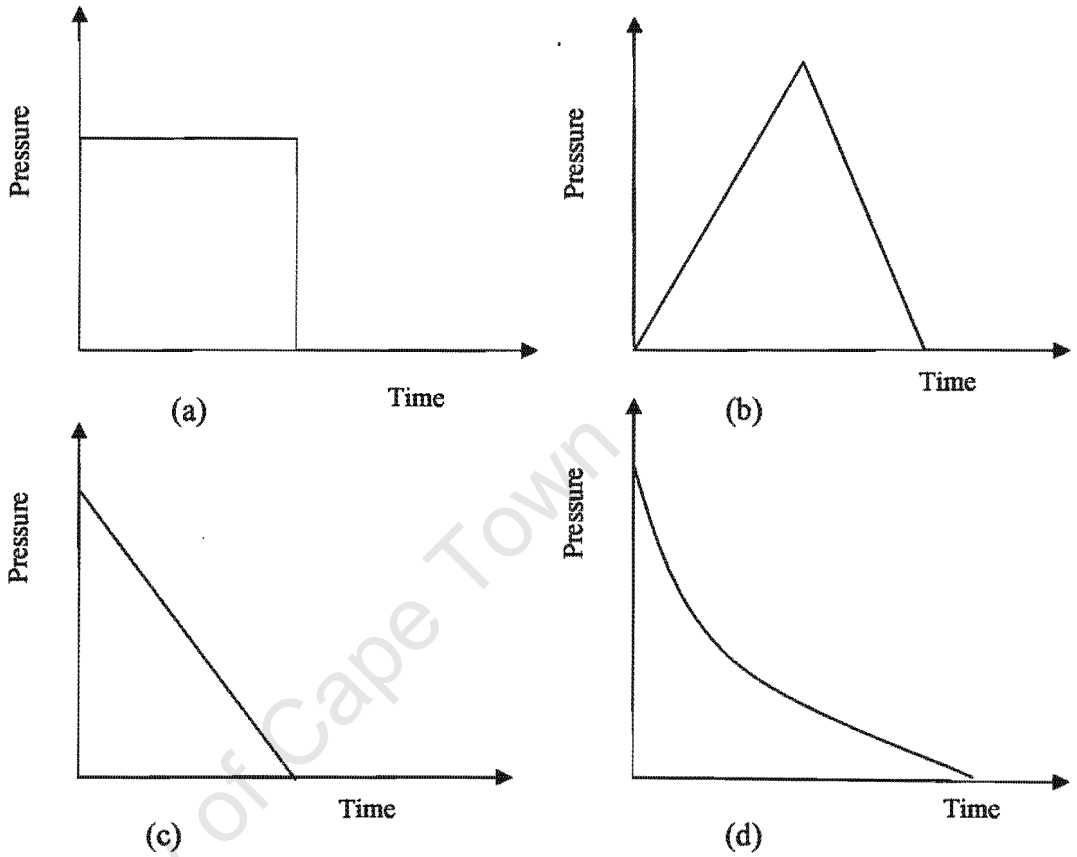

Figure 2.3 : Some "ideal" pressure-time impulsive loading history from the literature [18].

This study considers a rectangular pressure pulse (figure 2.3 (a)). In situations where the pressure pulse is not well approximated by a blast-type pulse, Youngdahl [19] method of representing the true pulse with a rectangular pulse of equivalent impulse gave good results. Farrow, Nurick and Mitchell [20] used both a triangular and a rectangular pulse to predict the plate deflections, deformation shapes, residual strains and dynamic yield stress of circular plates subjected to uniformly distributed explosive loading using the ABAQUS finite element code.

Three types of impulsive loading have been reported in the literature. The first type concerns structures subjected to underwater explosive charges. Nurick [21] reported that the earliest studies on this was by Taylor in 1950. The second type is concerned with

pressure waves created by an air-blast as reported by Nobel and Oxley [22]. The third type of impulsive loading involves the detonation of sheet explosives and the impulse measured using a ballistic pendulum, this was first investigated by Humphreys in 1965 as reported by Nurick [23].

The impulsive blast load generated was simulated in the finite element model by the application of a pressure pulse. This is considered to be better than specifying an initial velocity field for the model at the start of the analysis since this leads to numerical instability within the explicit scheme. The duration t_b of the pressure load P is taken to be the actual burn time of the explosive, and hence the magnitude of the pressure is calculated by

$$P = \frac{I}{(t_b . A_0)} \qquad 2.1$$

where the pressure is taken to be a uniformly distributed and square function of time, figure 2.3 (a).

A_o : area of plate or beam exposed to pressure loading,

I : impulse and

t_b : duration the pressure is applied.

2.2 Experimental procedure

The experimental procedure; the method of creating an impulsive load using plastic explosive and the measurement of the impulse on plates and beams using a ballistic pendulum reviewed herein are similar to those used in many experiments.

The basic apparatus used in the experiments can be grouped under the following headings:

. Ballistic pendulum used to measure the impulse
. Plastic explosive used to impart the impulse
. Test specimens.

• The ballistic pendulum

A ballistic pendulum was used to measure the impulse applied to the plates and beams. It is made up of a steel I-beam suspended from a solid concrete roof by four spring steel wires. The spring steel wires have adjustable screws attached to them, enabling the pendulum to be in a level position. At one end of the ballistic pendulum called the experimental rig, test specimens are positioned and at the other end balancing masses are attached. The balancing masses ensure that each spring steel wire carries approximately the same mass thus ensuring that the impulse acts through the centroid of the pendulum. A pen (recorder) is also attached to the pendulum at this end (end where balancing masses are attached). The pen records the oscillation amplitude of the pendulum on to a sheet of paper. The oscillation amplitude relates directly to the impulse imparted to the test specimen. A schematic diagram of the ballistic pendulum is shown in figure 2.4.

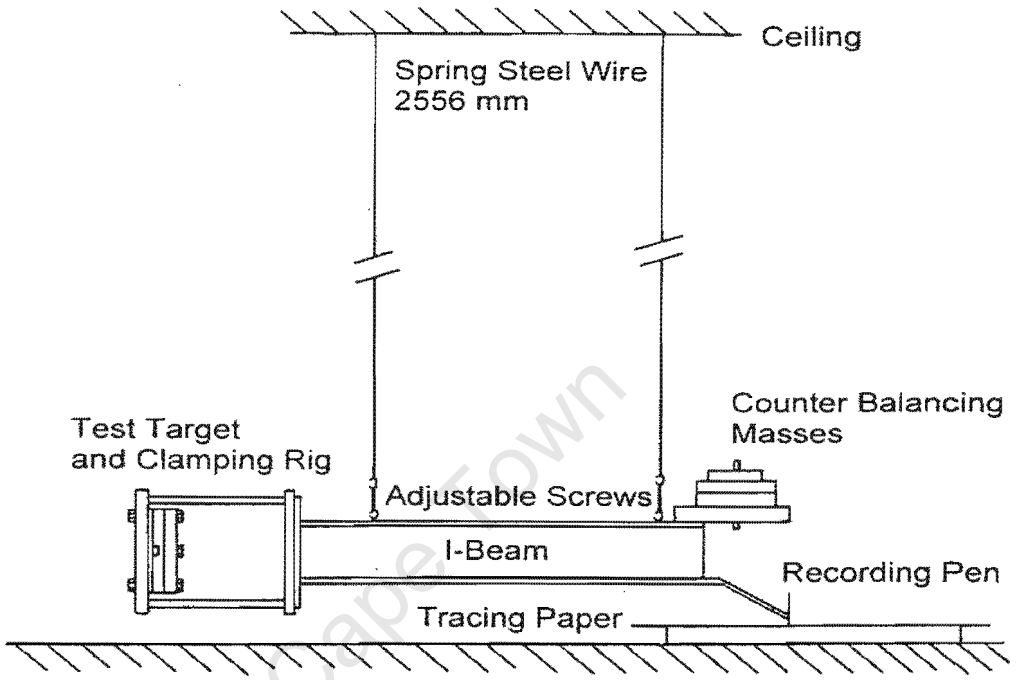

Figure 2.4 : Ballistic pendulum.

The impulse is calculated from the trace by measuring the following from the apparatus: mass of I-Beam, mass of clamping rig, mass of counter balance, total pendulum mass (M), R, Z, A and T are defined in appendix A.

- **Plastic explosive used to impart the impulse**

The plates and beams were loaded using sheet explosives. The speed of detonation is sufficiently large enough to assume that an ideal impulse is simultaneously applied over the whole plate or beam area.

The two ring configuration used by Nurick [23] in the experimental procedure for the explosive was applied for circular plates. The rings are modified to two concentric squares for the square plates investigated in this study. In the experiments the sheet explosive is arranged as shown in figures 2.5 and 2.6 for circular and square plates respectively.

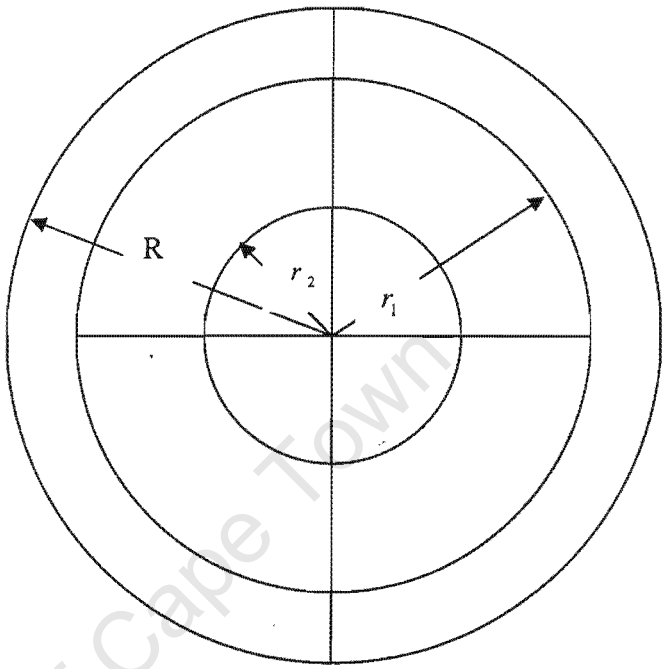

$r_1 = 0.82$ R, $r_2 = 0.41$ R

Figure 2.5 : Explosive configuration for circular plates.

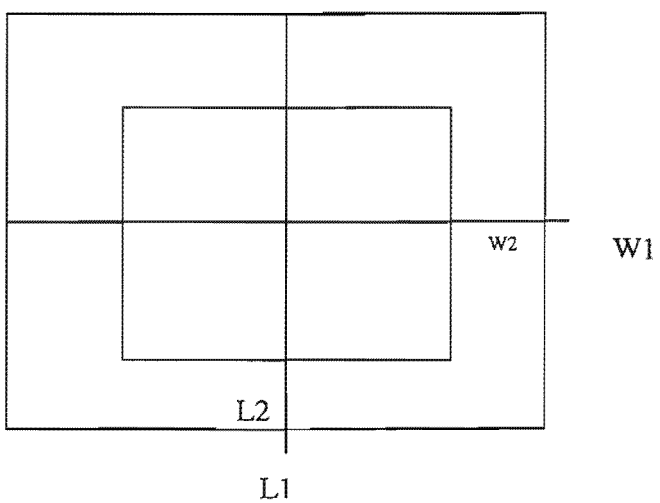

L1=W1=89mm and L2=W2=89mm.

Figure 2.6 : Explosive configuration for square plates

The load on plates was applied by strips of explosives laid out on a polystyrene pad in two concentric circular and square annuli which were interconnected by two perpendicular strips of explosive for circular and square plates respectively as reported by Nurick [23]. Sheet explosive in figure 2.5 and figure 2.6 are placed on a 14mm thick polystyrene pad. This attenuator is used to reduce the high peak pressure in the wave entering the plate and also to provide a uniform impulse and prevent spallation of the specimen.

For rectangular beams, the high pressure was provided by sheet explosive, which is cemented to a neoprene buffer which in turn, is bounded to the top surface of a clamped aluminium beam; Menkes and Opat [3]. The explosive was laid in such a way that it extended over the beam support. Menkes and Opat also used a 6.25 mm thick neoprene buffer was used to prevent rear-surface spallation. The high explosive used was Du Pont Detasheet D, and the adhesive was Du Pont 4684 cement, thin 1:1 with acetone. A schematic diagram of this lay out is shown in figure 2.7. The detonation point of the explosive is at B shown in figure 2.7.

For T-beams, a cylindrical strip of explosive was laid along a 25 mm thick polystyrene pad, the full length of the centerline of the beam flange. A pig-tail of explosive was placed at the center of the cylindrical strip, to which the detonation was attached; Nurick, Jones and Von Alten-Reuss [29]. Figure 2.7 is a schematic set-up of the explosive on beams. The detonation point of the explosive is at point A as shown in figure 2.7.

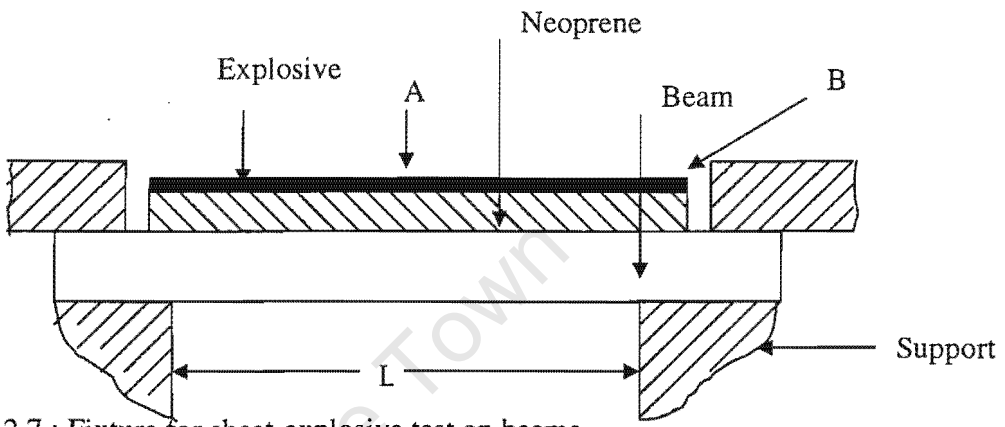

Figure 2.7 : Fixture for sheet-explosive test on beams .

2.3 Modes of failure

Menkes and Opat [3] reported different failure modes for fully camped metal beams loaded impulsively. They found that as the impulse increases three distinctly different damage modes were noted. These damage modes are: Mode I (large inelastic deformation), Mode II (tearing (tensile failure) in the outer fibers at or over the support) and Mode III (transverse shear failure at the supports). A schematic diagram of the failure modes is shown in figure 1.0.

Similar failure modes have also been observed for circular plates by Teeling-Smith and Nurick [24], Nurick, Gelman and Marshall [25]; in square plates by Nurick and Shave [26].

Three different phases of mode I (large inelastic deformation) failure were identified by Nurick, Gelman and Marshall[25]. The different phases were classified as follows:

Mode I : large inelastic deformation with no necking at the boundary

Mode Ia : large inelastic deformation with necking around part of the boundary

Mode Ib : large inelastic deformation with necking around the entire boundary.

Some sub-divisions of mode II damage were reported by Nurick and Shave [26]. These modes were classified as follows:

Mode II^* : partial tearing at the boundary

Mode IIa : complete tearing with increasing mid-point deformation

Mode IIb : complete tearing with decreasing mid point deformation.

The predictions have either assumed fully built-in (integral) or clamped conditions at the boundary of the plates. It is evident that most experiments have been carried out on plates considered fully clamped at the boundary, with fewer experiments on plates and beams with fully built-in conditions at the boundary.

Nurick and Radford [27] reported that the loading mechanism of the explosive determines the response of the plate and that the diameter and height of the explosive

were crucial parameters in the modelling procedure. Nurick and Radford [27] reported the refinement of the response modes of plates for localised loading conditions as:

Mode I	Large inelastic response
Mode Itc	Large inelastic response with thinning in the central area
Mode Ib	large inelastic response with thinning at the boundary
Mode II*c	Partial tearing in the central area
Mode IIc	Complete tearing in the central area – capping
Mode II	Complete tearing at the boundary.

The effect of the shape of explosive on the failure of plates and beams is currently being investigated.

Nurick and Jones [28], Nurick, Jones and Alten-Reuss [29] reported on the large inelastic deformations of T-beams subjected to uniform blast loads over the entire span. The resulting response of beams was categorised into global and local deformations. The global deformation referred to the transverse deflections of the beam mid-point while the local deformation referred to the bending and shear distortion of the flanges. The local deformations were small and occurred only at the mid-point. Nurick, Jones and Alten Reuss [29] observed that this was attributed to the effect of the blast created by the detonator and pig-tail lead of explosive. They further observed that compressive stress was developed in the web at the clamped boundary. At large impulses, there were signs of onset of tearing of the flanges at the supports. Nonaka [30] observed that bending action predominates in long beams under normal conditions of transverse loading, but there are certain situations where shearing action plays an important rule. The shear effect is significant in the case of blast loading, which involves large intensity of load in comparison with the load carrying capacity in shear. With this observation the effect of the length of beam was not very crucial in this investigation.

2.4 : The effect of boundary conditions on failure

Clamped and Built-in (integral) boundary conditions are implemented in this study. A comparison is made between failure at the clamped and integral boundaries. Experimental investigation on the effect of boundary conditions on failure of thin plates subjected to impulsive loading has been studied by Thomas [31]. Gelman, Nurick and Mitchell [10] investigated numerically the effect of boundary conditions on the failure of thin plates subjected to impulsive loading. Their results show that boundary conditions do not affect mode I failure but do affect modes Ia and Ib and the onset of mode II failure. These boundary conditions are crucial in assessing the tearing mechanisms which occur when the blast load is large enough to cause partial or complete tearing of the boundaries of plates and beams. It was observed that thinning at the boundary for plate diameters with sharp edge conditions and large deformations occur before thinning and tearing occur for relaxed boundary, conditions as reported by Nurick and Mitchell [10].

2.5 Computational Predictions

Predictions of large deformations of structural components as a result of blast loading using computational and numerical techniques have been well reported in the literature. Jacinto, Ambrosini Danesi [11] in their work cited the fact that suggestions to computational modelling of structures under impulsive loads arise from the comparison of numerical and experimental results. They carried out a computational and experimental analysis of plates under air blast loading. Numerical modelling was carried out using the ABAQUS code. The objectives of their work were, firstly, the comparison between testing and numerical responses in order to obtain guides to the numerical modelling and analysis of this phenomenon and, secondly to provide data that could be used for checking the accuracy of a variety of calculation methods. They presented a set of four tests at natural scale on two nonstiffened metallic steel plates with different boundary conditions subjected to the action of pressure waves originated by the detonation of explosive loads. They also carried out a linear dynamic analysis of the plate models using the ABAQUS code. They found out that the element size of computational models should agree with the quantity of modes that will be included in the response, the obtained results improved significantly when the used load was considered as the temporal superposition of the pressure over the anterior and posterior faces of the plate.

Using a computer program called NAPSSE (Non-linear Analysis of Plate Structures using Super Elements) Olson, Nurick, Levin and Fagnan [14, 15] successfully predicted both maximum deflection and deformation shape of uniformly blast loaded non-stiffened and stiffened plates. The displacement fields incorporated into these super elements were represented both analytically and by polynomial functions to reduce the number of elements used for design level accuracy.

Rudrapatna, Vaziri and Olson [32] carried out a numerical prediction on deformation and failure of thin clamped blast loaded square plates. The numerical analysis was based on a finite element formulation which includes the nonlinear effects of geometry and material as well as strain rate sensitivity. NAPSSE package was used for simulations. They

reported on a phenomenological interactive failure criterion comprising bending, tension and transverse shear to predict the various modes of failure. Nurick , Olson and Fagnan [15] also observed that the influence of strain rate through its effect on the yield stress and the plate response was a major factor. Figure 2.8 is a plot of the predicted strain rate, the dynamic yield stress and the time of occurrence for first yield versus impulse. The strain rates are very high, ranging from 850 to 3000 per second as the impulse increases from 5 to 30 Ns, with the corresponding dynamic yield stress varying from 750 to 890 MPa. The time to first yield decreases from 7 to 2.8 μ s, with increasing impulse, all less than the load duration of 15 μ s. Strain rate on pure aluminium has little effect on its central deflection. However for aluminium alloys strain rate effect can not be completely neglected.

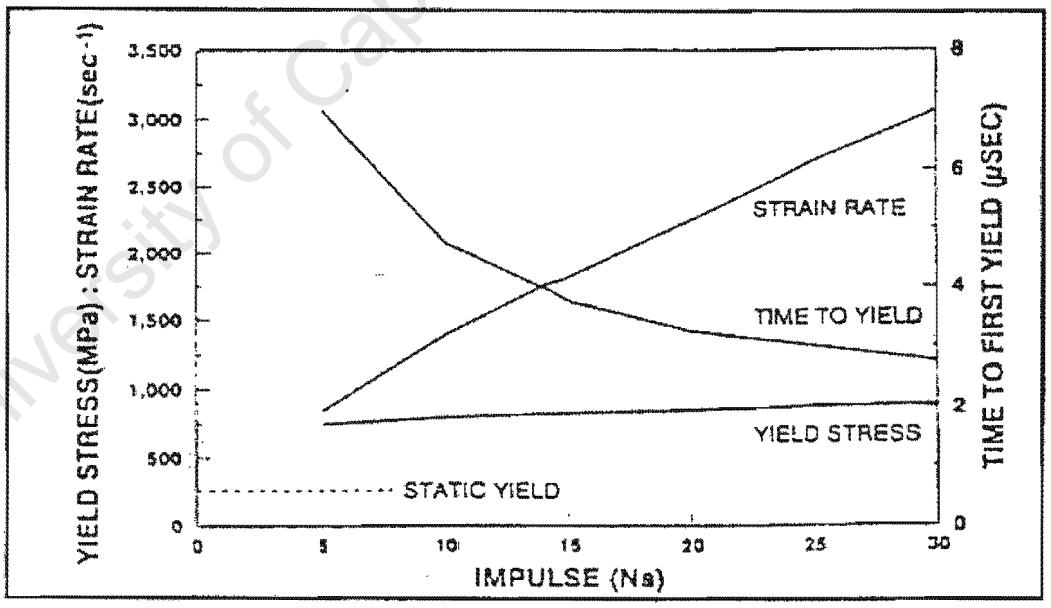

Figure 2.8: First yield results Vs impulse for a single 3x4mm single stiffened square plate [15].

Farrow, Nurick and Mitchell [20] also observed that the strain rate effect does not only decrease the maximum displacement but also the time to reach the maximum displacement. Figure 2.9 shows a comparison of the deflection-history of the mid-point displacement of a circular plate subjected to an impulsive load of 12Ns of a model with rate dependence excluded and included. It is evident from this that the strain rate dependence of mild steel has a large effect on its yield stress which can result in central deflection reductions of around 45%.

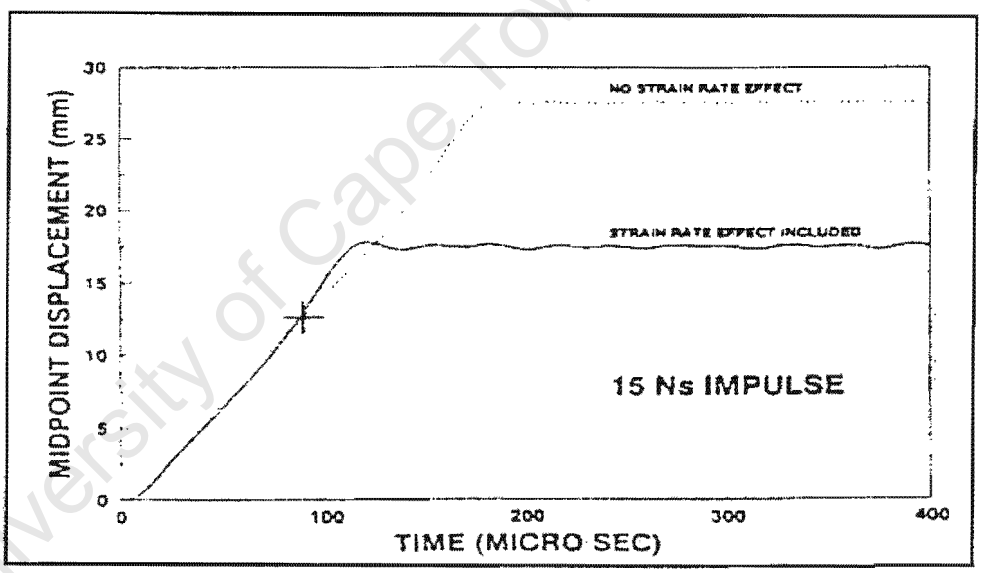

Figure 2.9: Plate Mid-point displacement response [15].

Farrow, Nurick and Mitchell [20] modelled the deformation of blast loaded fully clamped circular plates using the ABAQUS finite element code. It was suggested that mode II (tensile tearing) failure was likely to occur at higher impulses and at the boundary from the plastic strain distribution as shown in figure 2.10. The maximum predicted strain occurs at the clamped outer boundary with the strain reducing to a minimum and then increasing towards the centre of the plate.

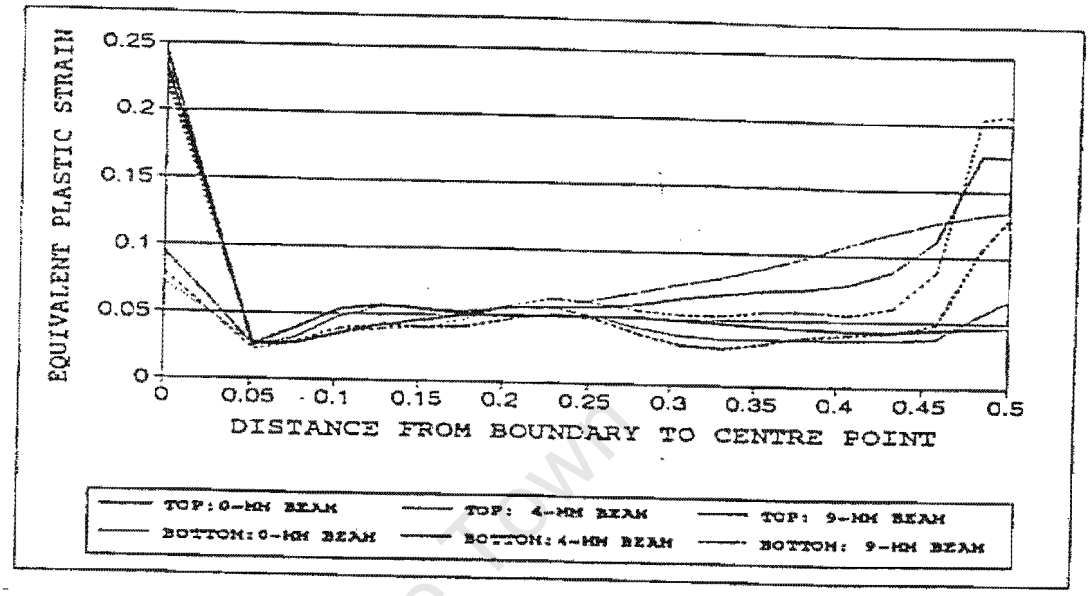

Figure 2.10 : Plastic strain distribution [20].

Wiehahn, Nurick and Bowles [8] used the temperature dependent material properties to show failure occurring as a result of a thermo-mechanical instability and localised shear banding. These localised shear banding provided new insights into the subsequent failure and tearing mechanism through the thickness of the plate undergoing deformation at strain rates in the range of $10^2 s^{-1}$ to $10^4 s^{-1}$. In their work, comparisons between experimental and numerical results gave favourable correlation with a temperature dependent simulation being a favourable correlation than a temperature independent simulation in situations where tearing did not occur. Deflections obtained from models using temperature dependent material properties are more than those using a temperature independent material. Simulations using temperature dependent properties showed severe necking as a result of unrealistically large strains in the localised region clearly indicating the point of failure for cases where tearing occurred when a coarse mesh was used. On the other hand, fine meshes predicted formations of shear bands at an angle of either 45^0 or 135^0 to the mid-plane for the same cases. The exact method of failure was highly dependent on mesh density. Figures 2.11 and 2.12 show this phenomenon.

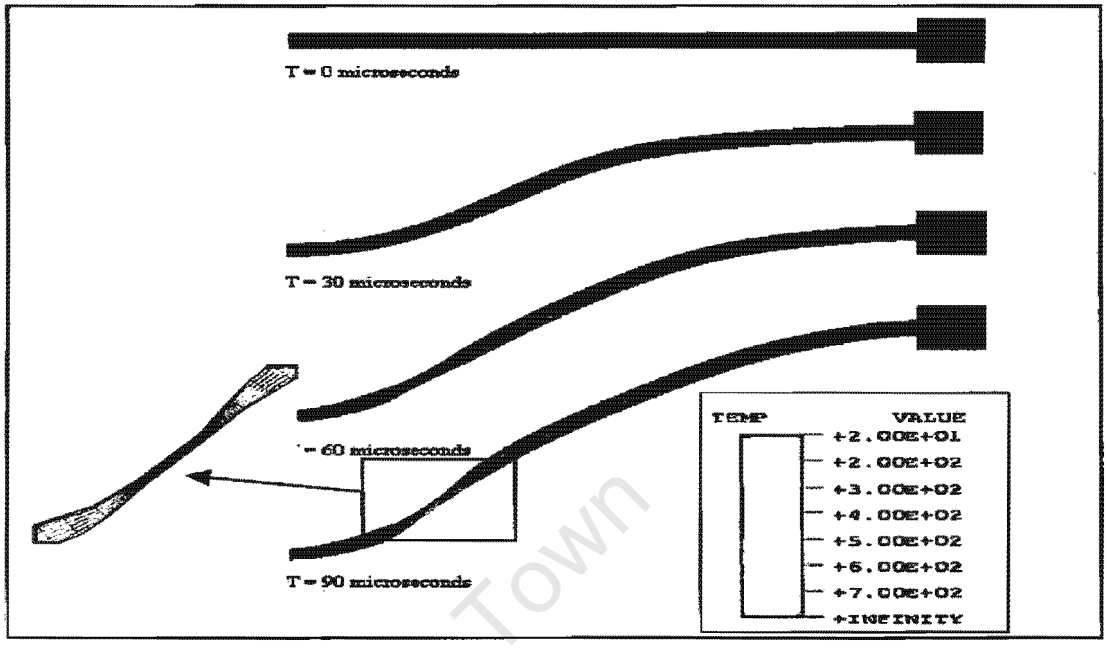

Figure 2.11: Severe element elongation predicting tearing [8]

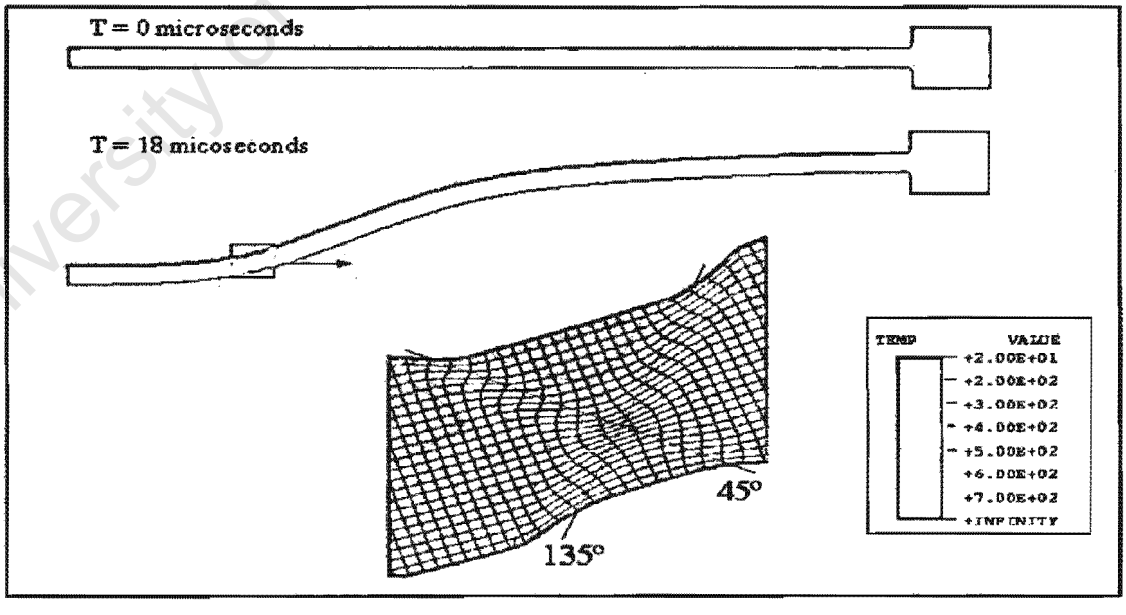

Figure 2.12 : Formation of shear band at 45^0 and 135^0 [8]

2.6 Circular Plates

2.6.1 Theoretical predictions

Taylor [13], Hudson [33], Richardson and Kirkwood [34] were the first to conduct theoretical studies into the influence of dynamic loads on the behaviour of circular plates. Hopkins and Prager [35] studied the dynamic behaviour of simply supported circular plates subjected to a rectangular pulse. The plate was idealised as a rigid-perfectly plastic material, and was assumed to obey the Tresca yield condition and associated flow rule. Florence [36] solved the problem of a circular clamped plate loaded with a central rectangular pulse. Witmer, Balmer, Leech and Pian [37] developed a numerical method, the predictions of which compared favourably with experimental values recorded for large dynamic deformations of beams, rings, plates and shells.

From the theoretical overview by Nurick and Martin [1], much effort has been concentrated on the dynamic deformation of plates in which either membrane forces or bending moments alone were believed to be important. Jones [12] attempted to link the two distinct stages of plastic strain and describe the behaviour of plates dynamically loaded with deflections in the range where both bending moments and membrane forces are important.

Nurick and Martin [38] reported on the response of impulsively loaded circular plates. They used a method based on a light interference technique to measure the displacement-time history. Final mid-point deflections up to 12 plate thicknesses were measured and a comparison of deflections and the time to peak response with the predicted membrane mode technique was made. Shen and Jones [17], presented an approximate theoretical analysis into the deformation and rupture of fully clamped circular plates. The analysis combines bending moments, membrane forces and transverse shear force and uses the Cowper-Symonds constitutive equation to include strain rate effects. Jones [39] presented an approximate theoretical procedure which includes strain rates to predict deflection. The maximum permanent transverse displacement (W_f) for a rigid, perfectly plastic membrane is given by:

$$\frac{W_f}{H_m} = \left(\frac{2\rho V_o^2 R_m^2}{3n\sigma_o H_m^2} \right)^{\frac{1}{2}} \qquad 2.2$$

where n introduces the strain rate effect and is given by:

$$n = 1 + \left(\frac{V_o W_f}{3\sqrt{2} D R_m^2} \right)^{\frac{1}{q}} \qquad 2.3$$

where

R_m : radius of the plastic membrane

H_m : thickness of the plastic membrane

W_f : maximum permanent transverse displacement

V_o : uniformly distributed impulsive velocity

ρ : density of material

σ_o : static yield stress

D and q are material constants.

2.6.2 Experimental studies

Nurick and Martin [2] noted that the number of theoretical predictions far outnumber the experiments performed. Consequently, most review papers on dynamic plastic behaviour of structures, and in particular of plates, subjected to impulsive loading have focused mainly on theoretical predictions.

Bodner and Symonds [40] investigated the response of fully clamped circular plates and measured the deflection-time history by using a condenser microphone placed near the centre of the plate. Nurick [41, 23] described experiments using annular rings of sheet explosive to simulate impulsive loading and in which the magnitude of the impulse is measured by means of a ballistic pendulum. The deflection-time history was recorded using a light-interference technique in which photo-voltaic diodes were used to measure

the light interference patterns obtained during deformation. Deflections of up to 20 mm during a time period of 200μs were observed on fully clamped circular, square and rectangular plates. An analysis of the experimental results provide a useful guideline for predicting maximum central deflection of impulsively loaded plate.

Teeling-Smith [42] has carried out an experimental study on clamped impulsively loaded circular plates which investigates the various modes of failure mentioned in section 2.3. Nurick, Gelman and Marshall [25] presented both experimental and numerical investigations on clamped circular plates with various boundary conditions. Investigation of the deformed plates identified several distinct observations at the boundary: Mode I (large inelastic deformation with no necking at the boundary); Mode Ia (large inelastic deformation with necking around part of the boundary); Mode Ib (large inelastic deformation with necking around the entire boundary); Mode II^* (tearing around part of the boundary); Mode II (tearing around entire boundary).

Gelman, Nurick and Mitchell [10] presented numerical investigations on impulsively loaded circular plates with various boundary conditions. They observed that the boundary condition has no effects on mode I failure but greatly affects failure modes II and III. They noted here that the occurrence of thinning and hence subsequent rupture is highly dependent on the boundary fixation conditions.

A dimensionless damage number, Φ is used to compare experimental results with other experiments, which have different target dimensions. Nurick and Martin [2] by considering the damage number defined by Johnson [43], modified the damage number for circular plates as follows:

$$\Phi_c = \frac{I\left(1 + In\left(\frac{R}{R_o}\right)\right)}{\Pi R t^2 (\rho \sigma_o)^{\frac{1}{2}}} \qquad 2.4$$

where

R : the radius of the plate

R_o : radius of the loaded area

t : plate thickness

ρ : density of material

σ_o : static yield stress

Nurick and Radford [27] carried out a series of experimental investigation into the deformation and tearing of clamped circular plates subjected to localised central blast loads. They observed that for circular plates subjected to a central blast load, the response is characterised by an inner dome surperimposed on the global dome. Nurick and Radford further analysed the micro response of the plates and noted that the grain elongation is high in areas where thinning or tearing occurs.

Circular plates on which numerical investigation for the work of this thesis is based on are those of Teeling-Smith [42]. He carried out the experimental work on plates by using test plates of 200mm square and clamping them between two 20mm thick heavy steel plates by means of eight M12 bolts. Both the heavy clamping plates had a 100mm diameter circular hole in the centre (figure 2.13), through which the thin test plates deformed when loaded impulsively.

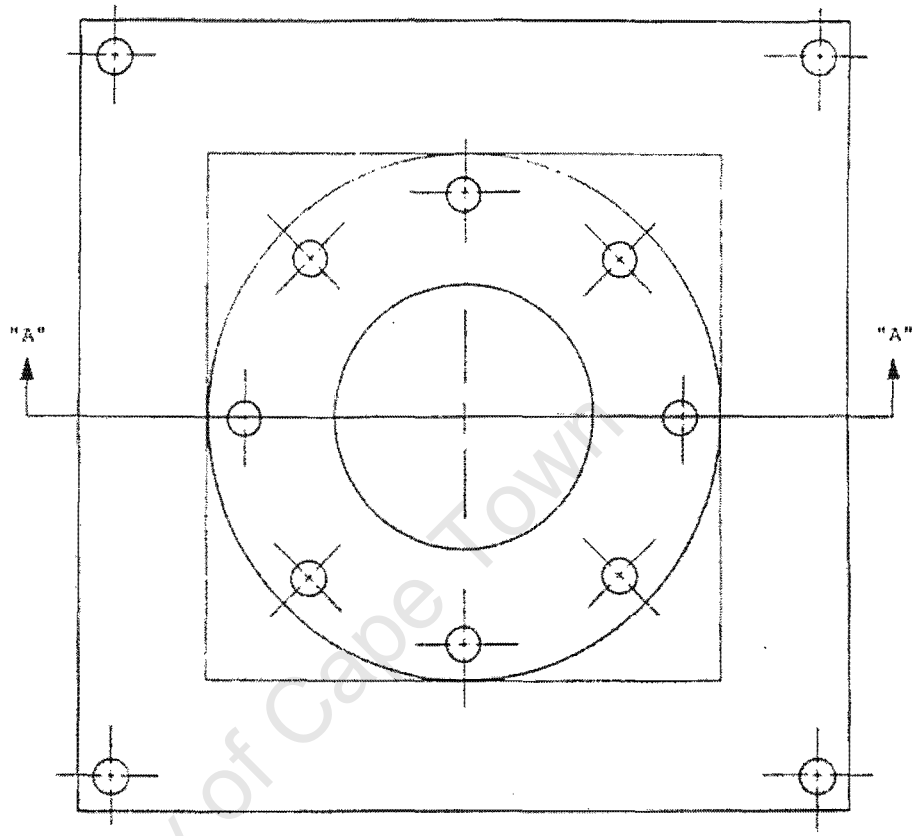

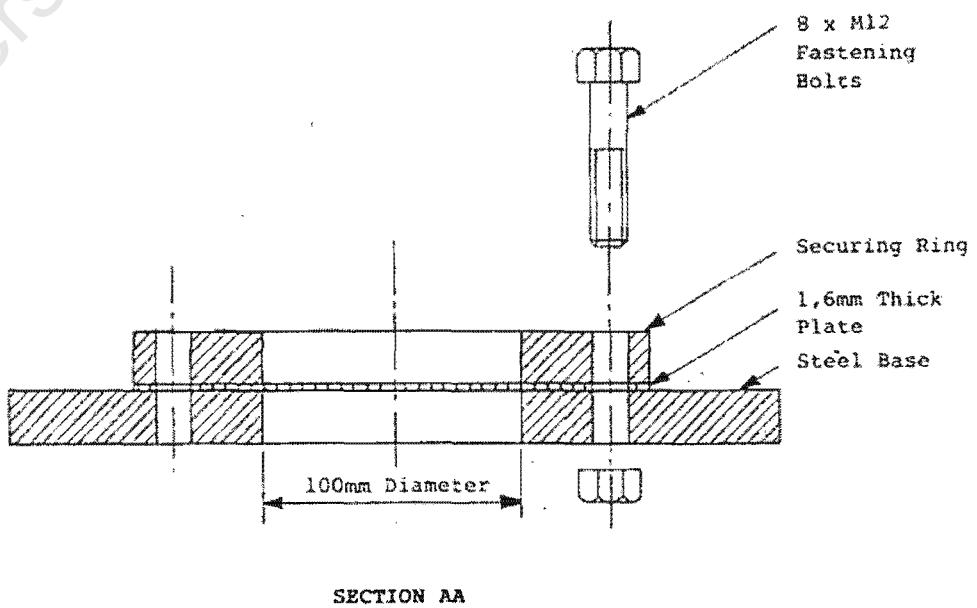

Figure 2.13 : Test plate and Clamping Device [42].

Teeling-Smith recorded three measurements for each experiment; firstly the impulse from which the initial velocity of the plate as well as the total energy input was determined. Secondly the velocity of circular disc from plates that under went complete tearing was recorded as this enabled the excess kinetic energy to be calculated and thirdly measurement of the final mid-point deflection and shape of the deformed plates. He measured the velocity of the circular disc by means of breakage of two fuse wires with a small voltage applied across each wire. As each wire is broken a signal is sent to a digital oscilloscope where the time taken for the disc to travel a certain distance is measured. The final mid-point deflection is measured using the digitising of approximately three hundred points on each plate, these are then interpolated and plotted. Contour paths and three-dimensional image are produced for a number of test plates and from the contour paths the deformed shape across selected cross-sections was determined.

2.7 Square Plates

2.7.1 Theoretical predictions

Nurick and Martin [1] reported that predictions on the deformation of quadrangular plates considered the bending action of plates, membrane effects, energy methods and approximate techniques. Due to the complex nature of the quadrangular plate problem, limited theoretical work has been presented on the deformation and rupture of square plates.

Jones [39] presented an approximate theoretical procedure which includes strain rate effects to predict deflection.

$$\frac{W_f}{H} = \left[\frac{(1+3\lambda)^{\frac{1}{2}} - 1}{4} \right] \qquad 2.5$$

with

$$\lambda = \frac{\mu V_o^2 L_B^{\ 2}}{M_o H} \qquad 2.6$$

where

μ : mass per unit length

V_o : initial impulsive velocity

L_B : beam half span

H : beam depth

M_o : fully plastic bending moment

This procedure gives a lower bound for the deflection-thickness ratio. An upper bound can be found by replacing σ with $0.618\sigma_o$. The constant 0.618 relates to the inscribing yield criterion of the plastic yield surface and is determined from the fully plastic bending moment- axial force (m-n) characteristic relation for a rectangular section. See figure 2.14.

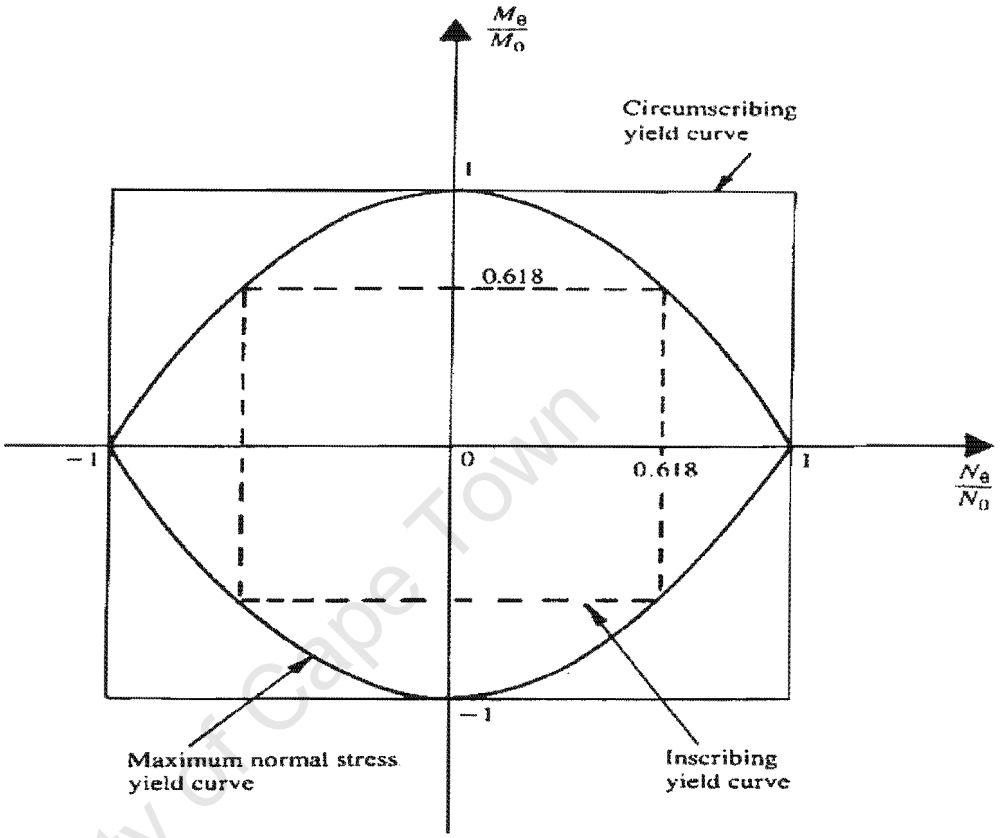

Figure 2.14 : Exact and approximate yield curves for a beam with a rectangular cross-section [39] .

For a quadrangular plate of length 2L and width 2B which is fully clamped around the entire boundary and subjected to a uniformly distributed impulsive velocity, V_o, the maximum permanent transverse displacement, W_f, is given by:

$$\frac{W_f}{H} = \frac{(3-\xi_o)\left\{\left(1+\frac{\Gamma}{n}\right)^{\frac{1}{2}}-1\right\}}{2\{1+(\xi_o-1)(\xi_o-2)\}} \qquad 2.7$$

where

loading parameter; $\Gamma = \frac{2\rho V_o^2 L^2 \beta^2}{3\sigma_o H^2}(3-2\xi_o)\left(1-\xi_o+\frac{1}{2-\xi_o}\right)$ 2.8

geometry parameter; $\xi_o = \beta\left\{(3+\beta)^{\frac{1}{2}}-\beta\right\}$ 2.9

strain rate enhancement; $n = 1+\left(\frac{V_o W_f}{3\sqrt{2}DB^2}\right)^{\frac{1}{q}}$ 2.10

and

aspect ratio; $\beta = \frac{B}{L}$ 2.11

Jones [40] also presented a dimensionless initial kinetic energy. This relationship is given by:-

$$\lambda = \frac{\mu V_o^2 L_B^{\ 2}}{M_o H} \quad 2.12$$

where

μ : mass per unit length

V_o : initial impulsive velocity

L_B : beam half span

H : beam depth

M_o : fully plastic bending moment

The static fully plastic bending moment is given by :

$$M_o = \frac{\sigma_o B_p H^2}{4} \quad 2.13$$

where

B_p : plate breath

These approximate theoretical procedures give reasonable correlation with experimental results in predicting mode I failure, Jones [40].

2.7.2 Experimental prediction

Nurick and Martin [2] presented an extensive experimental overview of the blast loading of plates. Nurick [1, 2] provides a method of relating the plate geometry, impulse and material properties of plates of different thicknesses using the damage number. The relation is given by :

$$\Phi_q = \frac{I}{2t^2\left(BL_p\rho\sigma_o\right)^{\frac{1}{2}}} \qquad 2.15$$

where

I : applied impulse

t : plate thickness

B_p : plate breath

L_p : plate length

σ_o : material static yield stress

ρ : material density.

This relationship is true for plates that have been deformed and showed no sign of tearing.

From the relationship in (equation 2.15) Martin and Nurick [1, 2] obtained an empirical relationship of the form:

$$\frac{\delta_f}{t} = 0.471\ \Phi_q + 0.001 \qquad 2.16$$

Theoretical techniques are based upon assumptions and simplifications and are therefore well suited to the preliminary design of blast-loaded structures and as a check to experimental and numerical results.

Nurick [44] presented an empirical solution for predicting maximum central deflection of impulsively loaded plates. An analysis of the experimental results of plates subjected to an impulsive load by means of sheet explosive was performed in order to predict with reasonable certainty the resulting mid-point deflections of the plate. Using the available experimental information, Nurick [44] showed that there is a 90% probability that the deflection-thickness ratio will be ± 1 deflection-thickness ratios of the least square fit. Thomas [31] investigated the effect of boundary conditions on the failure of thin plates and from his study the clamping or fixing conditions at the boundary determines the tearing mechanism encountered. He concluded as follows:

•Changing the plate from being clamped to being integral has negligible effect on mode Ia failure. Mode II failure occurred at lower impulse for integral plates, and appeared to have a higher shear component in their failure.

• Those theoretical solutions found to be valid for mode I failure for clamped plates are also valid for integral plates.

•The assumption of fully constrained edges does not accurately model the edge boundary conditions of clamped plates. Theoretical and numerical methods need to adjust the assumed boundary conditions to distinguish between clamped and integral plates.

Nurick, Olson, Fagnan and Levin [15] presented an investigation on the deformation and tearing of blast-loaded stiffened square plates. The experimental and numerical results were carried out on plate with integral boundary conditions. They observed that the predicted central displacement decrease with increasing stiffener size. Olson, Fagnan and Nurick [14], using numerical and experimental techniques for square plates respectively and assuming fixed end conditions have shown that in the experiments, the plates exhibited essentially the same modes of failure; I (permanent large deformation), II (tensile tearing) and III (shear rupture) as previously observed for circular plates. Chung [45] using stiffened square plates present both experimental and numerical investigations into the deformation and tearing of quadrangular plates using the approach that include and exclude temperature dependent material properties to determine modes II and III failure. The experimental results showed that the plates exhibited essentially mode I failure and only a few cases of mode II failure. Other phases in the mode II failure region exhibited were mode II-1, mode II-2 and mode II-3 which designate mode II^* failure at the number of sides of the plate that tore and mode II which is defined where partial tearing of the boundary occur.

Square plates investigated in this study are those studied by Nurick and Shave [26]. The experimental procedure they used was similar to that of Teeling-Smith [42], and the arrangement is as shown in figure 2.13 section 2.6.2. The only significant difference is that the experimental rig was arranged to accommodate square plates.

The test specimen were cut from 1.6 mm cold-rolled mild steel plates with dimensions of 240x240 mm. The area of the plate subjected to loading was 89x89 mm. These dimensions of the loaded area gave almost the same area loaded in circular plates in section 2.6 by Teeling-Smith. The test specimens were clamped between two 20 mm thick steel plates with eight 11 mm diameter high strength bolts on a bolt diameter of 175 mm.

The load on plates investigated by Nurick and Shave [26] was applied by strips of explosive laid out on a polystyrene pad in two concentric square annuli which were

interconnected by two perpendicular strips of explosive (figure 2.6 section 2.2). The detonator was attached to the centre of the perpendicular strip. The speed of detonation of the explosive was 6500 - 7500ms^{-1}. The impulse was increased by increasing only the mass of the annuli and not the cross piece. Figure 2.6 section 2.2 shows a schematic diagram of the explosive layout.

The failure modes observed by Menkes and Opat [3] were also reported by Nurick and Shave[26]. Mode II failure was defined into *II** (tensile tearing at the outer fibres over part of the support) and Mode II (tensile tearing at outer fibres over the entire support).Mode II was further identified as IIa (complete tearing of the sides with mid-point deflection of the plate increases with increasing impulse); and mode IIb (complete tearing of the plate with the mid-point decreases with increasing impulse).

2.8 Rectangular Beams

2.8.1 Theoretical predictions

Some of the earliest studies in dynamic plastic beam response were those of Lee and Symonds [46] and Symonds [47], which dealt with beams subjected to concentrated midspan pulse loads. The analysis uses a rigid-plastic material idealisation based on the assumption that elastic strains are much smaller than plastic strain and can therefore be neglected. Symonds [48] later used the rigid-plastic idealisation to obtain solutions for the response of simply supported and clamped beams subjected to uniformly distributed pulse loads. Schubak, Anderson and Olson [49] presented a simplified dynamic analysis of rigid-plastic beams in which the beams are assumed to have doubly symmetric cross-sections and obey a rigid-plastic material law. They also developed a simplified analytical procedure to predict the dynamic response of stiffened plates to high intensity load pulses by modelling the plates as rigid-plastic beams or grillages. The partial end fixity of a stiffened plate was modelled by connecting the beams to rigid supports with rigid-plastic links of zero length and reduced plastic capacities. The true beam yield curve was approximated by four segments. As a consequence, the response of the beam was divided into two distinct linear phases; an initial plastic hinge mechanism phase (small-displacement) where the beam resists the load primarily through bending and a later plastic string phase (large-displacement) where the beams bending resistance disappears as shown in figure 2.15.

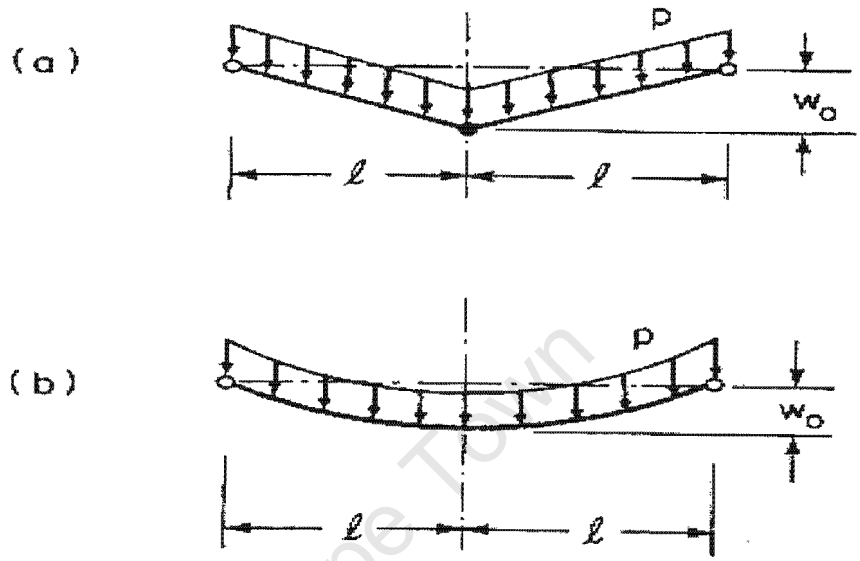

Figure 2.15 : Deflection modes: (a) single mid-span hinge (bending) mechanism; (b) plastic string [49].

This response was solved using two methods. In the first method, the two phases were governed by linear differential equations that were solved in closed form and in the second method, the response was approximated as a sequence of "instantaneous'' mode response, in which the velocity field was solved by an "instantaneous" mode solution algorithm wherein the "instantaneous" modes were taken to be over time steps of small but finite duration Δt.

He-Ming Wen [50] presented an approximate theoretical analysis based on a power law stress-strain relationship. The predicted rupture (tensile tearing) of the beams under impulsive loading by an effective strain failure criterion which takes into consideration the influence of the transverse shear on the axial tensile strain was considered. The theoretical predictions are in reasonable agreement with the experimental observations in

terms of the maximum permanent transverse displacement and the critical input impulse causing beam tensile failure when material rate sensitivity is taken into consideration.

Li and Jones [51] proposed an analytical model for studying the material failure in shear hinges which develop during the dynamic plastic response of beams. The modelling of the structural response outside a shear hinge using a rigid, perfectly plastic theory and within the shear hinge, strain hardening, strain rate and temperature effects were considered in order to obtain the conditions for an adiabatic shear failure.

Jones [39] presented the maximum permanent transverse displacement, W_f, of a beam which is fully clamped at both ends and impulsively loaded, with a uniform velocity, V_o, across the entire span, $2L_B$, by :

$$\frac{W_f}{H} = \frac{1}{2}\left\{\left(1+\frac{3\rho V_o^2 L_B^2}{n\sigma_o H^2}\right)^{\frac{1}{2}} - 1\right\} \qquad 2.17$$

where

strain rate enhancement is given by :

$$n = \frac{\sigma_o^1}{\sigma_o} = 1+\left(\frac{V_o W_f}{3\sqrt{2}DL_B^2}\right)^{\frac{1}{q}} \qquad 2.18$$

2.8.2 Experimental studies

Jones, Griffin and Van Duzer [52] describe experiments on end-clamped wide beams and rectangular plates in which the impulse was measured directly using a ballistic pendulum. Rectangular beams investigated in this study are those of Menkes and Opat [3]; aluminium 6061-T6. Figure 2.7 section 2.2 shows the experimental configuration. The high pressure was provided by sheet explosive, which is cemented to a neoprene buffer which in turn, is bonded to the top surface of a clamped aluminium beam. The explosive was laid in such a way that it extended over the beam supports. A 6.25 mm thick neoprene buffer was used to prevent rear-surface spallation. The high explosive used was Du pont Detasheet D, and the adhesive was Du pont 4684 cement, thin 1:1 with acetone; Menkes and Opat [3]. The detonation point for the rectangular beams was at the point B indicated in figure 2.7 section 2.2. No deformation asymmetry was observed with this particular method of set up of the explosive and the detonation point. Figure 2.16 shows typical results obtained from this by Menkes and Opat [3].

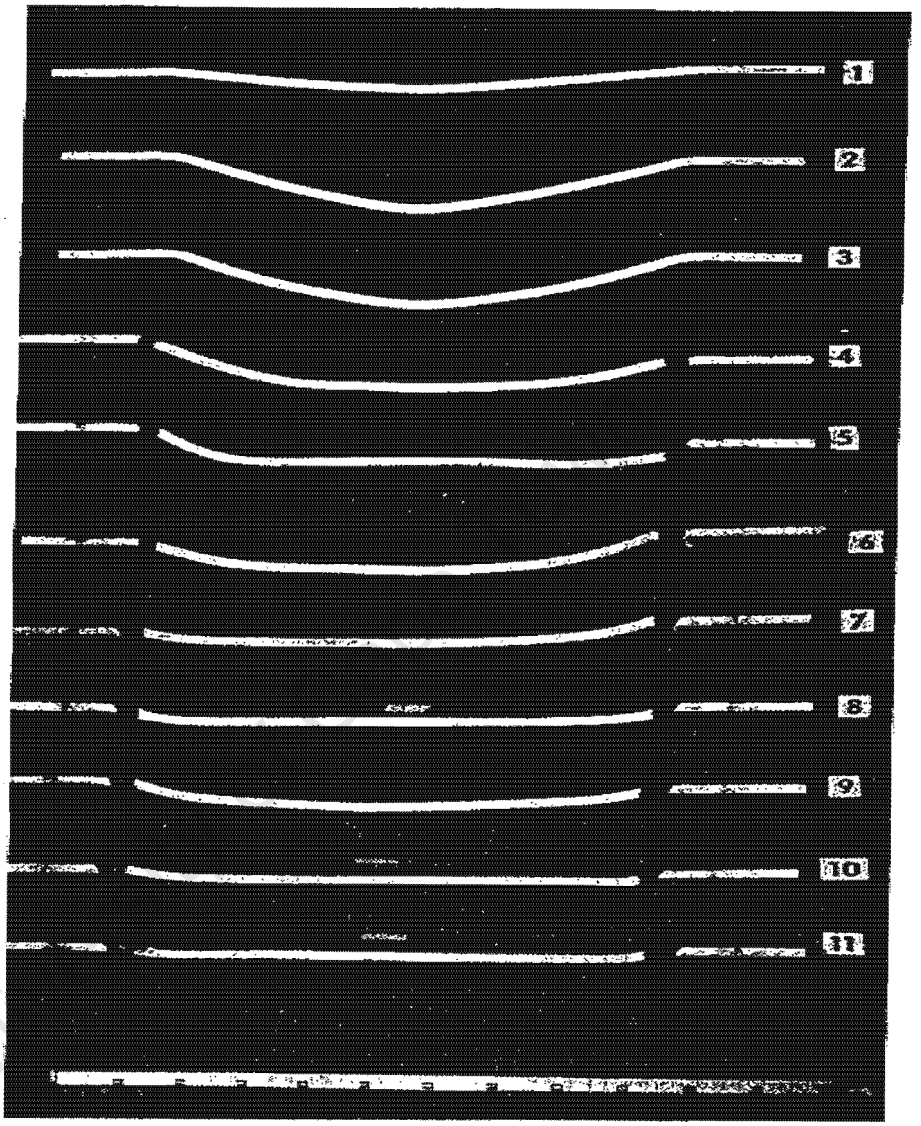

Figure 2.16 : Permanent deformed profiles of aluminium 6061-T6 beams examined by Menkes and Opat, illustrating the transition from a mode I to a mode III with increasing impulsive velocity [39].

2.9 T-Beams

2.9.1 Theoretical predictions

The theoretical rigid-plastic predictions for the dynamic plastic response of impulsively loaded fully clamped beams with rectangular cross-section have been found to give favourable correlation with the permanent transverse displacements recorded on metal beams. This method is used to provide an approximate solution for T-section beams with satisfactory agreements with experimental data. Nurick, Jones and Von Alten-Reuss [29] reported that "a satisfactory correlation is found between the theoretical predictions and the corresponding experimental results, with the experimental data generally bounded by the theoretical predictions which uses inscribing and circumscribing curves to the exact yield surfaces''. Interaction yield curves for T-sections have been used by Schubak, Anderson and Olson [49]. The moment-axial force interaction curves must be developed for the particular T-shaped cross-section. Using the procedure of Schubak, Anderson and Olson [49], figure 2.17 was obtained by Nurick, Jones and Von Alten-Reuss [29]. The shape of this interaction curve reflects the asymmetry of the cross-section. A simplified inscribing square yield criterion is based on the values m=n=0.566, that is σ_o in equation 2.20 is replaced by $0.566\,\sigma_o$ and equation 2.19 then predicts an approximate upper bound on the maximum permanent transverse displacement. This adjusted value of σ_o also inscribes the coordinates m=-n=0.688 shown in figure 2.17.

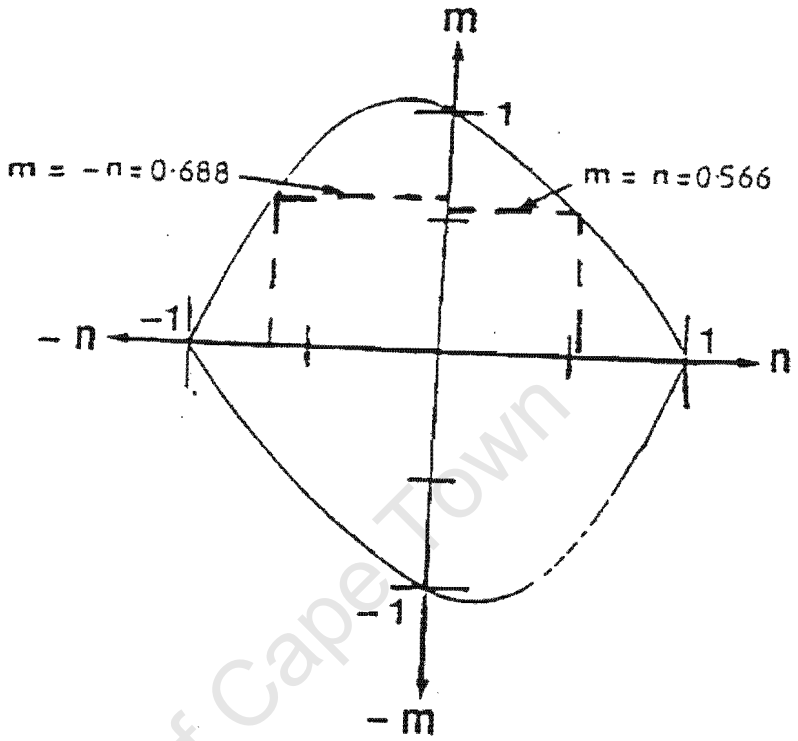

Figure 2.17 : Interaction Yield Curve for a T-section beam [29].

Nurick and Jones [28] presented an approximate theoretical analysis which accounts for asymmetry of the cross-section of T-beams which are subjected to uniform impulsive loads resulting in large inelastic deformations. Predictions have also been reported by Schubak, Anderson and Olson [49] using finite element analysis for beams with both rectangular and I shaped cross sections. Schubak, Anderson and Olson [49] further reported that the interaction relations of all practically doubly-symmetric sections can be accurately approximated by a linear interaction in m-n space in figure 2.14. Nurick and Jones [28] described the effect of the m-n interaction for T-beams subjected to impulsive loads causing large inelastic deformations. Their predictions were compared with five sets of experimental data having varying cross-section and lengths.

The maximum permanent transverse displacement of a rigid, perfectly plastic, fully clamped beam with a rectangular cross-section of depth H, which is subjected to an impulsive velocity across a span $2L_B$ given in equation 2.19 is modified to account for the asymmetry of the T-section beam as follow :

$$\frac{W_f}{H} = \frac{1}{2}\left[\left(1+\frac{3}{4}K\lambda\right)^{\frac{1}{2}} - 1\right] \qquad 2.19$$

where

$$\lambda = \frac{\mu V_o^2 L^2}{M_o H} \qquad 2.20$$

K is determined from the fully plastic axial force and bending moment carrying capacity and is given by:

$$K = \frac{HN_o}{4M_o} \qquad 2.21$$

When

K=1; equation 2.19 predicts the maximum permanent deflection of a rectangular beam.

2.9.2 Experimental studies.

T-beams considered in this study are those of Nurick, Jones and Von Alten-Reuss [29]. The test specimens were cut from extruded aluminium 6063 alloy sections to the dimensions shown in figure 2.17.

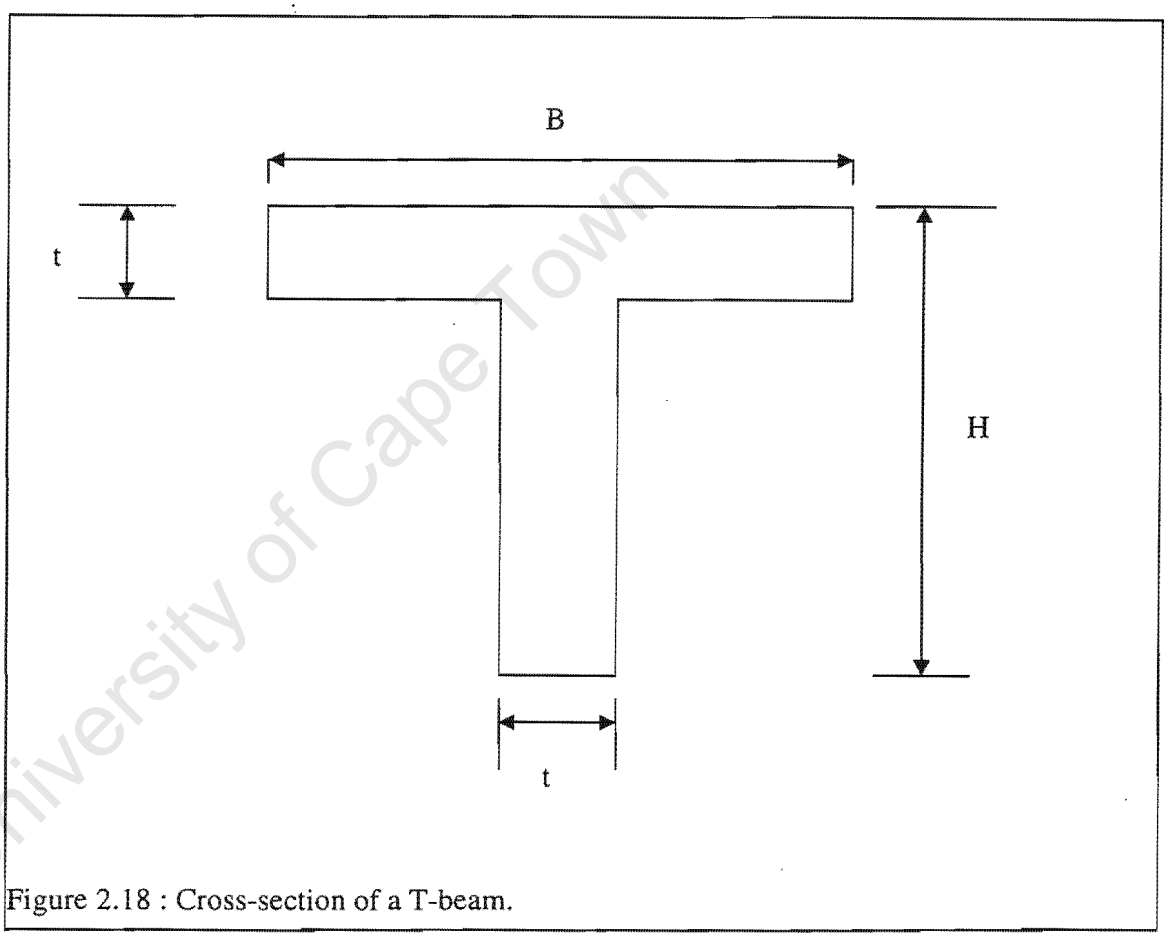

Figure 2.18 : Cross-section of a T-beam.

The test was performed on a ballistic pendulum using plastic explosive to initiate a uniform impulsive load. The rigid body displacement of the pendulum is used to determine the impulse and hence the magnitude of the initial velocity. A cylindrical strip of explosive was laid along a 25 mm thick polystyrene pad, the full length of the centerline of the beam flange. A short pig-tail of explosive was placed at the centre of the cylindrical strip, to which the detonator was attached. The speed of detonation of the explosive was 6500-7500m s^{-1} resulting in complete detonation in approximately 11 μs

to 15 μs for beam spans of 150 – 200 mm respectively. The detonation point of the explosive was at point A as shown in figure 2.7.

The specimens were clamped at both ends with serrated hardened steel, to prevent sliding during testing. A spacer was used to stabilize the section. The clamping blocks were clamped together using six bolts per support, three per side of the beam. The experimental set-up is shown in figure 2.18.

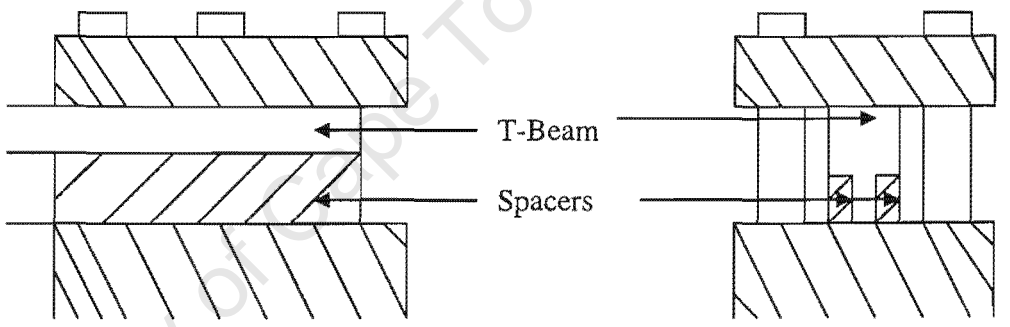

Figure 2.19 Clamping rig for blast loaded T-section aluminium beams.

3.0 Material Properties

To better understand the behaviour of steel plates and aluminium alloy beams investigated in this study, a better knowledge of the material properties of these metals is required. Stress strain curves were obtained from standard tensile tests and converted into true stress and logarithmic plastic strain according to the ABAQUS / Explicit code manual [53].

Mild steel plates and aluminium beams undergoing blast-loading conditions plastically deforming at high strain rates causing localised high temperatures as a result of high strain rate. Material properties at such strain rates and temperatures are under-going further research at the moment.

Two material models can be used to model such high strain rate deformations. They are:

- the classical metal plasticity model
- the Johnson-Cook plasticity model

3.1 Classical metal plasticity model

The classical metal plasticity model uses standard Mises or Hill yield surfaces associated with plasticity flow, which allows for isotropic and anisotropic yield, respectively. It can be used when rate-dependent effects are important. It is implemented by using stress-strain data from uni-axial tensile tests that are modified for yield hardening, strain rates and temperature dependencies with a strain based shear failure / predictor incorporated.

3.1.1 Yield hardening

Most materials with ductile bahaviour yield at stress levels that are orders of magnitude less than the elastic modulus of the material. This means that Young's modulus describes their elastic region. For the plastic region, logarithmic plastic strain and true stress are

required. For an isotropic material; mild steel and alumimum alloy considered in this study; the norminal stress-strain data obtained from uni-axial tests is converted to true stress and logarithmic plastic strain using the following equations:

$$\sigma_{true} = \sigma_{nom}(1+\varepsilon_{nom}) \qquad 3.1$$

$$\varepsilon_{In}^{pl} = In(1+\varepsilon_{nom}) - \frac{\sigma_{true}}{E} \qquad 3.2$$

Where

σ_{nom} : nominal stress; σ_{true} : true stress

ε_{nom} : nominal strain; ε_{In}^{pl} : logarithmic plastic strain and E : Young's Modulus.

Graphs of the logarithmic plastic strain and true stress for mild steel and aluminium alloy are shown in figures 3.1 and 3.2 respectively.

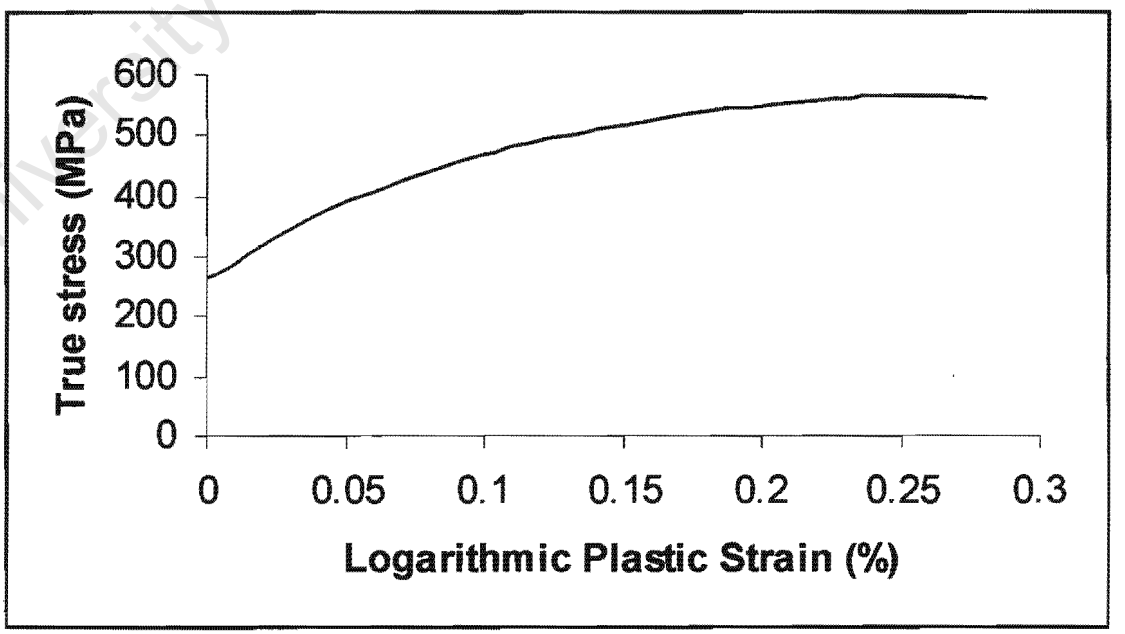

Figure 3.1: Graph of true stress vs. plastic strain (mild steel).

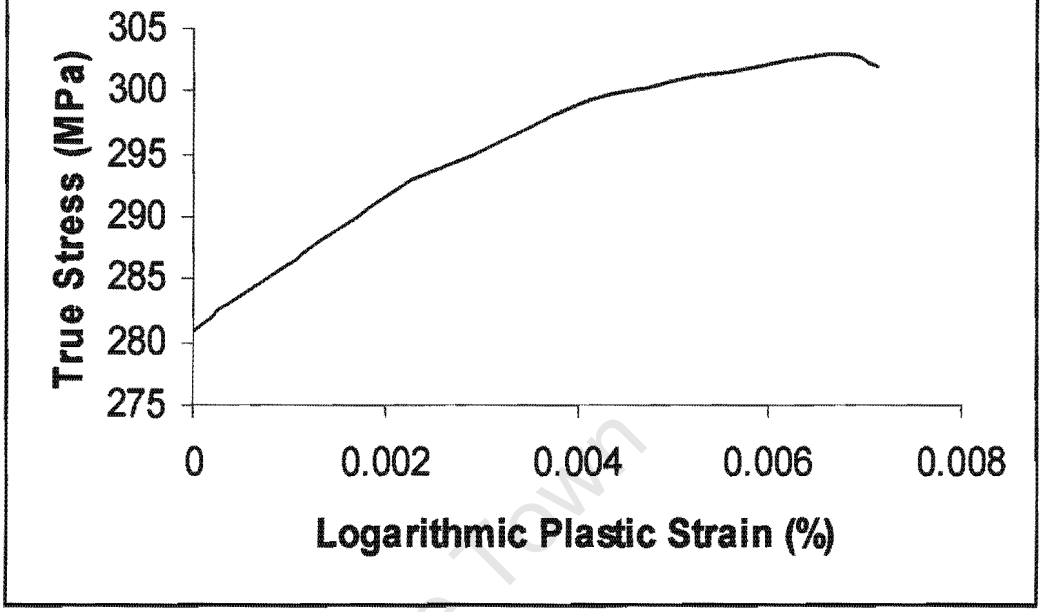

Figure 3.2 : Graph of true stress vs. plastic strain (aluminium 6061-T6).

3.1.2 Internal heat generation

Internal heat is generated through the dissipation of plastic work. Wiehahn, Nurick and Bowles [8] assumed that 90% of the plastic work in centrally uniformly loaded circular plates is converted to heat. This is essentially because of the short duration of the blast; (15 μ s) and the subsequent deformation of the plate; (150 μ s) allowing very little heat to be dissipated from the deformation area. They assumed further that the process was adiabatic and the density and specific heat of the material do not change with temperature.

3.1.3 Steel properties at high temperatures

Steel does not provide any significant resistance to heat transfer and, furthermore, the thermal properties of steel that are of interest do not vary significantly with temperature, as opposed to mechanical properties. The mechanical behaviour of steel can be described with one theoretical model since the effect of temperature on the stress-strain curves of steel is the same for all types of steel as reported by Soares, Gordo and Teixeira [4]. They further observed that when there is a temperature differential within the plate, this

generates thermal stresses increasing with temperature until they reach a level that induces the collapse of the plate. Initial temperature has a significant effect on the collapse of the plates. Figure 3.3 shows the behaviour of steel at high temperatures. It is observed from figure 3.3 that for temperatures higher than $200^{\circ}C$, the stress-strain characteristics of steel change by decreasing the yield stress and the modulus of elasticity. This effect combined with increase of stress associated with the temperature increase leads to the collapse of plates.

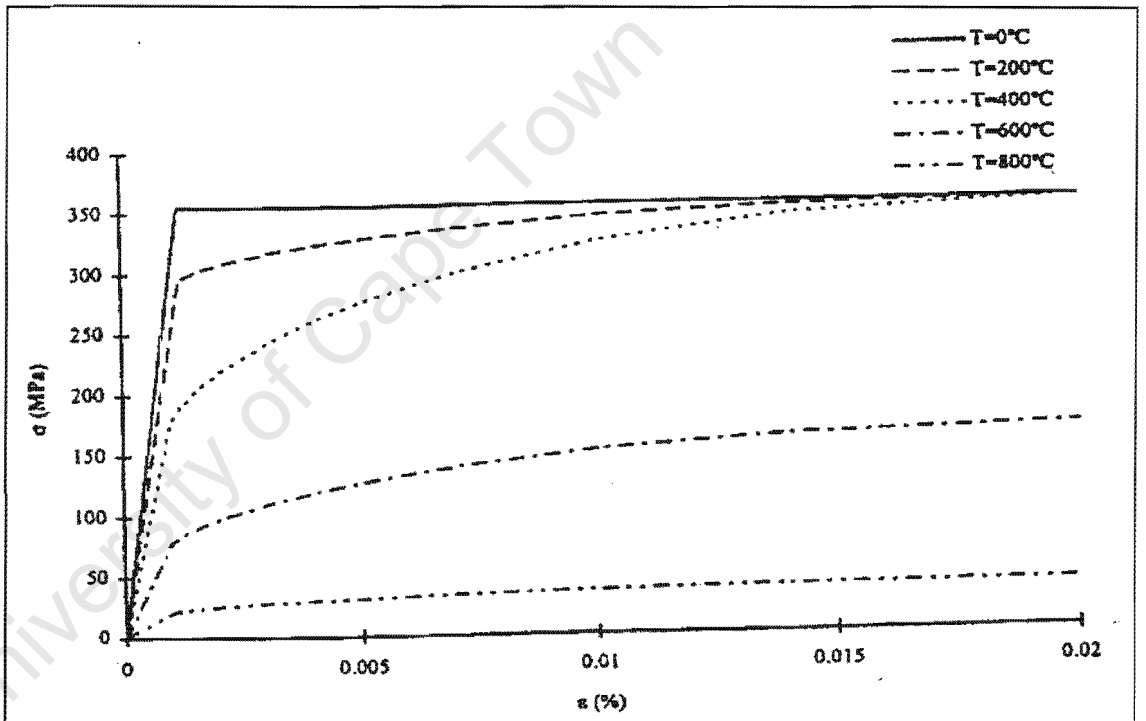

Figure 3.3: Variation of stress-strain relationship with temperature for steel [4].

3.1.4 Aluminium alloy properties at high temperature

The deformation and fracture characteristics of aluminium alloys, for example carbon fibre reinforced 7075-T6 matrix composite, is affected by temperature variations. The flow behaviour of the composite is strongly dependent on temperature and strain rate as reported by Woei-Shyan Lee, Wu-Chung Sue and Chi-Feng Lin [6]. Figure 3.4 shows this variation at different temperatures and strain rates.

There is a general tendency toward decrease in flow stress at increased temperature. Comparing the difference in flow stress resulting from both strain rate and temperature, it is observed that flow stress is strongly influenced by temperature.

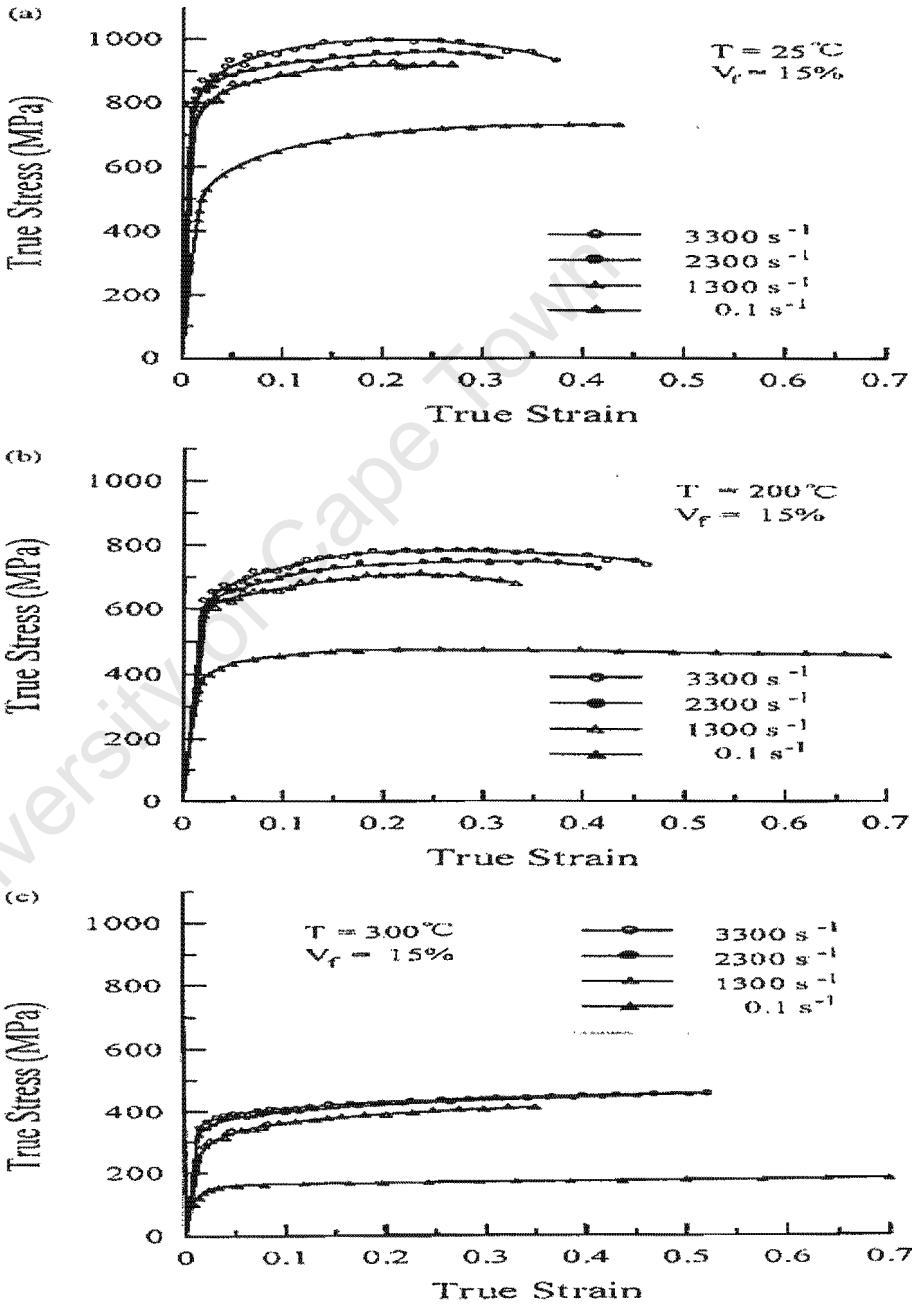

Figure: 3.4: Typical true stress / strain curves of 15%V_f carbon fibre reinforced 7075 al metal-matrix composite deformed at temperatures of (a) 25^0C, (b) 200^0C and (c) 300^0C under various strain rates [6].

Guedes, Gordo and Teixeira [4] observed that the maximum load carrying capacity of steel plates is often reached at temperatures ranging from 100^0C to 200^0 C, a situation in which the yield stress of the material has not decreased too much yet. They observed further that the elastic support of the plates are important until collapse is reached. The increase in temperature induces a tendency for the plates and beams to expand. For temperatures higher than 200^0C, the stress-strain characteristics of steel and aluminium change by decreasing the yield stress and the modulus of elasticity. These effects combined with increase of stresses associated with the temperature elevation leads to the collapse of the plates and beams. Guedes, Gordo and Teixerira [4] observed further that at ambient temperature the collapse strength of plates is governed mainly by the plate slenderness, although the boundary conditions, the aspect ratio and the initial distortions are important parameters.

Plastic work results in heat generation causing the degradation of material properties. Since ABAQUS / Explicit allows adiabatic stress analysis to be performed where heat is generated by the plastic strain, temperature dependent material properties were incorporated in the numerical analysis. Masui, Nunokawa and Hiramatsu [55] reported the temperature dependence of Young's modulus and yield stress for mild steel, as shown in the following equations.

$$E = 207x10^9 - 58.34x10^6.\tau \quad \text{for} \quad \tau \le 600^0C \qquad 3.3$$

$$E = 3.1x10^5.(\tau - 1100)^2 + 97x10^9 \quad \text{for} \quad 600^0C < \tau \le 1100^0C \qquad 3.4$$

$$\sigma_o = \sigma_{yo} \quad \text{for} \quad \tau \le 200^0C \qquad 3.5$$

$$\sigma_o = \sigma_{yo}x[1 - 0.00178.(\tau - 200)] \quad \text{for} \quad 200^0C < \tau < 700^0C \qquad 3.6$$

$$\sigma_o = \sigma_{yo}x[0.133 - (\tau - 700)x3.884x10^{-4}] \quad \text{for} \quad 700^0C \le \tau \le 1000^0C \qquad 3.7$$

where

E : Young's Modulus; τ : material temperature;

σ_o : static yield stress; σ_{yo} : static yield stress at the reference temperature of the tensile test.

The temperature rise due to the plastic strain is computed using the specific heat of the material while Young's modulus and true stress and logarithmic plastic strain data are put in tabular form for different temperatures. ABAQUS / Explicit determines the exact Young's Modulus and strain by linear interpolation of the tabulated values.

Young's Modulus as a function of temperature is shown in figure 3.5. The Young's Modulus gradually decrease linearly from a value of 207GPa at room temperature to 175GPa at 600^0C. It then decays quadratically to 100.1GPa at 1000^0C.

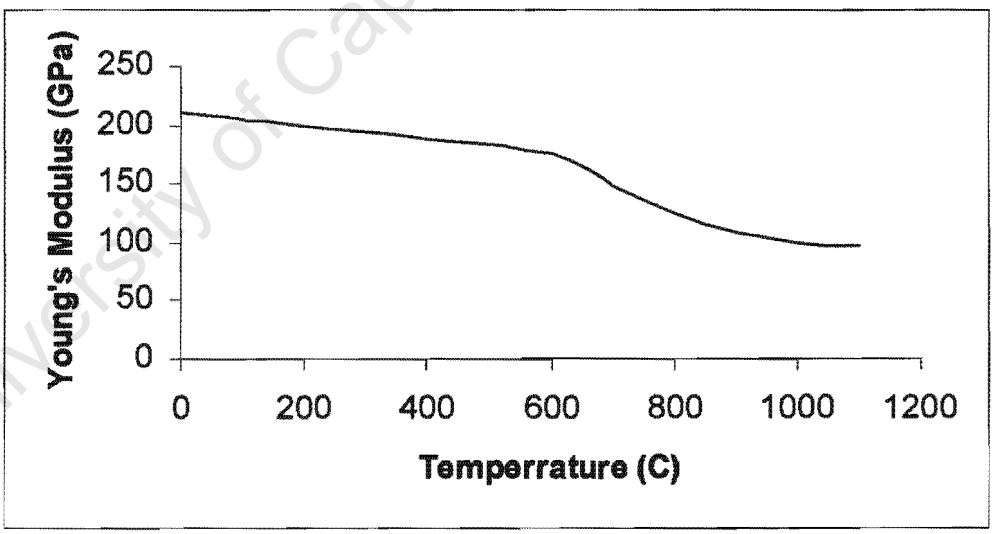

Figure 3.5: Graph of temperature vs. Young's Modulus (mild steel).

The yield stress is not affected by temperatures below 200^0C. In this case, the yield stress remains constant until a temperature of 200^0C, at which point it decays at a rate of $449KPa/^0C$ to a temperature of 700^0C. From 700^0C to 1000^0C, the yield stress further decreases but at a slower rate of $100KPa/^0C$. A graph of yield stress vs. temperature is shown in figure 3.6.

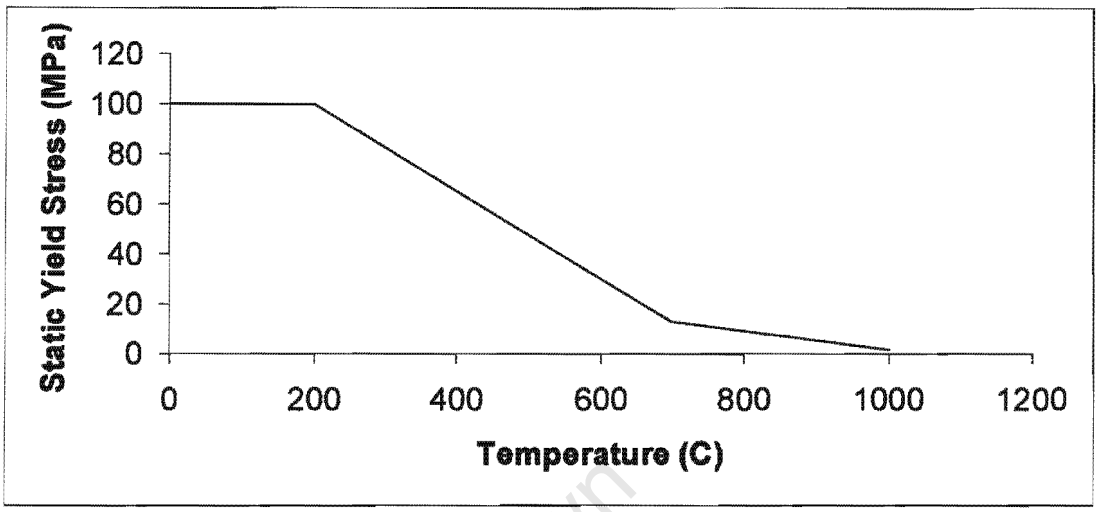

Figure 3.6 : Graph of temperature vs. yield stress (Mild steel).

A comparison of the temperature effect on the yield stress and Young's Modulus is shown in figure 3.7. The yield stress and Young's modulus were normalised by dividing the Young's Modulus and the yield stress at any temperature by Young's Modulus and yield stress at $0°C$ respectively. It can be seen from the graph that the yield stress is more affected than Young's Modulus.

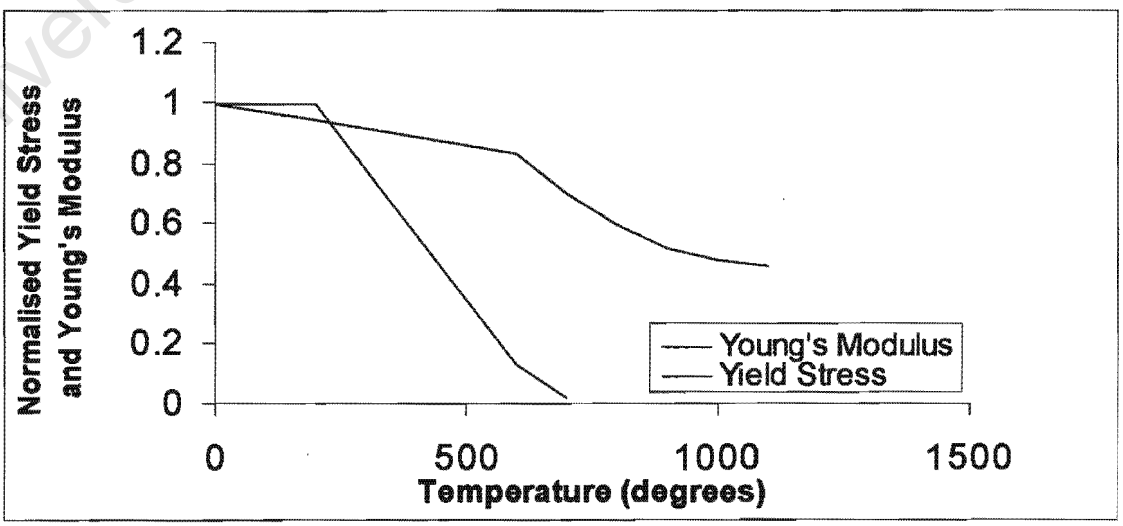

Figure 3.7 : A comparison of the normalized static yield stress and Young's Modulus vs. temperature (mild steel).

In figure 3.7, it is observed that the yield stress decays faster than Young's modulus. Young's Modulus and yield stress for aluminium is also affected by high temperatures.

Aluminium melts at temperatures above $600^{o}C$. Equations 3.3 to 3.7 were modified to include temperatures above which aluminium fail as follows. Because of the limited material data on this metal to the author, temperatures used by Woei-Shyan Lee, Wu-Chung Sue and Chi-Feng Lin [6] were considered in this study.

$$E = 207x10^{9} - 58.34x10^{6}.\tau \quad \text{for} \quad \tau \le 25^{0}C \qquad 3.8$$

$$E = 3.1x10^{5}.(\tau - 1100)^{2} + 97x10^{9} \quad \text{for} \quad 25^{0}C < \tau \le 300^{0}C \qquad 3.9$$

$$\sigma_{o} = \sigma_{yo} \quad \text{for} \quad \tau \le 25^{0}C \qquad 3.10$$

$$\sigma_{o} = \sigma_{yo}x[1 - 0.00178.(\tau - 200)] \quad \text{for} \quad 25^{0}C < \tau < 200^{0}C \qquad 3.11$$

$$\sigma_{o} = \sigma_{yo}x[0.133 - (\tau - 300)X3.884X10^{-4}] \quad \text{for} \quad 200^{0}C \le \tau \le 300^{0}C \qquad 3.12$$

Figures 3.8 and 3.9 shows the effect of temperature on Young's Modulus and the true stress on aluminium 6061-T6 alloy.

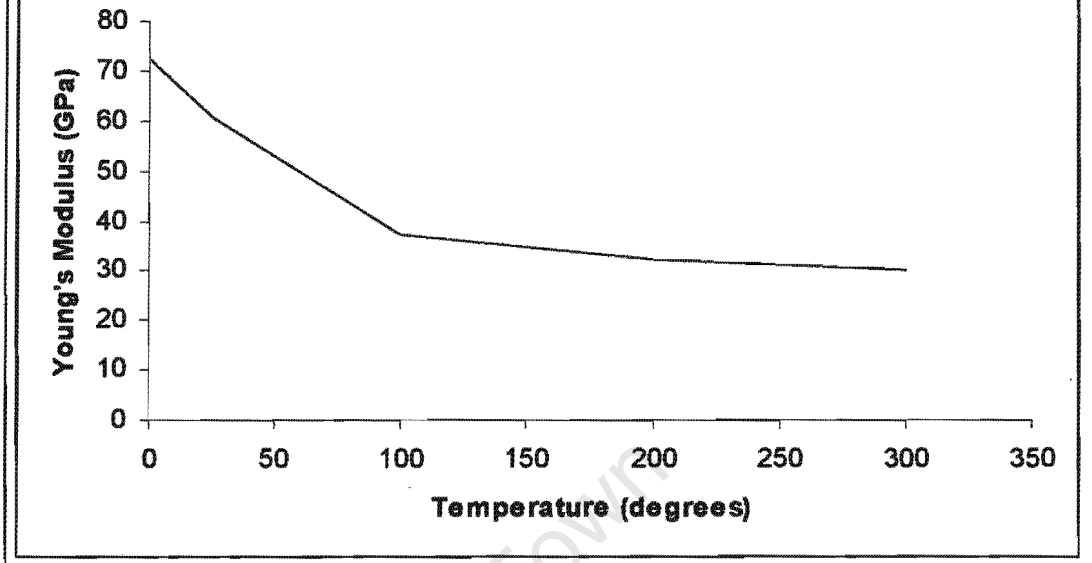

Figure 3.8: Graph of temperature Vs. Young's modulus (aluminium).

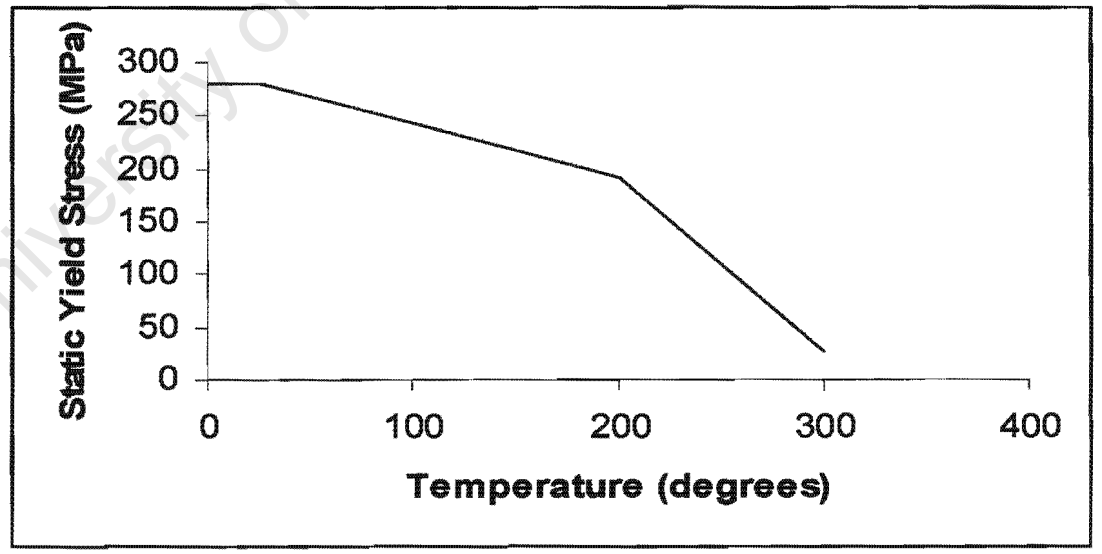

Figure 3.9: Graph of temperature Vs. yield stress (aluminium).

3.1.5 Strain rate dependence

Pure aluminium is not very sensitive to strain rate effect, but aluminium alloys such as 6063-T6 considered in this study is strain rate sensitive. Mild steel typically exhibits linear elastic and isotropic strain hardening plastic behaviour with a significant dependence on strain rate. The Von Mises yield criterion with isotropic hardening is an appropriate model to describe the elasto-plastic properties of the plates and beams. Hardening as a result of the strain rate effect was modelled using the Cowper-Symond relation given in equation 3.14.

$$\frac{\sigma_o^1}{\sigma_o} = 1 + \left(\frac{\dot{\varepsilon}}{D} \right)^{\frac{1}{q}} \qquad 3.14$$

Where

σ_o^1 : Dynamic yield stress; σ_o : Static yield stress; $\dot{\varepsilon}$: Strain rate;

D and q are material constants. D = 40.1 s^{-1}, q = 5 for steel and D = 6500 s^{-1}, q = 4 for aluminium 6063-T6 and 6061 are acceptable values and are used in this study [24,17] respectively.

It is observed that the strain rate effect on aluminium is less pronounced compared to steel. Figure 4.3 shows the stress – strain curve for aluminium 6061 -T6 with strain rate effects included. Lee, Shyu and Chiou [55] observed that the flow stress of a material depends not only on the strain and strain-rate but also on its microstructure at the dislocation level.

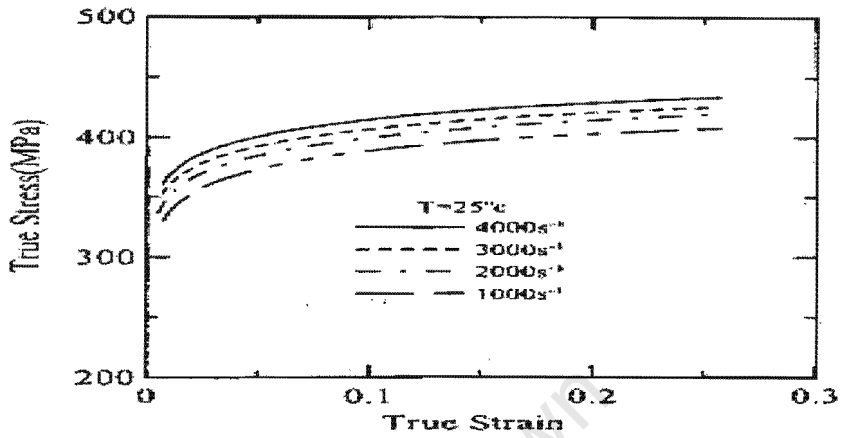

Figure 3.10: Dependence of strain-rate on the flow stress of 6061-T6 Al alloy [53].

3.2 Strain based shear failure criteria

The failure criterion is based on the value of equivalent plastic strain at element integration points. Failure is assumed to occur when the damage parameter exceed 1. The damage parameter, ϖ, is defined as:

$$\varpi = \sum \left(\frac{\Delta \bar{\varepsilon}^{pl}}{\bar{\varepsilon}_f^{pl}} \right) \qquad 3.15$$

where

$\Delta \bar{\varepsilon}^{pl}$: increment of the equivalent plastic strain.

$\bar{\varepsilon}_f^{pl}$: strain at failure.

The summation above is performed over all increments in the analysis. The shear failure criterion gives two failure choices, including the removal of elements from the mesh as a result of tearing or ripping of the structure. This criterion was not employed in this study.

It should also be noted that from the classical plasticity model, the equivalent plastic strain can be given in tabular form as a function of the equivalent plastic strain rate, a dimensionless pressure deviatoric stress ratio, the temperature and other predefined field variables.

A summary of the material properties of the plates and beams used in simulation is presented in tables 3.1, 3.2, 3.3 and 3.4.

Property	**Symbol**	**Value**
Young's Modulus (GPa)	E	$210x10^9$
Poisson's Ratio	ν	0.33
Specific heat (J/Kg ^oC)	c(T)	660
Density (Kg/m^3)	ρ	7850
Static yield stress (N/m^2)	σ_o	$264x10^8$

Table 3.1 : Material properties of test plates (circular mild steel plates) [42]

Property	**Symbol**	**Value**
Young's Modulus (GPa)	E	$210x10^9$
Poisson's Ratio	ν	0.33
Specific heat (J/Kg ^oC)	c(T)	660
Density (Kg/m^3)	ρ	7850
Static yield stress (N/m^2)	σ_o	$237x10^8$

Table 3.2 : Material properties of test plates (square mild steel plates) [26]

Property	**Symbol**	**Value**
Young's Modulus (GPa)	E	$72.4x10^9$
Poisson's Ratio	ν	0.32
Specific heat (J/Kg ^oC)	c(T)	937.4
Density (Kg/m^3)	ρ	2686
Static yield stress (N/m^2)	σ_o	$281x10^8$

Table 3.3 : Material properties of test beams (rectangular 6061-T6 aluminium alloy beams) [17]

Property	**Symbol**	**Value**
Young's Modulus (GPa)	E	72.4×10^9
Poisson's Ratio	ν	0.32
Specific heat (J/Kg ^oC)	c(T)	937.4
Density (Kg/m^3)	ρ	2686
Static yield stress (N/m^2)	σ_o	195×10^8

Table 3.4 : Material properties of test beams (T-beam 6063 aluminium alloy beams) [17,29] .

3.3 Johnson-Cook plasticity model

The Johnson-Cook plasticity model is a particular type of Mises plasticity model with analytical forms of the hardening law and rate dependence. It is suitable for high-strain-rate deformation of many metal and in adiabatic transient dynamic simulations. Johnson-Cook hardening is a particular type of isotropic hardening where the static yield stress; is assumed to be in the form:

$$\sigma_o = \left[A^1 + S\left(\bar{\varepsilon}^{pl}\right)^b\right]\left[1-\left(\hat{\theta}\right)^m\right], \qquad 3.16$$

where

A^1, S, b and m : material parameters measured at or below the transient temperature, $\theta_{transient}$.

$\bar{\varepsilon}^{pl}$: equivalent plastic strain

$\hat{\theta}$: non-dimensional temperature

The non-dimensional temperature is defined as:

$$\hat{\theta} \equiv \begin{cases} 0 for \theta \le \theta_{transint} \\ \dfrac{(\theta - \theta_{transient})}{(\theta_{melt} - \theta_{transient})} for \theta_{transient} \le \theta \le \theta_{melt} \\ 1 for \theta > \theta_{melt} \end{cases} \qquad 3.10$$

where

θ : current temperature

θ_{melt} : melting temperature

$\theta_{transition}$: transition temperature defined as the one at or below which there is no temperature dependence on the expression of the yield stress.

The Johnson-Cook model is valid up to the melting temperature.

The classical metal plasticity model was chosen over Johnson-Cook plasticity model because of the many parameters that have to be defined and the material data for these parameters not readily available to the author of this work.

4.0 FINITE ELEMENT SIMULATIONS

This chapter outlines the finite element method and data used for the numerical simulation of the mild steel plates and aluminium alloy beams.

4.1 Finite element analysis method

The numerical analysis was carried out using ABAQUS; a suite of powerful engineering simulation program, based on finite element method that can solve problems ranging from relatively simple linear analyses to the most complicated nonlinear problems. ABAQUS contains an extensive library of elements that can model virtually any geometry and an extensive library of material models, which can simulate the behaviour of most engineering materials, including metals, rubber, polymers, composites, reinforced concrete, crushable and resilient foams and geotechnical materials such as soil and rock. A general-purpose finite element program, ABAQUS / explicit rather than ABAQUS / Standard was used because it is computationally efficient for the analysis of large models with relatively short dynamic response time as is the case with blast loading, incorporates non-linear geometry, material effects, strain rate sensitivity, temperature effects, performs adiabatic stress analysis and requiring no iterations and tolerances or global tangent stiffness matrix. Numerical implementation is carried out by solving the governing equations using an explicit integration scheme together with the use of diagonal ("Lump") element mass matrices. The explicit integration performs a large number of small time increments efficiently with an explicit central difference time rule. The dynamic equilibrium equation is satisfied at the beginning of the increment, t; the accelerations calculated at time t are used to advance the velocity solution to time $t + \Delta t/2$ (as opposed to direct-integration available in ABAQUS / Standard); and the displacement solution time to $t + \Delta t$. The explicit procedure integrates through time by using many small time increments. Such a numerical integration is however, conditionally stable, with the stability being governed by the time step taken in the integration scheme. In the application of blast loaded plates and beams, high frequency waves are propagated through the specimen. To correct these high frequency components, the time step in the

solution scheme must be smaller than the time it takes for a dilatation wave to cover the length of an element. The critical time increment to ensure stability is represented by

$$\Delta t \leq \min\left(L^{el} \sqrt{\frac{\rho}{\lambda + 2\mu}} \right) \qquad 4.1$$

where

L^{el} : characteristic element length

ρ : the material density

μ and λ Lame's constants

Convergence in ABAQUS / Explicit is not implemented after each time increment, thus the time stepping in the explicit scheme is very small to maintain accuracy. Thus the explicit scheme is suited for short duration and high-speed dynamic events like blast loading.

4.2 Geometrical modelling of the plates and beams

The structure being model is discretised into a number of elements. The discretisation depends on the type of analysis and the geometry of the structure. A vast number of elements are available in the ABAQUS element library. It is also possible to formulate and implement a user defined element. This was not necessary in this study because the elements in the ABAQUS element library were sufficient for the various models considered herein. The following elements described in section 4.2.1 where used in this study.

4.2.1 Circular plates

An axisymmetric model using four noded, reduced integration, solid elements (CAX4R) with hourglass control was used for modelling the circular plates. A typical element is as shown in figure 4.1. A CAX4R element has three degrees of freedom at each node which are rotation in the R-Z plane and translational in the R and Z directions respectively. The

axis of symmetry is defined at R=0. Rigid bodies were used in clamping the plates as shown in section 4.5.

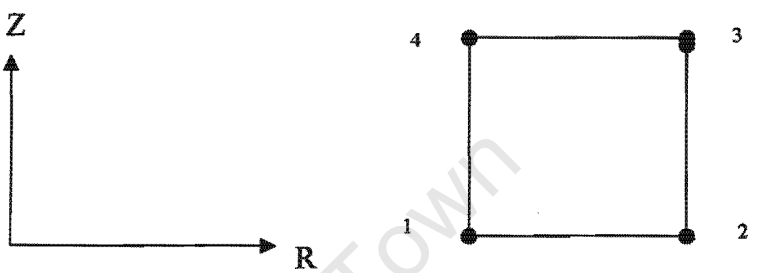

Figure 4.1: A schematic of a CAX4R element, showing co-ordinate system and node numbering.

4.2.2 Square Plates and Beams

An 8-noded linear brick, 3-d continuum element with reduced integration and hourglass control (C3D8R) elements were used to model the square plates and beams. A typical element is as shown below in figure 4.2.

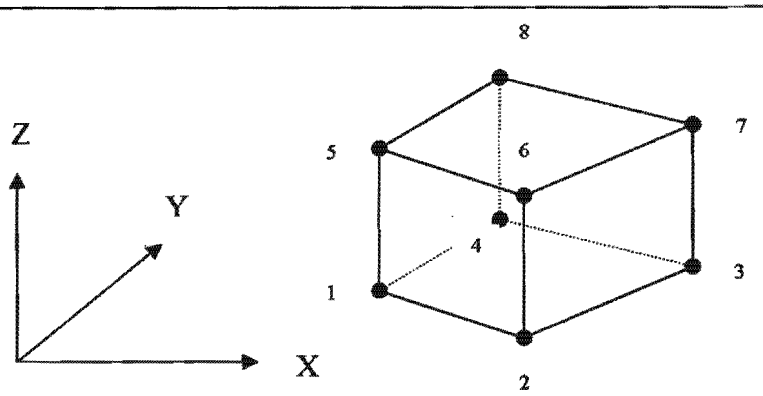

Figure 4.2: A schematic of a C3D8R element, showing node numbering and co-ordinate system

4.3 Type of mesh used

An ideal model must have sufficient elements to accurately describe the model history and also be able to minimise these elements to reduce computational expense. Another constraint on the model is the aspect ratio; the ratio between the longer and shorter dimensions of an element. If the aspect ratio exceeds by a factor of four, the element is considered excessively distorted and the analysis will be terminated.

The number of elements used in the model has a significant effect on the finite element analysis. The solution approaches the exact solution of the governing equations as the number of elements increases in the model. Thus a satisfactory representation of the exact solution can be obtained by using sufficient number of elements. However, the increase in the number of elements results in an increase in computational expense and time. The increase in computational time can be attributed to the following factors:

- The stable time increment for the numerical integration decreases.
- The number of degrees of freedom needing to be analysed increases.

Modelling the plate and beams using axisymmetric and symmetric formulations respectively reduces both computational time and the size of the files to be analysed. These reduced models decrease the computational time by a factor of four or more with the results unaffected.

4.4 Modelling the blast load

In modelling the blast load, the uniform blast load generated by the use of plastic explosive in the experiments, was modelled as a pressure applied to the exposed area of plates and beams over a given time in the finite element model. The pressure distribution and area over which the explosive act is complex for the actual explosive, but the time is fixed by the properties and geometry. The following assumptions were used to simplify the modelling of the blast load.

- The duration of the pressure distribution; τ, was calculated from the burn time of the explosive .

- In reality, the pressure distribution with time is complex, and consist of both an over-pressure and under-pressure. The over-pressure is relatively large compared to the under-pressure. The under-pressure and its contribution to the deformation can thus be neglected.

- The over-pressure is constant for the duration of the burn time.

The above assumptions gives a rectangular pressure distribution with time which is shown in figure 4.3. The magnitude of the pressure; P is then calculated from equation 4.2.

$$P = \frac{I_m}{A_o.\tau_b} \qquad 4.2$$

where

τ_b : duration of pressure distribution

I_m : measured impulse

A_o : plate or beam area exposed to blast load.

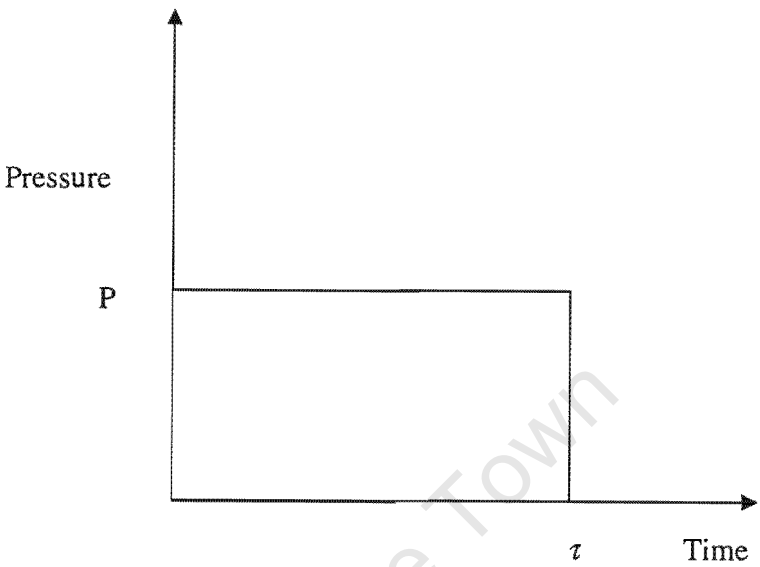

Figure 4.3: Pressure distribution with respect to time.

Tables 4.1, 4.2, 4.3 and 4.4 give some typical pressure values for circular and square plates, rectangular beams and T-beams used in this study.

Impulse (Ns)	Pressure (Pa)
4.76	4.04×10^7
13.28	1.13×10^8
16.85	1.43×10^8
17.75	1.51×10^8
18.65	1.58×10^8
21.69	1.84×10^8
24.56	2.08×10^8
29.24	2.48×10^8
30.67	2.60×10^8
52.05	4.42×10^8

Table 4.1: Typical values of pressure for circular plates

Impulse (Ns)	Pressure (Pa)
9.1	7.66×10^7
9.4	7.91×10^7
9.7	8.16×10^7
9.9	8.33×10^7
10.2	8.58×10^7
10.5	8.84×10^7
11.1	9.34×10^7
11.5	9.68×10^7
11.9	1.00×10^8
14.4	1.21×10^8
24.4	2.05×10^8
49.0	4.12×10^8

Table 4.2: Typical values of pressure for square plate

Impulse (Ns)	Pressure (Pa)
9.16	5.92×10^7
11.22	7.25×10^7
13.18	8.51×10^7
14.77	9.54×10^7
17.19	1.11×10^8
18.07	1.17×10^8
20.39	1.32×10^8
22.08	1.43×10^8
23.14	1.49×10^8
33.14	2.17×10^8

Table 4.3 : Typical values of pressure for rectangular beams.

Impulse (Ns)	Pressure (Pa)
Length of 200mm	
1.132	$3.59x10^7$
1.167	$3.70x10^7$
1.409	$4.47x10^7$
1.487	$4.72x10^7$
1.527	$4.85x10^7$
1.665	$5.29x10^7$
1.735	$5.51x10^7$
1.831	$5.81x10^7$
1.871	$5.94x10^7$
2.024	$6.43x10^7$
2.07	$6.57x10^7$
Length of 150mm	
1.002	$8.68x10^7$
1.116	$9.66x10^7$
1.279	$1.11x10^8$
1.306	$1.13x10^8$
1.395	$1.21x10^8$
1.576	$1.36x10^8$
1.745	$1.51x10^8$
1.867	$1.62x10^8$
1.928	$1.67x10^8$
1.966	$1.70x10^8$
2.070	$1.79x10^8$
2.184	$1.89x10^8$

Table 4.4 : Typical values of pressure for T-beams

4.5 Modelling the plates and beams

Circular plates were modelled in ABAQUS using an axisymmetric formulation with clamped and built-in boundaries as shown in figures 4.4 and 4.5 respectively. Square plates, rectangular beams and T-beams were modelled by making use of the symmetry as shown in figures 4.6, 4.7, 4.8, 4.9 and 4.10 respectively. Rigid bodies were used in clamping the plates and beams while encastre boundary conditions was applied for the built-in plates and beams. Symmetric boundary conditions were applied in the regions of the plates and beams that were not clamped or encastre.

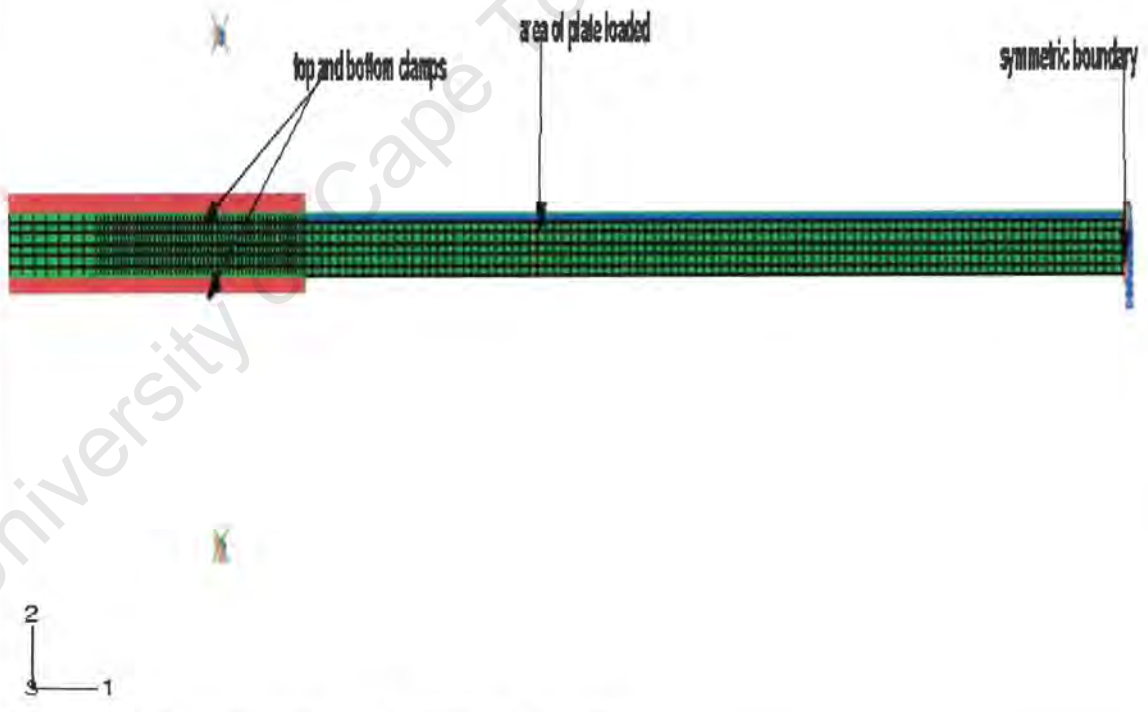

Figure 4.4: Circular plate with clamped boundary.

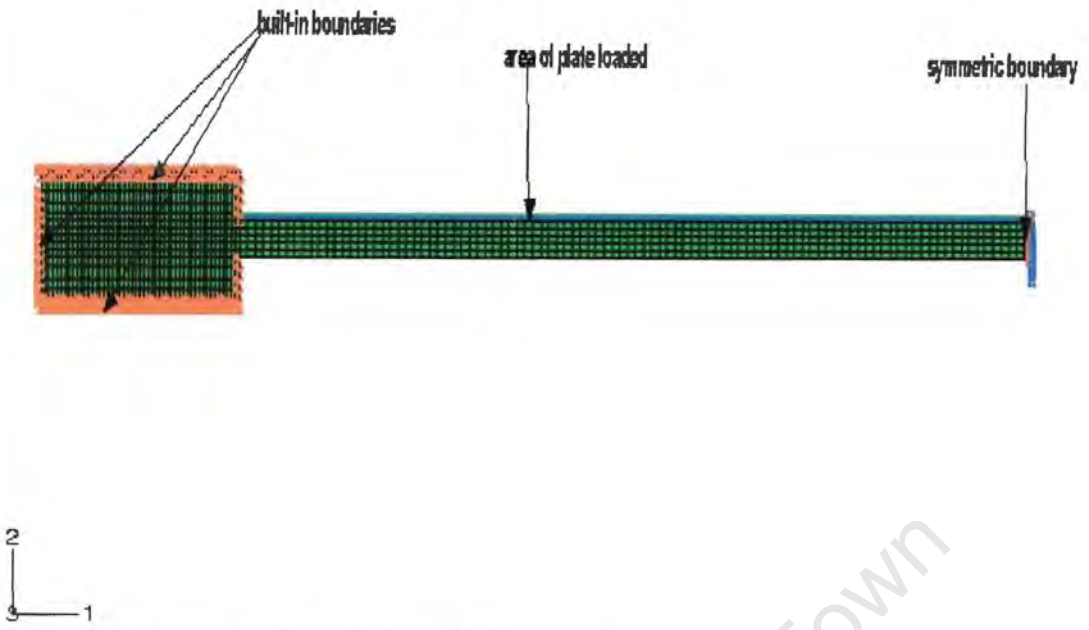

Figure 4.5: Circular plate with built-in boundary.

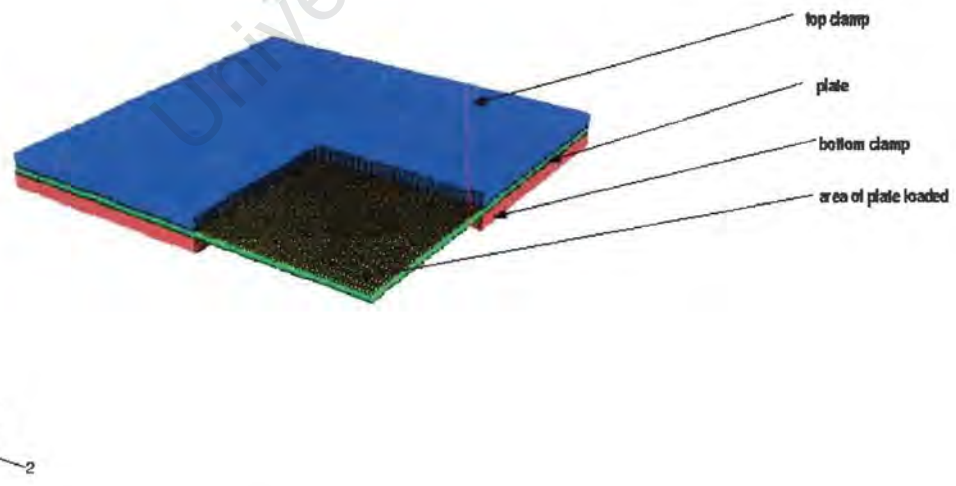

Figure 4.6: Square plate with clamped boundary condition.

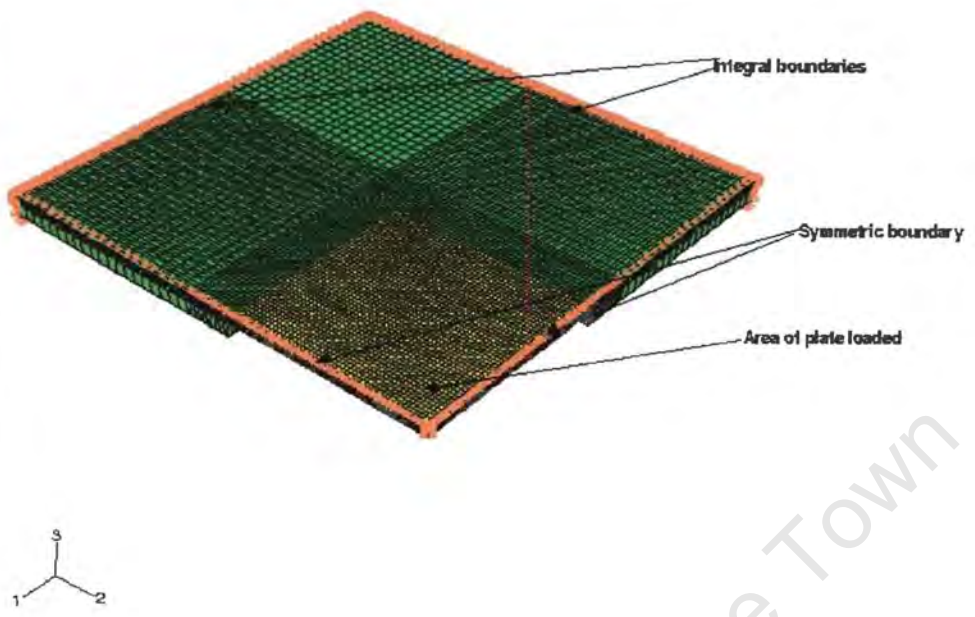

Figure 4.7: Square plate with integral boundary condition.

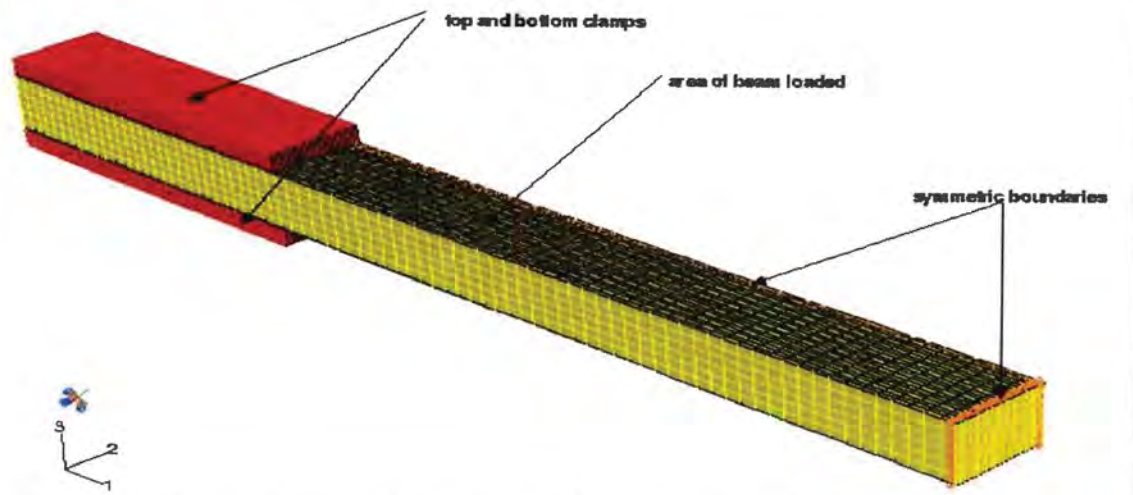

Figure 4.8: Rectangular beam with clamped boundary condition.

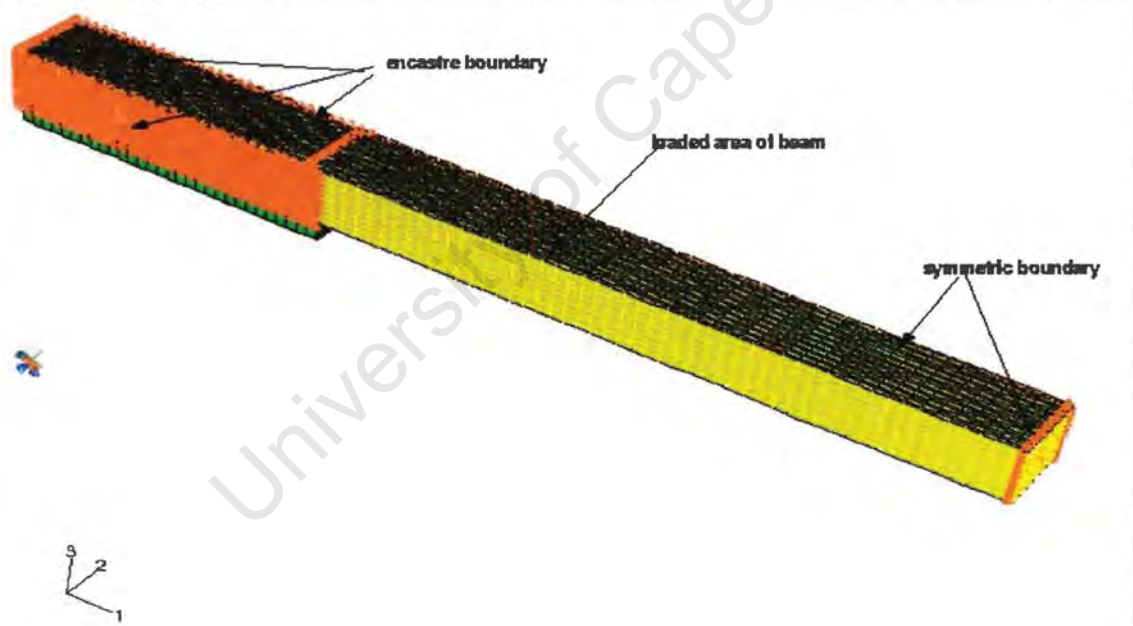

Figure 4.9: Rectangular beam with integral boundary condition.

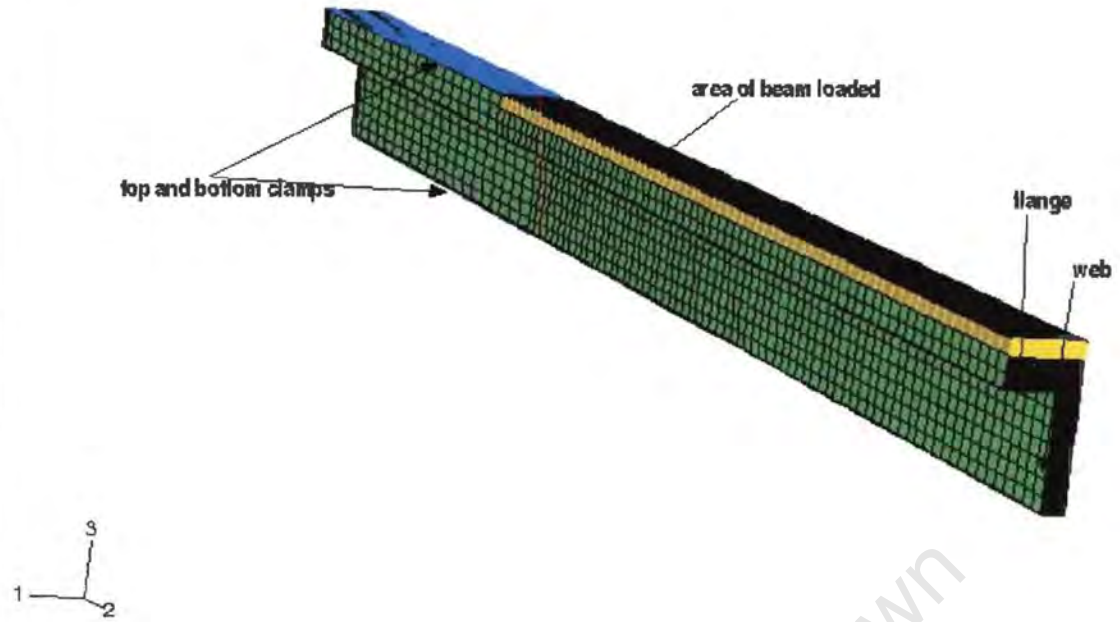

Figure 4.10: T-beams with clamped boundary condition.

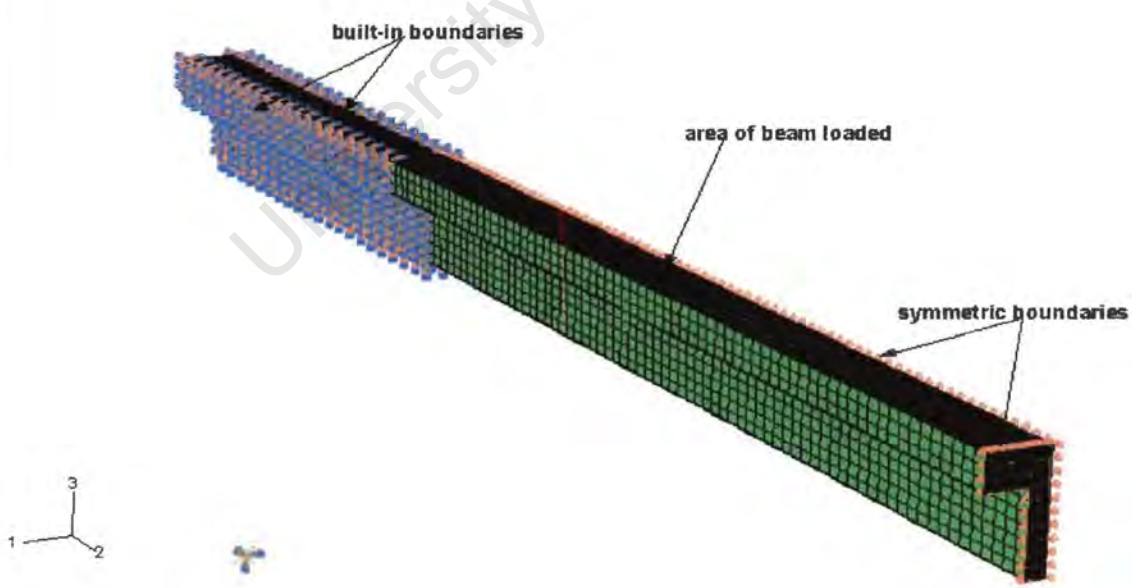

Figure 4.11: T-beams with built-n boundary condition.

The general goal of an ABAQUS simulation is to determine the response of a model to applied loads. In ABAQUS, the user divides the complete load history of the simulation into a number of steps. Each step is a period of "time" specified by the user for which ABAQUS calculates the response of the model to a particular set of loads and boundary conditions. A multiple step concept is employed in the history data section by ABAQUS /Explicit to accurately define the different conditions to which the model is exposed.

5.0 Simulation Results

Numerical simulation results obtained from circular and square mild steel plates, aluminium alloy rectangular beams and T-beams undergoing uniform blast loading are presented in this chapter. Before modelling more complex behaviour of plates and beams, such as failure through rupture; it is imperative to establish the level of correlation between the ABAQUS models and experiments for a range of impulse causing only permanent inelastic deformation (mode I failure). The level of correlation was established by comparing the final mid-point displacement obtained from numerical analysis with experiments. Contour plots and graphs of mid-point displacement and temperature for clamped and built-in plates and beams for mode I are also included. For modes II and III failure, outline plots of the failed plates and beams are presented with a comparison of solutions obtained from models that were clamped and built-in at the boundary. The ABAQUS input decks for the various models investigated in this thesis are presented in appendices B to E.

5.1 Circular plates

The simulation results presented in this section have a uniform mesh size of 100x6 elements in the plate resulting in a mesh density of approximately 0.5x0.267 mm. The diameter and thickness of the plates were 100mm and 1.6mm respectively.

5.1.1 Mode I failure

Mode I response is concerned with large inelastic deformation with no tearing. The analysis was carried out for a range of impulse from 4.76Ns to 29.24Ns. The investigation considered material properties that include and exclude temperature dependency and boundary fixation of the circular plates. It is primordial to ensure that the analysis continues for a period long enough for the plates to reach equilibrium. Figure 5.1.1 show the displacement history for six points; taken at equal intervals along the plate profile from the centre to the boundary (represented by curves 1 to 6 in figure 5.1.1). The displacement history plot represents a clamped circular plate that underwent an impulsive load of 4.76Ns. The displacement history for a built-in circular plate was also examined

and it was found to reach equilibrium at the same time. From figure 5.1.1, it is observed that all points monitored along the plate profile reached equilibrium at approximately the same time; 300 μ s. The displacement history plot shows that plates with clamped and integral boundary conditions responded to deformation linearly with time, reached a maximum and exhibited a small amount of residual elastic vibration about a mean displacement after approximately 300 μ s, and thereafter, the magnitude of the vibration slowly decays. It was thus sufficient to stop the analysis after 550 μ s.

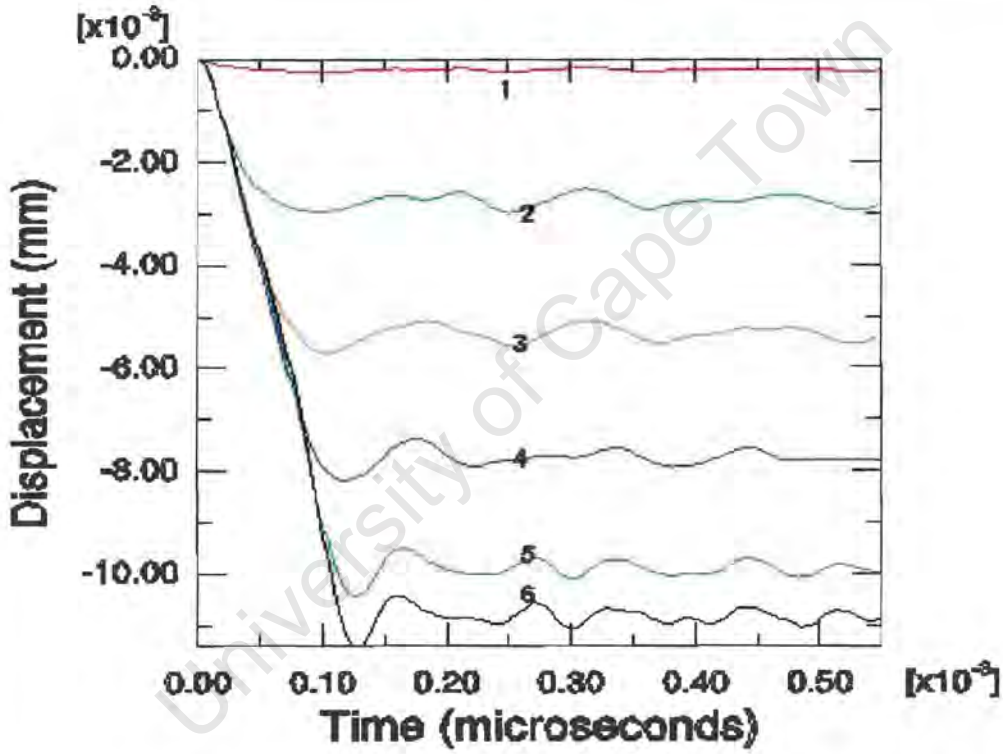

Figure 5.1.1 : Displacement history at various points along the profile of a clamped circular plate at an impulse of 4.76Ns.

Tables 5.1.1 and 5.1.2 shows the results of a comparison of the mid-point displacement of clamped and built-in circular plates respectively for models that include and exclude temperature dependent material properties. In tables 5.1.1 and 5.1.2, t represents the thickness of the plates (1.6mm).

1 **Impulse (Ns)**	2 **Measured Mid-point Displacement (mm)**	3 **Predicted Mid-point Displacement (mm) Model Including Temperature**	4 **Difference between Including temperature & measured mid-point displacement to plate thickness ratio (mm) (3-2)/t**	5 **Predicted Mid-point Displacement (mm) Model Excluding Temperature**	6 **Difference between Excluding temperature & measured mid-point displacement to plate thickness ratio (mm) (5-2)/t**	7 **Difference in mid-point displacement Between Model Including & Excluding Temperature (mm) (3-5)**
4.76	3.6	3.4	-0.1	3.5	-0.1	-0.1
13.28	12.5	11.0	-0.9	11.2	-0.8	-0.2
16.85	16.5	14.7	-1.1	14.3	-1.3	0.4
17.75	18.2	16.2	-1.3	16.0	-1.3	0.2
18.65	18.9	17	-1.2	16.6	-1.4	0.4
21.69	22.7	20.1	-1.6	19.8	-1.8	0.3
24.56	25.3	22.6	-1.7	21.4	-2.4	1.2
29.24	30.1	ABAQUS predicts mode II				

Table 5.1.1 : Comparison of predicted mid-point displacement with experiment for models that include and exclude temperature dependent material properties (clamped boundary condition).

From table 5.1.1, the difference in mid-point displacement-thickness ratio (column 4) is less than one plate thickness for impulses from 4.76Ns to 18.65Ns for a model that includes temperature dependent material properties. This range of impulse gives temperatures ranging from $83\,^{\circ}C$ to $228\,^{\circ}C$ as tabulated in table 5.1.4. This ratio shows that at this temperature the material properties of the plate are not affected by temperature as the yield stress of the material has not decreased much, as reported by Guedes, Gordo and Teireira [4]. In table 5.1.1, the ratio exceeds one plate thickness from an impulse of 24.56 and a temperature of 504 $^{\circ}C$ is recorded in table 5.1.4. The difference in mid-point displacement-thickness ratio between a model that includes temperature dependent material properties and one that excludes temperature dependent material properties is less than one plate thickness (Column 7 table 5.1.1). This ratio shows that mode I failure is not affected by temperature. It is also observed from table 5.1.1 that both models including and excluding temperature dependent material properties predicts mode I favourably as the difference ratio lies within the variation of ± 1 deflection-thickness ratio of Nurick [45].

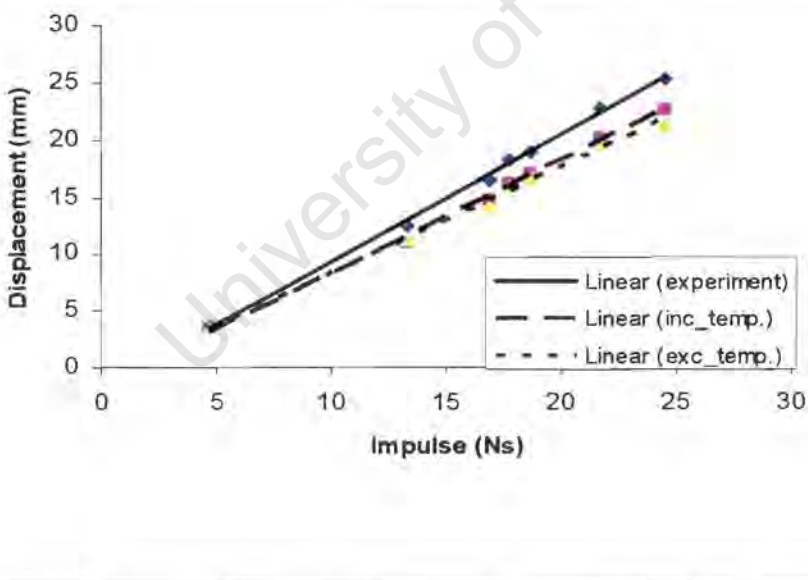

Figure 5.1.2 : Comparison of measured and predicted mid-point displacement as a function of impulse (clamped boundary condition).

From figure 5.1.2, a linear behaviour is observed between the plate deformation and applied impulse.

1 Impulse (Ns)	2 Measured Mid-point Displacement (mm)	3 Predicted Mid-point Displacement (mm) Model Including Temperature	4 Difference between Including temperature & measured mid-point displacement to plate thickness ratio (mm) (3-2)/t	5 Predicted Mid-point Displacement (mm) Model Excluding Temperature	6 Difference between Excluding temperature & measured mid-point displacement to plate thickness ratio (mm) (5-2)/t	7 Difference in mid-point displacement Between Model Including & Excluding Temperature (mm) (3-5)
4.76	3.6	3.2	-0.3	3.2	-0.3	0.0
13.28	12.5	10.7	-1.1	10.9	-1.0	-0.2
16.85	16.5	15.1	-0.9	14.1	-1.5	1.0
17.75	18.2	17.3	-0.6	15.1	-1.9	2.2
18.65	18.9	18.1	-0.5	16.2	-1.7	1.9
21.69	22.7	22.2	-0.3	18.4	-2.9	3.8
24.56	25.3	ABAQUS predicts mode II				
29.24	30.1					

Table 5.1.2: Comparison of predicted mid-point displacement with experiment for models that include and exclude temperature dependent material properties (built-in boundary condition).

From tables 5.1.1 and 5.1.2, it is observed that mid-point displacement is higher for a model with clamped boundary compared to one with built-in boundary. This might be as a result of the "pull-in" observed in this model (figure 5.1.5). Mode II is predicted at an impulse of 24.56Ns (table 5.1.2) for plates with built-in boundaries compared to a higher impulse of 29.24Ns (table 5.1.1) for plates with clamped boundaries.

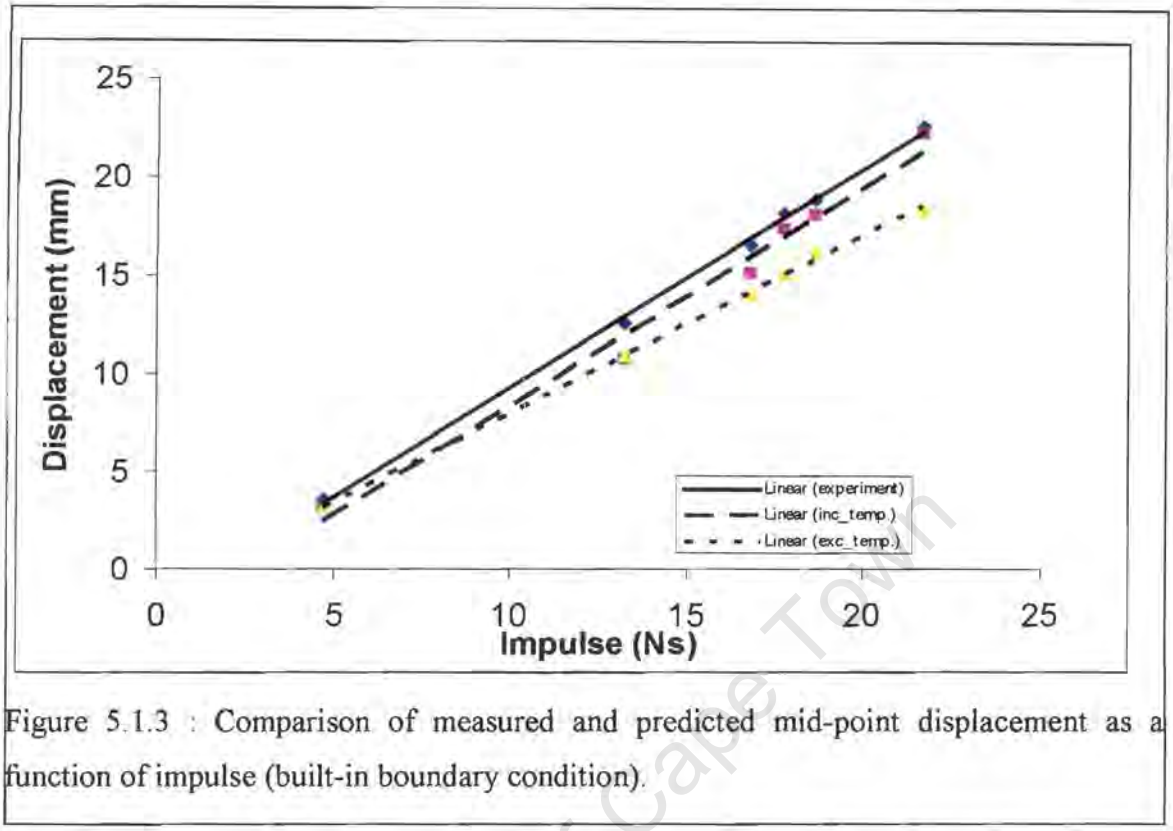

Figure 5.1.3 : Comparison of measured and predicted mid-point displacement as a function of impulse (built-in boundary condition).

From figure 5.1.3, a linear behaviour which was observed between the plate deformation and applied impulse in figure 5.1.2 is repeated in figure 5.1.3. This is in agreement with experimental observations that mid-point displacement increases with increase in impulse.

Impulse (Ns)	**Measured Mid-point Displacement (mm)**	**Predicted Mid-point Displacement (mm) Clamped Model Including Temperature**	**Predicted Mid-point Displacement (mm) Built-in Model including Temperature**
4.76	3.6	3.4	3.2
13.28	12.5	11.0	10.7
16.85	16.5	14.7	15.1
17.75	18.2	16.2	17.3
18.65	18.9	17	18.1
21.69	22.7	20.1	22.2
24.56	25.3	22.6	ABAQUS Predicts mode II
29.24	30.1	ABAQUS Predicts mode II	ABAQUS Predicts mode II

Table 5.1.3: Comparison of predicted mid-point displacement with experiment for models that include temperature dependent material properties (clamped and built-in boundary).

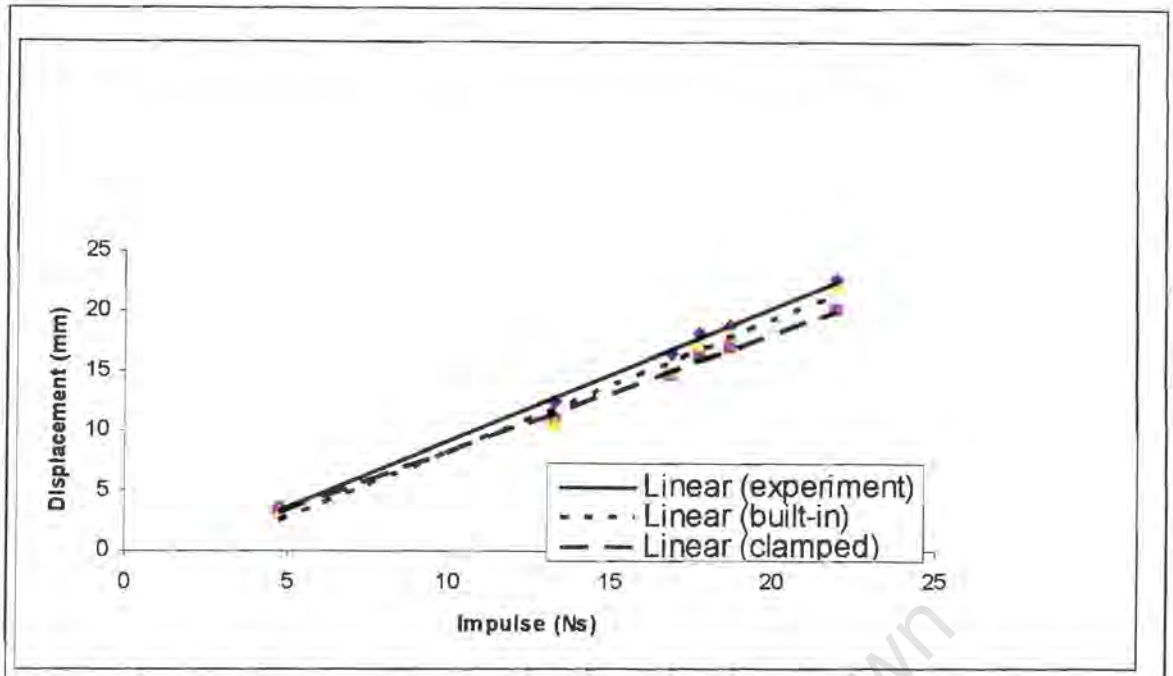

Figure 5.1.4 : A plot of variation of mid-point displacement with impulse for a plate with clamped and built-in boundary condition (models including temperature).

From figure 5.1.4, it is observed that both clamped and built-in models under estimate the mid-point displacement compared to the experimental values.

A similar behaviour for models excluding temperature dependent material properties was observed for plates clamped and built-in at the boundary and has not been included in this work.

The plates' response to an uniform explosive blast load for clamped and built-in models are shown in figures 5.1.5 and 5.1.6 respectively. The models show the response of the plate from time 0.005 μ s (clamped model) and 0 (built-in) μ s respectively to 300 μ s. In figure 5.1.5, at time t=0.005 μ s the top clamp is moved onto the plate just before the application of the pressure load. At t=15 μ s, the plate deforms with no visible separation between the top surface of plate and the top clamp. As the plate continues to deform, at t=50 μ s the top clamp starts separating from the plate and the bottom clamp denting the unloaded side of the plate. Thinning at the boundary is observed at t=100 μ s and at

t=220 μ s the plate records its maximum mid-point displacement. The separation of the plate from the clamp might have contributed to the "pull-in" effect observed in the model.

In figure 5.1.6, from t=0 μ s to 15 μ s the pressure load is applied to the plate. At t=50 μ s, no visible sign of thinning at the boundary is observed. As the plate continues to deform, thinning at the boundary of the plate is observed at t=100 μ s and at t=220 μ s the plate reaches maximum mid-point displacement. It was observed that thinning of plates with built-in boundaries is higher than that for plates clamped at the boundaries. This might be a possible course for early occurrence of mode II failure in built-in plates.

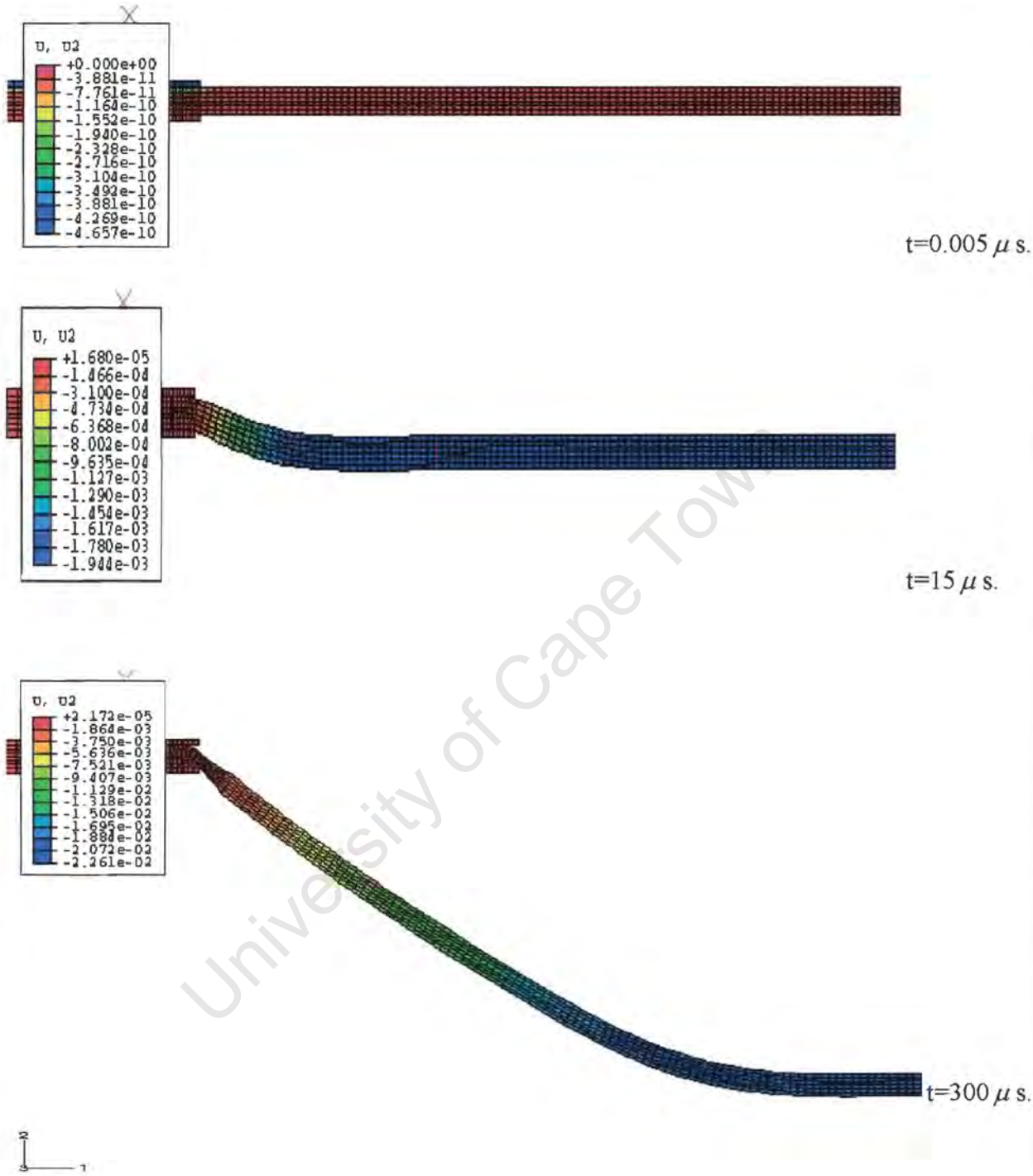

Figure 5.1.5 : Response of a clamped circular plate at an impulse of 21.69Ns showing displacement in the -2-direction.

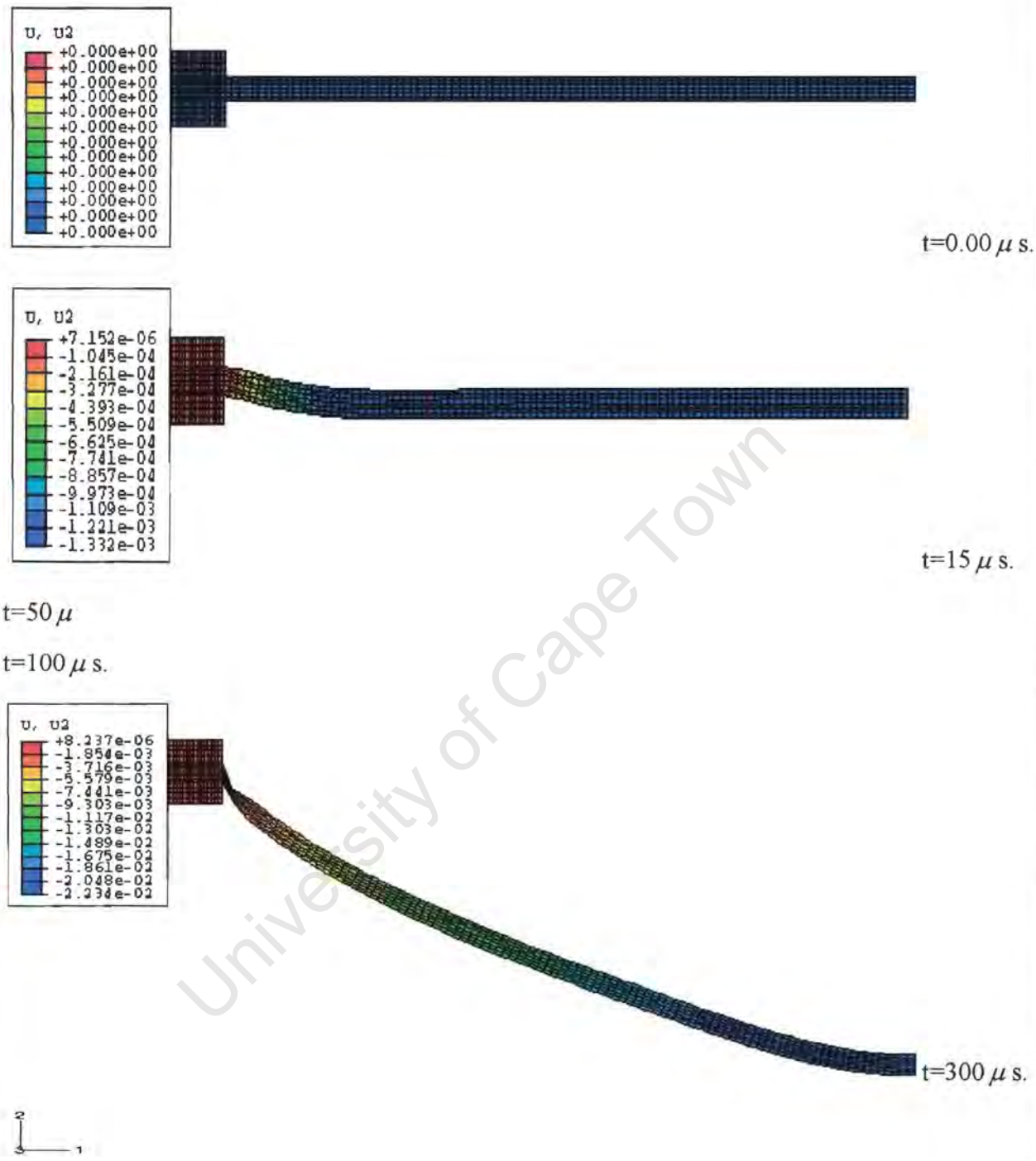

Figure 5.1.6 : Response of a built-in circular plate at an impulse of 21.69Ns showing displacement in the -2-direction.

Impulse (Ns)	**Temperature Model With Clamped Boundary** (^{o}C)	**Temperature Model With built-in Boundary** (^{o}C)
4.76	83	95
13.28	89	126
16.85	103	206
17.75	216	304
18.65	228	321
21.69	504	511
24.56	523	703
29.24	701	711

Table 5.1.4 : Temperature variation at the boundary with impulse for models with clamped and built-in boundaries.

Temperature increases with increase in impulse as shown in table 5.1.4 and figure 5.1.7, this might be the reason for an increase in the difference ratio of mid-point displacement-thickness observed in tables 5.1.1 and 5.1.2.

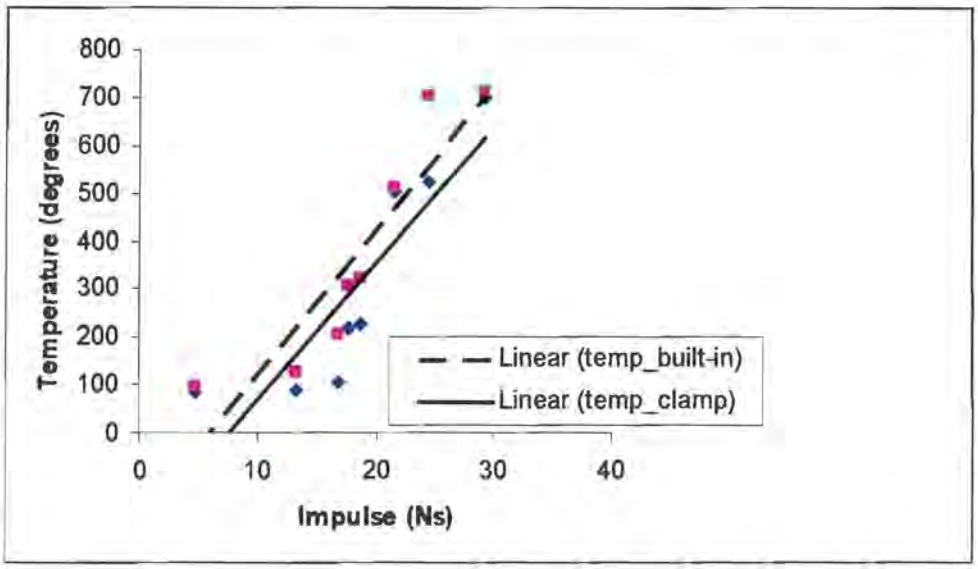

Figure 5.1.7 : A plot of highest temperature at the boundary against impulse for plates clamped and built-in at the boundary.

It is observed from figure 5.1.7 that temperatures of both clamped and built-in models increase with increase in impulse. Model built-in at the boundary has a higher temperature compared to a model clamped at the boundary.

High temperatures and strains are observed at the boundary and the centre of the plate. As time increases, the temperature at the boundary increases faster than that at the centre. The temperatures and strains observed in figures 5.1.8 and 5.1.9 results in thinning of the plates at the boundary.

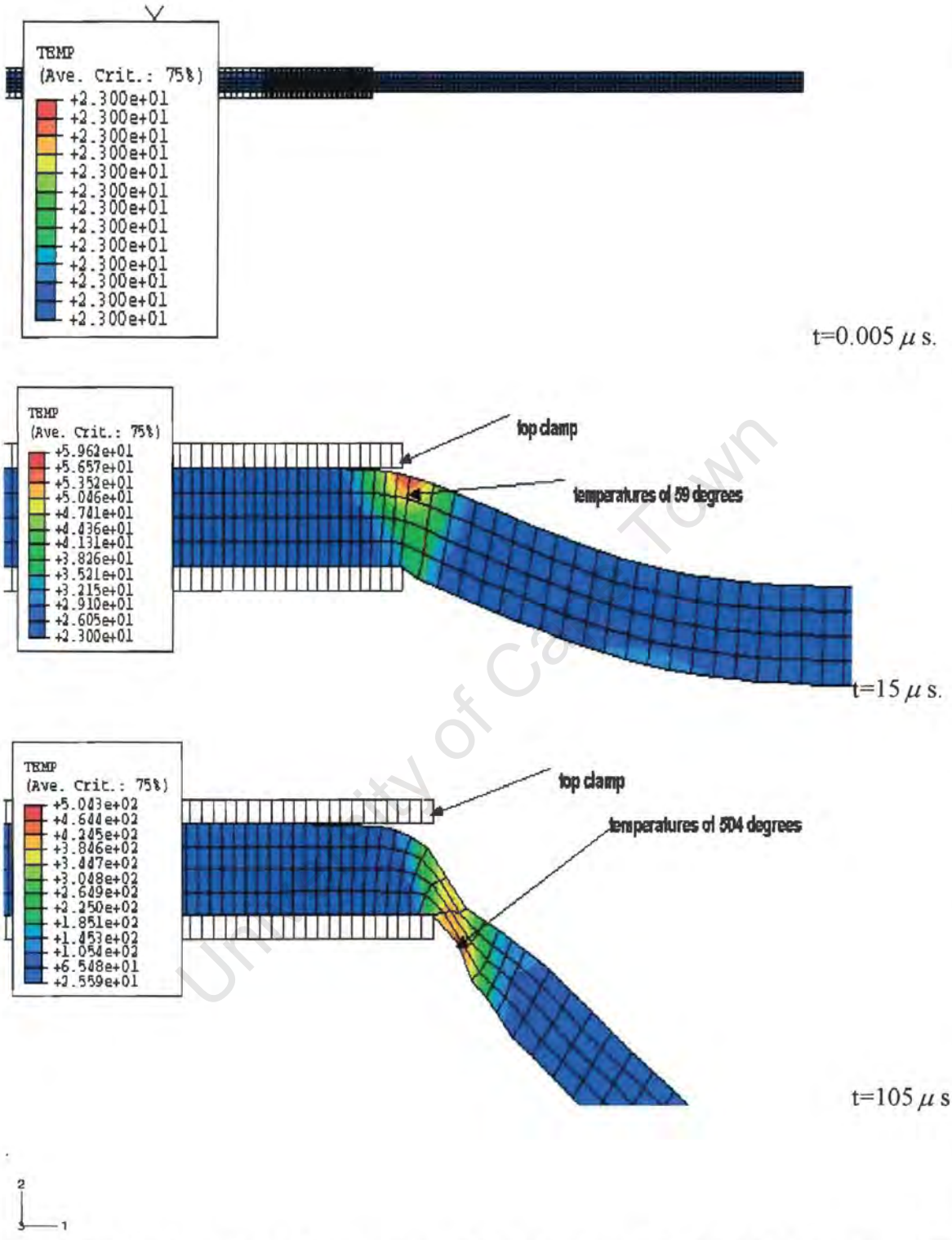

Figure 5.1.8 : Variation of temperature at the boundary with time for an impulse of 21.69Ns (clamped boundary).

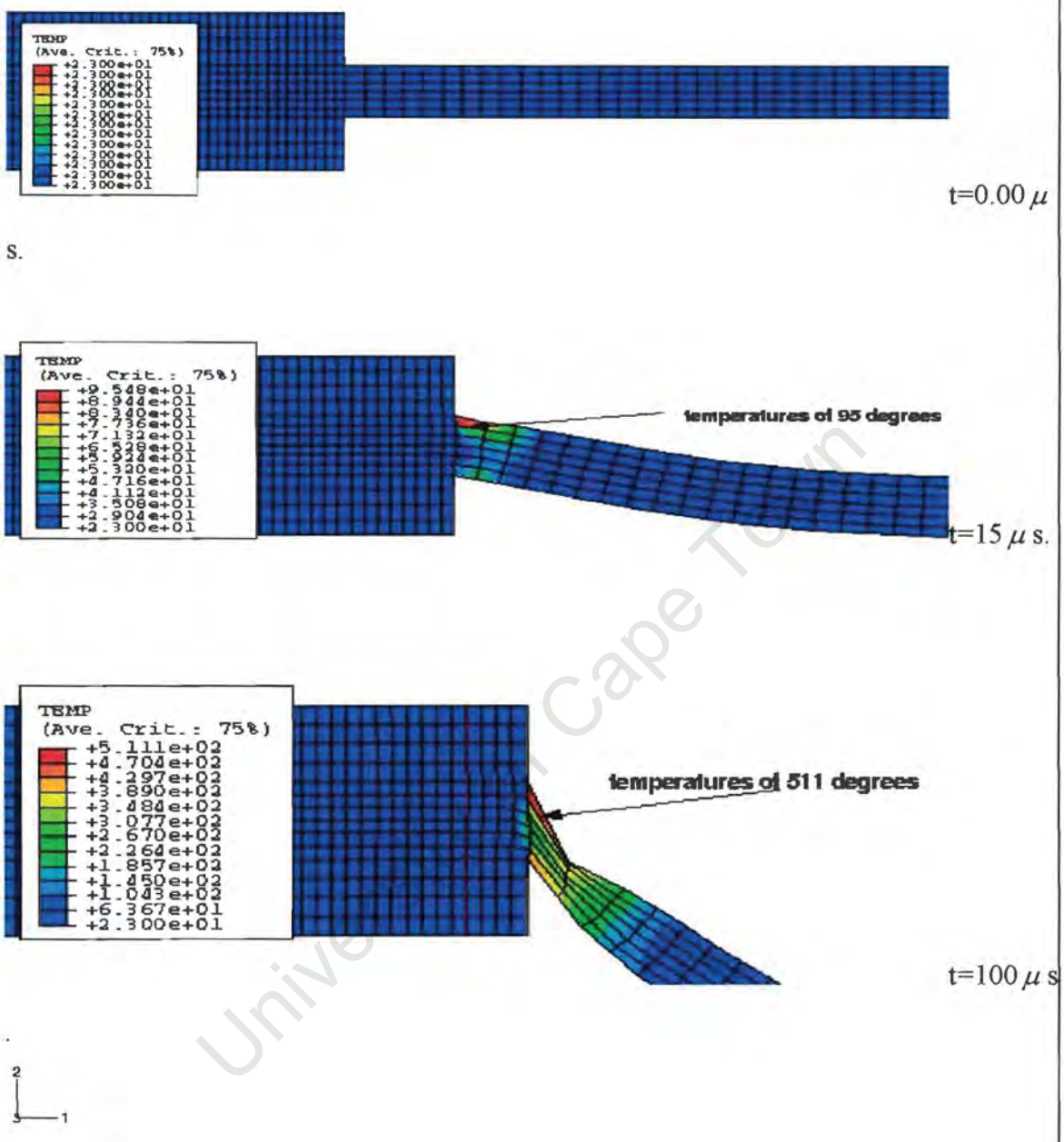

Figure 5.1.9 : Variation of temperature at the boundary with time for an impulse of 21.69Ns (built-in boundary).

5.1.2 Tearing mode response

The response of steel to blast loading depends greatly upon the temperature and the strain rate at which the deformation is taking place. According to Woei-Shyan Lee and Gen-Wang Yeh [56] temperature and strain rate are coupled, since one influences the other. They observed that temperature affects the rate of deformation, which is controlled mainly by a thermally-activated mechanism. At the same time, the deformation at high strain rate can generate significant heating and cause a temperature increase. This leads to various modes of failure in blast loaded structures. Experimental evidence has shown three distinct modes of failure of steel plates occurring in blast loading conditions. Mode I failure involves the large inelastic deformation of the plates without any sign of tearing, and has been discussed in section 5.1.1. The onset of mode II failure is defined by the first sign of tearing occurring in the plates at the boundary. Thereafter all the tearing behaviour is described as mode II until the mode III failure where the energy of the blast is sufficient enough to cause shearing around the entire perimeter of the plates before any significant displacement has taken place in the remainder of the plates. The result of such a failure mode is an almost flat disk of the size of the circular plate.

5.1.3 Method of plate failure

When tearing occurs the model is subjected to severe temperature rises in the region of fracture, forming a band of high temperature due to a slightly higher amount of strain rate in the band compared to the surrounding areas. As a result of greater adiabatic heating due to the large amount of plastic work the material properties weaken. The weakening of material properties results in larger strains, higher temperatures and lower stresses until unrealistic element elongation occurs. As the temperature of the band increases, the elements in this band undergo extensive elongation in the direction of displacement exceeding realistic strain (70%-300%). Hence, indicating that failure will occur within the high temperature band.

The reason for the severe element elongation can thus be ascribed to the effects of the temperature dependent material properties. During plastic deformation, most of the plastic work is converted into heat. If the rate is high, or if the material concern has a poor thermal conductivity, there is not sufficient time for this heat to dissipate to the surrounding material, and the increase in temperature will then cause thermal softening. If the thermal softening effect is greater than the strain-hardening effect, an unstable localized material flow will occur, a narrow band with very large shear deformation being formed. Because of the thermal softening a 200% failure strain criterion was imposed by Wiehahm, Nurick and Bowles [8], Chung [45], Grobbelaar [57] on the models they investigated to ensure failure after extensive adiabatic heating in the localised region and hence used in this study. If the failure criterion is not imposed, the elements in the localised area will keep on deforming as a result of the decaying material properties.

5.1.4 Plate response

Figures 5.1.10 to 5.1.15 show the response of clamped and built-in circular plates which were torn at the boundary (mode II) while figure 5.1.16 and 5.1.17 show plates that sheared at the boundary (mode III). The plates are considered torn when a temperature of $700^{\circ}C$ and a logarithmic strain of 70% is observed through out the thickness of the plate.

A temperature of $587^{\circ}C$ and logarithmic strain of 64% (figure 5.1.10) indicates that the plate is about to fail at this region. At this temperature, the rate of strain hardening is still greater than the rate of thermal softening, Woei-Shyan lee and Gen-Wang Yeh [56]. A temperature of $607^{\circ}C$ and logarithmic strain of 77%, figure 5.1.11 in the outer elements through thickness at the boundary of the plate show that the plate will fail at these elements. A further high temperature increase and strain of $706^{\circ}C$ and 122%, figure 5.1.12 indicate that tearing has taken place through the thickness of the plate at the boundary.

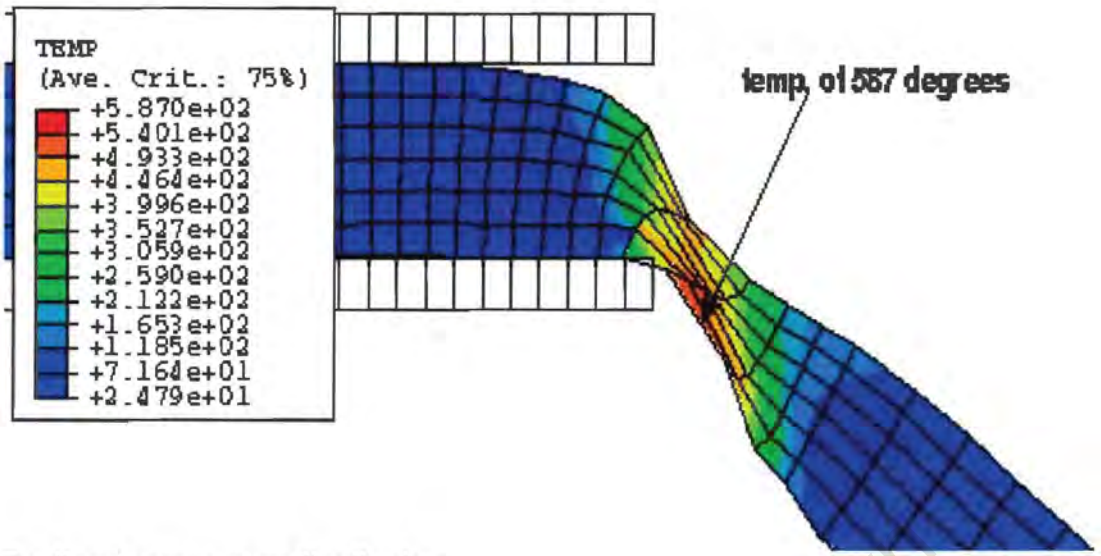

Predicted temperature distribution.

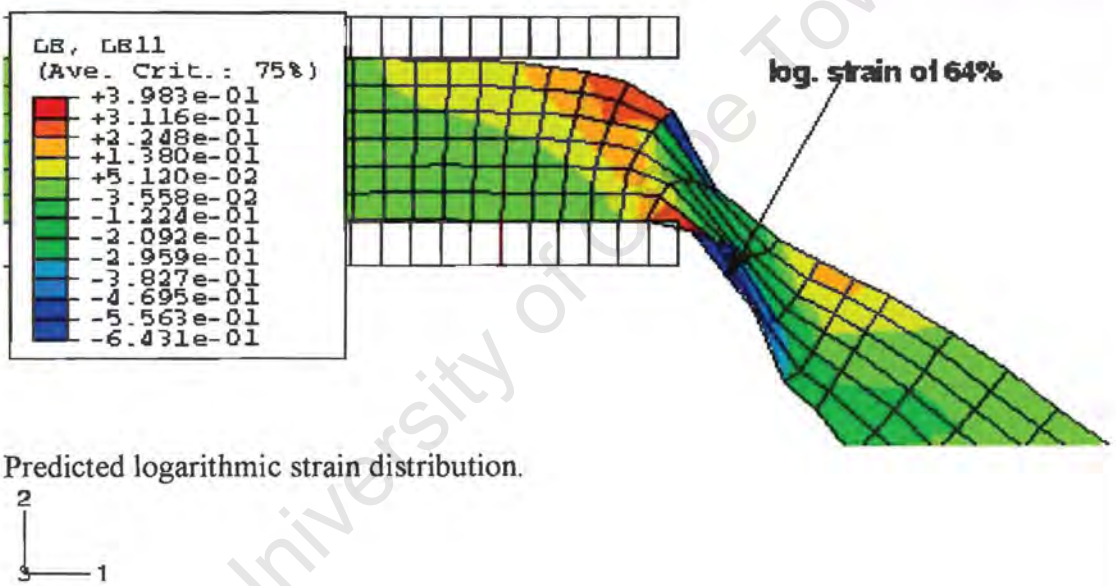

Predicted logarithmic strain distribution.

Figure 5.1.10: Initiation of mode II at an impulse of 30.67Ns at time t= 43 μs for a plate clamped at the boundary.

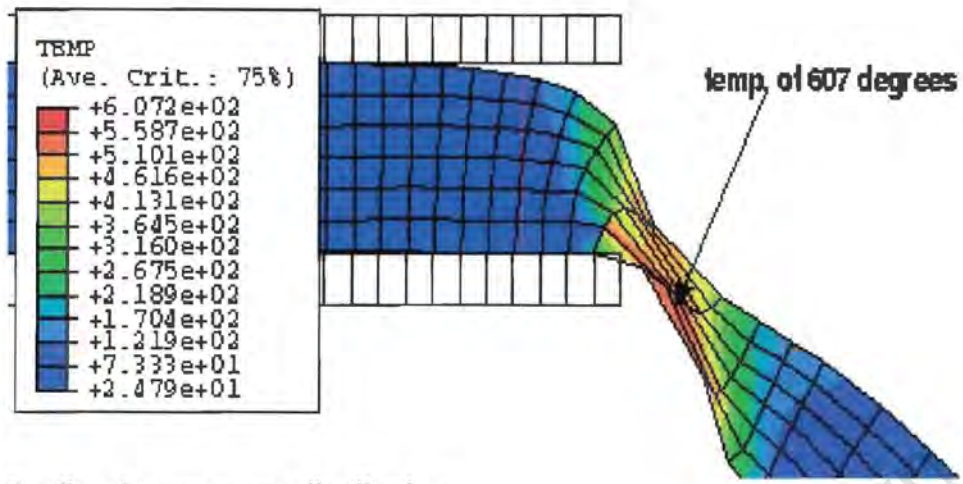

Predicted temperature distribution.

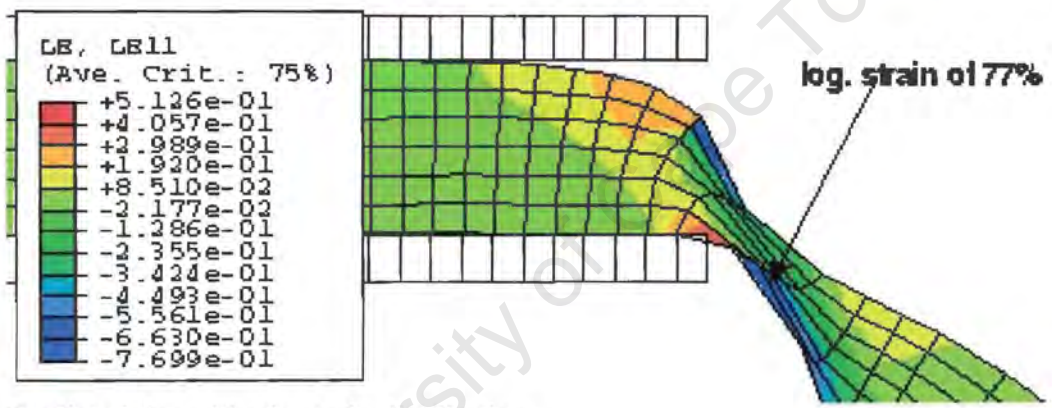

Predicted logarithmic strain distribution.

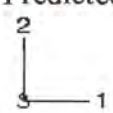

Figure 5.1.11 : Predicted mode II response at an impulse of 30.67Ns at t= 47 μs for a plate clamped at the boundary.

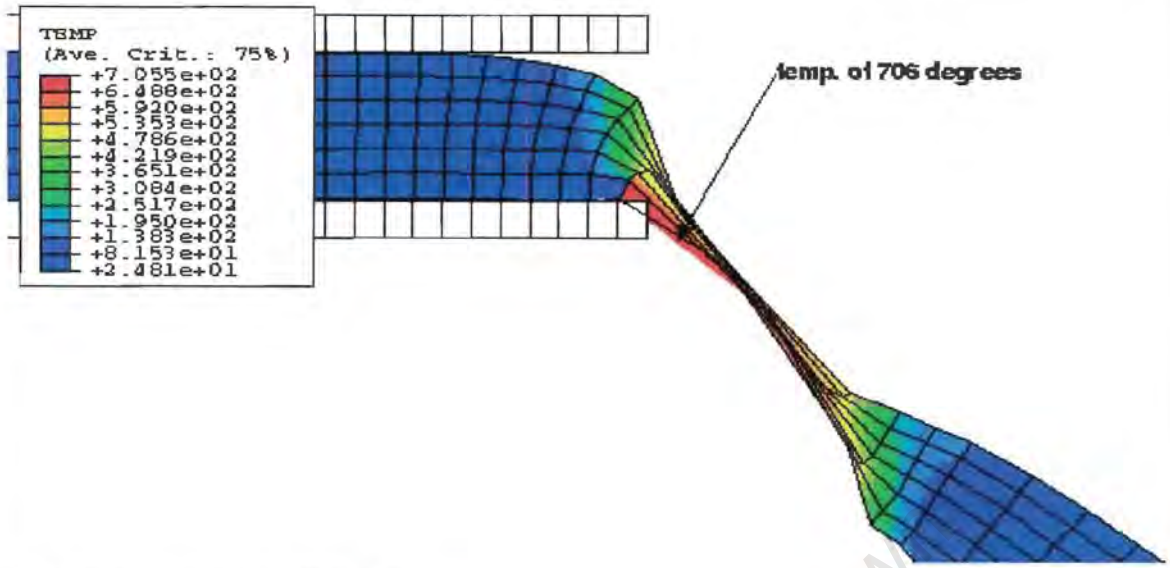

Predicted temperature distribution.

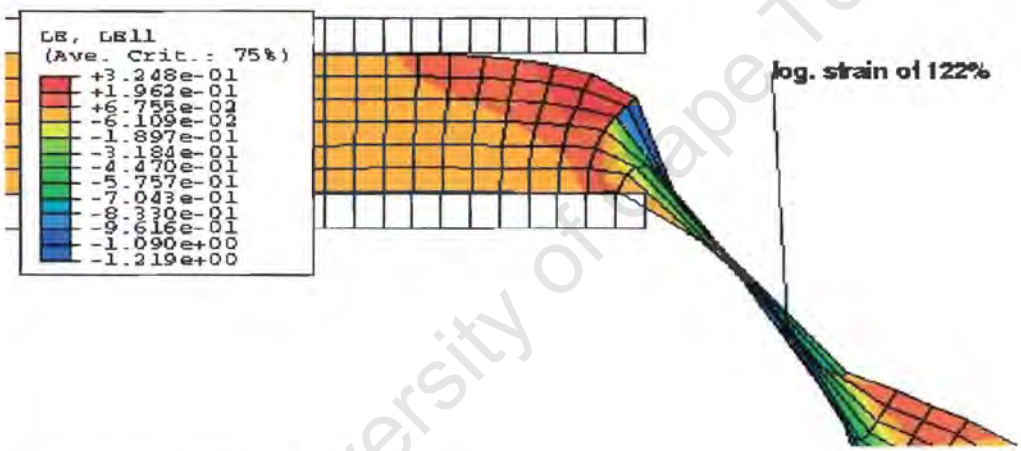

Predicted logarithmic distribution.

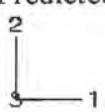

Figure 5.1.12 : Predicted mode II response at an impulse of 30.67Ns at time t= 52 μs for a plate clamped at the boundary.

A temperature of $604^{\circ}C$ and logarithmic strain of 102% figure 5.1.13 in the outer elements indicate that the plate will fail at these elements. A temperature of $717^{\circ}C$ and logarithmic strain of 164% through the plate thickness shows that tearing has occurred in the model, figure 5.1.15.

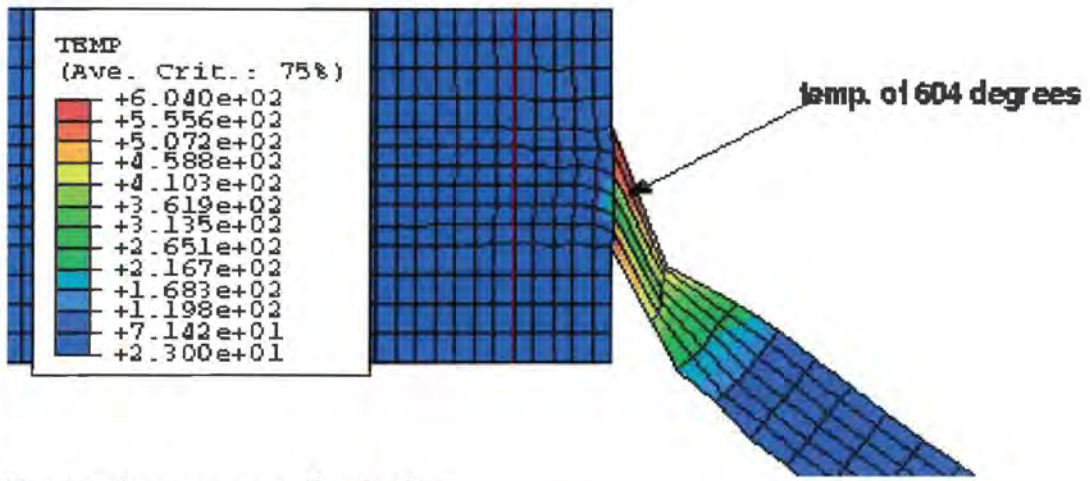

Predicted temperature distribution.

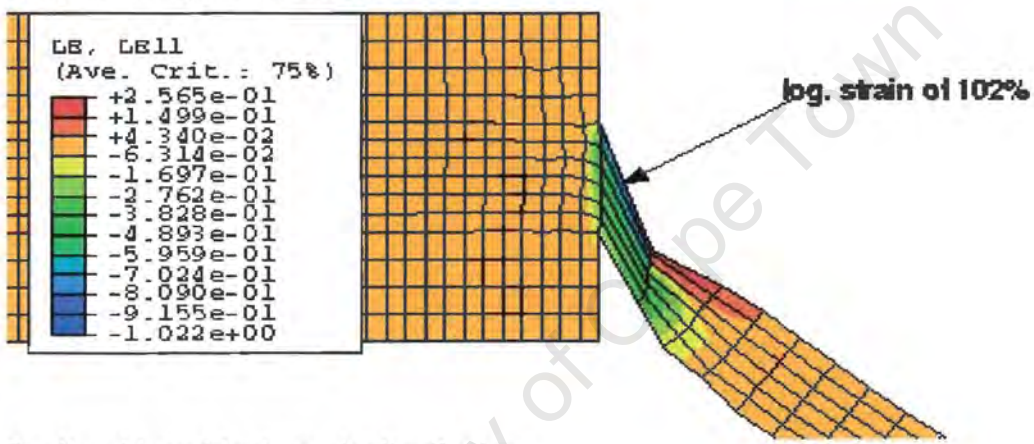

Predicted logarithmic strain distribution.

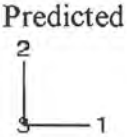

Figure 5.1.13: Initiation of mode II at an impulse of 30.67Ns at time t=38 μs for a plate built-in at the boundary.

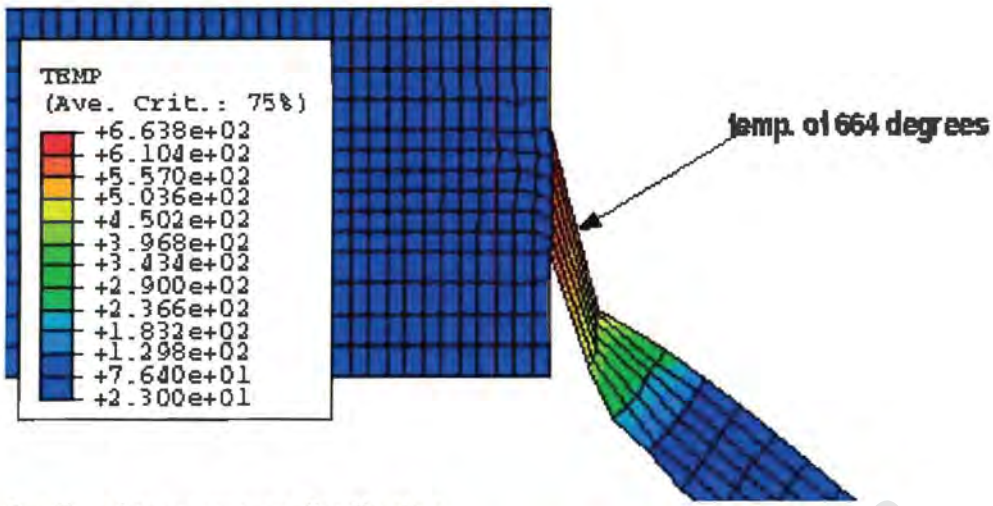

Predicted temperature distribution.

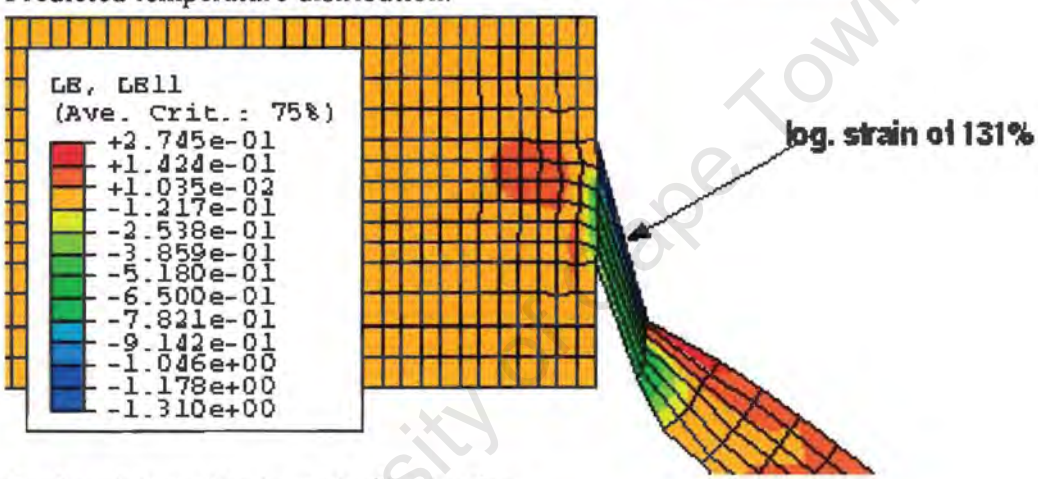

Predicted logarithmic strain distribution.

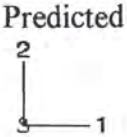

Figure 5.1.14: Predicted mode II at an impulse of 30.67Ns at time t=46 μs for a plate built-in at the boundary.

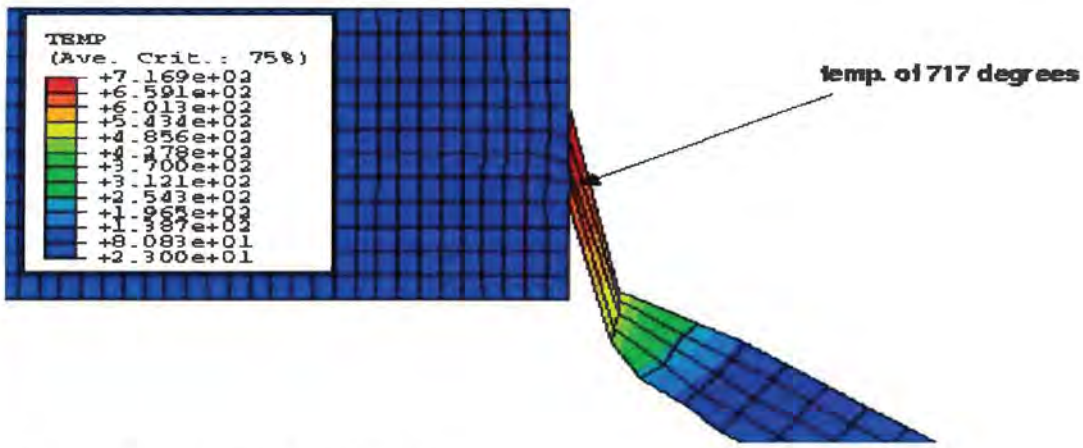

Predicted temperature distribution.

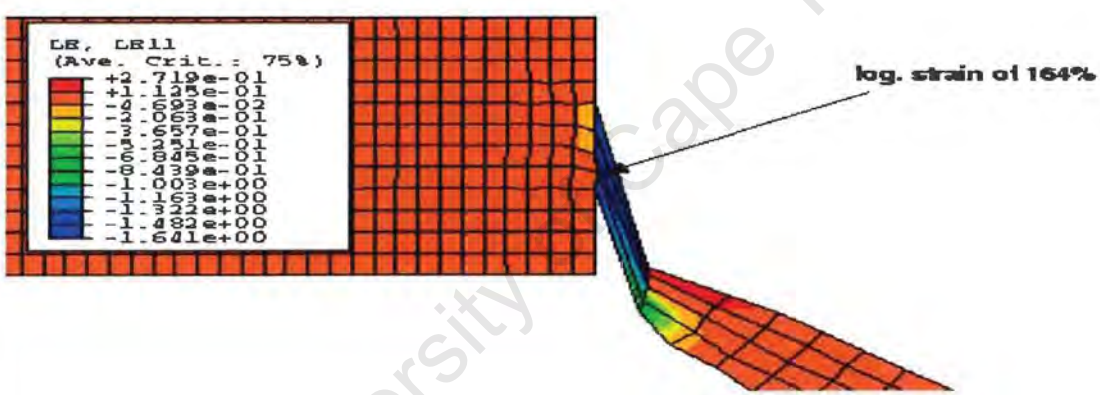

Predicted logarithmic distribution.

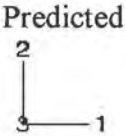

Figure 5.1.15 : Predicted mode II response at an impulse of 30.67 at time t=47 μs Ns for a plate built-in at the boundary.

Mode II is observed to occur at an early time of $47\,\mu s$ in a model fully built-in at the boundary compared to a time of $52\,\mu s$ for a model clamped at the boundary.

To determine transverse shear, equivalent plastic strain and temperature were used. The plates are considered to be transversely sheared when a temperature of $700\,^{o}C$ and equivalent plastic strains of more than 70% is observed across the plate thickness.

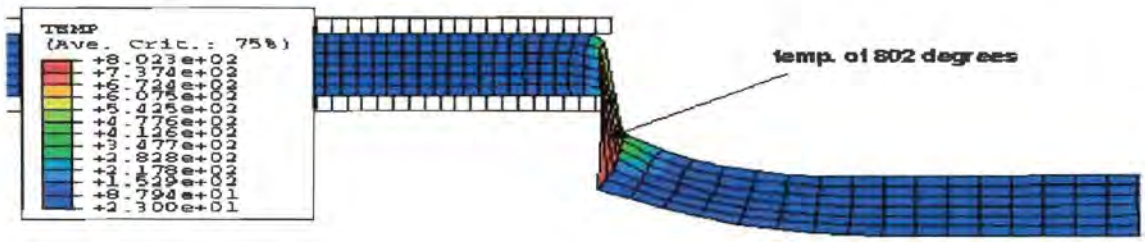

Predicted logarithmic distribution.

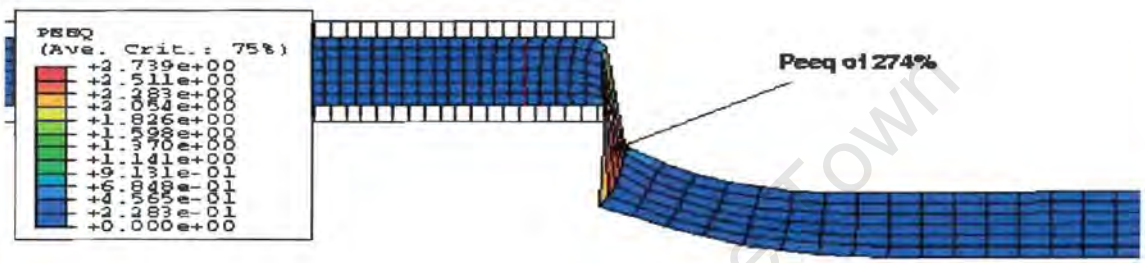

Predicted Equivalent plastic strain distribution.

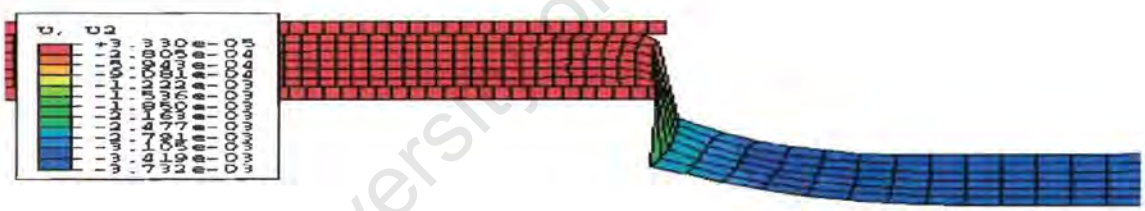

Predicted Mid-point displacement.

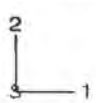

Figure 5.1.16 : Predicted mode III response at an impulse of 52.05Ns for a plate clamped at the boundary at time t=4.2 μs.

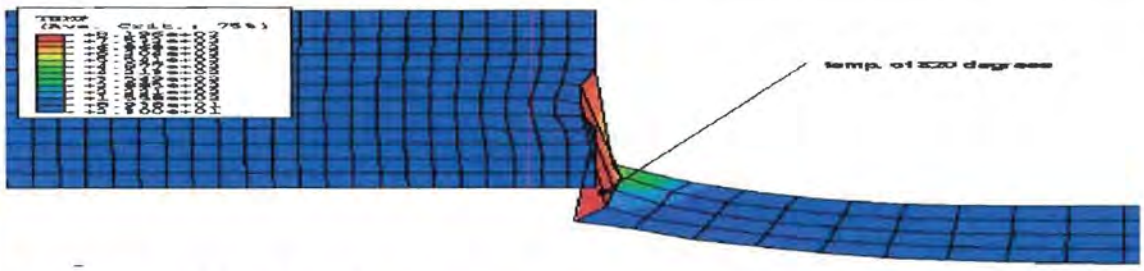

Predicted logarithmic distribution.

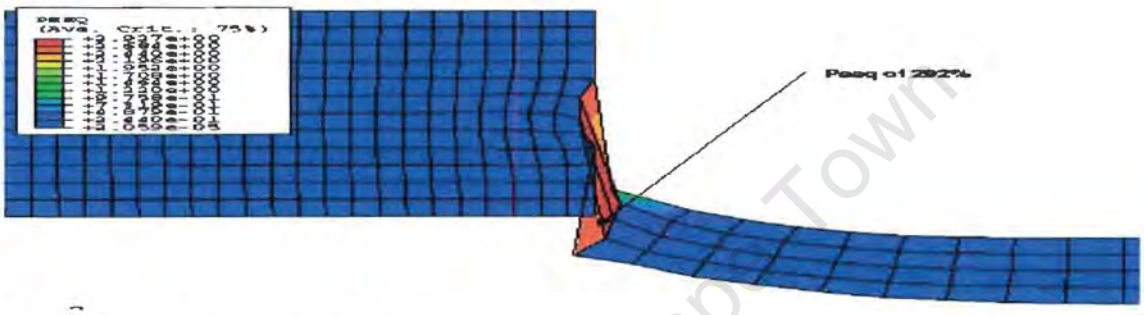

Equivalent plastic strain distribution.

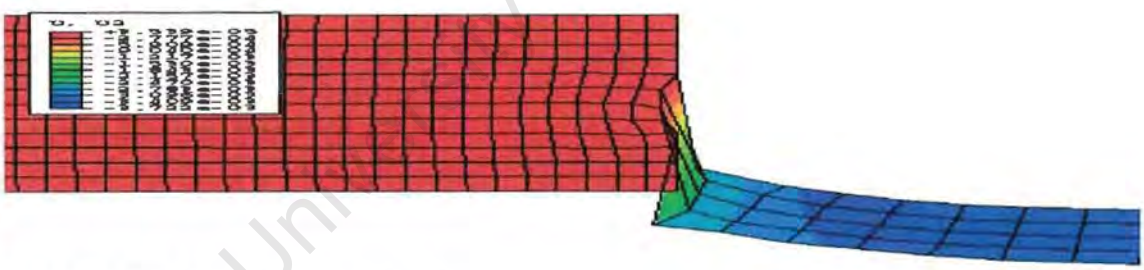

Predicted Mid-point displacement.

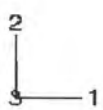

Figure 5.1.17 : Predicted mode III response at an impulse of 52.05Ns for a plate built-in at the boundary at time t=3.2 μs.

Figures 5.1.16 and 5.1.17 show the predicted mode III response of clamped and fully built-in circular plates respectively. High temperatures of $802^{o}C$ (figure 5.1.16), $820^{o}C$ (figure 5.1.16) and equivalent plastic strains of 274% (figure 5.1.16), 292% (figure 5.1.17) respectively indicate that shearing has taken place in the models. A mid-point deflection of 3.72mm and 3.73mm (figures 5.1.16 and 5.1.17) respectively at the time of plates shearing compares well with the experimental mid-point deflection of 5.00mm [24]. Transverse shearing occurs early (at time t=3.2 $\mu s.$) in a model built-in at the boundary compared to a clamped boundary model (at time t 4.2 $\mu s.$).

5.2 Square plates

The simulation results presented in this section are for clamped and built-in square plates having a uniform mesh size of 50x50x4 elements giving a mesh density of 0.89x0.89x0.267. The square plates considered here have length and width of 89mm.

5.2.1 Mode I failure

The analysis was carried out for a range of impulse from 9.1Ns to 11.9Ns. The investigation considered material properties that include and exclude temperature dependency and boundary fixation of the square plates. The duration of the analysis was investigated and it was found out that it takes the same time for clamped and built-in square plates to reach equilibrium as circular plates (section 5.1.1, figure 5.1.1), thus the analysis was allowed to run for 550 μs .

Tables 5.2.1 and 5.2.2 show the results of a comparison of mid-point displacement obtained from models clamped and built-in at the boundary including and excluding temperature dependent material properties with the experiment. In tables 5.2.1 and 5.2.2, t represents the thickness of the plate (1.6mm).

1 Impulse (Ns)	2 Measured Mid-point Displacement (mm)	3 Predicted Mid-point Displacement (mm) Model Including Temperature	4 Difference between Including temperature & measured mid- point displacement to plate thickness ratio (mm) (3-2)/t	5 Predicted Mid-point Displacement (mm) Model Excluding Temperature	6 Difference between Excluding temperature & measured mid- point displacement to plate thickness ratio (mm) (5-2)/t	7 Difference in mid-point displacement Between Model Including & Excluding Temperature (mm) (3-5)
9.1	10.3	11.0	0.2	10.9	0.2	-0.1
9.4	9.4	10.9	0.9	10.9	0.9	0.0
9.7	11.0	11.3	0.2	11.0	0.0	-0.3
9.9	10.6	11.4	0.5	11.3	0.4	-0.1
10.2	11.1	11.9	0.5	11.3	0.5	-0.6
10.5	11.5	12.5	0.6	11.4	-0.1	-1.1
11.1	11.4	12.9	0.9	11.7	0.1	-1.2
11.5	11.5	13.9	1.5	12.7	0.8	-1.2
11.9	11.8	ABAQUS predicts mode II				

Table 5.2.1 : Comparison of predicted mid-point displacement with experiment for models that include and exclude temperature dependent material properties (clamped boundary condition).

From table 5.2.1, the difference in mid-point displacement thickness ratio is less than one plate thickness showing good correlation between predicted and measured mid-point displacement. Both models including and excluding temperature dependent material properties predict mode I failure with a good degree of accuracy as the difference ratio lies within the variation of ± 1 deflection-thickness ratio of Nurick [44]. ABAQUS models predict mode II failure at an impulse (11.9Ns) lower than that of the experiment (14.4Ns).

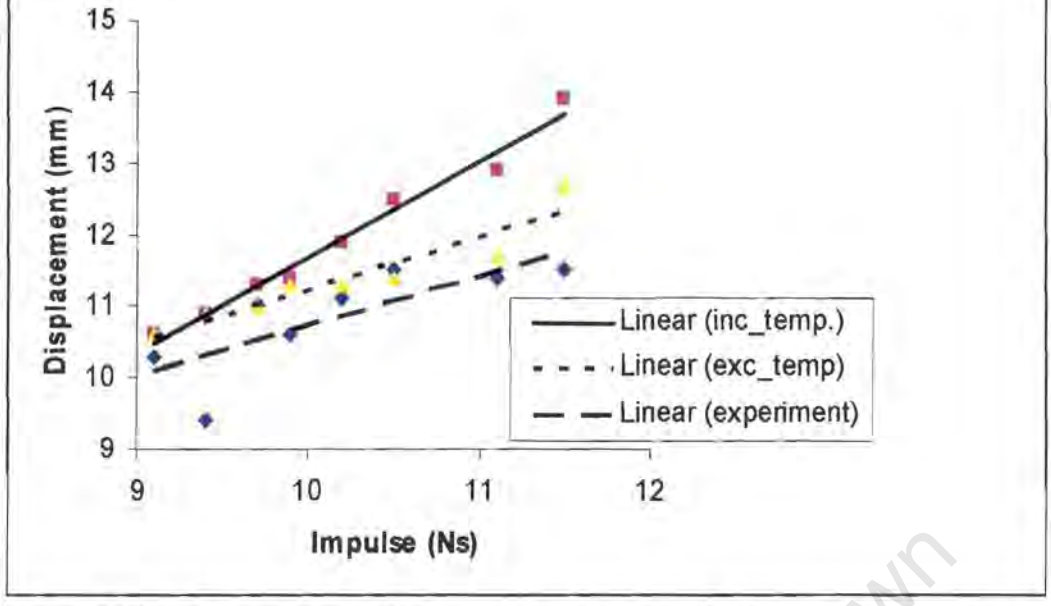

Figure 5.2.1 : A comparison of measured and predicted mid-point displacement as a function of impulse (clamped boundary).

From figure 5.2.2, it is observed that models including and excluding temperature dependent material properties responded linearly to impulse for mode I failure. It is also observed that both models over estimate the mid-point displacement compared to the experimental.

1 Impulse (Ns)	2 Measured Mid-point Displacement (mm)	3 Predicted Mid-point Displacement (mm) Model Including Temperature	4 Difference between Including temperature & measured mid-point displacement to plate thickness ratio (mm) (3-2)/t	5 Predicted Mid-point Displacement (mm) Model Excluding Temperature	6 Difference between Excluding temperature & measured mid-point displacement to plate thickness ratio (mm) (5-2)/t	7 Difference in mid-point displacement Between Model Including & Excluding Temperature (mm) (3-5)
9.1	10.3	10.4	0.1	10.4	0.1	0
9.4	9.4	10.7	0.8	10.7	0.8	0
9.7	11.0	10.8	-0.1	10.8	-0.1	0
9.9	10.6	11.5	0.5	11.2	0.3	-0.3
10.2	11.1	11.7	0.3	11.5	0.3	-0.2
10.5	11.5	11.9	0.3	11.6	0.1	-0.3
11.1	11.4	12.4	0.6	11.9	0.3	0.5
11.5	11.5	ABAQUS predicts mode II				
11.9	11.8					

Table 5.2.2 : Comparison of predicted mid-point displacement with experiment for models that include and exclude temperature dependent material properties (built-in boundary condition).

From tables 5.2.2, it is observed that mode II failure is predicted at an impulse of 11.5Ns compared to a higher impulse of 11.9Ns in table 5.2.1. This observation shows that boundary fixation has an effect on mode II failure.

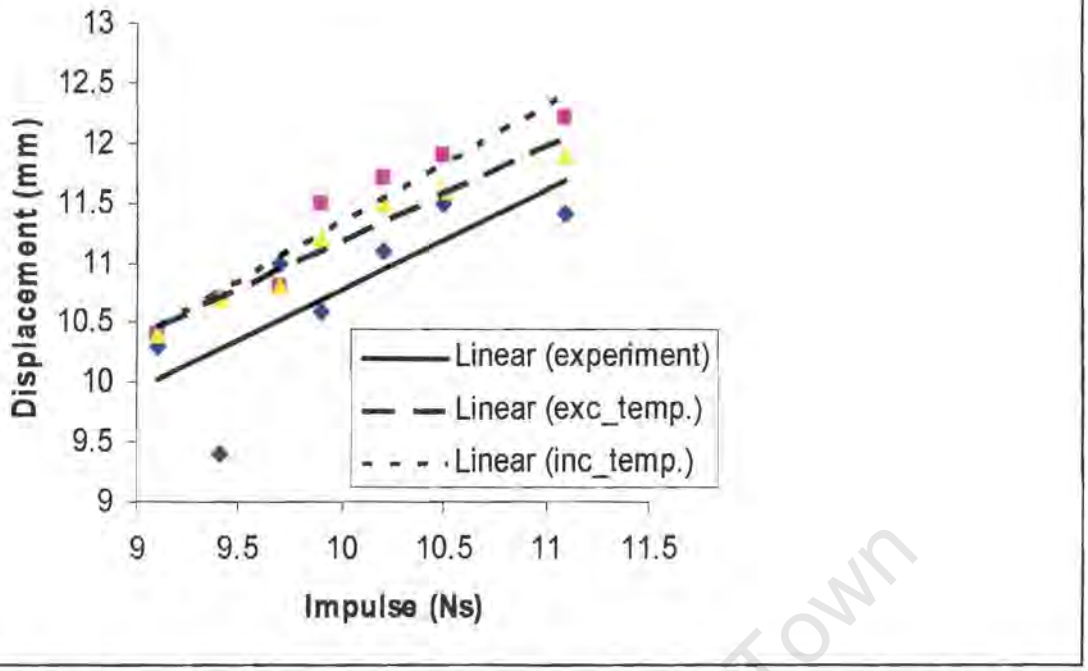

Figure 5.2.2 : A plot of mid-point displacement against impulse for plates with clamped and built-in boundary condition (models including temperature).

In figure 5.2.2, mid-point displacement predicted by a plate clamped at the boundary is higher than for a plate built-in at the boundary. This difference might be as a result of the "pull-in" effect observed in clamped plates (figures 5.2.3 and 5.2.4).

The plates' response to an uniform explosive blast load for a square plate clamped and built-in at the boundary is shown in figures 5.2.3 and 5.2.4 respectively. The models show the plates response from just detonation of the explosive to the final deformed shape. After 300 μs, both models vibrate about the equilibrium position and settle to final mid-point displacements of 11.0mm and 10.9mm respectively.

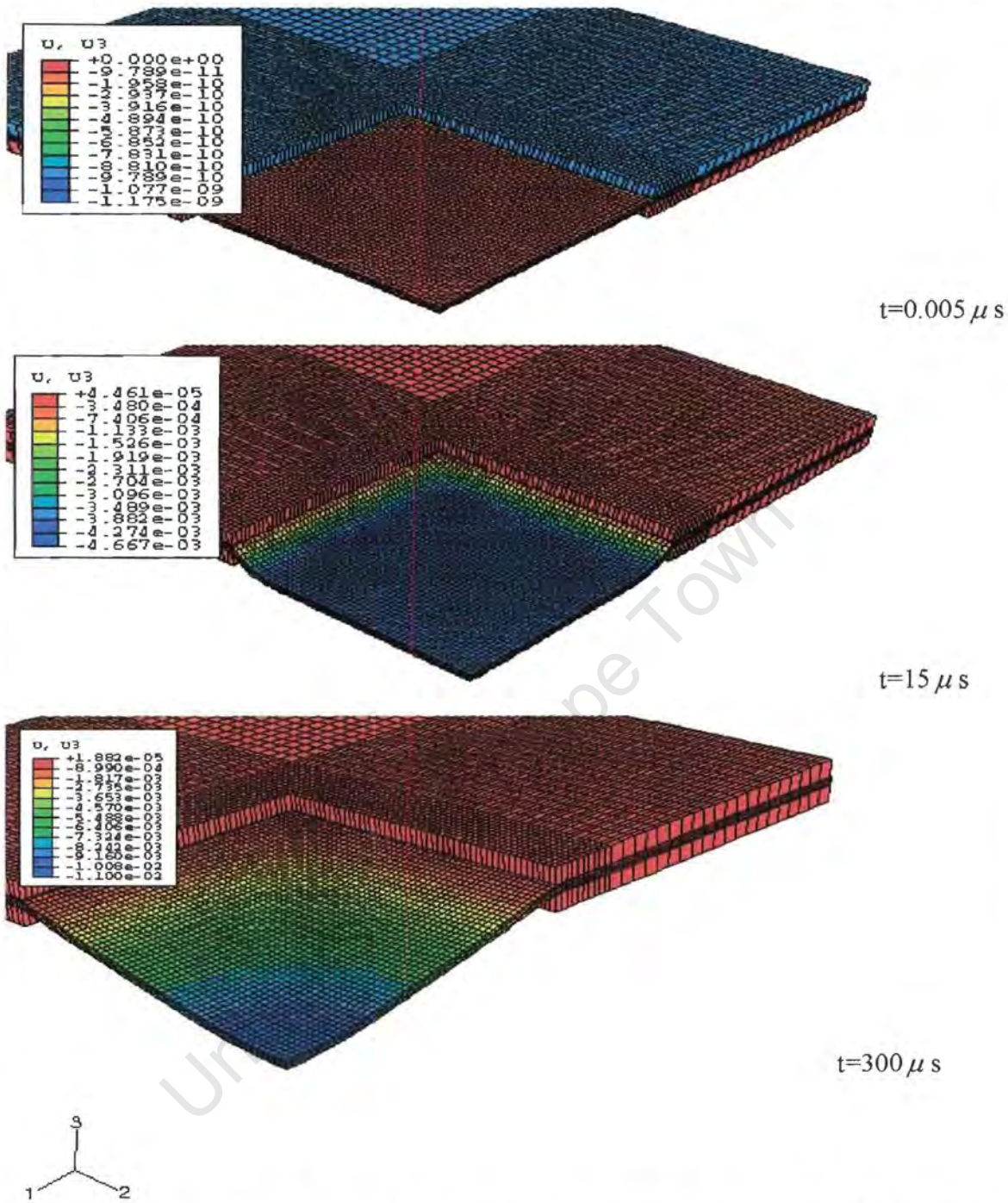

Figure 5.2.3 : Response of a clamped square plate at impulse of 9.1Ns showing displacement in the -3-direction.

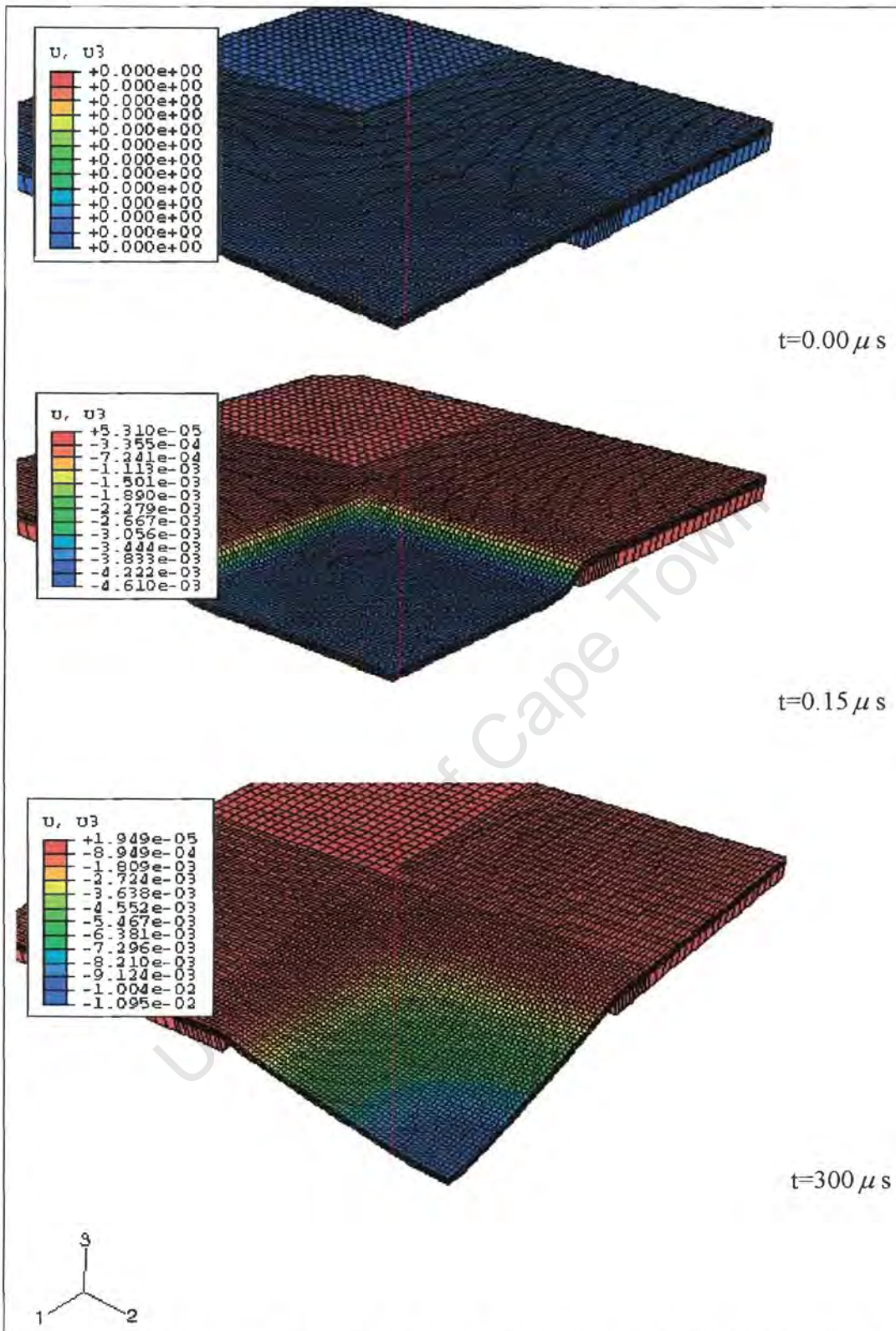

Figure 5.2.4 : Response of a built-in square plate at impulse of 9.1Ns showing in displacement the -3-direction.

Impulse (Ns)	Temperature Model With Clamped Boundary (^{o}C)	Temperature Model With built-in Boundary (^{o}C)
9.1	112	132
9.4	122	137
9.7	194	203
9.9	236	257
10.2	305	346
10.5	351	403
11.1	408	511
11.5	514	609
11.9	602	689

Table 5.2.3 : Temperature variation at the boundary with impulse for models with clamped and built-in boundaries.

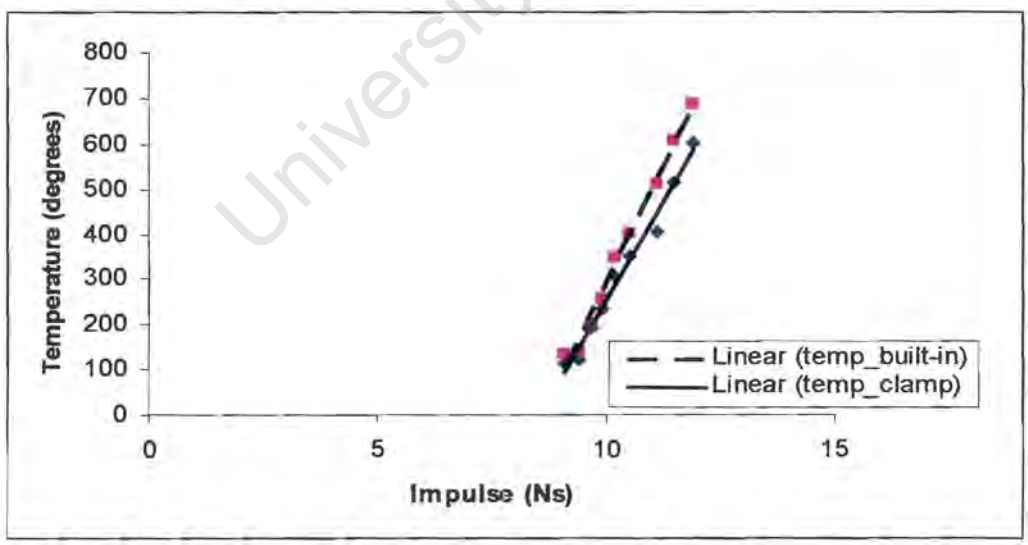

Figure 5.2.5 : A plot of highest temperature at the boundary against impulse for plates clamped and built-in at the boundary.

From figure 5.2.5, it can be observed that a model with built-in boundary has a temperature higher than one clamped at the boundary. This might be an indication that plates with built-in boundary will fail at a time earlier than plates with clamped boundary.

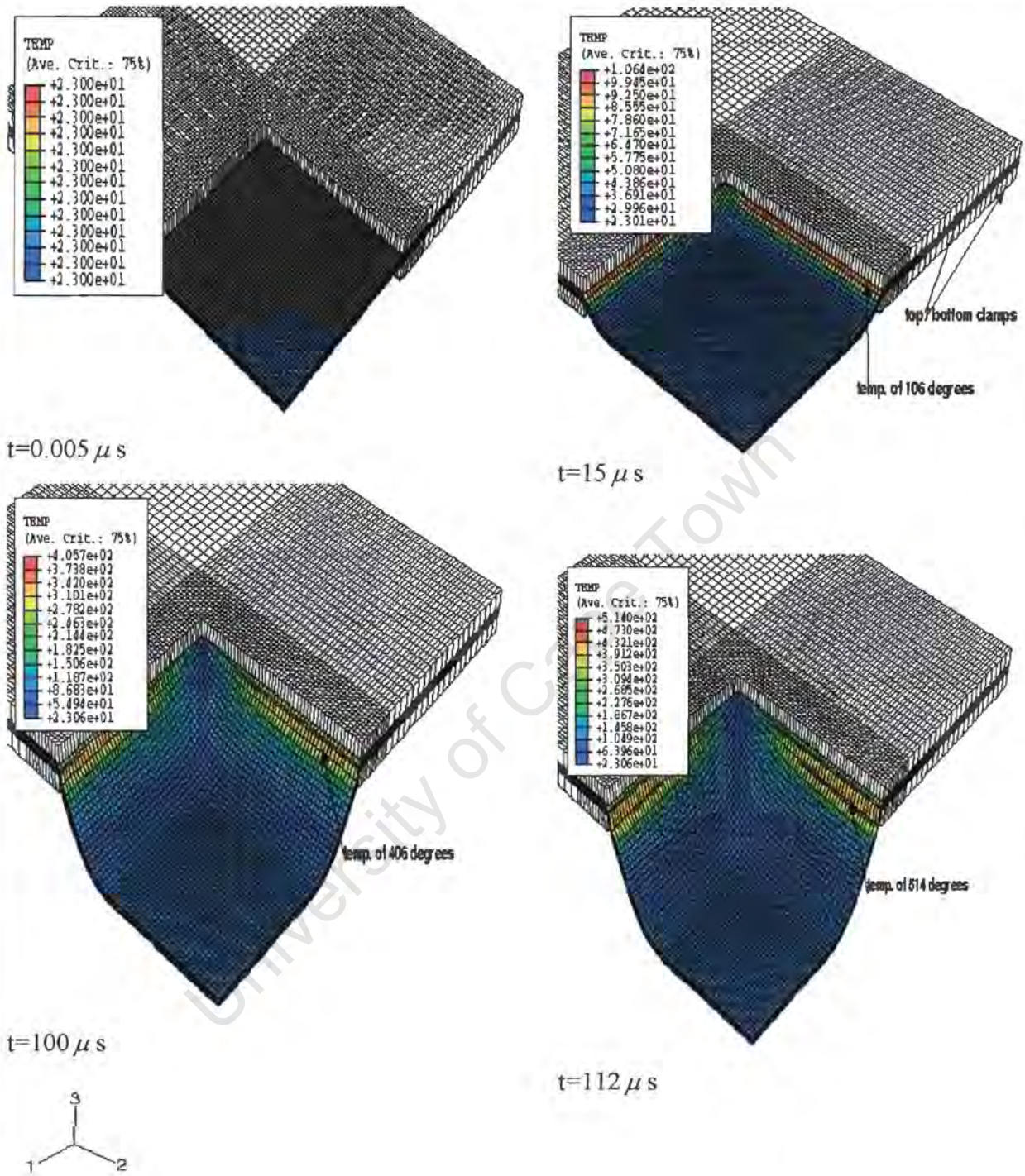

Figure 5.2.6 : Variation of temperature at the boundary with time for an impulse of 11.5Ns.

5.2.2 Tearing mode response

Experimental evidence has shown three distinct modes of failure for square plates undergoing blast loading. These failure modes are discussed in section 5.1.2.

5.2.3 Plate response

Figures 5.2.7 to 5.2.12 show the response of clamped and built-in square plates which were partially or completely torn at the boundary (mode II* and mode II) while figure 5.2.13 to 5.2.16 shows plate that underwent transverse shearing at the boundary. In general, the finite element models show good correlation with the experimental results. In the experiments, tearing is not symmetric due to the complex nature of the loading conditions involving explosives. However, because of the symmetry conditions applied in the simulation models, the predictions fail to show how mode II failure progresses from one side of the plate to two sides, three sides before the exposed area of the plate is blown out of the boundary as observed in the experiment.

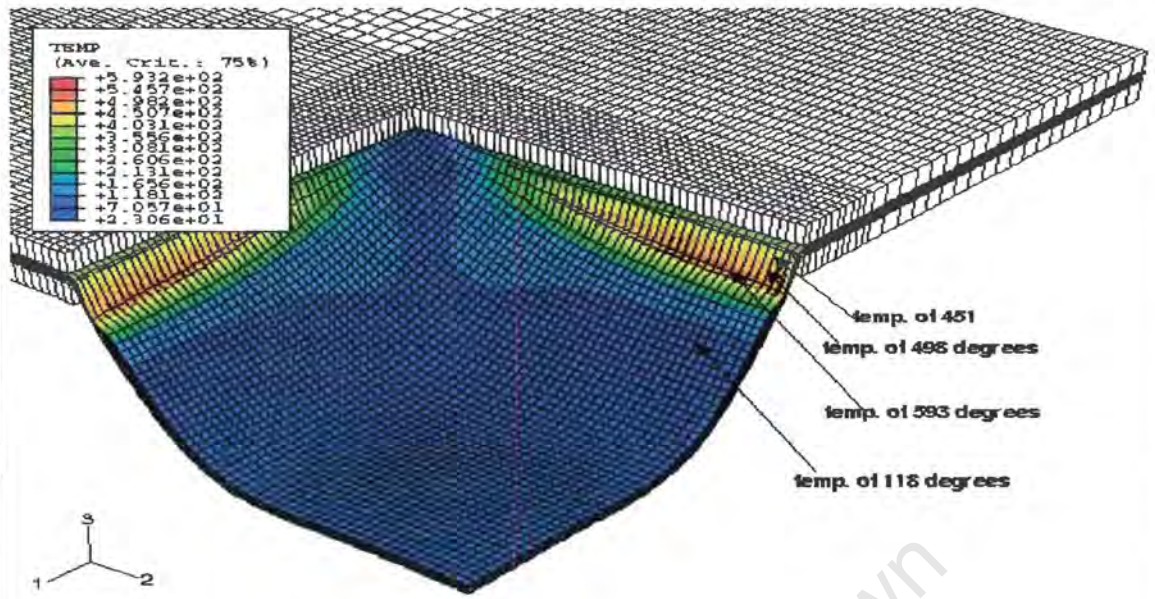

Predicted temperature distribution.

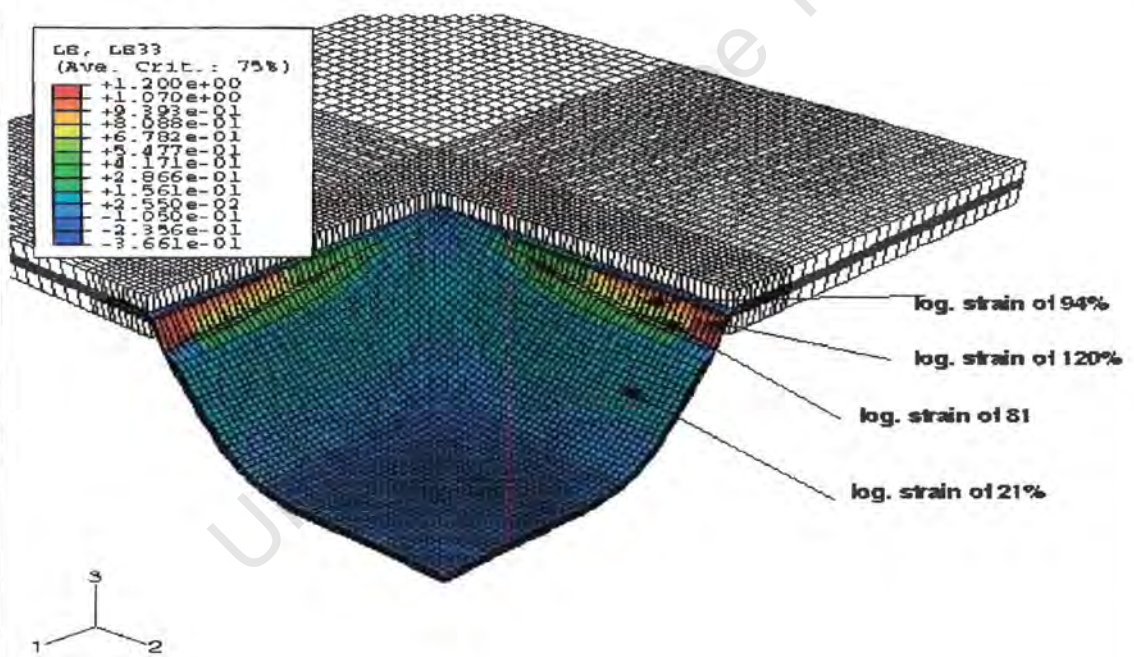

Predicted logarithmic strain distribution.

Figure 5.2.7 : Initiation of mode II* at an impulse of 14.4 Ns at time t=63 μs for a plate clamped at the boundary.

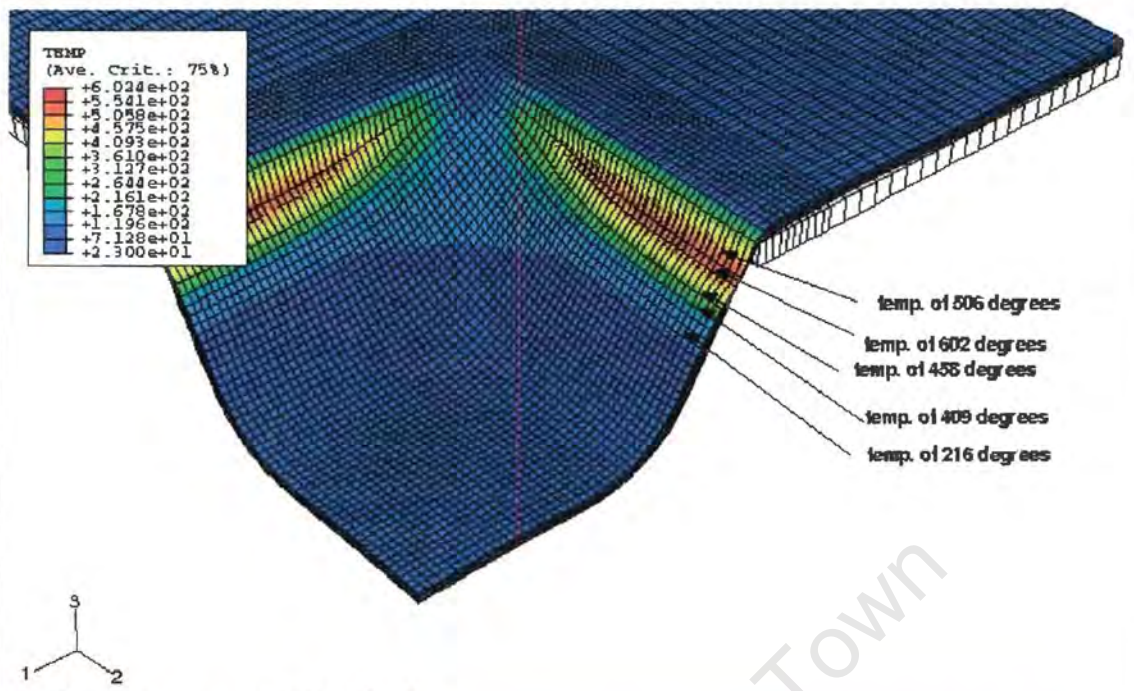

Predicted temperature distribution.

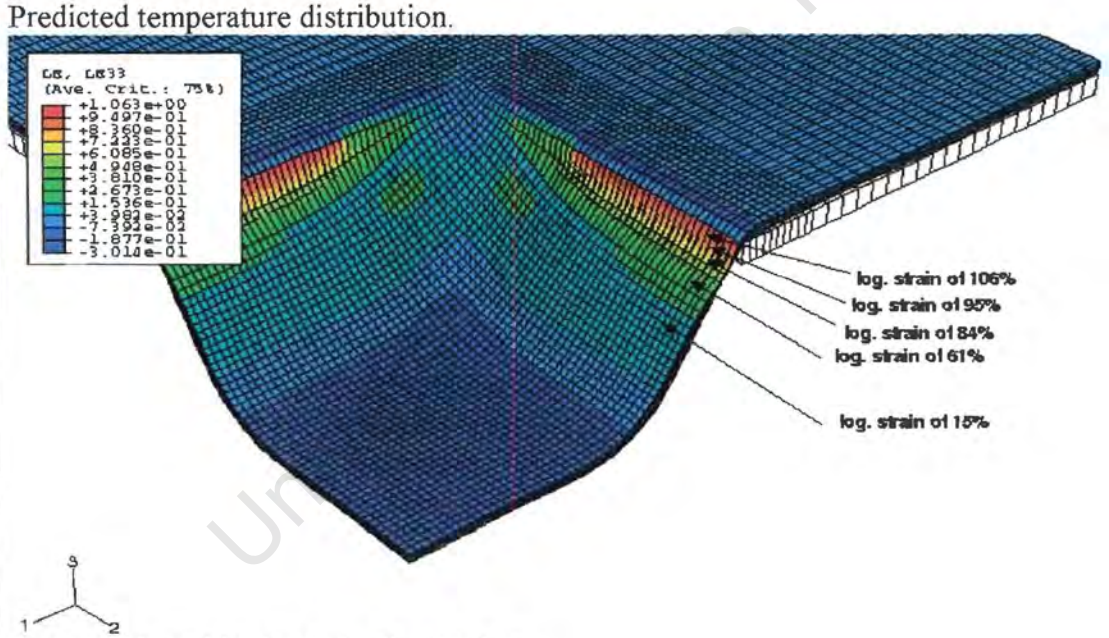

Predicted logarithmic strain distribution.

Figure 5.2.8 : Initiation of mode II* at an impulse of 14.4 Ns at time, t=51 μs for a plate built-in at the boundary.

A temperature of $593^{0}C$ and logarithmic strain of 120% (figure 5.2.7) indicates that the plate is about to fail and most likely starting at the centre of each side where highest temperatures and logarithmic strains are recorded. At this temperature and strain, the rate of strain hardening is still greater than the rate of thermal softening, Woei-Shyan lee and Gen-Wang Yeh [56]. A temperature of $602^{0}C$ and logarithmic strain of 106% (figure 5.2.8) indicates that the plate will fail and tearing will take place in the regions of high temperature and strain starting from the centre. From figures 5.2.7 and 5.2.8, it is observed that at time, t=51 μs tearing sets in for a plate built-in at the boundary compared to a time of 63 μs (figure 5.2.9) for a plate clamped at the boundary. This shows that boundary conditions have an effect on failure mode II*.

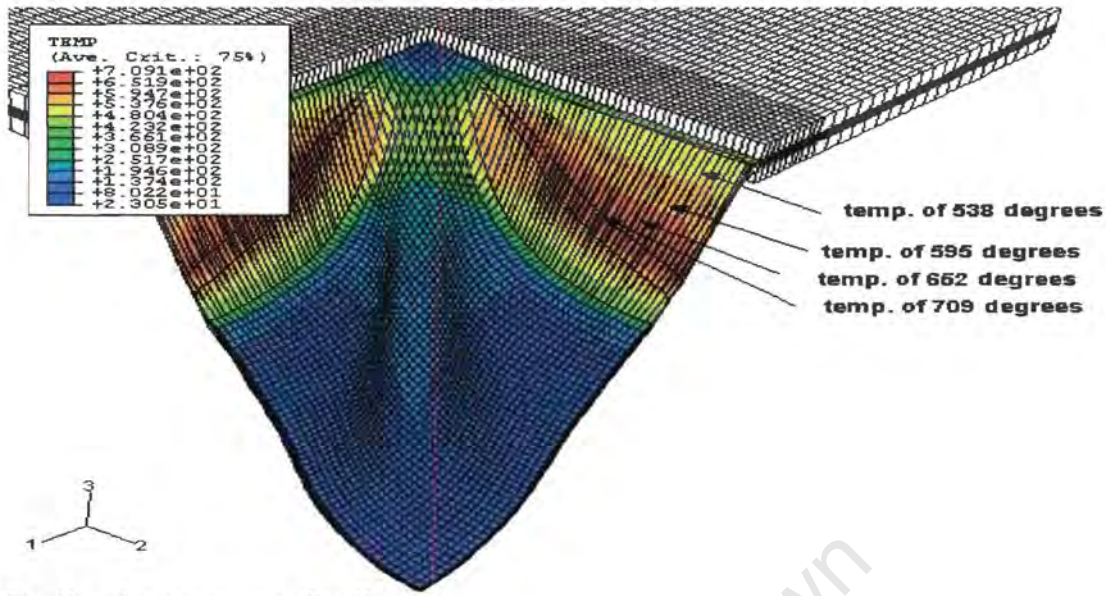

Predicted temperature distribution.

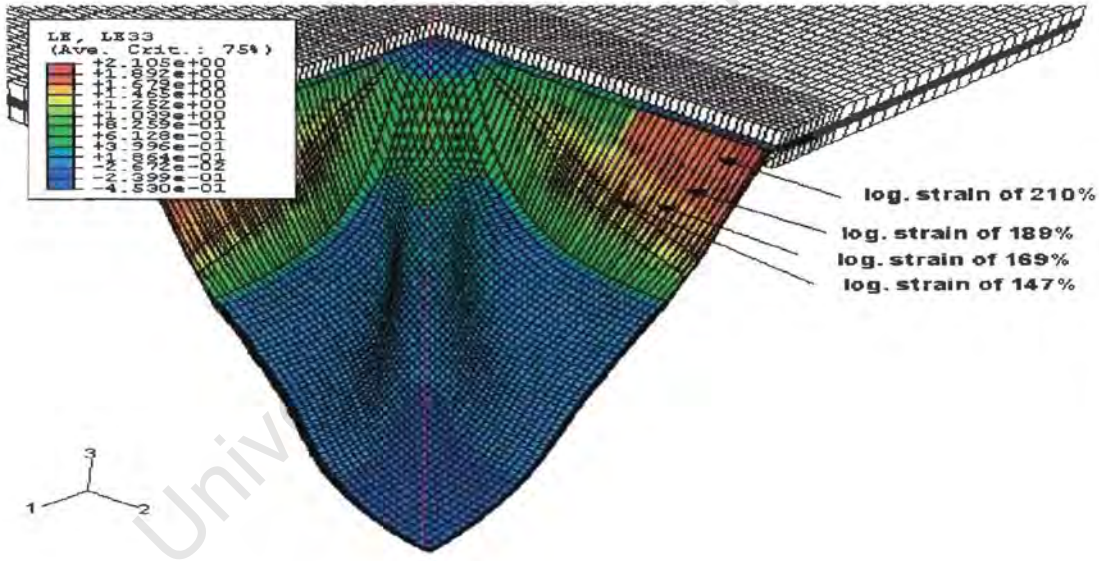

Predicted logarithmic strain distribution.

Figure 5.2.9 : Predicted mode Π* response at an impulse of 14.4 Ns at time, t=89 μs for a plate clamped at the boundary.

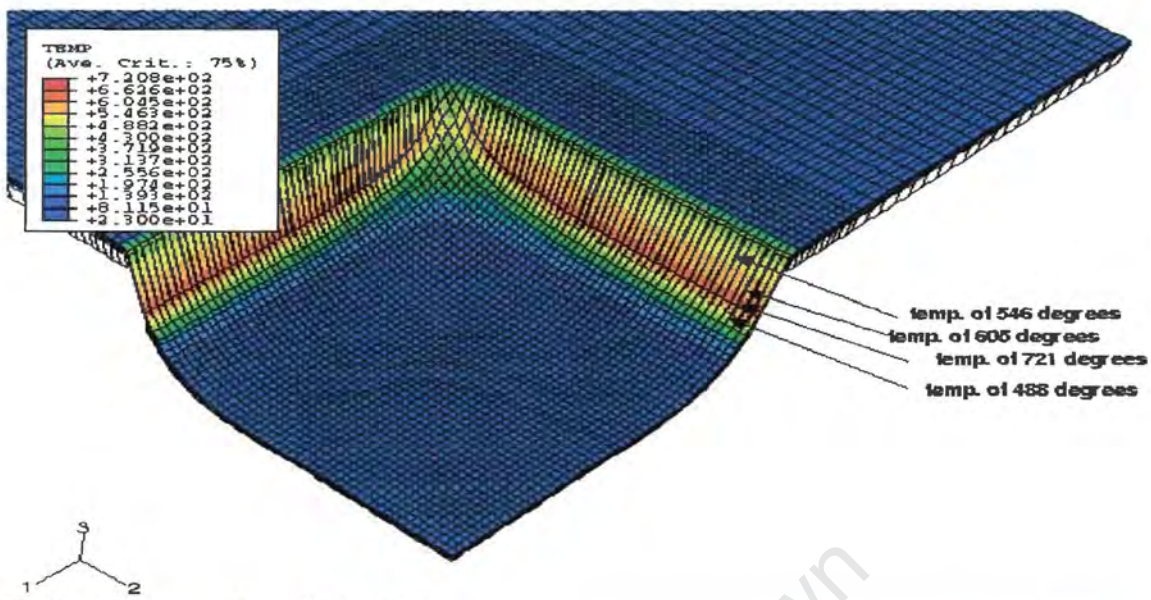

Predicted temperature distribution.

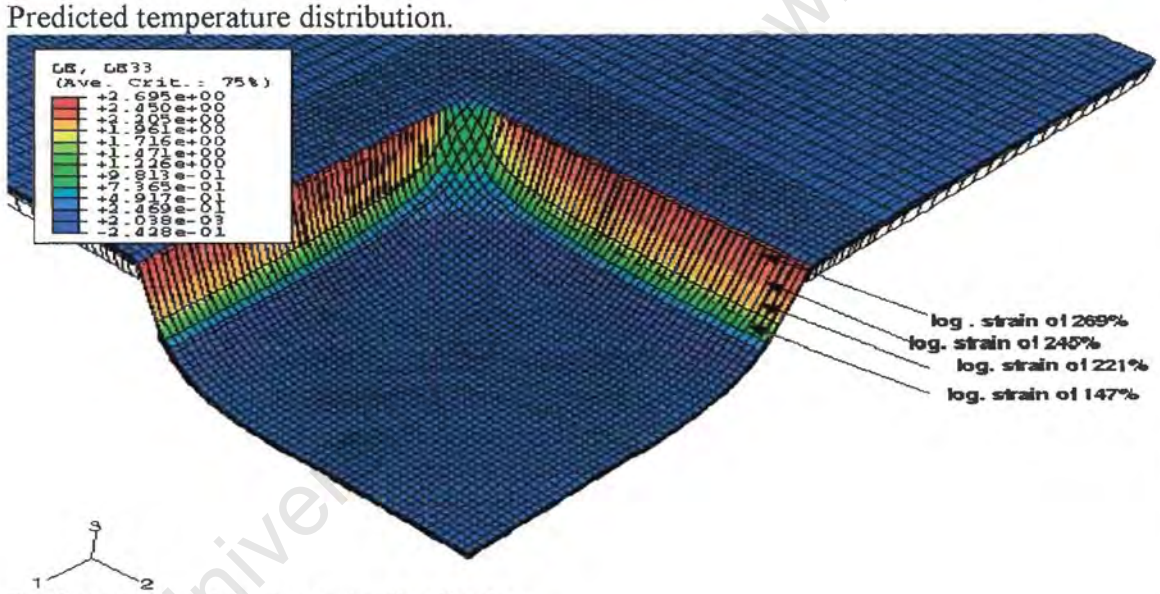

Predicted logarithmic strain distribution.

Figure 5.2.10 : Predicted mode II* response at an impulse of 14.4 Ns at time, t=89 μs for a plate built-in at the boundary.

Figures 5.2.9 and 5.2.10 show the predicted response of clamped and built-in square plates respectively which were partially torn at the boundary (mode II*) under an uniform impulsive load of 14.4Ns. Temperature and logarithmic strain values of $709^{0}C$ and 210% (figure 5.2.9), $721^{0}C$ and 269% (figure 5.2.10) respectively at the elongated elements show that tearing occurred in the models. A predicted total length of tear is given in table 5.2.4 for the models. The torn length per side in ABAQUS was calculated by multiplying the length of one element given in section 5.2.1 by the number of torn elements. Elements are considered to be torn when a temperature of $700^{0}C$ or more and logarithmic strain of 70% or more is reached. It should be noted here that the predicted torn length was assumed to be the same on all sides of the plates since symmetric conditions were used in the models.

Sides of plate	1	2	3	4	Total Length(mm)	% Torn
Experiment	61	59	58	53	231	65%
Clamped plate	55	55	55	55	220	62%
Built-in plate	85	85	85	85	341	96%

Table 5.2.4 : Comparison of torn length of clamped and built-in plates with experimental torn length [26].

From table 5.2.5, a torn length of 62% for a clamped plate is comparable to the experimental torn length of 65% observed by Shave and Nurick [26]. A torn length of 96% is obtained for a built-in plate, indicating the effect of boundary condition on mode II* failure.

Figures 5.2.11 and 5.2.12 show the predicted mode II response for clamped and built-in plates at an impulse of 24.4Ns.

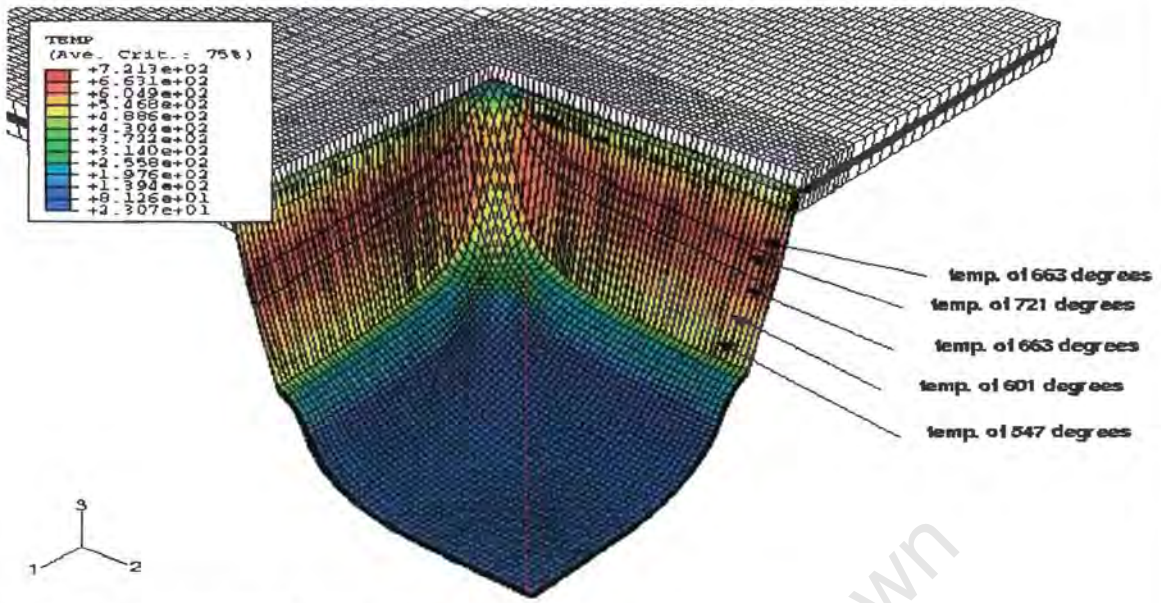

Predicted temperature distribution.

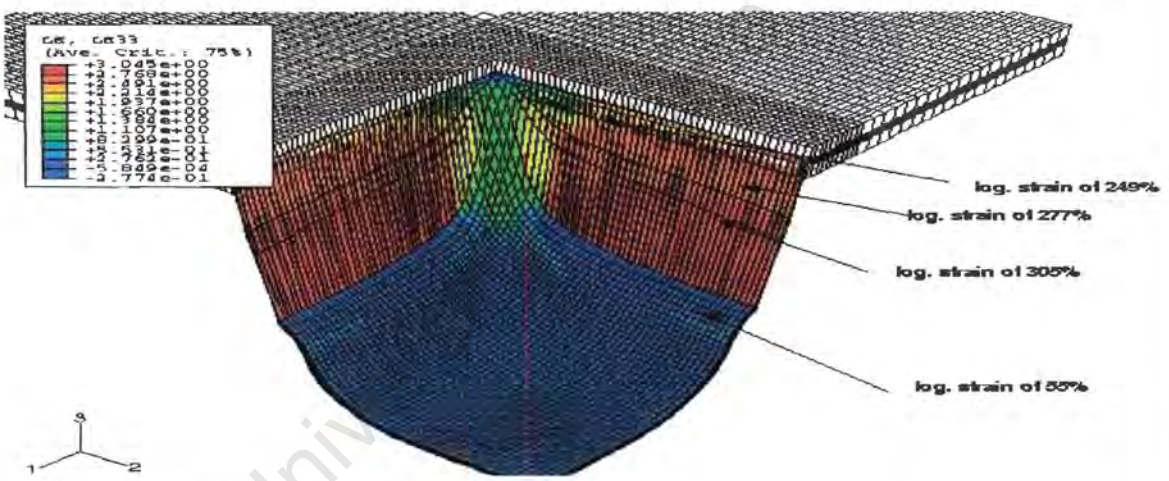

Predicted logarithmic strain distribution.

Figure 5.2.11 : Predicted mode II response at an impulse of 24.4Ns for a plate clamped at the boundary at time t=89 μs .

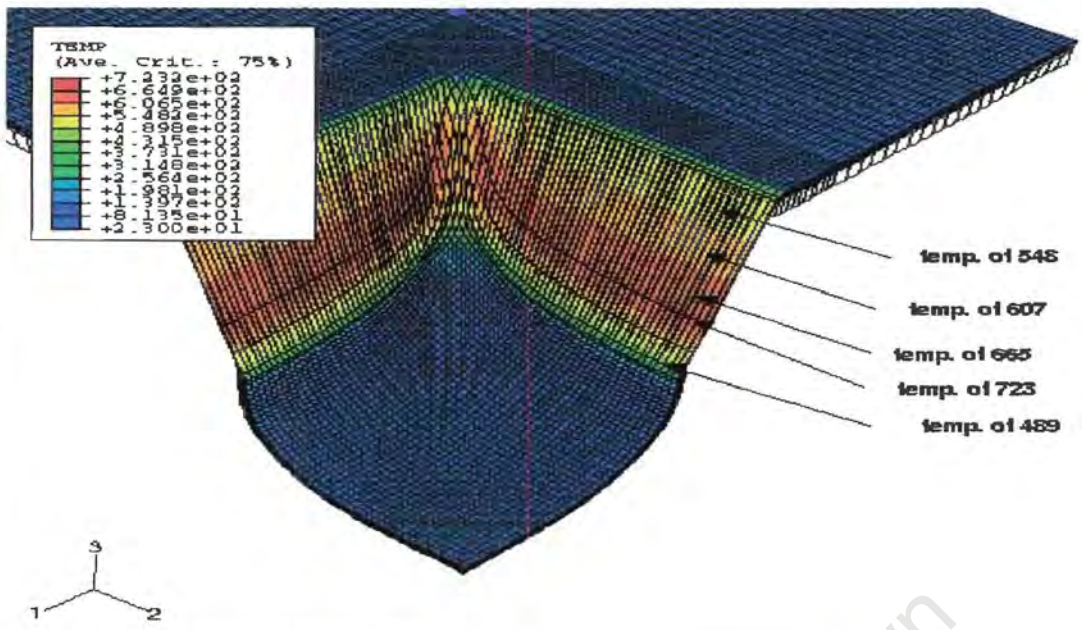

Predicted temperature distribution.

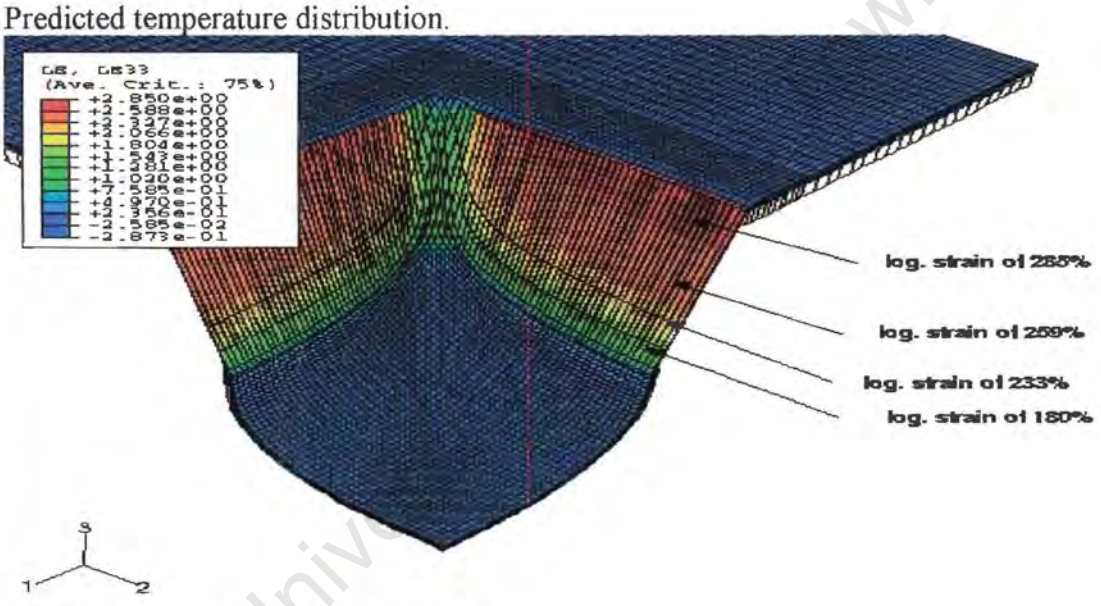

Predicted logarithmic strain distribution.

Figure 5.2.12 : Predicted mode II response at an impulse of 24.4Ns for a plate built-in at the boundary at time t=75 μs .

Figures 5.2.11 and 5.2.12 show the predicted response of clamped and built-in plates that were completely torn at the boundary (mode II) under an uniform impulse of 24.4Ns. Temperatures and logarithmic strains of $721^{0}C$ and 249% (figure 5.2.11), $723^{0}C$ and 285% (figure 5.2.12) respectively at the elongated elements show that tearing occurred in the models.

Figures 5.2.13 and 5.2.14 show the predicted mode III response for clamped and built-in plates at an impulse of 49Ns.

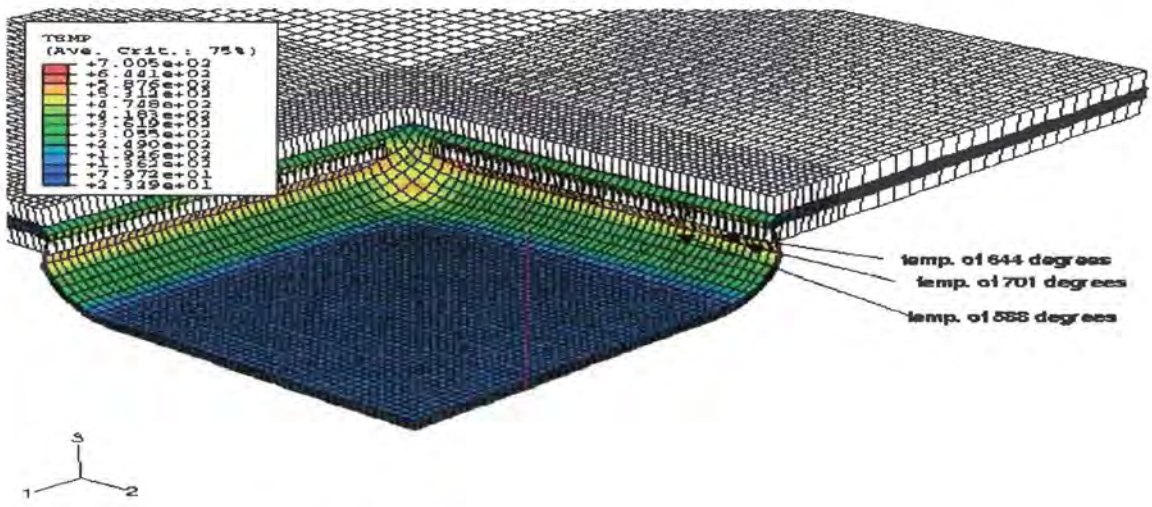

Predicted temperature distribution.

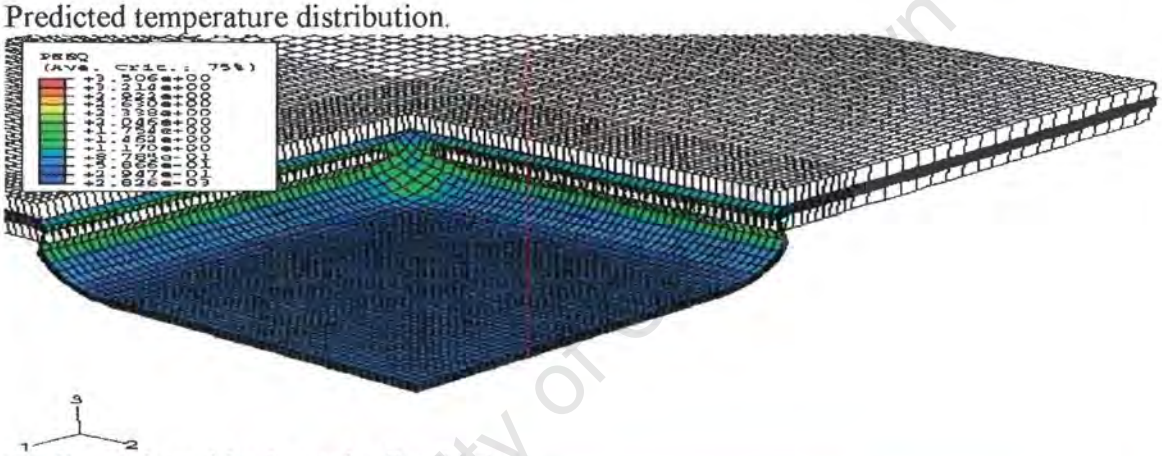

Predicted logarithmic strain distribution.

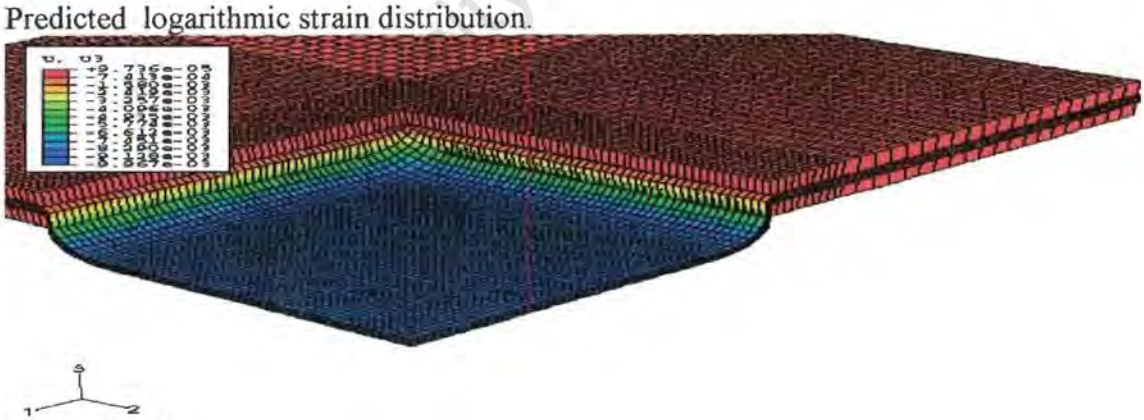

Mid-point displacement.

Figure 5.2.13 : Predicted mode III response at an impulse of 49Ns for a plate clamped at the boundary time t=13.95 μs .

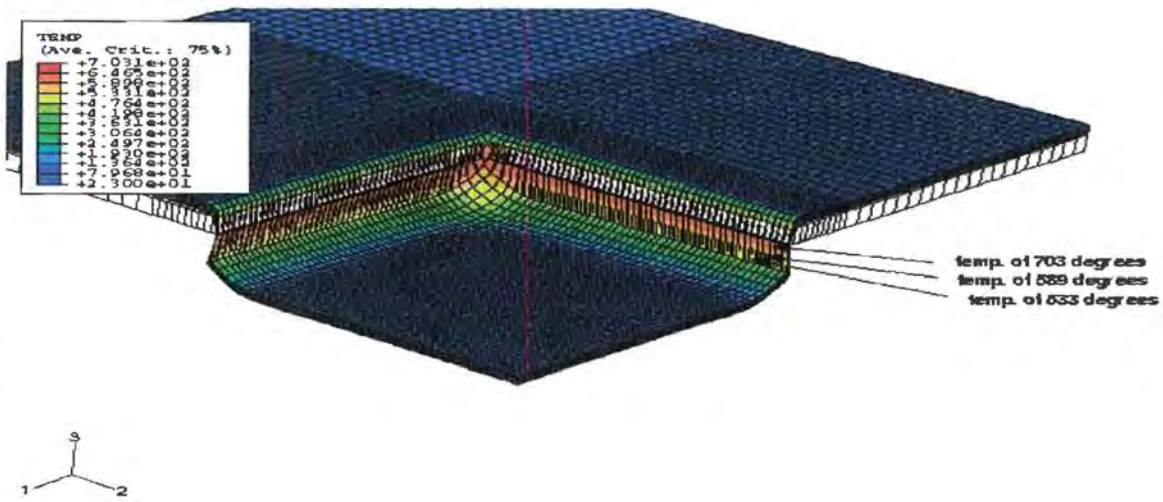

Predicted temperature distribution.

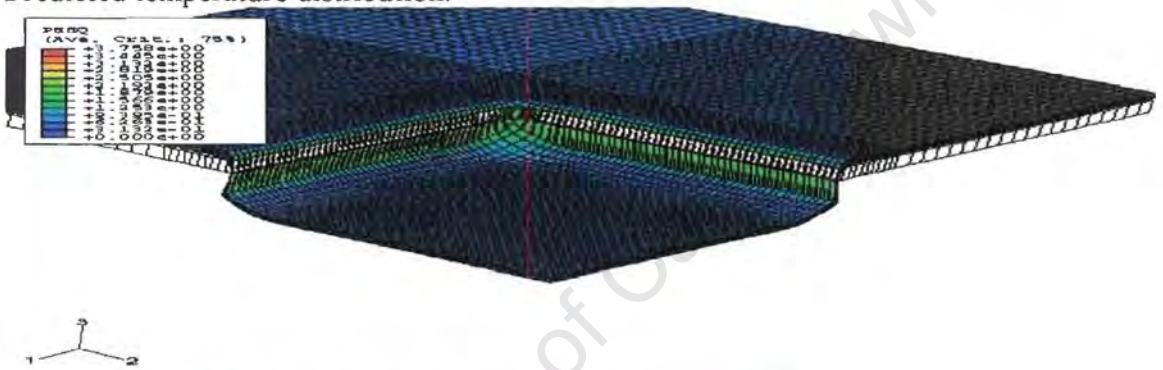

Predicted logarithmic strain distribution.

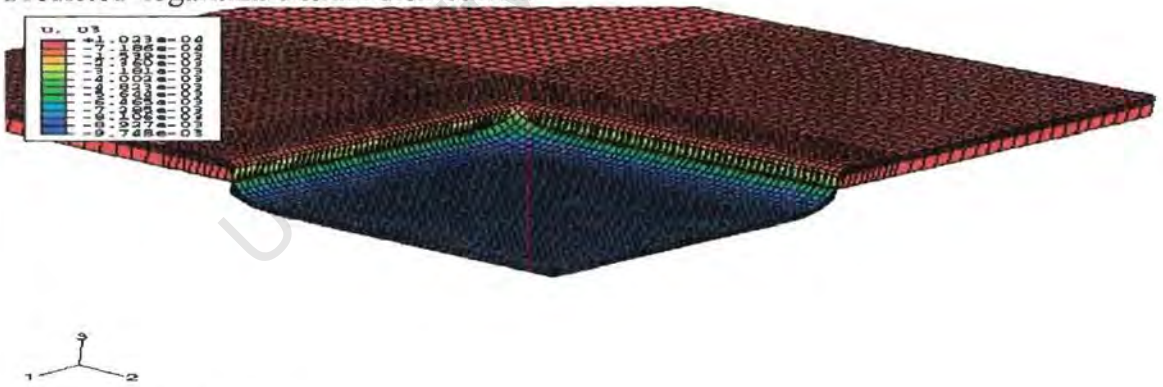

Mid-point displacement.

Figure 5.2.14 : Predicted mode III response at an impulse of 49Ns for a plate built-in at the boundary at time t=13.95 μs .

High temperatures of 701^0C and equivalent plastic strain of 351% (figure 5.2.15), 703^0C and 376% (figure 5.2.16) respectively at the entire boundary of the plates indicate that transverse shearing will take place at the boundary. A deflection of 9.97mm (figure 5.2.15) and 9.75mm (figure 5.2.16) respectively is also predicted at this time which is comparable to the experimental deflection in the range of 0 to 5mm.

Figures 5.2.15 and 5.2.16 shows flat square plates almost of the same size as the blast loaded plates sheared from the boundary as a result of the high impulse.

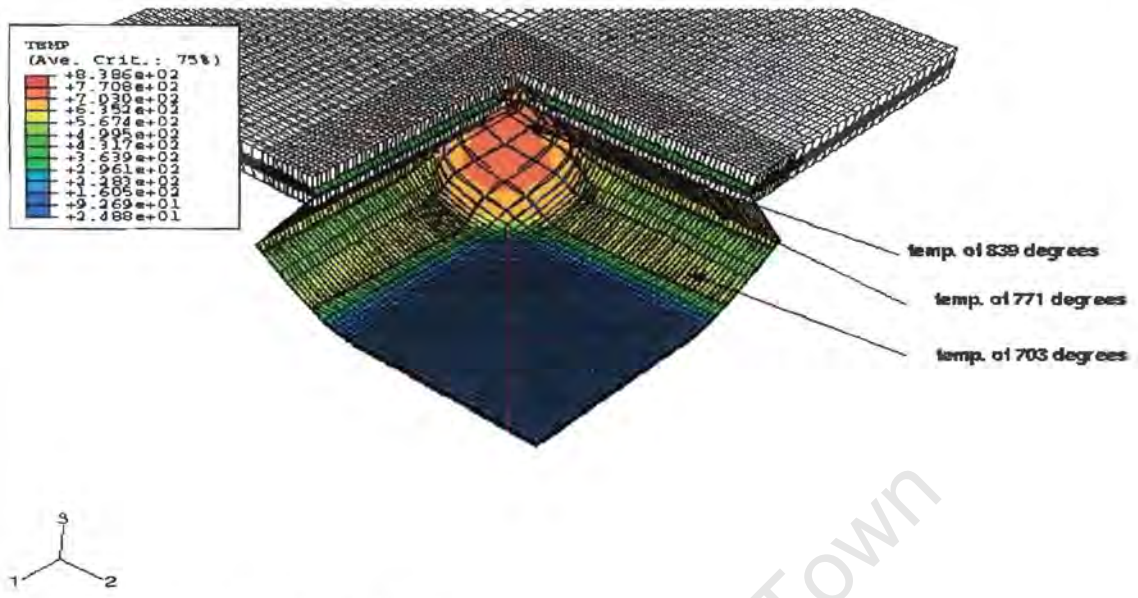

Predicted temperature distribution.

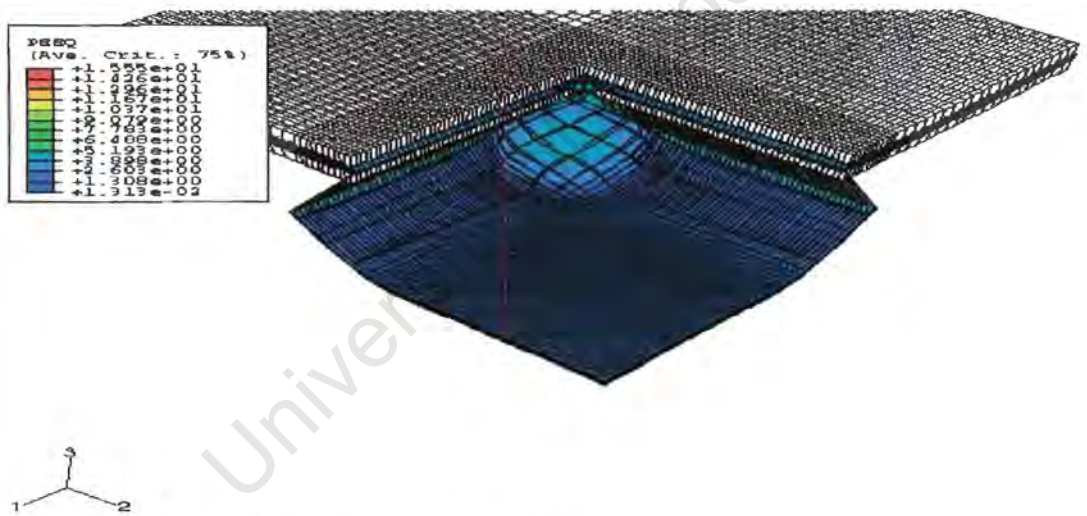

Predicted equivalent plastic strain distribution.

Figure 5.2.15 : Contour plot of an almost flat plate ripped from the clamped base plate at an impulse of 49Ns at time t=15.3 μs .

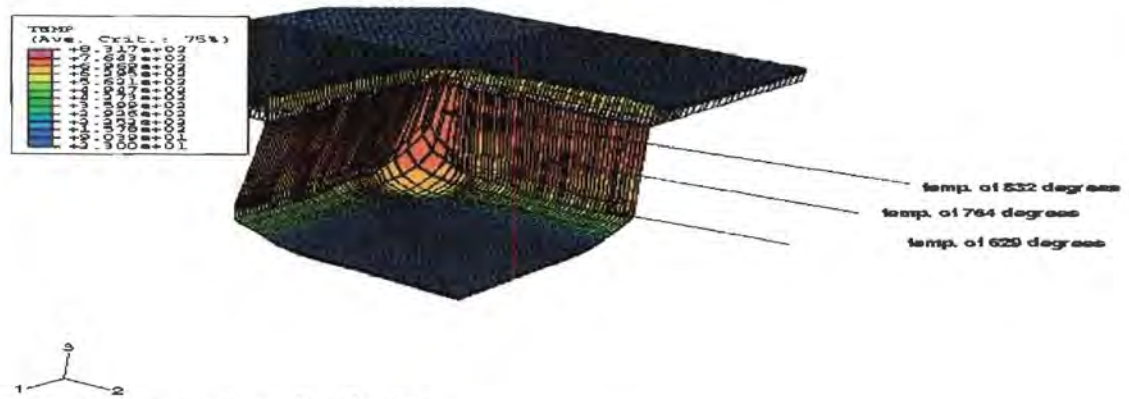

Predicted temperature distribution.

Predicted temperature distribution.

Figure 5.2.16 : Contour plot of an almost flat plate ripped from the built-in base plate at an impulse of 49Ns at time t=15.3 μs

5.3 Rectangular beams

The simulation results presented in this section have a uniform mesh size of 50x20x10 and 25x20x10 elements in beam spans of 203.2mm and 101.6mm respectively resulting in a mesh density of approximately 2.032x0.25x0.95mm. The finite element code SLAM used by Costantino [58] to verify the experimental results performed on rectangular beams by Menkes and Opat [3] was not considered in this section since the finite element code (ABAQUS / Explicit) used in this study is an improved package.

5.3.1 Mode I failure

The analysis was carried out for a range of impulse from 9.16Ns to 22.08Ns. The investigation considered material properties that include and exclude temperature dependency and boundary fixation of the beams. Figure 5.3.1 shows the displacement history for five points (represented by curves 1 to 5); taken from the mid-point of the beam to a distance 10mm from the boundary. The displacement history plot represents a clamped rectangular beam span of 203.2mm that underwent an impulsive load of 9.16Ns. The displacement history for a built-in rectangular beam was also examined and it was found to behave the same. From figure 5.3.1, it was observed that all points monitored along the beam profile reach equilibrium at approximately the same time; 800 μs. The displacement history plot shows that beam spans of 203.2mm and 101.6mm with clamped and integral boundary conditions responded to deformation linearly with time, reached a maximum and exhibited a small amount of residual elastic vibration about a mean displacement after approximately 800 μs, and thereafter, the magnitude of the vibration slowly decays. This same behaviour was also observed in steel plates discussed earlier in this work. It was thus sufficient to stop the analysis after 850 μs.

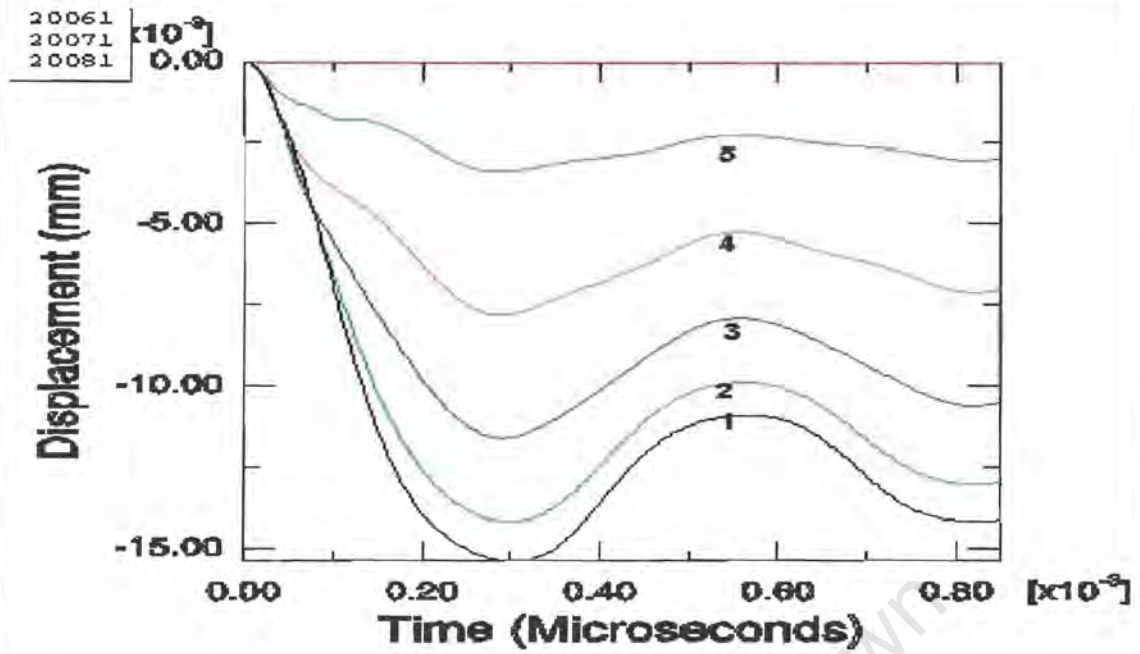

Figure 5.3.1 : Displacement history at various points along the profile of a clamped rectangular beam at an impulse of 9.16Ns.

Tables 5.3.1 and 5.3.2 show the results of a comparison of the mid-point displacement of clamped and built-in rectangular beams respectively for models that include and exclude temperature dependent material properties. Beam lengths of 203.2mm and 101.6mm where examined in this section.

1 Impulse (Ns)	2 Measured Mid-point Displacement (mm)	3 Predicted Mid-point Displacement (mm) Model Including Temperature	4 Difference between Including temperature & measured mid-point displacement (mm) (3-2)	5 Predicted Mid-point Displacement (mm) Model Excluding Temperature	6 Difference between Excluding temperature & measured mid-point displacement (mm) (5-2)	7 Difference in mid-point displacement Between Model Including & Excluding Temperature (mm) (3-5)
Length=203.2mm						
9.16	12.7	14.53	1.83	14.50	1.80	-0.03
11.22	19.05	20.33	1.28	20.30	1.25	-0.03
13.18	22.35	23.64	1.29	23.65	1.30	0.01
14.78	31.75	33.10	1.35	32.30	0.55	-0.80
17.19	33.27	35.26	1.99	34.9	1.63	-0.36
18.08	38.1	39.92	1.82	39.10	1.00	-0.82
20.39	38.1	41.11	2.93	40.10	2.00	-0.93
22.08	36.58	ABAQUS predicts mode II				
Length=101.6mm						
9.16	4.57	6.81	2.33	6.90	2.33	0.09
11.22	7.87	7.95	-0.07	7.80	-0.07	-0.15
13.18	7.87	9.16	0.23	8.10	0.23	-1.06
14.78	9.65	10.09	0.15	9.80	0.15	-0.29
17.19	14.22	16.10	0.98	15.20	0.98	-0.9
18.08	20.57	22.4	0.73	21.30	0.73	-1.1
20.39	19.05	24.1	3.6	22.60	3.6	-1.5
22.08	20.57	ABAQUS predicts mode II				

Table 5.3.1 : Comparison of predicted mid-point displacement with experiment for models that include and exclude temperature dependent material properties (clamped boundary condition).

The difference between measured and predicted mid-point displacement for models that include and exclude temperature is less than the beam thickness (columns 4 and 6 of table 5.3.1). This shows that both models predict mode I failure reasonably well. It is also observed from table 5.3.1 that the difference in mid-point displacement between both models (column 7) is also less than one beam thickness indicating that temperature has no effect on mode I failure on rectangular beams.

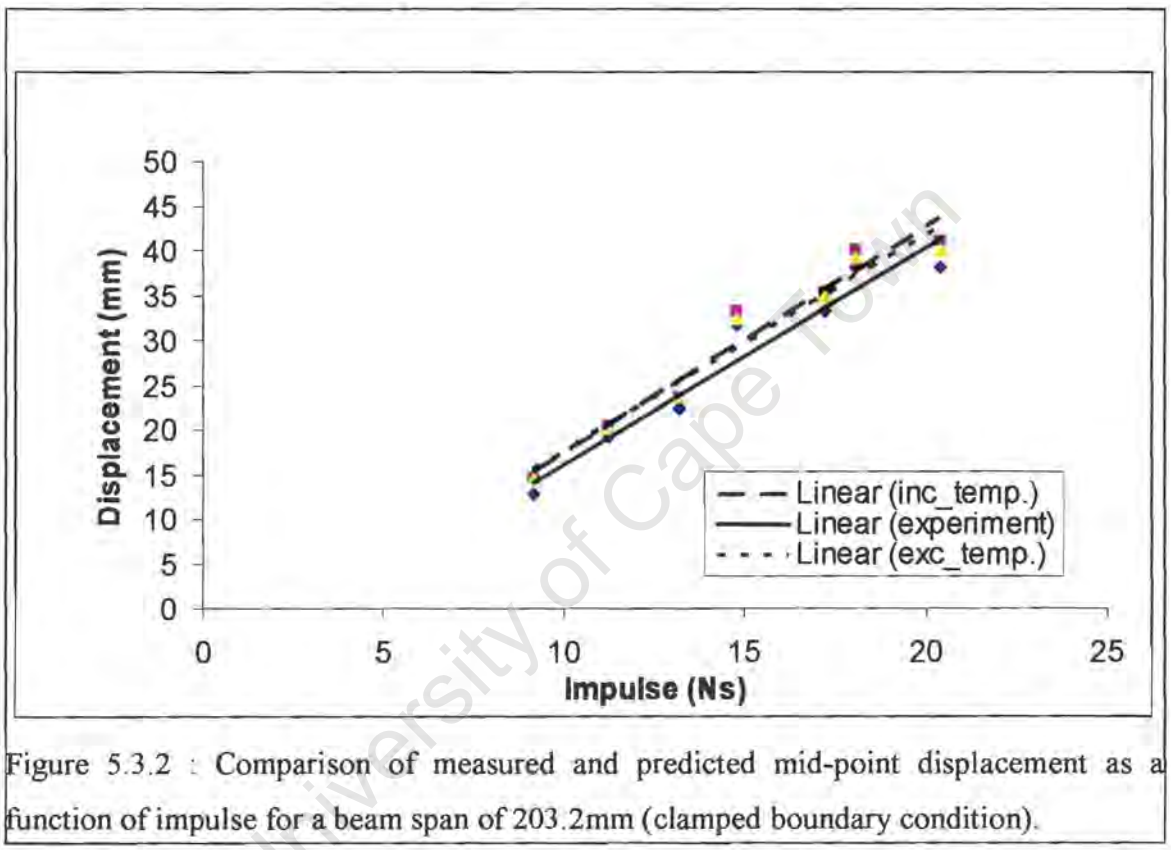

Figure 5.3.2 : Comparison of measured and predicted mid-point displacement as a function of impulse for a beam span of 203.2mm (clamped boundary condition).

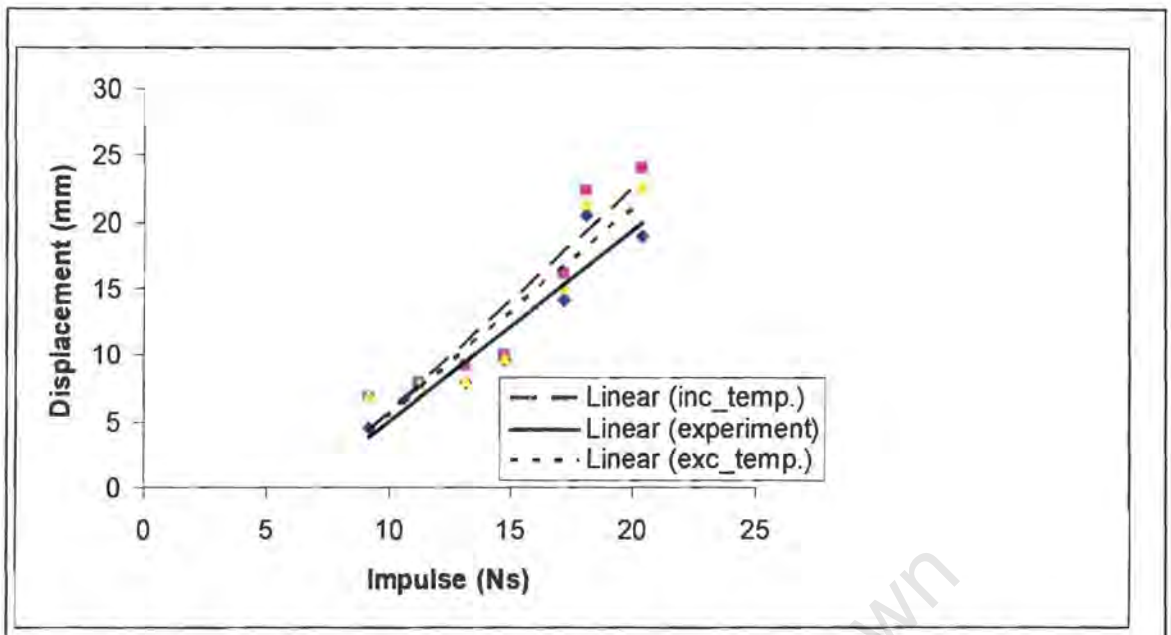

Figure 5.3.3 : Comparison of measured and predicted mid-point displacement as a function of impulse for a beam span of 101.6mm (clamped boundary condition).

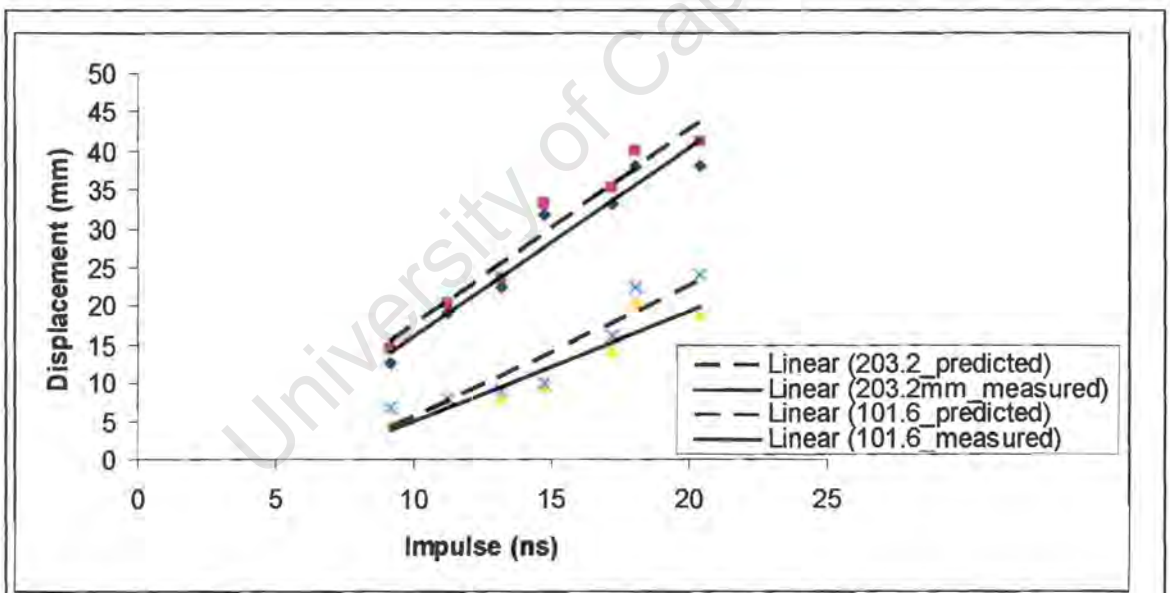

Figure 5.3.4 : A comparison of mid-point displacement for beam spans of 203.2mm and 101.6mm as a function of impulse.

From figures 5.3.2, 5.3.3, and 5.3.4, it is observed that the length of the beam influences the final mid-point displacement as observed in the experiments by Menkes and Opat [3]. A beam with a longer length (203.2mm) has a higher mid-point displacement compared to one with a shorter length (150mm). It is observed from these figures that the predicted mid-point displacement is higher than the measured mid-point displacement with model including temperature dependent material properties having a slightly higher mid-point displacement compared to a model excluding temperature dependent material properties at higher impulses.

1 Impulse (Ns)	2 Measured Mid-point Displacement (mm)	3 Predicted Mid-point Displacement (mm) Model Including Temperature	4 Difference between Including temperature & measured mid- point displacement (mm) (3-2)	5 Predicted Mid-point Displacement (mm) Model Excluding Temperature	6 Difference between Excluding temperature & measured mid- point displacement (mm) (5-2)	7 Difference in mid-point displacement Between Model Including & Excluding Temperature (mm) (3-5)
Length=203.2mm						
9.16	12.70	13.52	8.82	13.49	0.79	-0.03
11.22	19.05	20.30	1.25	20.10	1.05	-0.20
13.18	22.35	23.65	1.30	23.20	0.85	-0.45
14.78	31.75	32.90	1.15	32.40	0.65	-0.50
17.19	33.27	34.90	1.63	32.90	-0.37	-2.00
18.08	38.10	39.10	1.00	34.01	-4.09	-5.09
20.39	38.10	40.10	2.00	36.30	-1.8	-3.80
22.08	36.58	ABAQUS predicts mode II				
Length=101.6mm						
9.16	4.57	5.01	0.44	5.01	0.44	0.00
11.22	7.87	9.10	1.23	9.10	1.23	0.00
13.18	7.87	10.90	3.03	10.01	2.14	0.00
14.78	9.65	12.6	2.95	12.20	2.55	-0.89
17.19	14.22	17.81	3.59	16.40	2.18	-0.40
18.08	20.57	22.90	2.33	22.20	1.63	-1.41
20.39	19.05	23.40	4.40	23.10	4.10	-0.70
22.08	20.57	ABAQUS predicts mode II				

Table 5.3.2: Comparison of predicted mid-point displacement with experiment for models that include and exclude temperature dependent material properties (built-in boundary condition).

From tables 5.3.1 and 5.3.2, it is observed that mid-point displacement is higher for a model with clamped boundary compared to one with built-in boundary. This might be as a result of the "pull-in'' observed in this model.

Impulse (Ns)	Measured Mid-point Displacement (mm)	Predicted Mid-point Displacement (mm) Clamped Model Including Temperature	Predicted Mid-point Displacement (mm) Built-in Model Including Temperature
9.16	12.70	14.53	13.52
11.22	19.05	20.33	20.30
13.18	22.35	23.64	23.65
14.78	31.75	33.10	32.90
17.19	33.27	35.26	34.90
18.08	38.10	39.92	39.10
20.39	38.10	41.11	40.10
22.08	36.58	Mode II	Mode II

Table 5.3.3: Comparison of predicted mid-point displacement for a beam span of 203.2mm with experiment for models that include temperature dependent material properties (clamped and built-in boundary).

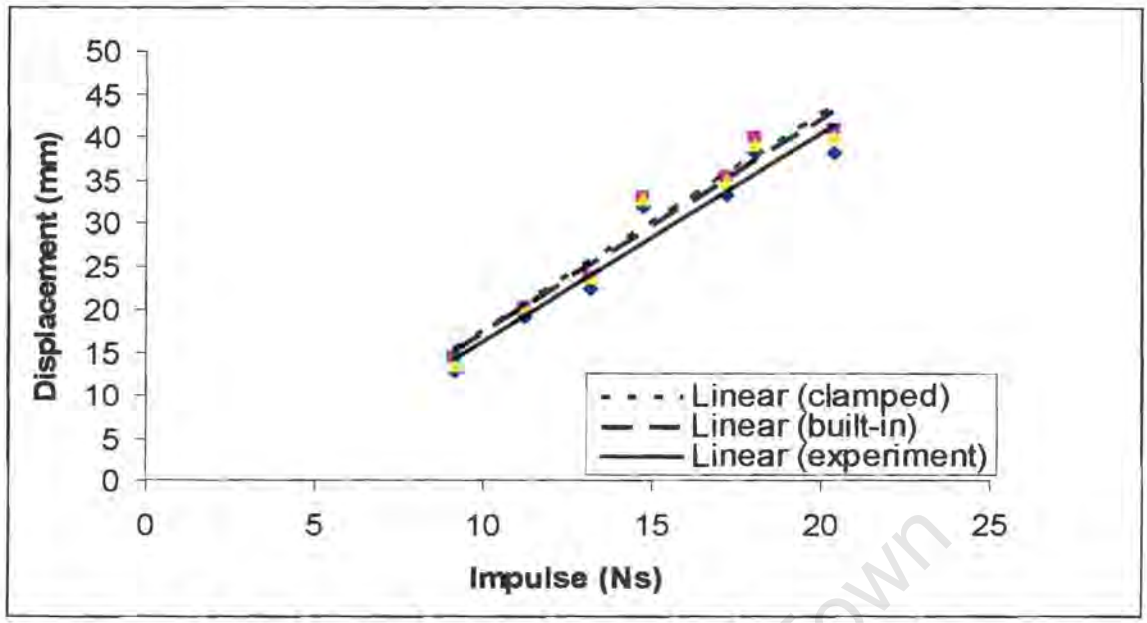

Figure 5.3.5 : A plot of mid-point displacement against impulse for a beam span of 203.2mm with clamped and built-in boundary conditions (models including temperature).

From figure 5.3.5, it is observed that a model with clamped boundary has a higher mid-point displacement compared to one with built-in boundary. Beam span of 101.6mm showed same bahaviour and thus was not included here.

Beams' response to an uniform explosive blast load for clamped and built-in models are shown in figures 5.3.6 and 5.3.7 respectively. The models show the response of the beam at time 0.005 μ s (clamped beams) and 0.0 μ s (built-in beams) to 800 μ s.

t=0.005 μ s.

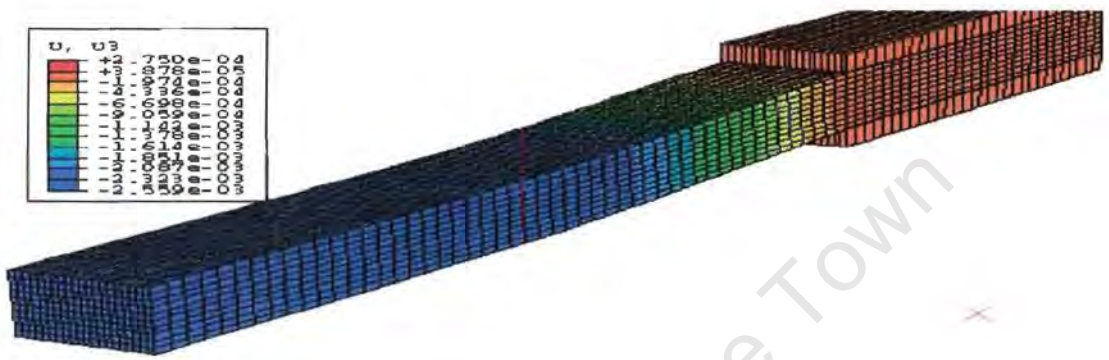

t=30 μ

t=800 μ s.

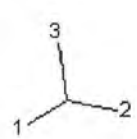

Figure 5.3.6 : Response of a clamped rectangular beam span of 203.2mm at an impulse of 9.16Ns showing displacement in the -3-direction.

Figure 5.3.7 : Response of a built-in rectangular beam span of 203.2mm at an impulse of 9.16Ns showing displacement in the -3-direction.

Impulse (Ns)	Temperature Model With Clamped Boundary (^{o}C)	Temperature Model With built-in Boundary (^{o}C)
9.16	69	71
11.22	74	74
13.18	91	102
14.78	97	111
17.19	118	123
18.08	153	162
20.39	231	238
22.08	317	326

Table 5.3.4 : Temperature variation at the boundary with impulse for models with clamped and built-in boundaries.

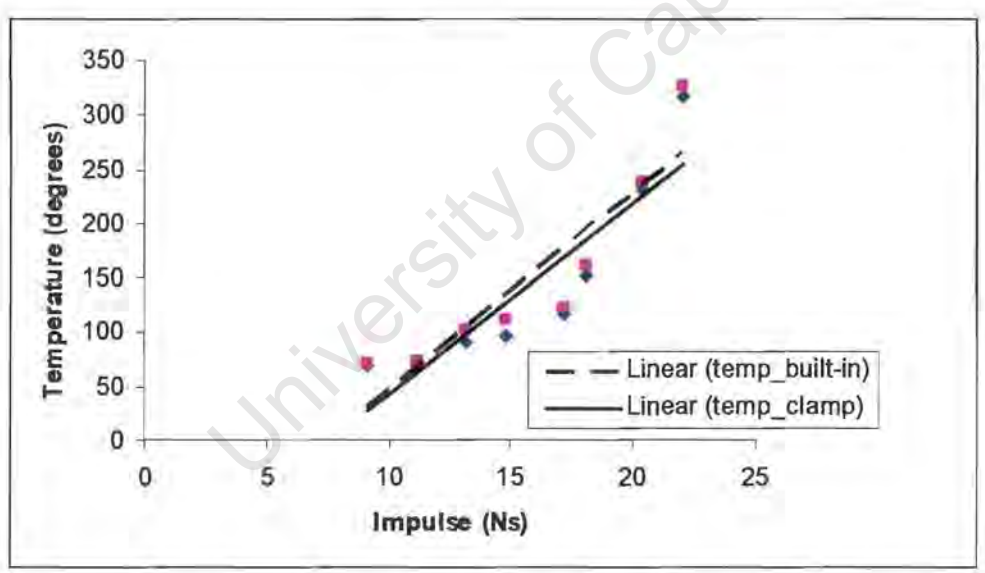

Figure 5.3.8 : A plot of highest temperature at the boundary against impulse for beam span of 203.2mm clamped and built-in at the boundary.

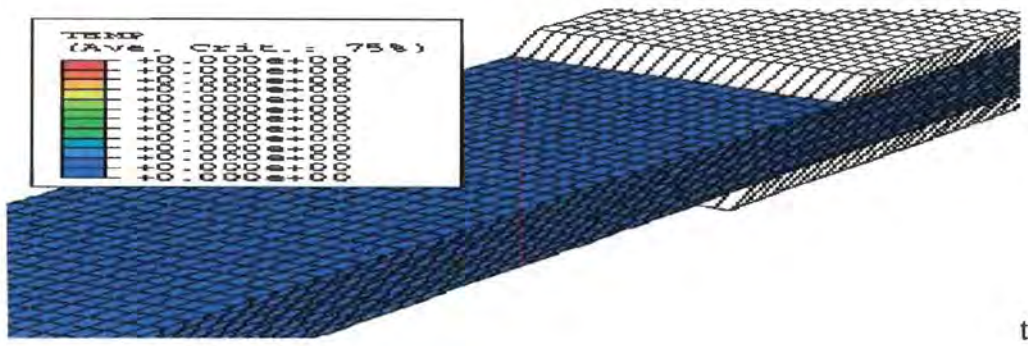

t=0.005 μ s

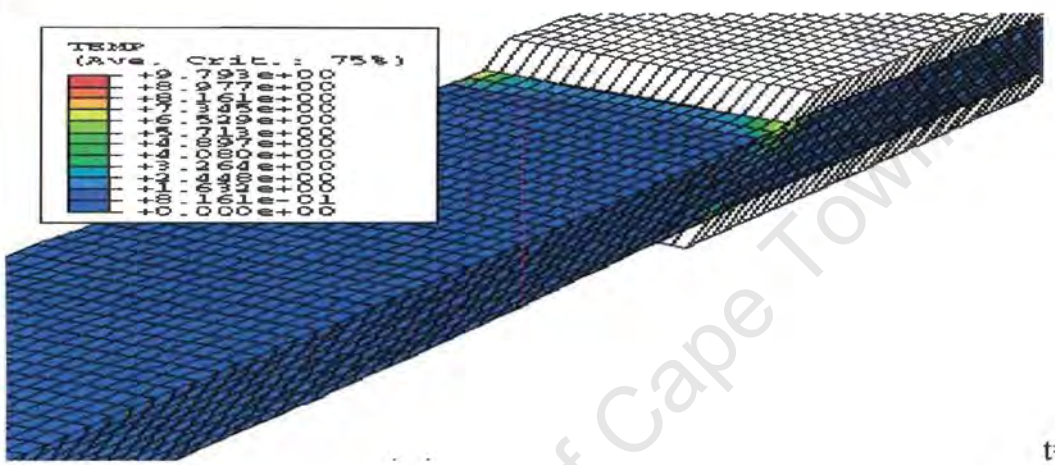

t=30 μ s.

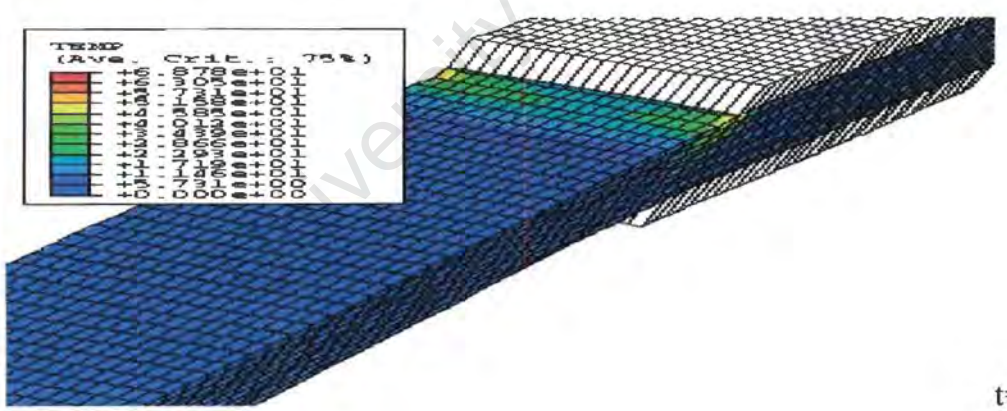

t=800 μ s

Figure 5.3.9 : Variation of temperature at the boundary with time for an impulse of 9.16Ns (clamped boundary) for beam span of 203.2mm.

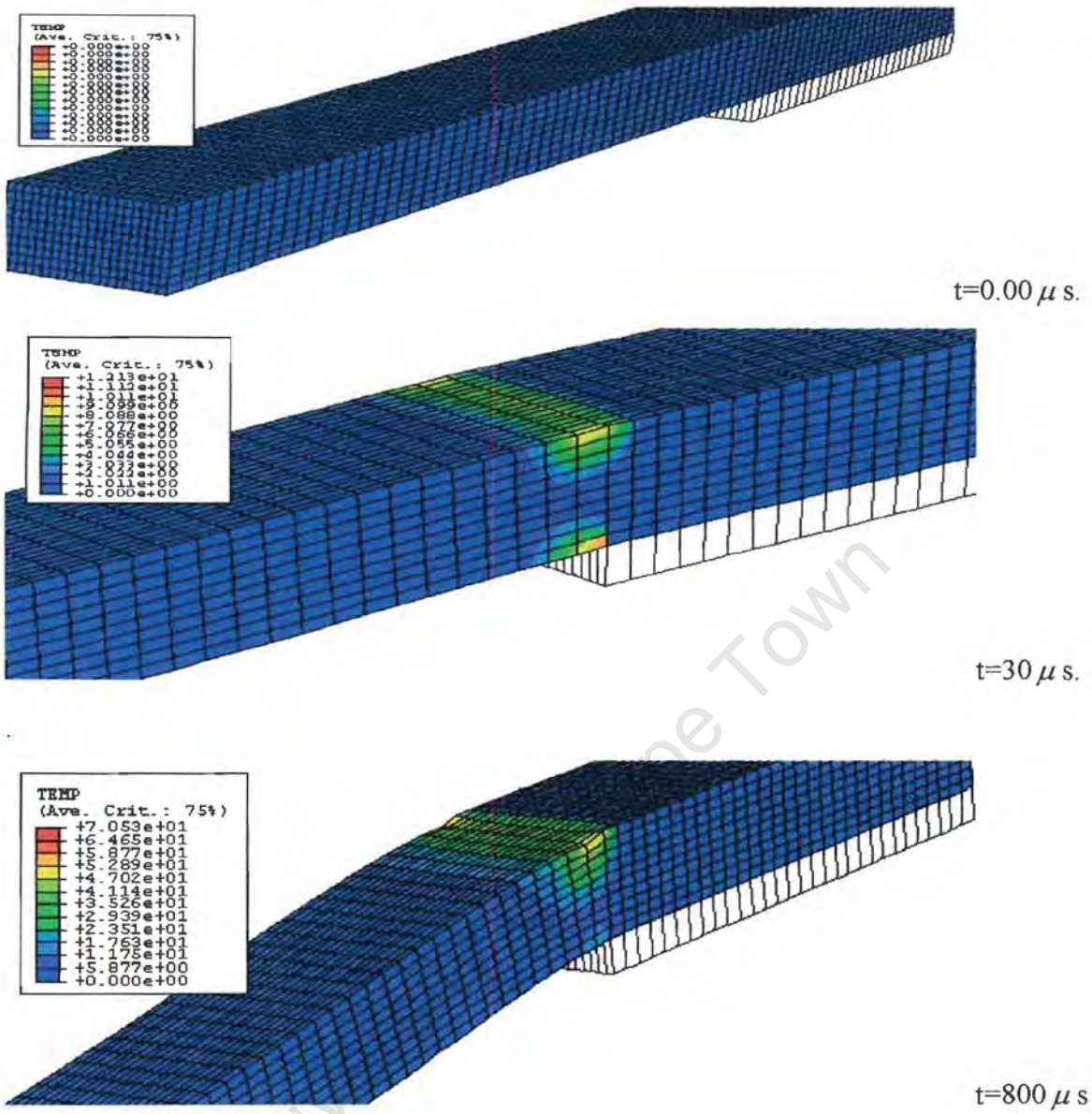

Figure 5.3.10 : Variation of temperature at the boundary with time for an impulse of 9.16Ns (built-in boundary) for beam span of 203.2mm.

From figures 5.3.9 and 5.3.10, it is observed that high temperatures are recorded at the boundary for both clamped and built-in models with built-in model having a slightly higher temperature than clamped model.

5.3.2 Tearing mode response

The response of aluminium alloy beams to blast load depends greatly upon the temperature and to a lesser extend the strain rate at which the deformation is taking place. Experimental evidence has shown three distinct modes of failure of aluminium beams as reported by Menkes and Opat [3] occurring in blast loading conditions. Mode I failure has been discussed in section 5.3.1. The onset of mode II failure in rectangular beams is defined by the first sign of tearing occurring at the boundary. Thereafter all the tearing behaviour is described as mode II until the mode III failure where the energy of the blast is sufficient enough to cause shearing around the entire boundary of the beam before any significant displacement has taken place in the remainder of the beam. The result of such a failure mode is an almost flat beam with width and length close to that of the loaded beam. Elements in the beam are considered to be torn when a temperature of $300^{\circ}C$ and logarithmic strain of 70% is reached.

5.3.3 Beam response

Figures 5.3.11 and 5.3.12 show the response of clamped and built-in rectangular beams of span 203.2mm which were completely torn at the boundary (mode II). Beam spans of 101.6mm were examined and a similar behaviour was observed, indicating that beam length has no effect on mode II failure. This was also observed in the experiments be Menkes and Opat [3].

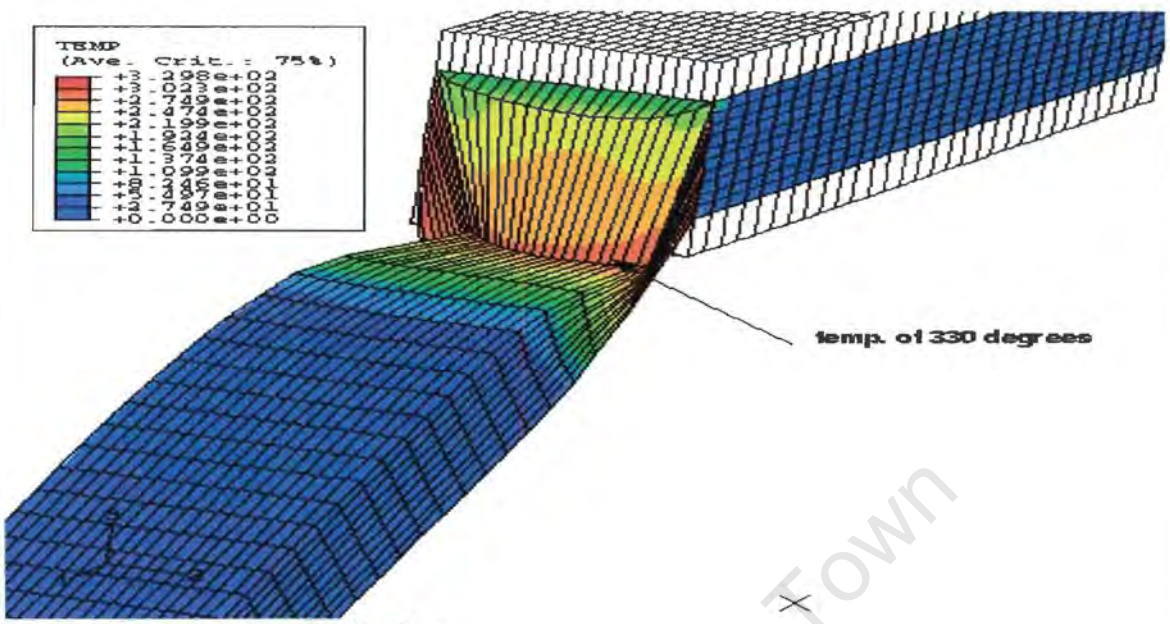

Predicted temperature distribution.

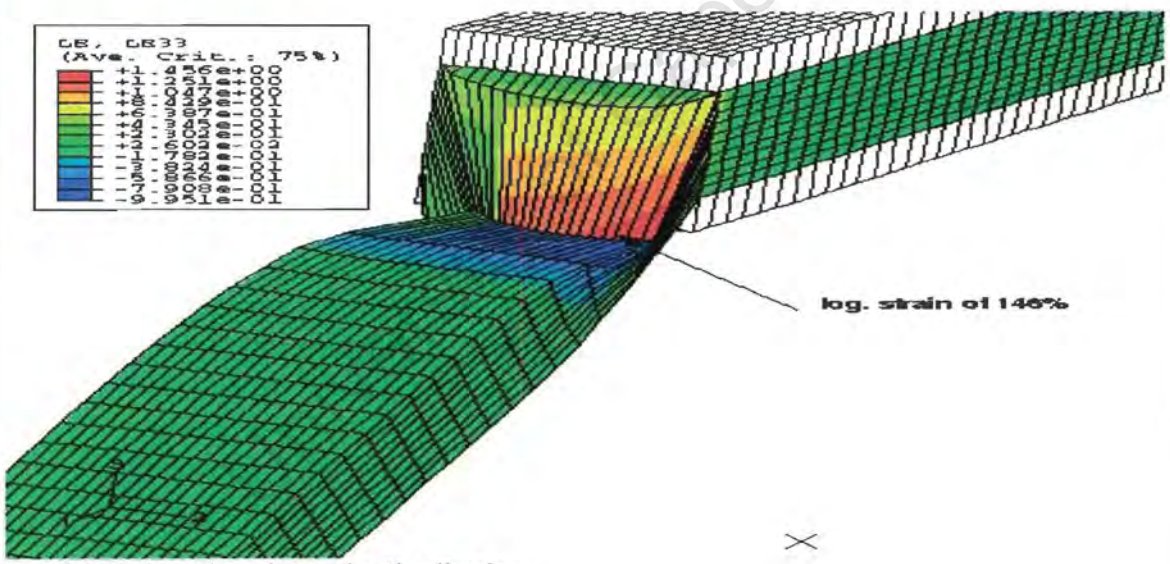

Predicted logarithmic strain distribution.

Figure 5.3.11 : Predicted mode II response at an impulse of 23.14Ns at time, t= 97 μs for a beam clamped at the boundary.

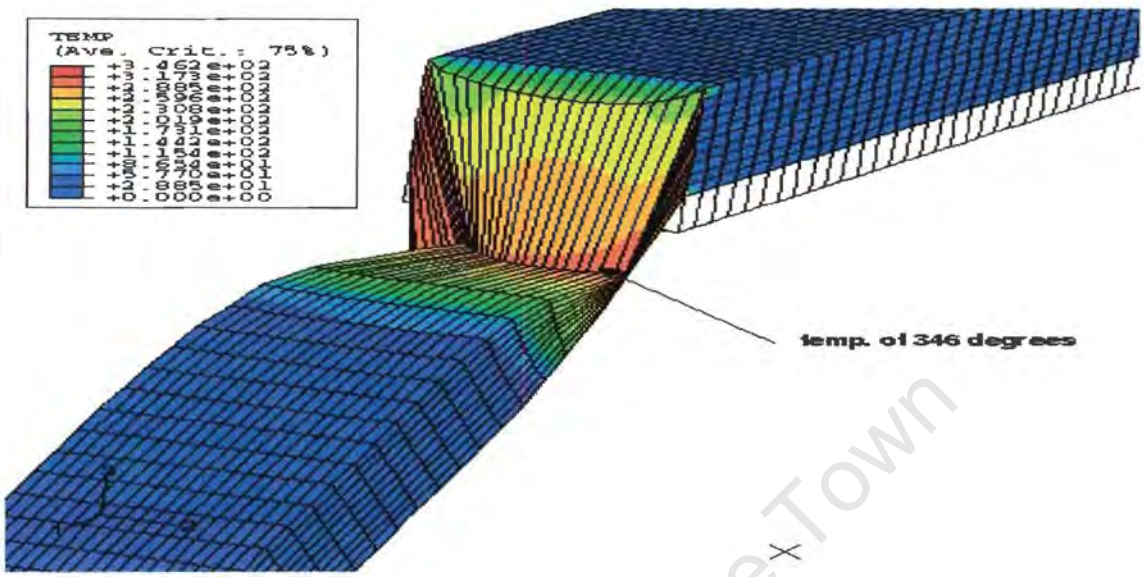

Predicted temperature distribution.

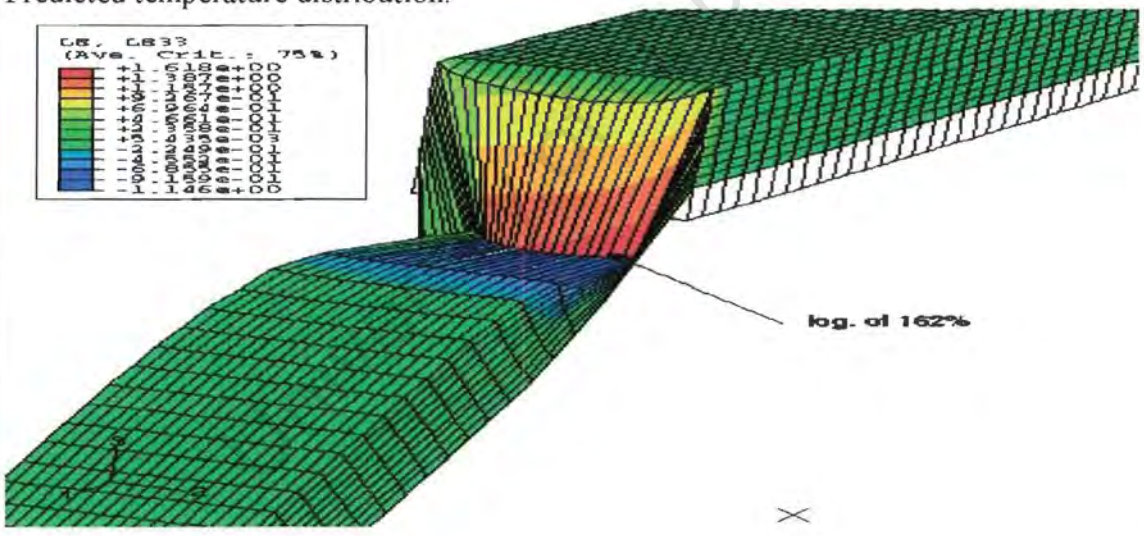

Predicted logarithmic distribution.

Figure 5.3.12 : Predicted mode II response at an impulse of 23.14Ns at time, t= 97 μs for a beam built-in at the boundary.

A temperature of $330^{\circ}C$ and logarithmic strain of 146% through the beam thickness (figure 5.3.11), $346^{\circ}C$ and logarithmic strains of 162% (figure 5.3.12) indicates that tearing has occurred in the models. From figures 5.3.11 and 5.3.12, it is observed that mode II has occurred in both models at a time of $97\,\mu s$.

Figures 5.3.13 and 5.3.14 show failure mode III for clamped and built-in rectangular beams of span 203.2mm.

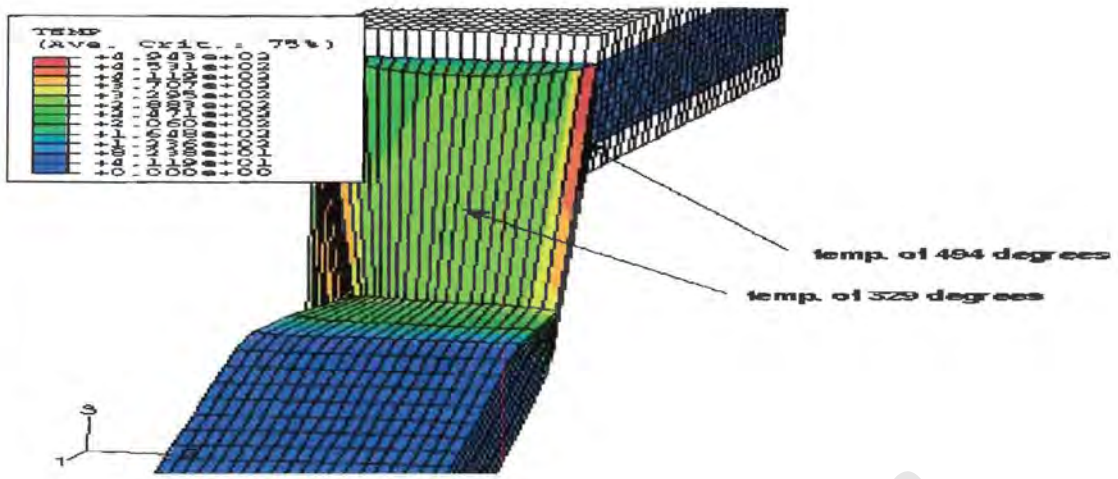

Predicted temperature distribution

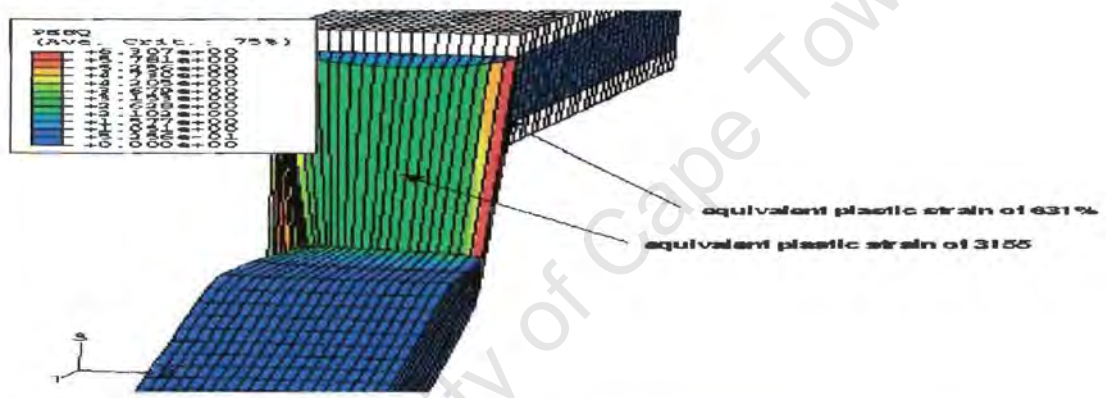

Predicted Equivalent plastic strain distribution

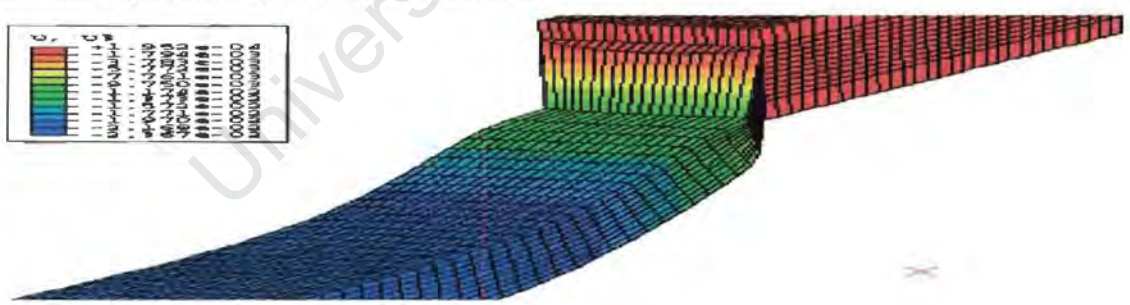

Predicted Mid-point displacement

Figure 5.3.13 : Predicted mode III response at an impulse of 33.54Ns for a rectangular beam clamped at the boundary at time 48 μs .

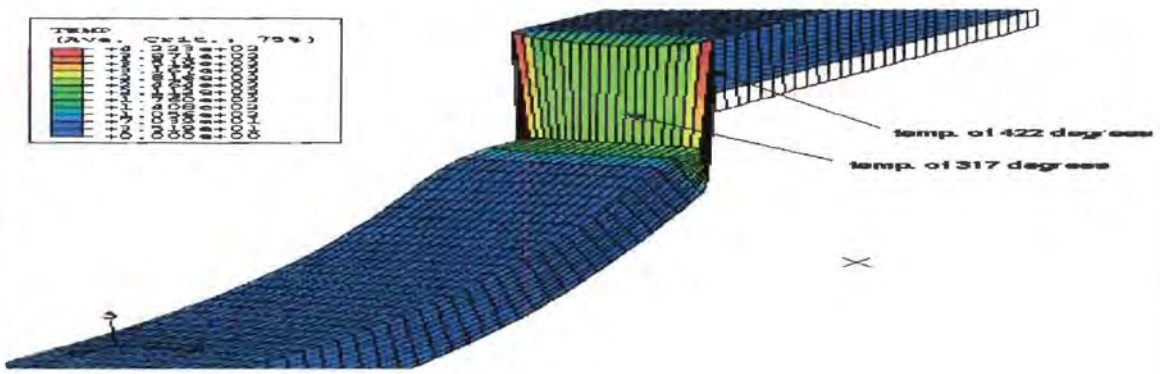

Predicted temperature distribution

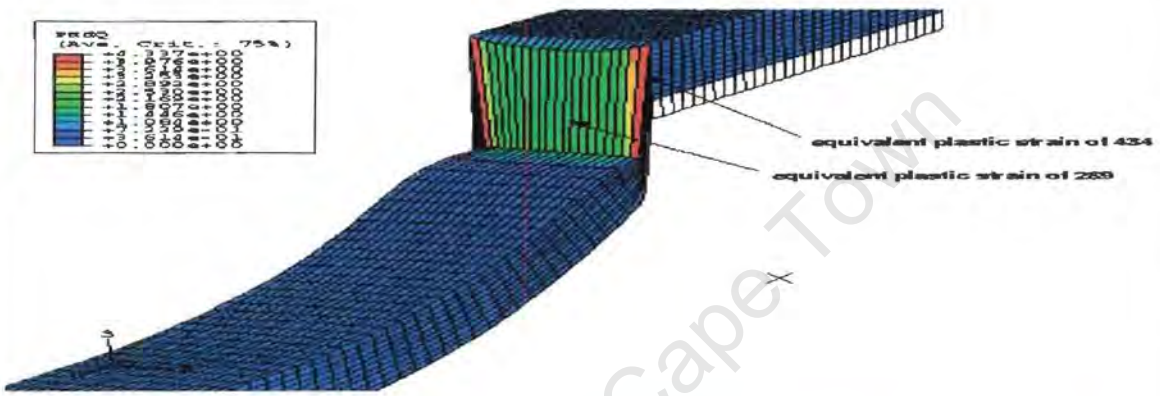

Equivalent plastic strain distribution

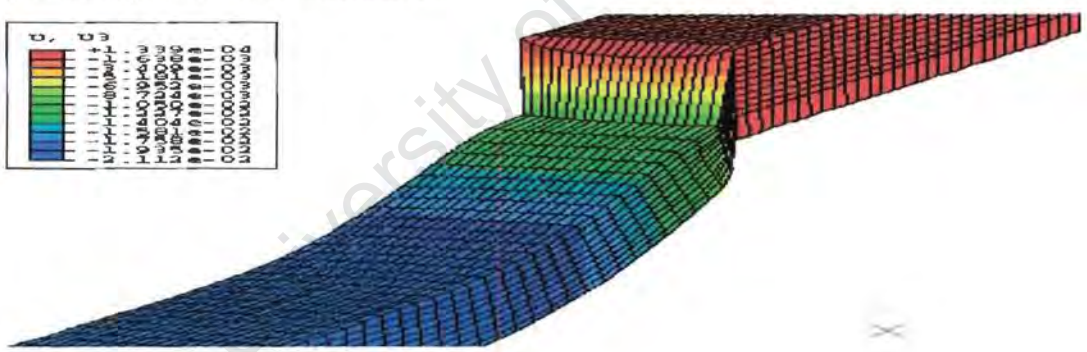

Predicted Mid-point displacement

Figure 5.3.14 : Predicted mode III response at an impulse of 33.54Ns for a rectangular beam built-in at the boundary at time 34 μs .

Figures 5.3.13 and 5.3.14 show the predicted mode III response of clamped and fully built-in rectangular beams respectively. A temperature of $494^{0}C$ and equivalent plastic strain of 631% (figure 5.3.13) indicates that shearing has taken place in the models. A mid-point displacement of 23.67mm is also recorded but no experimental data was available for comparison. A temperature of $422^{0}C$ and equivalent plastic strain of 434% was observed in built-in beams which also indicates shearing in the model (figure 5.3.14). A mid-point displacement of 21.12mm was recorded with no experimental data to compare. It is observed that shearing occurs early in a model clamped at the boundary (figure 5.3.13) compared to a model clamped at the boundary (figure 5.3.14)

5.4 T-beams

The simulation results presented in this section have a uniform mesh size of 50x50x10 and 70x50x10 elements in beam spans of 200mm and 150mm respectively resulting in mesh densities of approximately 1.5x0.21x1.12mm and 1.43x0.21x1.12 respectively. Beam spans of 150mm and 200mm having a flange width of 10.5mm, nominal total height of 11.2mm and flange and web thicknesses of 3.2mm were considered in this section. Only mode I was investigated on T-beams as there was no experimental data available for modes II and III failure.

5.4.1 Mode I Failure

The analysis was carried out for a range of impulse from 1.132Ns to 2.184Ns. The investigation considered material properties that include and exclude temperature dependency and boundary fixation of the T-beams. The mid-point displacement time history for T-beams was similar to that of rectangular beams and was not included in this section. The analysis was allowed to run for 850 μs.

Tables 5.4.1 and 5.4.2 shows the results of a comparison of the mid-point displacement of clamped and built-in T-beams respectively for models that include and exclude temperature dependent material properties.

1 Impulse (Ns)	2 Measured Mid-point Displacement (mm)	3 Predicted Mid-point Displacement (mm) Model Including Temperature	4 Difference between Including temperature & measured mid-point displacement (mm) (3-2)	5 Predicted Mid-point Displacement (mm) Model Excluding Temperature	6 Difference between Excluding temperature & measured mid-point displacement (mm) (5-2)	7 Difference in mid-point displacement Between Model Including & Excluding Temperature (mm) (3-5)
Length of 200mm						
1.132	7.64	8.75	1.1	8.70	1.06	-0.05
1.167	7.66	9.27	1.61	9.13	1.47	-0.14
1.409	10.76	11.62	0.86	11.81	1.05	0.19
1.487	10.2	12.25	2.05	12.30	2.10	0.05
1.527	10.8	12.84	2.04	12.01	1.21	-0.83
1.665	12.1	13.37	1.27	12.94	0.84	-0.43
1.735	14.34	15.10	0.76	15.80	1.46	0.70
1.831	14.72	16.20	1.48	15.04	0.32	-1.16
1.871	16.10	16.77	0.67	16.13	0.03	-0.64
2.024	16.50	17.83	1.33	16.91	0.41	-0.92
2.07	15.78	19.01	3.23	17.08	1.30	-1.93
2.073	17.72	25.16	7.44	18.42	0.70	-6.74
Length of 150mm						
1.002	7.66	8.04	0.38	8.14	0.48	0.10
1.116	9.36	9.14	-0.22	9.23	-0.13	0.09
1.279	10.52	11.02	0.50	11.00	0.48	-0.02
1.306	9.66	12.41	2.75	12.06	2.40	-0.35
1.395	9.30	12.92	3.62	12.26	2.96	-0.66
1.576	11.68	13.42	1.74	12.11	0.43	-1.31
1.745	12.72	14.11	1.39	13.60	0.88	-0.51
1.867	14.10	14.96	0.86	13.95	-0.15	-1.01
1.928	13.70	15.03	1.33	14.30	0.60	-0.51
1.966	13.60	17.47	3.89	14.90	1.30	-0.73
2.070	15.72	22.91	7.19	18.21	2.49	-4.70
2.184	15.00	23.67	8.67	18.90	3.90	-4.77

Table 5.4.1 : Comparison of predicted mid-point displacement with experiment for models that include and exclude temperature dependent material properties (clamped boundary condition).

From table 5.4.1, the difference between measured and predicted mid-point displacement is less than one beam thickness for both models including and excluding temperature dependent material properties. This might be an indication that temperature has less influence on failure mode I for T-beams.

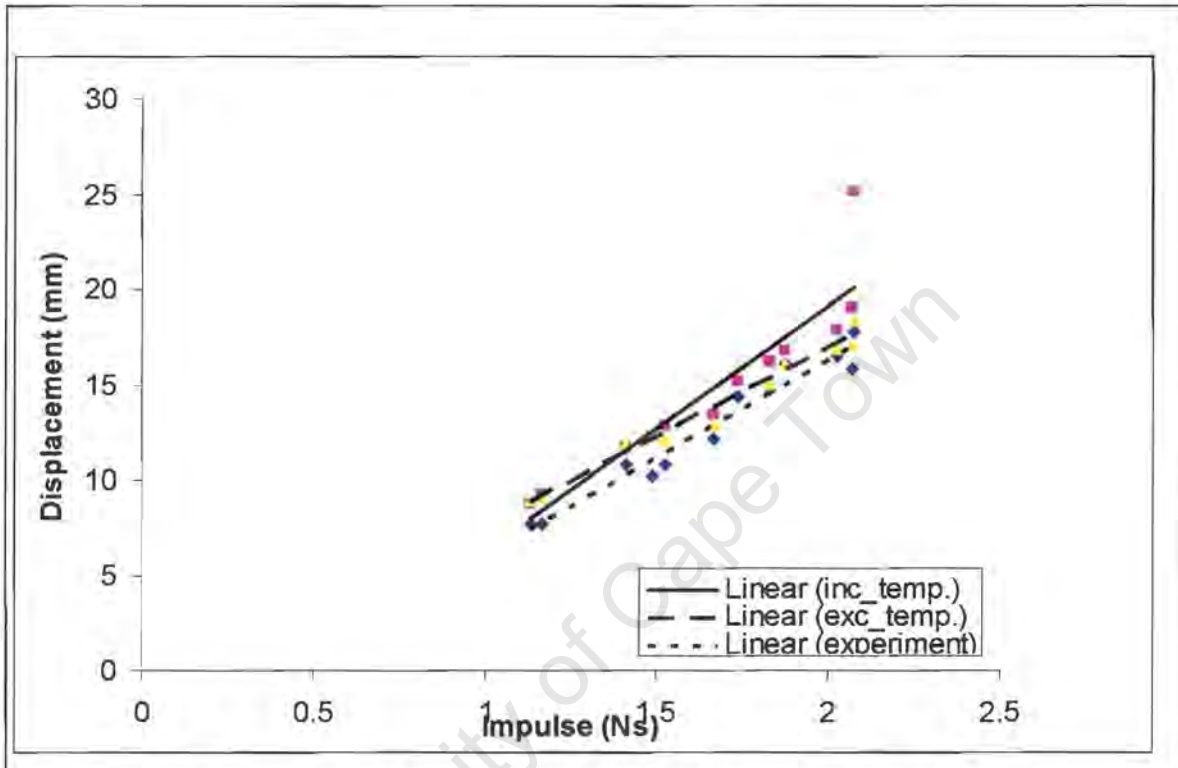

Figure 5.4.1 : Comparison of measured and predicted mid-point displacement as a function of impulse for a beam span of 200mm (clamped boundary condition).

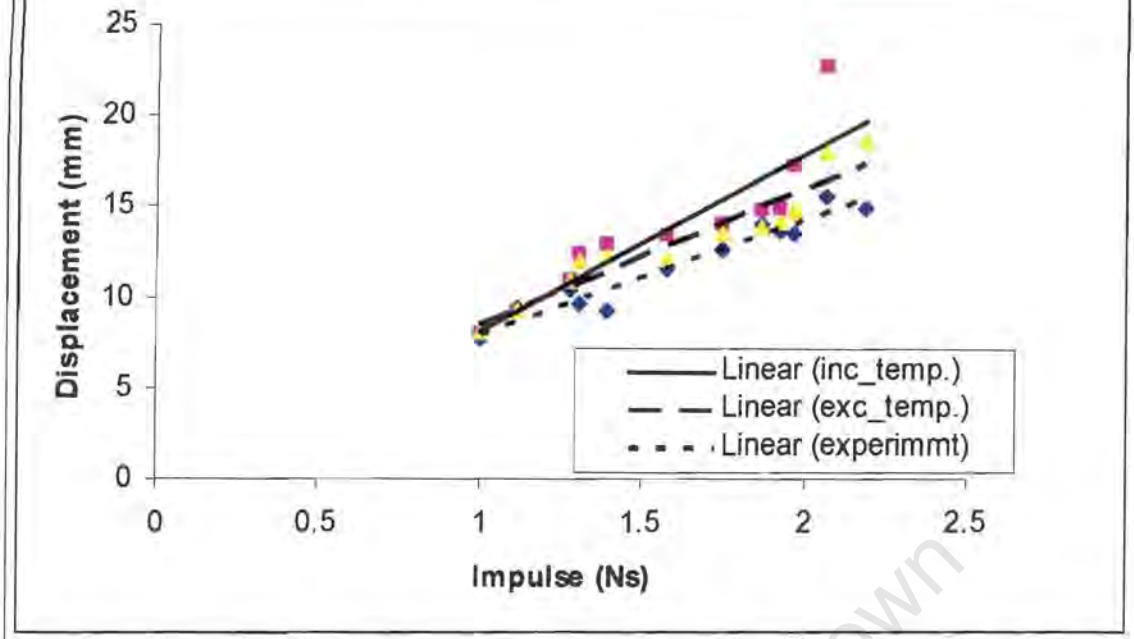

Figure 5.4.2 : Comparison of measured and predicted mid-point displacement as a function of impulse for a beam span of 150mm (clamped boundary condition).

It is observed from figures 5.4.1 and 5.4.2 that the predicted mid-point displacement for both beam lengths of 200mm and 150mm are higher than the measured mid-point displacement.

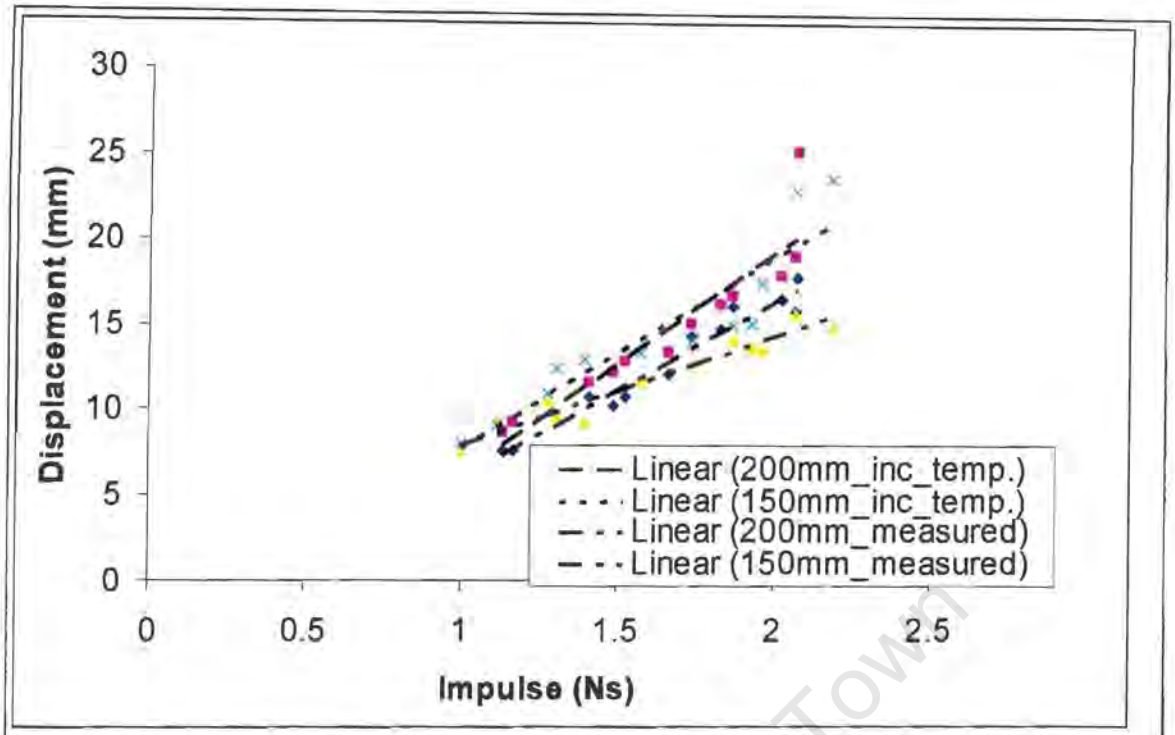

Figure 5.4.3 : A comparison of mid-point displacement for beam spans of 200mm and 150mm as a function of impulse.

It is observed from figure 5.4.3 that beam span of 200mm has a higher mid-point displacement compared to beam span of 150mm. This shows that length of T-beams has an influence on mode I failure as observed in section 4.3.1 and reported by Menkes and Opat [3].

1 Impulse (Ns)	2 Measured Mid-point Displacement (mm)	3 Predicted Mid-point Displacement (mm) Model Including Temperature	4 Difference between Including temperature & measured mid-point displacement (3-2)	5 Predicted Mid-point Displacement (mm) Model Excluding Temperature	6 Difference between Excluding temperature & measured mid-point displacement (5-2)	7 Difference in mid-point displacement Between Model Including & Excluding Temperature (mm) (3-5)
Length of 200mm						
1.132	7.64	8.71	0.28	7.92	0.28	-0.07
1.167	7.66	9.27	0.47	8.13	0.47	-1.14
1.409	10.76	11.2	1.05	11.81	1.05	6.10
1.487	10.2	12.2	2.10	12.30	2.10	1.00
1.527	10.8	12.04	1.21	12.01	1.21	-3.00
1.527	12.1	12.37	0.84	12.94	0.84	5.70
1.665	14.34	15.09	0.46	14.80	0.46	-2.90
1.735	14.72	15.20	0.12	14.84	0.12	-3.60
1.831	16.10	15.77	0.80	16.90	0.80	1.13
1.871	16.50	16.13	0.41	16.91	0.41	7.80
2.024	15.78	17.01	1.30	17.08	1.30	7.00
2.07	17.72	21.19	0.70	18.42	0.70	-2.77
Length of 150mm						
1.002	7.66	8.13	0.47	8.14	0.48	0.01
1.116	9.36	8.91	-0.45	9.10	-0.26	0.19
1.279	10.52	10.46	-0.06	10.30	-0.22	-0.16
1.306	9.66	12.10	2.44	12.00	2.34	-0.10
1.395	9.30	12.92	3.62	12.50	3.20	-0.42
1.576	11.68	13.46	1.78	12.96	1.28	-0.50
1.745	12.72	13.81	1.09	13.00	0.28	-0.81
1.867	14.10	14.06	-0.04	14.10	0.00	0.04
1.928	13.70	14.55	0.85	14.60	0.90	0.05
1.966	13.60	16.17	2.57	15.21	1.61	-0.96
2.070	15.72	19.91	4.19	17.40	1.68	-2.51
2.184	15.00	21.97	6.97	18.01	3.01	-3.96

Table 5.4.2: Comparison of predicted mid-point displacement with experiment for models that include and exclude temperature dependent material properties (built-in boundary condition).

From tables 5.4.1 and 5.4.2, it is observed that mid-point displacement is higher for a model with clamped boundary compared to one with built-in boundary. This might be as a result of the "pull-in'' observed in a model clamped at the boundary.

From figures 5.4.4 and 5.4.5 it is observed that predicted mid-point displacement is higher than measured mid-point displacement.

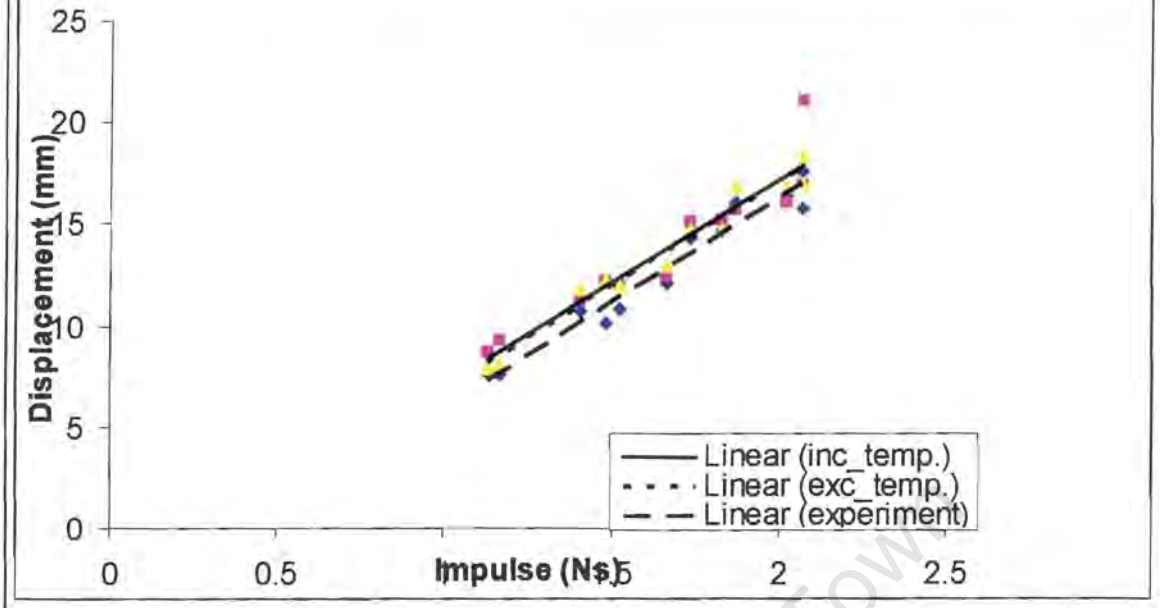

Figure 5.4.4 : Comparison of measured and predicted mid-point displacement as a function of impulse for a beam span of 200mm (built-in boundary condition).

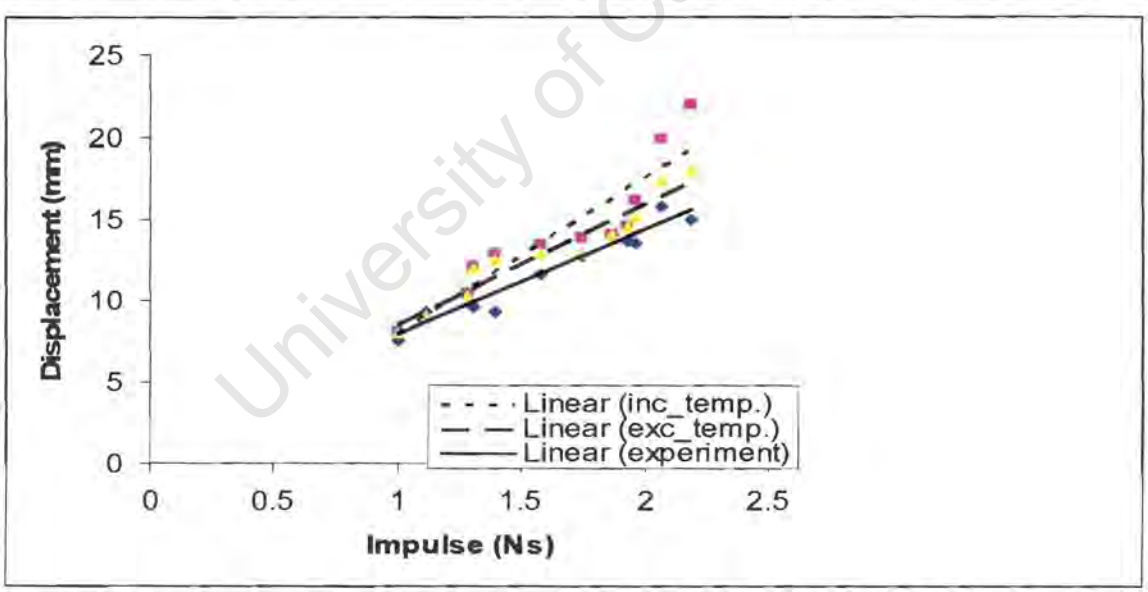

Figure 5.4.5 : Comparison of measured and predicted mid-point displacement as a function of impulse for a beam span of 150mm (built-in boundary condition).

1 Impulse (Ns)	2 Measured Mid-point Displacement (mm)	3 Predicted Mid-point Displacement (mm) Clamped Model Including Temperature	5 Predicted Mid-point Displacement (mm) Built-in Model Including Temperature
200mm			
1.132	7.64	8.75	8.71
1.167	7.66	9.27	9.27
1.409	10.76	11.62	11.2
1.487	10.2	12.25	12.2
1.527	10.8	12.84	12.04
1.665	12.1	13.37	12.37
1.735	14.34	15.10	15.09
1.831	14.72	16.20	15.20
1.871	16.10	16.77	15.77
2.024	16.50	17.83	16.13
2.07	15.78	19.01	17.01
150mm			
1.002	7.66	8.04	8.14
1.116	9.36	9.14	9.10
1.279	10.52	11.02	10.30
1.306	9.66	12.41	12.00
1.395	9.30	12.92	12.50
1.576	11.68	13.42	12.96
1.745	12.72	14.11	13.00
1.867	14.10	14.96	14.10
1.928	13.70	15.03	14.60
1.966	13.60	17.47	15.21
2.070	15.72	22.91	17.40
2.184	15.00	23.67	18.01

Table 5.4.3: Comparison of predicted mid-point displacement with experiment for models that include temperature dependent material properties (clamped and built-in boundary).

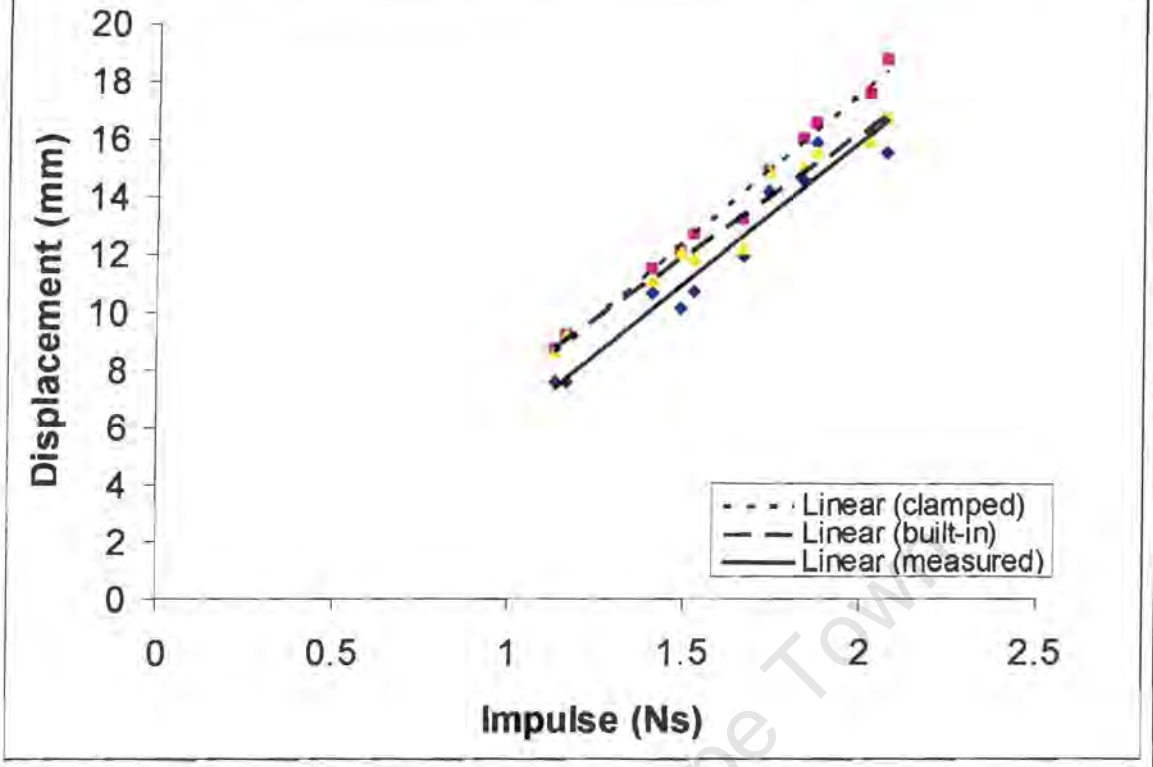

Figure 5.4.6: A plot of mid-point displacement against impulse for a T-beam of span 200mm with clamped and built-in boundary conditions (models including temperature).

From table 5.4.3 and figure 5.4.6 it is observed that a higher mid-point displacement is recorded by a model clamped at the boundary compared to a model built-in at the boundary.

T-beams' response to an uniform explosive blast load for clamped and built-in models are shown in figures 5.4.7 and 5.4.8 respectively. Beam spans of 150mm showed a similar behaviour and are not include here.

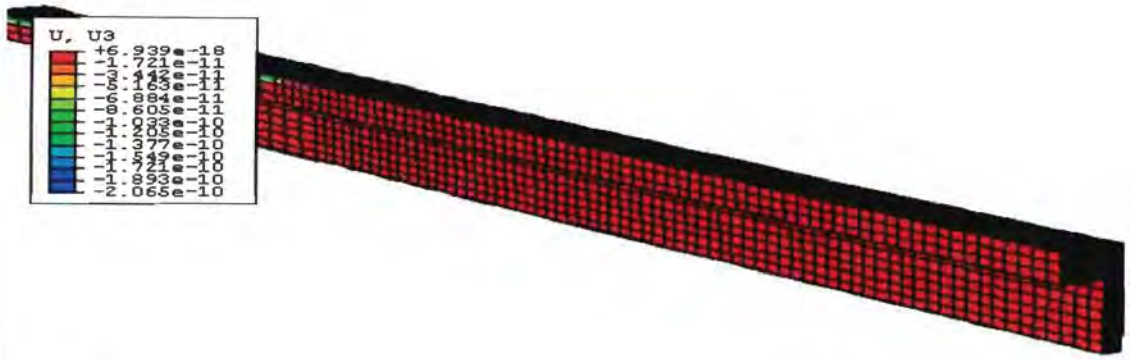

t=0.005 μ s.

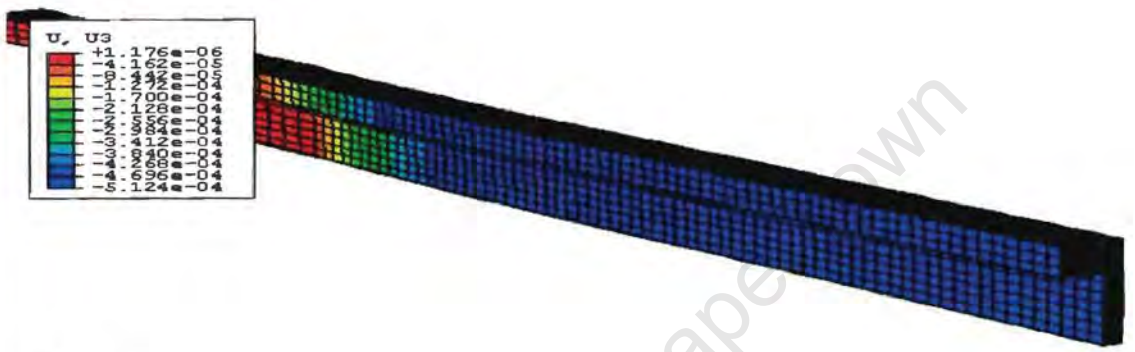

t=15 μ s.

t=800 μ

Figure 5.4.7 : Response of a clamped T-beam (200mm) at an impulse of 1.132Ns showing displacement in the -3-direction.

t=0.00 μ s.

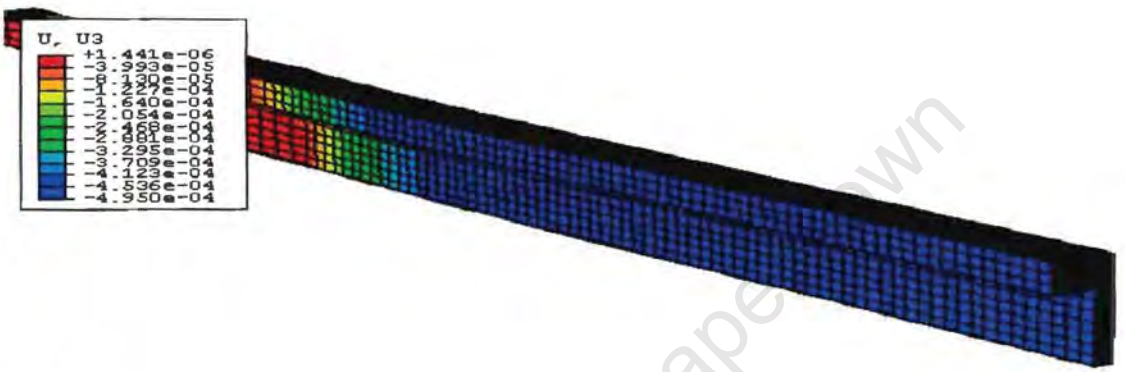

t=15 μ s.

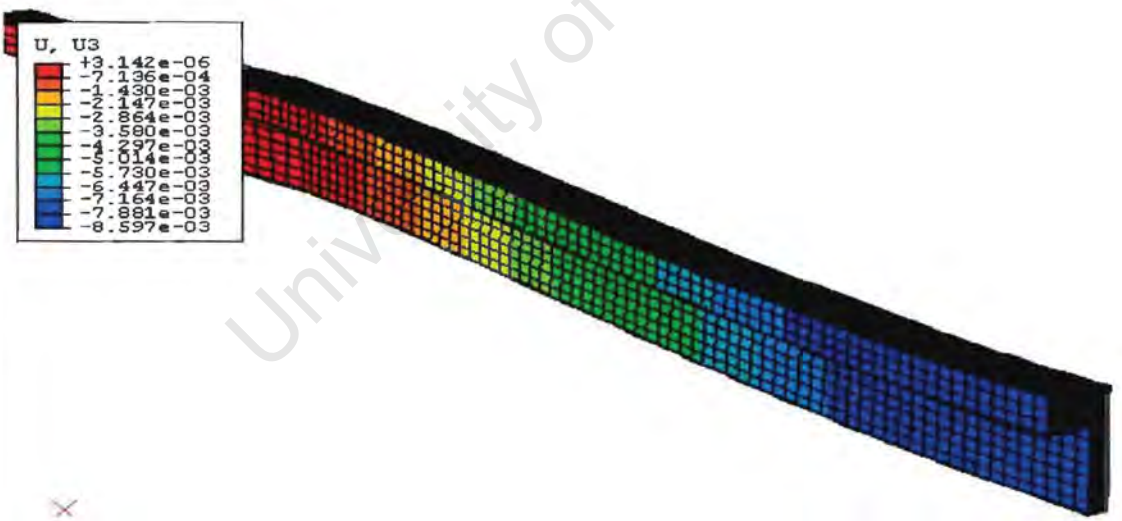

t=800 μ s.

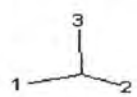

Figure 5.4.8 : Response of a built-in T-beam (200mm) at an impulse of 1.132Ns showing displacement in the -3-direction.

Impulse (Ns)	Temperature Model With Clamped Boundary (^{o}C)	Temperature Model With built-in Boundary (^{o}C)
200mm		
1.132	4	4
1.167	6	6
1.409	6	6
1.487	6	7
1.527	10	10
1.665	13	13
1.735	13	12
1.831	14	13
1.871	14	16
2.024	18	19
2.07	18	19
150mm		
1.002	3	3
1.116	3	4
1.279	5	4
1.306	5	6
1.395	7	9
1.576	10	10
1.745	13	16
1.867	14	16
1.928	17	19
1.966	17	19
2.070	19	19
2.184	21	21

Table 5.4.4 : Temperature variation at the boundary with impulse for models with clamped and built-in boundaries (Beam spans of 150mm and 200mm).

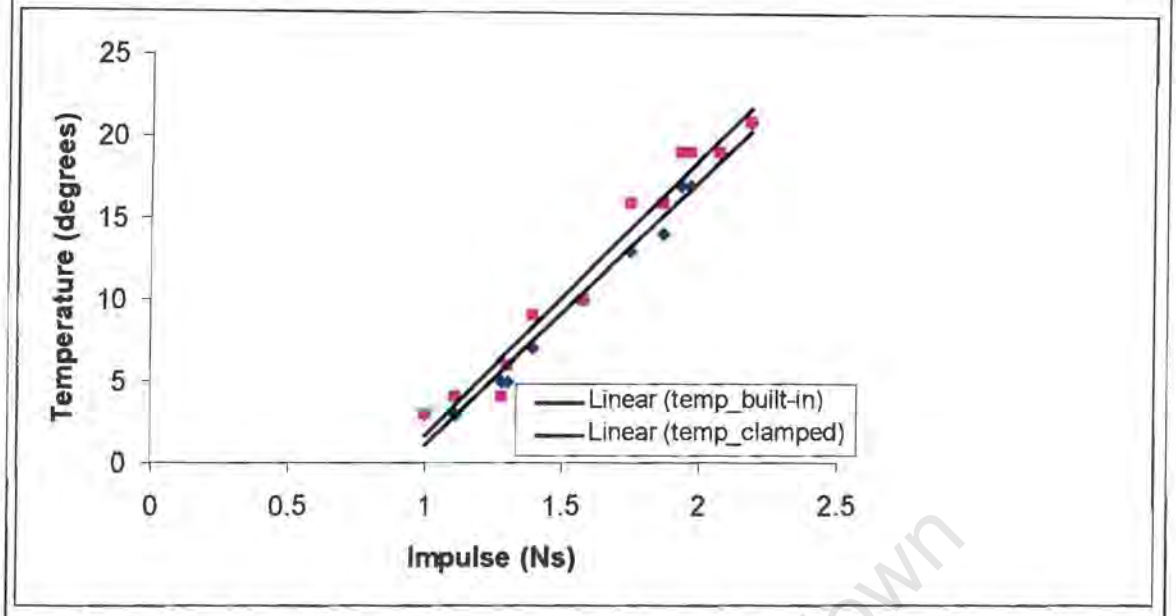

Figure 5.4.9 : A plot of highest temperature at the boundary against impulse for T-beam clamped and built-in at the boundary (beam span of 150mm).

From figures 5.4.10 and 5.4.11, high temperatures are observed at the boundaries in the web of both clamped and built-in beams.

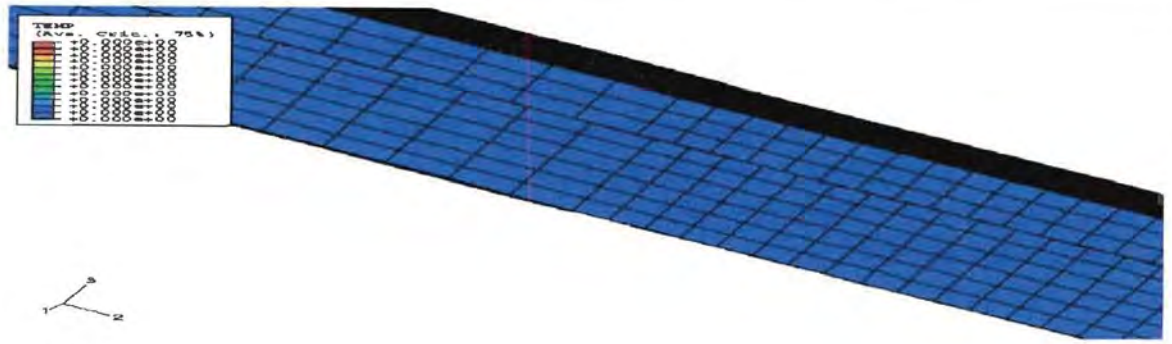

t=0.005 μ s.

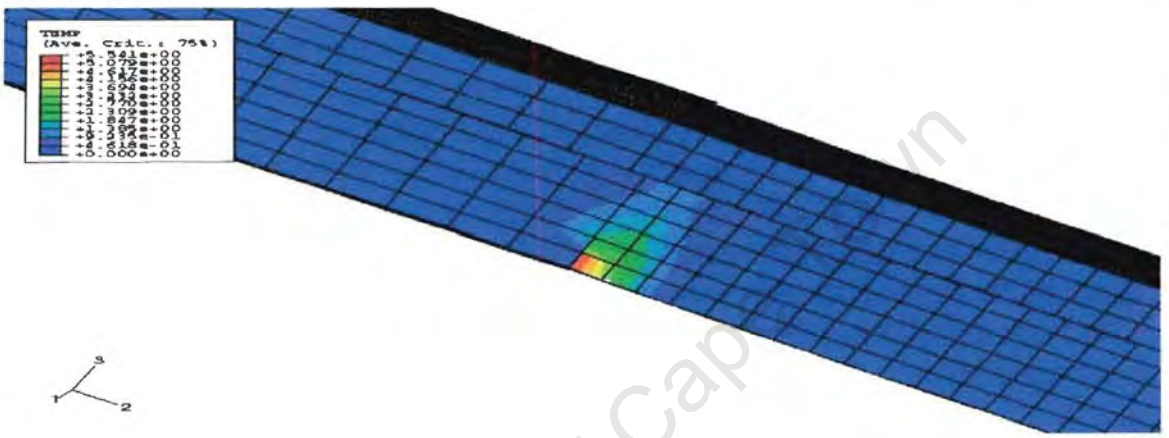

t=15 μ s.

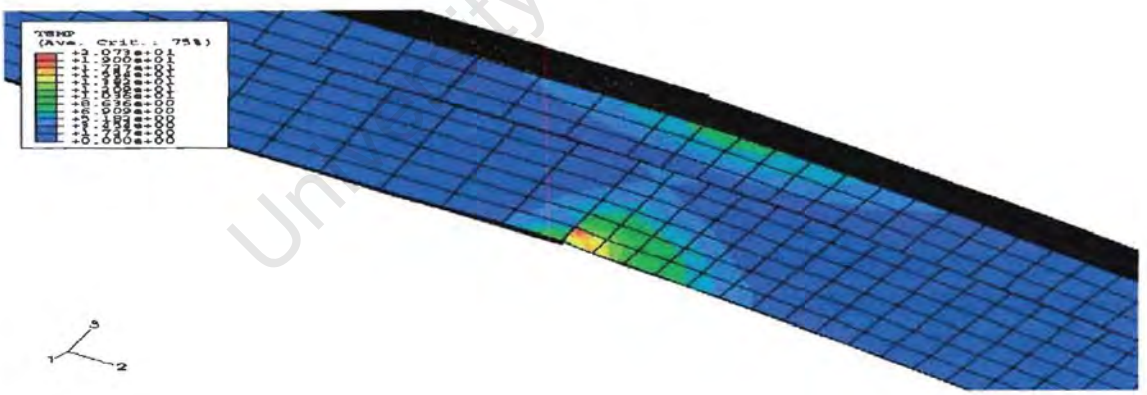

t=800 μ s.

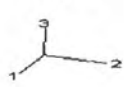

Figure 5.4.10 : Variation of temperature at the boundary with time for an impulse of 2.184Ns (clamped boundary) for a beam span of 150mm.

t=0.00 μ s.

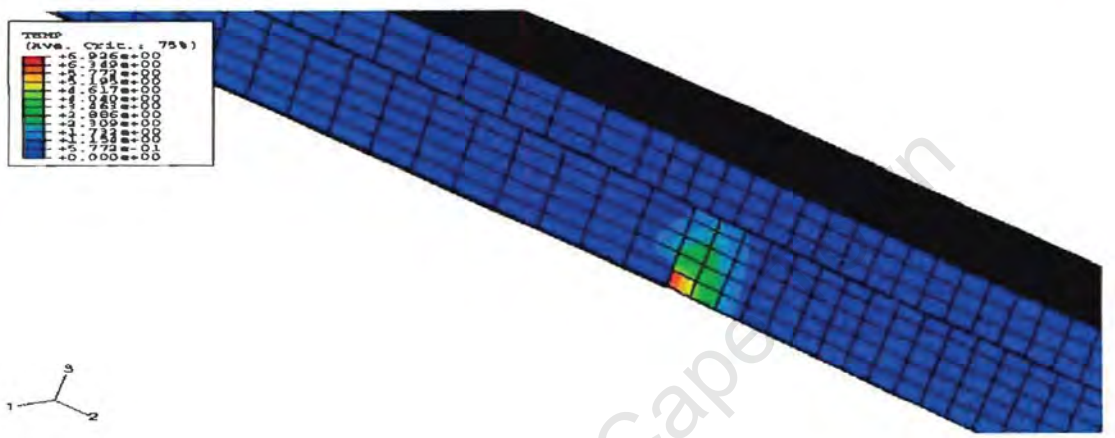

t=15 μ s.

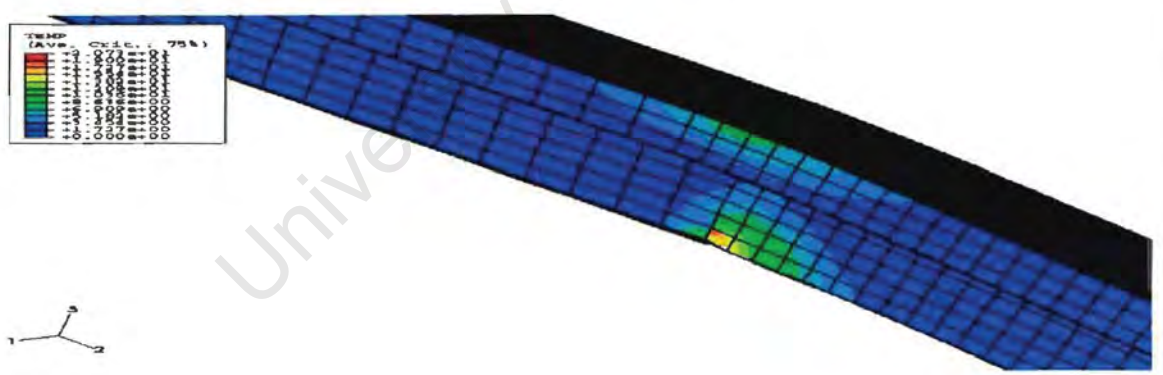

t=800 μ s.

Figure 5.4.11 : Variation of temperature at the boundary with time for an impulse of 2.184Ns (built-in boundary) for a beam span of 150mm.

From figures 5.4.10 and 5.4.11, a maximum temperature of $21\,^{\circ}C$ is observed at the boundaries of both clamped and built-in T-beams indicating thinning in this area. The predictions failed to show the local deformation (the bending and shear distortions of the flanges) and global deformation (the transverse deflections of the beam mid-span) observed in the experiment.

6.0 Conclusions

The deformation and tearing of uniformly blast-loaded circular and square steel plates, aluminium alloy rectangular beams and T-beams were investigated numerically with emphasis laid on the effect of temperature dependent material properties, clamped and built-in boundaries. Finite element models using material properties that include and exclude temperature dependency were applied in the simulations. Based on the findings of this work, the following conclusions may be drawn.

The ABAQUS / Explicit package has proved to be successful in the analysis of circular and square plates, rectangular beams and T-beams exposed to uniform blast loading, which involves highly non-linear material and geometric behaviour. The level of correlation between the predicted and the experimental results is encouraging.

Modes of failure

The results obtained from this investigation show that the plates and rectangular beams exhibited failure modes I, II and III while T-beams were investigated only for mode I failure

Mode I predictions

The analysis for mode I failure was investigated using material properties that included and excluded temperature dependence and boundary fixation. Mode I failure was observed to be well predicted for the various models considered in this study. Mid-point displacement appeared to be dependent on impulse applied to the plates and beams. Mid-point displacement increases with increase in impulse. Comparison with experimental data for mid-point displacement, contour plots of models clamped and built-in at the boundary showed a closed relationship for the range of impulse investigated. Predicted mid-point displacement for both models including and excluding temperature dependent material properties was higher than the measured mid-point displacement for square plates, rectangular beams and T-beams. Predicted mid-point displacement for circular plates was less than measured mid-point displacement. This might be an indication that axisymmetric modelling of the circular plate results in less "pull-in" compared to three dimensional modelling used in square plates, rectangular beams and T-beams. Using material properties that depend on temperature, it was observed that mode II failure was predicted at an impulse lower than the experimental impulse that caused mode II failure. This might be as a result of the weakening of the material properties with increasing temperature. Models clamped at the boundary for both plates and beams predicted a higher mid-point displacement compared to models built-in at the boundary. This might be as a result of the "pull-in" effect observed in clamped plates and beams. The length of rectangular beams and T-beams was observed to influence the mid-point displacement.

Mode II predictions

In the analysis, the prediction for mode II failure is based on a criterion of maximum logarithmic strain in conjunction with a strain rate and temperature dependent effects. At a critical impulse, this failure mode is observed first at the boundary for circular plates and rectangular beams. First sign of mode II failure in square plates is observed at the middle of the side boundaries. Failure mode II* (partial tearing at the boundaries) was observed in square plates and the predicted failure compared favourably with the experimental result. At higher impulses, complete tearing of the boundaries is predicted to occur by means of high strain and temperature values or severely elongated elements caused by the imposition of an unrealistic strain of 200% failure criterion. Simulation results obtain herein compares favourably with experimental data for failure mode II. The predicted critical impulse for failure mode II at the boundary was observed to be dependent on the boundary fixation of the plates and beams.

Mode III predictions

The prediction for mode III failure was based on a criterion of maximum equivalent plastic strain and high temperatures. Shearing was observed to start earlier in plates and beams built-in at the boundary compared to clamped plates and beams. Predicted results compared favourably with experimental results.

7.0 Recommendations

The following recommendations are made based on the results and conclusions of this thesis.

. Further investigations on boundary fixation on plates and beams investigated in this study should be carried out. This might give some insight on how to reduce the penetration of the plates and beams by the rigid bodies used for clamping. Clamped and built-in boundaries with various fillet radii may be considered.

. Experimental investigation should be carried out to determine the strain and equivalent plastic strain at which mode II and III occur. These strains could then be used to validate simulation results.

. Other types of loading conditions such as localised blast loads should be investigated especially on T-beams.

. The finite element models should be further investigated using techniques that implement Jones-Wilkins-Lee (JWL) equation of state to determine the material behaviour of the explosive. This will enable the implementation of a contact to contact boundary interaction between the explosive and the plate / beam as opposed to pressure loading technique used in this study.

- Further work should be carried out on aluminium to properly characterise its material behaviour at high strain and temperature.

8.0 Reference

1. G. N. Nurick and J. B. Martin, **Deformation of thin plates subjected to impulsive loading** – a review. Part I: Theoretical Considerations, International Journal of Impact Engineering, 1989, 8(2), 159-169.
2. G. N. Nurick and J. B. Martin, **Deformation of thin plates subjected to impulsive loading** – a review. Part II: Experimental Studies, International Journal of Impact Engineering, 1989, 8(2), 171-186.
3. S. B. Menkes, and H. J. Opat, **Tearing and shear failure in explosively loaded clamped beams**, Explosion Mechanics, 1973, 13, 480-486.
4. C. Guedes Soares, J. M. Gordo & A. P. Teixeira, **Elasto – Plastic Behavior of Plates Subjected to Heat Loads**, J. Construction Steel Res. 1998, 45(2), 179 – 198.
5. Ji-Lin Yu, **Numerical simulation of impact loaded steel beams and the failure criteria**, International Journal of Solids Structures, 1997, 34(30), 3677-4004.
6. Woei-Shyan Lee, Wu-Chung Sue, Chi-Feng Lin, **The effect of temperature and strain rate on the properties of carbon-fibre-reinforced 7075 aluminium alloy metal-matrix composite**, Composites Science and Technology, 2000, 60, 1975-1983.
7. F. Grimpe, J. Heyer and W. Dahl, **Influence of temperature, strain rate and specimen geometry on the microscopic cleavage fracture stress**, Nuclear Engineering and Design, 1999, 188, 155-160.
8. M. A. Wiehahn, G. N. Nurick and H. C. Bowles, **Some Insights into the mechanism of the deformation and tearing of thin plates at high strain rates incorporating temperature dependent material properties**, Department of Mechanical Engineering, university of Cape Town, South Africa.
9. K. Ramajeyathilagam, C. P. Vendhan and V. Bhujanga Rao, **Non-linear dynamic response of rectangular plates under shock loading**, International Journal of Impact Engineering, 2000, 24, 999-1015.
10. M. E. Gelman, G. N. Nurick and G. P. Mitchell, **A numerical study of inelastic failure of impulsively loaded circular plates, with various boundary conditions**, Proceedings of the 1st South African Conference on Applied Mechanics (SACAM) July 1996, '96, Gauteng, 223-234.

11. Abel Carlos Jacinto, Ricardo Daniel Ambrosini and Rodolfo Francisco Danesi, **Experimental and computational analysis of plates under air blast loading**, International Journal of Impact Engineering, 2001, 25, 927-947.

12. N. Jones, Impulsive **loading of a simply supported circular rigid-plastic plate**. Trans. ASME, J. Applied Mechanics, 1968, 3, 59-65.

13. G. I. Taylor, **The distortion under pressure of a diaphragm which is clamped along its edge and stressed beyond its elastic limit**. Underwater Explosion Research, Vol. 3, The Damage Process, PP. 107-121. Office of Naval Research (1950, originally written 1942).

14. M. D. Olson, J. R. Fagnan and G. N. Nurick, **Deformation and rupture of blast loaded square plates-predictions and experiments**. International Journal of Impact Engineering, 1993, 12(2), 279-291.

15. G. N. Nurick, M. D. Olson, J. R. Fagnan and A. Levin, **Deformation and tearing of blast-loaded stiffened square plates**, International Journal of Impact Engineering, 1995, 16(2), 273-291.

16. J. Richard Martin, Ali Reza, Larry W. Anderson, **What is an explosive? A case history of an investigation for the insurance industry**, Journal of Loss Prevention in the Process Industries, 2000, 13(13), 491 – 497.

17. W. Q. Shen, and N. Jones, **Dynamic response and failure of fully clamped circular plates under impulsive loading,** International Journal of Impact Engineering, 199, 13(2), 259-278.

18. The Steel Construction Institute, **The effect of simplification of the explosive pressure-time history**, British Gas Research and Technology, 1992.

19. C. K. Youngdahl, **Correlation parameters for eliminating the effect of pulse shape on dynamic deformation**, Journal of Applied Mechanics, ASME, 1970, 3, 744-752.

20. G. H. Farrow, G. N. Nurick, G. P. Mitchell, **Modeling of impulsively loaded circular plates using the finite element code**, Proc. 13th Symp. Finite element Methods in South Africa, Stellenbosch, South Africa, January, 1995, 1995.

21. G. N. Nurick, **Large deformations of thin plates subjected to impulsive loading**, PhD. Thesis University of Cape Town, 1987.

22. C. F. Noble, PLB Oxley, **Estimating the charge size in explosive forming of sheet metal**, The College of Aeronautics, Cranfield, 1964.
23. G. N Nurick., **The measurement of the deformation response of a structure subjected to an explosive load using a light interference technique**, proceedings of the 1986 SEM Spring Conference on Experimental Mechanics, 1986, 105-114.
24. R. G. Teeling-Smith and G. N. Nurick, **The deformation and tearing of thin circular plates subjected to impulsive loads**, International Journal of impact Engineering, 1991, 11(1), 77-91.
25. G. N. Nurick, M. E. Gelman and N. S. Marshall, **Tearing of blast loaded plates with clamped boundary conditions**, International Journal of Impact Engineering, 1996, 18(7), 803-827.
26. G. N. Nurick and G. C. Shave, **The deformation and tearing of thin square plates subjected to impulsive loads – An experimental study**, International Journal of Impact Engineering, 1996, 18(1), 99 – 116.
27. G. N. Nurick and A. M. Radford, **Deformation and tearing of clamped circular plates subjected to localized central blast loads, Recent developments in computational and applied mechanics**, 1997.
28. G. N. Nurick and N. Jones, **Prediction of large inelastic deformations of T-beams subjected to uniform impulsive loads, high strain rate effects on polymer, metal and ceramic matrix composites and other advanced materials**, ASME, 1995, AD-Vol.48.
29. G. N. Nurick, N. Jones and G. V. Von Alten-Reuss, **Large inelastic deformations of T-beams subjected to impulsive loads**, Structures Under Shock and Impact (SUSI), (ED. P Bulson), published by computational mechanics publications, 1994, 191-206.
30. T. Nonaka, **Shear failure of a steel member due to a blast**, International Journal of Impact Engineering, 2000, .24, 231-238.
31. B. M. Thomas, **The effect of boundary conditions on the failure of thin plates subjected to impulsive loading**, M.Sc. thesis, University of Cape Town, 1995.
32. N. S. Rudrapatna, R. Vaziri and M. D. Olson, **Deformation and failure of blast-loaded square plates**, International Journal of Impact Engineering, 1999, 22, 449-467.

33. G. E. Hudson, **A theory of the dynamic plastic deformation of a diaphragm**. Journal of Applied Physics, 1951, 22, 1-11.

34. J. M. Richardson and J. D. Kirkwood, **Theory of the plastic deformation of thin plates by underwater explosions**. Underwater Explosion Research, Vol. 3, The Damage process, PP 305-421. Office of Naval Research, 1950.

35. H. G. Hopkins and W. Prager, **On the dynamics of plastic circular plates**, ZAMP (Journal of Applied Mechanics And Phys.), 1954, 5, 317-330.

36. A. L. Florence, **Clamped circular rigid-plastic plates under central blast loading**. International Journal of Solid Structures, 1966, 2, 319-335.

37. E. A. Witmer, N. M. Balmer, J. W. Leech and T. N. N. Pian, **Large dynamic deformations of beams, rings, plates and shells**, ALAA J. I., 1963, 1848-1857.

38. G. N. Nurick and J. B. Martin, **The measurement of the response of clamped circular plates to impulsive loading, Mechanical properties at high rates of strain**, (Ed. J. Harding) Published by the Institute of Physics, 1984, 495-500.

39. N. Jones, **Structural Impact**, Cambridge University Press, 1989.

40. S. R. Bodner and P. S. Symonds, **Experiments on viscoplastic response of circular plates to impulsive loading**, Journal of Mech. Phys. Solid, 1979, 27, 91-113.

41. G. N. Nurick, **A new technique to measure the deflection-time history of material subjected to high strain rates**, International Journal of Impact Engineering, 1985, 3, 17-26.

42. R. G. Teeling-Smith, **An investigation into the deformation and tearing of thin circular plates subjected to impulsive loads**, M.Sc. Thesis, University of Cape Town, 1989.

43. W. Johnson, **Impact Strength of Materials**, Edward Arnold, Londaon ,1972.

44. G. N. Nurick, "**An empirical solution for predicting maximum central deflections of impulsively loaded plates". Mechanical Properties at high strain rate**, Institute of Physics, (Edited by J. Harding), 1989 ,457-464.

45. Steeve Chung Kim Yuen, **Deformation and tearing of uniformly blast loaded quadrangular stiffened plates**, M.Sc. Thesis, University of Cape Town, 2000.

46. E. H. Lee and P. S. Symonds, **large plastic deformations of beams under transverse impact**. ASME Journal of Applied Mechanics, 1952, 19, 308-315.

47. P. S. Symonds, **Dynamic load characteristics in plastic bending of beams**. ASME, Journal of Applied Mechanics, 1953, 20, 475-482.

48. P. S. Symonds, **Large plastic deformations of beams under blast type loading**. Proc. 2nd U. S. Natl. Cong. Applied Mechanics, ASME, 1954, 505-515.

49. R. B. Schubak, D.L. Anderson and M.D. Olson, **Simplified dynamic analysis of rigid-plastic beams**, International Journal of Impact Engineering, 1988, 8(1), 27-42.

50. He – Ming Wen, **Deformation and tearing of clamped work – hardening beams subjected to impulsive loads**, International Journal of Impact Engineering, 1996, 18(4), 425 – 433.

51. Q. M. Li, Norman Jones, **Formation of a shear localization in structural elements under transverse dynamic loads**, International Journal of Impact Engineering, 1999, 22(22), 589 – 607.

52. N. Jones, R. N. Griffin and R. E. Van Duzer, **An experimental study into the dynamic plastic behaviour of wide beams and rectangular plates**, International Journal of Mechanical Science, 1971, 13, 721-735.

53. Hibbit, Karlson and Sorenson, INC. **ABAQUS / Explicit User's manual,** 1998, 1 v5.8, 10.1-1 – 1-.24-1.

54. T. Masui, T. Nunokawa and T. Hiramatsu, **Shape correction of hot rolled steel using an on line leveler**, Journal of Japan Society for Technology of Plasticity,1987, 1.

55. Woei-Shyan Lee, Jia-Chyuan Shyu and Su-Tang Chiou, **Effect of strain rate on impact response and dislocation substructure of 6061-T6 aluminium alloy**, Scripta Mater, 2000, 42, 51-56.

56. Woei-Shyan Lee and Gen-Wang Yeh, **The plastic deformation behaviour of AISI 4340 alloy steel subjected to high temperature and high strain rate loading conditions**, Journal of Material Processing Technology, 1997, 71, 224-234.

57. W.P. Grobbelaar, **An investigation of structures subjected to blast loads incorporating an equation of state to model the material behaviour of the explosive,** M.Sc. Thesis, University of Cape Town, 1999.

58. C. J. Costantino, "**Two-dimensional wave propagation through non-linear media**," Journal of Computational Physics,1969, 4(2), 147-170.

Appendix A-Ballistic Pendulum

A general set up of the pendulum is shown in figure A.1.

The linearised equation of motion of the ballistic pendulum, assuming viscous damping is

$$\ddot{X} + 2\beta.\dot{X} + \omega_n^2.X = 0 \qquad (A.1)$$

where

$\beta = \frac{C}{2M}$, $\omega_n = \frac{2\pi}{T}$ and $\omega_d = \left(\omega_n^2 - \beta^2\right)^{\frac{1}{2}}$ and

C is the damping coefficient, M is the total mass of the pendulum including the test rig, I-beam and balancing mass, and T is the natural period of the pendulum.

The solution of the equation A.1 is given by

$$X = \frac{e^{-\beta.t}.x_o.\sin(\omega_d.t)}{\omega_d} \qquad (A.2)$$

where

$\dot{x}$ is the initial velocity of the pendulum.

Let x_1 be the horizontal displacement at $t = \frac{T}{4}$

and x_2 be the horizontal displacement at $t = \frac{3T}{4}$

Substituting into equation A.2 gives

$$x_1 = \frac{x_o.T}{2\pi}.e^{-0.25\beta.T} \qquad (A.3)$$

$$x_2 = \frac{x_o.T}{2\pi}.e^{-0.75\beta.T} \qquad (A.4)$$

Hence $$\frac{x_1}{x_2}e^{0.5\beta.T} \qquad (A.5)$$

giving $$\beta = \frac{2}{T} In\left(\frac{x_1}{x_2}\right) \quad \text{(A.6)}$$

and

$$x_o = \frac{2\pi}{T} . x_1 . e^{0.25\beta . T} \quad \text{(A.7)}$$

The impulse can therefore be calculated from

$$I = M . x_o \quad \text{(A.8)}$$

The natural period T is simply determined by averaging a number of measured pendulum oscillations. The damping constant; β ; is calculated from equation A.6 where x_1 and x_2 are calculated from the measurements taken from several pendulum oscillations in which the pendulum was drawn back and release.

From the pendulum; figure A.1, it can be seen that the distance moved by the pendulum and that measured by the pen are not the same, and this must be accounted for.

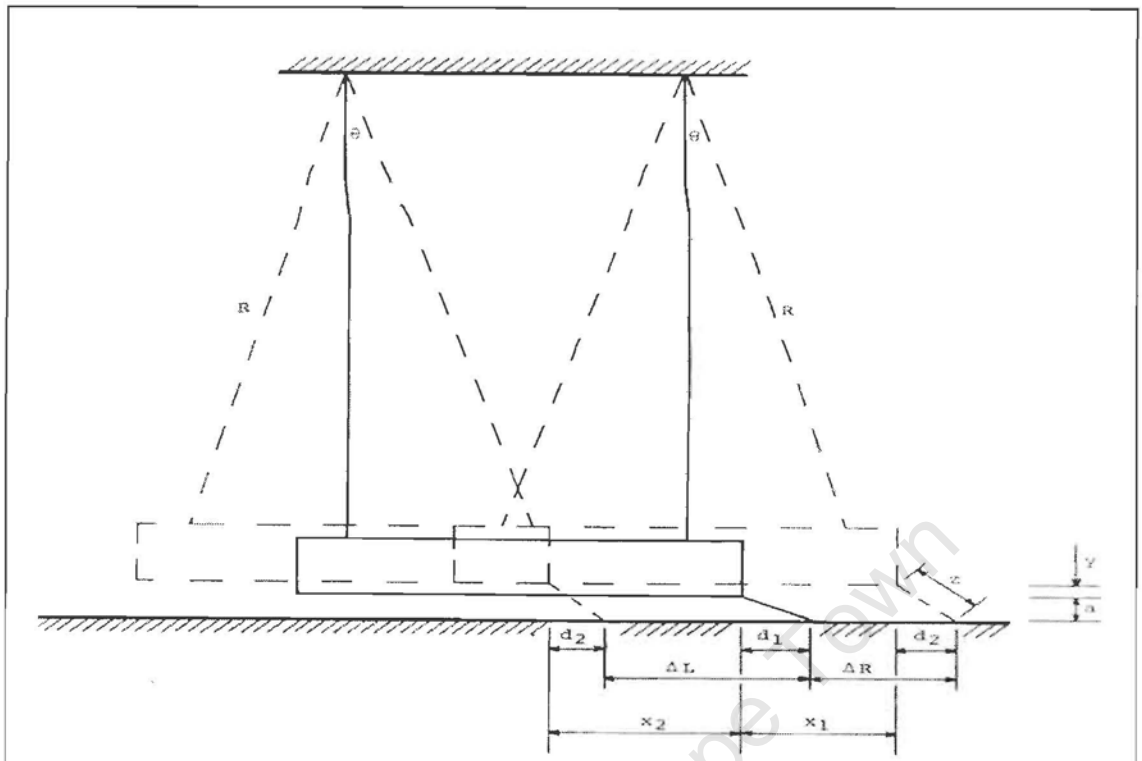

Figure A.1: Ballistic pendulum geometry.

From figure A.1, the horizontal distance between the end of the pendulum and the pen when the pendulum is stationary is giving by

$$d_1 = \left(Z^2 - a^2\right)^{\frac{1}{2}} \tag{A.9}$$

while at its maximum amplitude, the distance decreases and is giving by

$$d_2 = \left(Z - (aa = y)^2\right)^{\frac{1}{2}} \tag{A.10}$$

During testing, the pendulum oscillates to a very low amplitude thus giving a very small angle; 6 and therefore it can be assumed that

$$x_1 = R.6 \quad \text{and} \quad y = \frac{R.\theta_2}{2}$$

Hence

$$y = \frac{x_1^2}{2.R} \tag{A.11}$$

and

$$d_2 = \left(Z^2 - \left(a + \frac{x_1^2}{2.R} \right)^2 \right)^{\frac{1}{2}} \tag{A.12}$$

From figure A.1:

$$x_1 = \Delta R + d_1 - d_2$$

$$x_2 = \Delta L - d_1 + d_2$$

Substituting for d_1 and d_2, we have

$$x_1 = \Delta R + \left(Z^2 - a^2\right)^{\frac{1}{2}} - \left(Z^2 - \left(a + \frac{x_1^2}{2.R} \right)^2 \right)^{\frac{1}{2}} \tag{A.13}$$

and

$$x_2 = \Delta L - \left(Z^2 - a^2\right)^{\frac{1}{2}} + \left(Z^2 - \left(a + \frac{x_1^2}{2.R} \right)^2 \right)^{\frac{1}{2}} \tag{A.14}$$

where

ΔL, ΔR, Z, a and R are measured and therefore x_1 and x_2 can be calculated.

The data of the ballistic pendulum is shown in table A.1

Mass of I-beam	28155g
Mass of clamping rig	15385g
Mass of counter balance	23690g
Total pendulum mass	67230g
(M)	
R	2584mm
Z	119.62mm
A	62.7mm
T	3.19s

Table A.1: Ballistic pendulum details.

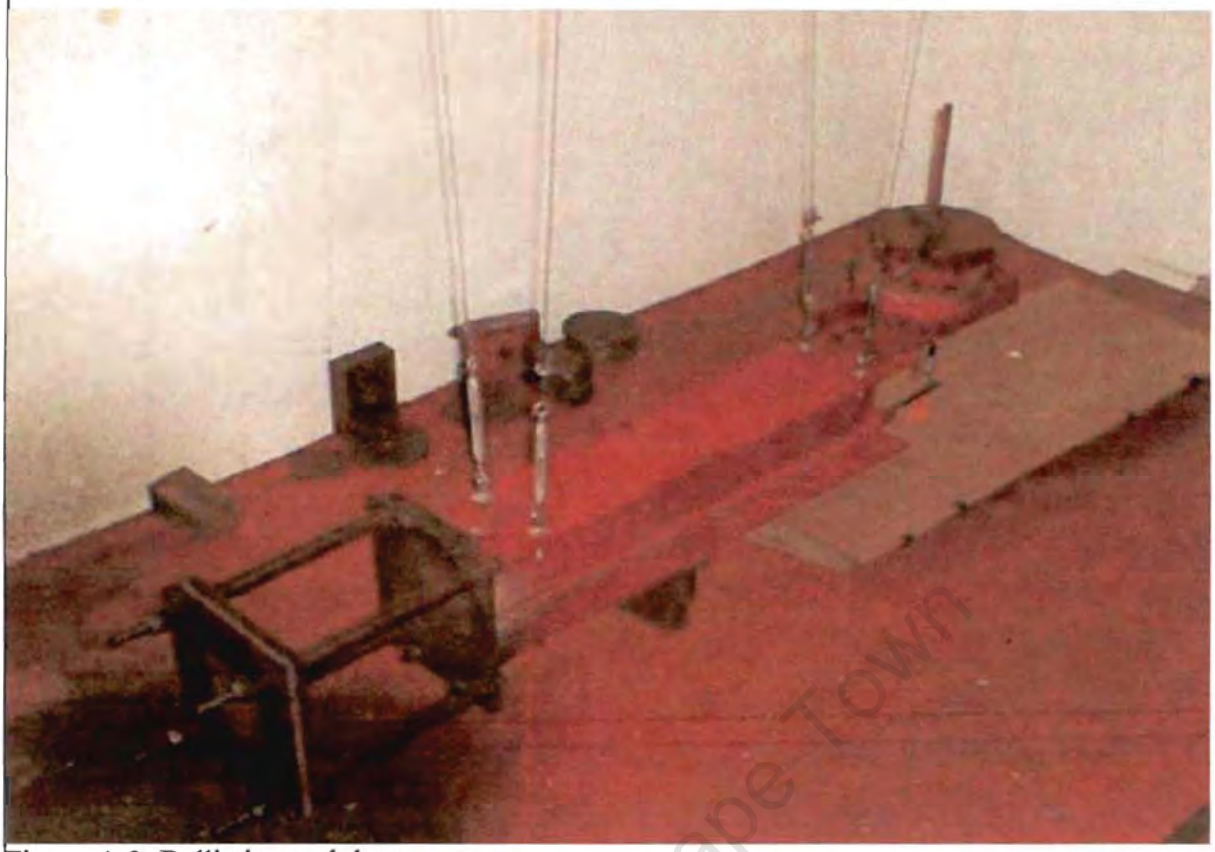

Figure A.2: Ballistic pendulum.

UNIFORM BLAST LOADING ON CLAMPED CIRCULAR PLATE USING MATERIAL PROPERTIES THAT INCLUDE TEMPERATURE DEPENDENCY

```
*HEADING
CIAMPED CIRCULAR PLATE SUBJECTED TO BLAST LOADING
SI UNITS (Kg, M, S, N)
*PREPRINT, ECHO=NO, MODEL=NO
**----------------------------------------DEFINITION OF NODES
*NODE
1,     0.0000,  0.0
51,    0.0375,  0.0
101,   0.0500,  0.0
201,   0.1000,  0.0
**----------------------------------------
*NGEN, NSET=EDGE1
1,   51,   1
51,  101,  1
101, 201, 1
**----------------------------------------COPING EDGE1 FOR EACH OF THE  EDGES
*NCOPY, SHIFT, OLDSET=EDGE1, CHANGE NUMBER=1000, NEWSET=EDGE2
0.0, 0.0004, 0.0
0.0, 0.0, 0.0, 0.0, 0.0, 0.0, 0.0
*NCOPY, SHIFT, OLDSET=EDGE1, CHANGE NUMBER=2000, NEWSET=EDGE3
0.0, 0.0004, 0.0
0.0, 0.0, 0.0, 0.0, 0.0, 0.0, 0.0
*NCOPY, SHIFT, OLDSET=EDGE1, CHANGE NUMBER=8000, NEWSET=EDGE4
0.0, 0.002, 0.0
0.0, 0.0, 0.0, 0.0, 0.0, 0.0, 0.0
*NCOPY, SHIFT, OLDSET=EDGE1, CHANGE NUMBER=9000, NEWSET=EDGE5
0.0, 0.002, 0.0
0.0, 0.0, 0.0, 0.0, 0.0, 0.0, 0.0
*NCOPY, SHIFT, OLDSET=EDGE1, CHANGE NUMBER=10000, NEWSET=EDGE6
0.0, 0.0024, 0.0
0.0, 0.0000, 0.0, 0.0, 0.0, 0.0, 0.0
*NFILL, NSET=PLATE
EDGE1, EDGE2, 1, 1000
EDGE3, EDGE4, 6, 1000
EDGE5, EDGE6, 1, 1000
**
*NSET, NSET=OUTER-R, GENERATE
2200,8200, 1000


**----------------------------------------DEFINITION OF ELEMENTS

*ELEMENT, TYPE=CAX4R, ELSET=CLAMP_BOT
```

```
1, 1, 2, 1002, 1001
*ELGEN, ELSET=CLAMP_BOT
1, 100, 1, 1, 1, 1000, 1000
**-----------------------------------------
*ELEMENT, TYPE=CAX4R, ELSET=PLATE
1010, 2010, 2011, 3011, 3010
*ELGEN, ELSET=PLATE
1010, 190, 1, 1, 6, 1000, 1000
**-----------------------------------------
*ELEMENT, TYPE=CAX4R, ELSET=CLAMP_TOP
7001, 9001, 9002, 10002, 10001
*ELGEN, ELSET=CLAMP_TOP
7001, 100, 1, 1, 1, 1000, 1000
**-----------------------------------------DEFINITION OF SECTIONS
*SOLID SECTION, ELSET=PLATE, MATERIAL=STEEL
*SOLID SECTION, ELSET=CLAMP_BOT, MATERIAL=RIGID
*SOLID SECTION, ELSET=CLAMP_TOP, MATERIAL=RIGID
**-----------------------------------------DEFINITION OF RIGID BODY NODES
*NODE, NSET=NS_REFNODE
3000000, 0.045,  0.0064
4000000, 0.045, -0.0064
**-----------------------------------------DEFINITION OF SURFACES
*RIGID BODY, REFNODE=3000000, ELSET=CLAMP_TOP
*ELSET, ELSET=CLAMP_TOP_FACEP2
7100
*ELSET, ELSET=CLAMP_TOP_FACEP4
7001
*SURFACE, TYPE=ELEMENT, NAME=SURF_CLAMP_TOP
CLAMP_TOP, S1
CLAMP_TOP_FACEP2, S2
CLAMP_TOP_FACEP4, S4
**-----------------------------------------
*RIGID BODY, REFNODE=4000000, ELSET=CLAMP_BOT
*ELSET, ELSET=CLAMP_BOT_FACEP2
100
*ELSET, ELSET=CLAMP_BOT_FACEP4
1
*SURFACE, TYPE=ELEMENT, NAME=SURF_CLAMP_BOT
CLAMP_BOT, S3
CLAMP_BOT_FACEP2, S2
CLAMP_BOT_FACEP4, S4
**-----------------------------------------

*ELSET, ELSET=TOPSURF, GENERATE
6101, 6200, 1
*SURFACE, TYPE=ELEMENT, NAME=LOAD_PLATE
```

```
TOPSURF, S3
**----------------------------DEFINATION OF UPPER CONTACT SURFACE FOR BC
*ELSET, ELSET=PLATE_TOP, GENERATE
6010, 6100, 1
*SURFACE, TYPE=ELEMENT, NAME=SURF_PLATE_TOP
PLATE_TOP, S3
**----------------------------DEFINATION OF LOWER CONTACT SURFACE FOR BC
*ELSET, ELSET=PLATE_BOT, GENERATE
1010, 1100, 1
*SURFACE, TYPE=ELEMENT, NAME=SURF_PLATE_BOT
PLATE_BOT, S1
**----------------------------DEFINITION OF MATERIAL PROPERTIES
*MATERIAL, NAME=STEEL
*INELASTIC HEAT FRACTION
0.9
*ELASTIC
2.10E11, .33, 0
1.98E11, .33, 200
1.75E11, .33, 600
1.47E11, .33, 700
1.25E11, .33, 800
9.09E10, .33, 900
1.00E11, .33, 1000
9.70E10, .33, 1100
*PLASTIC
2.64E8, 0.000000, 0
2.79E8, 0.007185, 0
3.31E8, 0.025556, 0
3.92E8, 0.051413, 0
4.57E8, 0.091745, 0
4.84E8, 0.115659, 0
5.16E8, 0.150734, 0
5.33E8, 0.174145, 0
5.51E8, 0.204152, 0
5.62E8, 0.226766, 0
5.69E8, 0.247764, 0
5.59E8, 0.280197, 0
2.64E8, 0.000000, 200
2.79E8, 0.007185, 200
3.31E8, 0.025556, 200
3.92E8, 0.051413, 200
4.57E8, 0.091745, 200
4.84E8, 0.115659, 200
5.16E8, 0.150734, 200
5.33E8, 0.174145, 200
5.51E8, 0.204152, 200
```

```
5.62E8, 0.226766, 200
5.69E8, 0.247764, 200
5.59E8, 0.280197, 200
3.51E7, 0.000000, 700
3.71E7, 0.007185, 700
4.40E7, 0.025556, 700
5.22E7, 0.051413, 700
6.08E7, 0.091745, 700
6.44E7, 0.115659, 700
6.86E7, 0.150734, 700
7.09E7, 0.174145, 700
7.33E7, 0.204152, 700
7.47E7, 0.226766, 700
7.56E7, 0.247764, 700
7.43E7, 0.280197, 700
4.38E6, 0.000000, 1000
4.63E6, 0.007185, 1000
5.50E6, 0.025556, 1000
6.51E6, 0.051413, 1000
7.58E6, 0.091745, 1000
8.04E6, 0.115659, 1000
8.56E6, 0.150734, 1000
8.85E6, 0.174145, 1000
9.15E6, 0.204152, 1000
9.33E6, 0.226766, 1000
9.44E6, 0.247764, 1000
9.28E6, 0.280197, 1000
*SPECIFIC HEAT
660
*RATE DEPENDENT
40, 5
*DENSITY
7850
**
*MATERIAL, NAME=RIGID
*ELASTIC
200E9, 0.3
*DENSITY
7800
**--------------------------DEFINITION OF BOUNDARY CONDITIONS
*BOUNDARY
OUTER-R, XSYMM
3000000, 1,1,0.0
3000000, 3,6,0.0
4000000, 1,6,0.0
*NSET, NSET=ALL, ELSET=PLATE
```

```
*INITIAL CONDITION, TYPE=TEMPERATURE
PLATE, 23.
**----------------------------DEFINITION OF LOAD
*AMPLITUDE, NAME=BLAST, DEFINITION=TABULAR
0.0,1.0,  15E-6,1, 15.1E-6,0.0
**----------------------------ANALYSIS STEPS BEGIN
*STEP
*DYNAMIC, EXPLICIT, ADIABATICS
,0.005E-6
*CONTACT PAIR, INTERACTION=SMOOTH
SURF_CLAMP_BOT, SURF_PLATE_BOT
**
SURF_CLAMP_TOP, SURF_PLATE_TOP
**
*SURFACE INTERACTION, NAME=SMOOTH
*FRICTION
0.25
*CLOAD
3000000,2,-1.2E6
*OUTPUT, FIELD, VARIABLE=ALL,OP=NEW, NUMBER INTERVAL=1
**
*END STEP
**-----------------------------------------------------
*STEP
*DYNAMIC, EXPLICIT, ADIABATICS
,15E-6
*DLOAD, AMPLITUDE=BLAST
TOPSURF, P3, 4.04E7
*OUTPUT, FIELD, VARIABLE=ALL,OP=NEW, NUMBER INTERVAL=100
*END STEP
*STEP
*DYNAMIC, EXPLICIT, ADIABATICS
,235E-6
*DLOAD, OP=NEW
*END STEP
*STEP
*DYNAMIC, EXPLICIT, ADIABATICS
,300E-6
*DLOAD, OP=NEW
*END STEP
**END OF ANALYSIS
```

UNIFORM BLAST LOADING ON CLAMPED CIRCULAR PLATE USING MATERIAL PROPERTIES THAT EXCLUDE TEMPERATURE DEPENDENCY

```
*HEADING
CIAMPED CIRCULAR PLATE SUBJECTED TO BLAST LOADING
SI UNITS (Kg, M, S, N)
*PREPRINT, ECHO=NO, MODEL=NO
**----------------------------------------DEFINITION OF NODES
*NODE
1,      0.0000,  0.0
51,     0.0375,  0.0
101,    0.0500,  0.0
201,    0.1000,  0.0
**----------------------------------------
*NGEN, NSET=EDGE1
1,  51,  1
51, 101, 1
101,201, 1
**----------------------------------------COPING  EDGE1 FOR EACH OF THE 6 EDGES
*NCOPY, SHIFT, OLDSET=EDGE1, CHANGE NUMBER=1000, NEWSET=EDGE2
0.0, 0.0004, 0.0
0.0, 0.0, 0.0, 0.0, 0.0, 0.0, 0.0
*NCOPY, SHIFT, OLDSET=EDGE1, CHANGE NUMBER=2000, NEWSET=EDGE3
0.0, 0.0004, 0.0
0.0, 0.0, 0.0, 0.0, 0.0, 0.0, 0.0
*NCOPY, SHIFT, OLDSET=EDGE1, CHANGE NUMBER=8000, NEWSET=EDGE4
0.0, 0.002, 0.0
0.0, 0.0, 0.0, 0.0, 0.0, 0.0, 0.0
*NCOPY, SHIFT, OLDSET=EDGE1, CHANGE NUMBER=9000, NEWSET=EDGE5
0.0, 0.002, 0.0
0.0, 0.0, 0.0, 0.0, 0.0, 0.0, 0.0
*NCOPY, SHIFT, OLDSET=EDGE1, CHANGE NUMBER=10000, NEWSET=EDGE6
0.0, 0.0024, 0.0
0.0, 0.0000, 0.0, 0.0, 0.0, 0.0, 0.0
*NFILL, NSET=PLATE
EDGE1, EDGE2, 1, 1000
EDGE3, EDGE4, 6, 1000
EDGE5, EDGE6, 1, 1000
**
*NSET, NSET=OUTER-R, GENERATE
2200,8200, 1000
```

```
**----------------------------------------DEFINITION OF ELEMENTS
*ELEMENT, TYPE=CAX4R, ELSET=CLAMP_BOT
1, 1, 2, 1002, 1001
*ELGEN, ELSET=CLAMP_BOT
1, 100, 1, 1, 1, 1000, 1000
**----------------------------------------
*ELEMENT, TYPE=CAX4R, ELSET=PLATE
1010, 2010, 2011, 3011, 3010
*ELGEN, ELSET=PLATE
1010, 190, 1, 1, 6, 1000, 1000
**----------------------------------------
*ELEMENT, TYPE=CAX4R, ELSET=CLAMP_TOP
7001, 9001, 9002, 10002, 10001
*ELGEN, ELSET=CLAMP_TOP
7001, 100, 1, 1, 1, 1000, 1000
**---------------------------------DEFINITION OD SECTIONS
*SOLID SECTION, ELSET=PLATE, MATERIAL=STEEL
*SOLID SECTION, ELSET=CLAMP_BOT, MATERIAL=RIGID
*SOLID SECTION, ELSET=CLAMP_TOP, MATERIAL=RIGID
**---------------------------------DEFINITION OF RIGID BODY NODES
*NODE, NSET=NS_REFNODE
3000000, 0.045,  0.0064
4000000, 0.045, -0.0064
**-----------------------------------DFINITION OF SURFACES
*RIGID BODY, REFNODE=3000000, ELSET=CLAMP_TOP
*ELSET, ELSET=CLAMP_TOP_FACEP2
7100
*ELSET, ELSET=CLAMP_TOP_FACEP4
7001
*SURFACE, TYPE=ELEMENT, NAME=SURF_CLAMP_TOP
CLAMP_TOP, S1
CLAMP_TOP_FACEP2, S2
CLAMP_TOP_FACEP4, S4
**----------------------------------------
*RIGID BODY, REFNODE=4000000, ELSET=CLAMP_BOT
*ELSET, ELSET=CLAMP_BOT_FACEP2
100
*ELSET, ELSET=CLAMP_BOT_FACEP4
1
*SURFACE, TYPE=ELEMENT, NAME=SURF_CLAMP_BOT
CLAMP_BOT, S3
CLAMP_BOT_FACEP2, S2
CLAMP_BOT_FACEP4, S4
**----------------------------------------
*ELSET, ELSET=TOPSURF, GENERATE
6101, 6200, 1
```

```
*SURFACE, TYPE=ELEMENT, NAME=LOAD_PLATE
TOPSURF, S3
**------------------------------DEFINATION OF UPPER CONTACT SURFACE FOR BC
*ELSET, ELSET=PLATE_TOP, GENERATE
6010, 6100, 1
*SURFACE, TYPE=ELEMENT, NAME=SURF_PLATE_TOP
PLATE_TOP, S3
**------------------------------DEFINATION OF LOWER CONTACT SURFACE FOR BC
*ELSET, ELSET=PLATE_BOT, GENERATE
1010, 1100, 1
*SURFACE, TYPE=ELEMENT, NAME=SURF_PLATE_BOT
PLATE_BOT, S1
**------------------------------DEFINITION OF MATERIAL PROPERTIES
*MATERIAL, NAME=STEEL
*INELASTIC HEAT FRACTION
0.9
*ELASTIC
2.10E11, .33
*PLASTIC
2.64E8, 0.000000
2.79E8, 0.007185
3.31E8, 0.025556
3.92E8, 0.051413
4.57E8, 0.091745
4.84E8, 0.115659
5.16E8, 0.150734
5.33E8, 0.174145
5.51E8, 0.204152
5.62E8, 0.226766
5.69E8, 0.247764
5.59E8, 0.280197
*SPECIFIC HEAT
660
*RATE DEPENDENT
40, 5
*DENSITY
7850
**
*MATERIAL, NAME=RIGID
*ELASTIC
200E9, 0.3
*DENSITY
7800


**-------------------------DEFINITION OF BOUNDARY CONDITIONS
```

```
*BOUNDARY
OUTER-R, XSYMM
3000000, 1,1,0.0
3000000, 3,6,0.0
4000000, 1,6,0.0
**-------------------------DEFINITION OF LOAD
*AMPLITUDE, NAME=BLAST, DEFINITION=TABULAR
0.0,1.0,  15E-6,1, 15.1E-6,0.0
**-----------------------ANALYSIS STEPS BEGIN
*STEP
*DYNAMIC, EXPLICIT
,0.005E-6
*CONTACT PAIR, INTERACTION=SMOOTH
SURF_CLAMP_BOT, SURF_PLATE_BOT
**
SURF_CLAMP_TOP, SURF_PLATE_TOP
**
*SURFACE INTERACTION, NAME=SMOOTH
*FRICTION
0.25
**
*CLOAD
3000000,2,-1.2E6
*OUTPUT, FIELD, VARIABLE=ALL,OP=NEW, NUMBER INTERVAL=1
*END STEP
**----------------------------------------
*STEP
*DYNAMIC, EXPLICIT
,15E-6
*DLOAD, AMPLITUDE=BLAST
TOPSURF, P3, 4.04E7
*OUTPUT, FIELD, VARIABLE=ALL,OP=NEW, NUMBER INTERVAL=100
*END STEP
*STEP
*DYNAMIC, EXPLICIT
,35E-6
*DLOAD, OP=NEW
*END STEP
*STEP
*DYNAMIC, EXPLICIT
,250E-6
*DLOAD, OP=NEW
*END STEP
*END OF ANALYSIS
```

UNIFORM BLAST LOADING ON BUILT-IN CIRCULAR PLATE USING MATERIAL PROPERTIES THAT INCLUDE TEMPERATURE DEPENDENCY

```
*HEADING
BUILT-IN CIRCULAR PLATE SUBJECTED TO BLAST LOADING
SI UNITS (Kg, M, S, N)
*PREPRINT, ECHO=NO, MODEL=NO
**-------------------------------------DEFINITION OF NODES
*NODE
1,      0.0000, 0.0
51,     0.0125, 0.0
151,    0.0625, 0.0
**-----------------------------------
*NGEN, NSET=EDGE1
1,   51,   1
51,  151, 1
**-----------------------------------------COPING  EDGE1 FOR EACH OF THE EDGES
*NCOPY, SHIFT, OLDSET=EDGE1, CHANGE NUMBER=4000, NEWSET=EDGE2
0.0, 0.0016, 0.0
0.0, 0.0, 0.0, 0.0, 0.0, 0.0, 0.0
*NCOPY, SHIFT, OLDSET=EDGE1, CHANGE NUMBER=10000, NEWSET=EDGE3
0.0, 0.0032, 0.0
0.0, 0.0, 0.0, 0.0, 0.0, 0.0, 0.0
*NCOPY, SHIFT, OLDSET=EDGE1, CHANGE NUMBER=14000, NEWSET=EDGE4
0.0, 0.0048, 0.0
0.0, 0.0, 0.0, 0.0, 0.0, 0.0, 0.0
**
*NFILL, NSET=PLATE
EDGE1, EDGE2, 4, 1000
EDGE2, EDGE3, 6, 1000
EDGE3, EDGE4, 4, 1000
**
*NGEN, NSET=OUTER-R
4151,10151, 1000
**-----------------------------------------DEFINITION OF ELEMENTS
*ELEMENT, TYPE=CAX4R, ELSET=PLATE
1, 1, 2, 1002, 1001
4001, 4001, 4002, 5002, 5001
10001, 10001, 10002, 11002, 11001
*ELGEN, ELSET=PLATE
1, 50, 1, 1, 4, 1000, 1000
4001, 150, 1, 1, 6, 1000, 1000
10001, 50, 1, 1, 4, 1000, 1000
```

```
**DEFINITION OF SURFACES
*ELSET, ELSET=TOPSURF, GENERATE
9051, 9200, 1
*SURFACE, TYPE=ELEMENT, NAME=LOAD_PLATE
TOPSURF, S3
**----------------------------------DEFINATION OF BUILT-IN BC NSETS
*NGEN, NSET=BOUND1
1, 51, 1
*NGEN, NSET=BOUND2
51, 4051, 1000
*NGEN, NSET=BOUND3
10051, 14051, 1000
*NGEN, NSET=BOUND4
14001, 14051, 1
*NGEN, NSET=BOUND5
1, 12001, 1000
**--------------------------------------DEFINITION OF MATERIAL PROPERTIES
*SOLID SECTION, MATERIAL=STEEL, ELSET=PLATE
*MATERIAL, NAME=STEEL
*INELASTIC HEAT FRACTION
0.9
*ELASTIC
2.10E11, .33, 0
1.98E11, .33, 200
1.75E11, .33, 600
1.47E11, .33, 700
1.25E11, .33, 800
9.09E10, .33, 900
1.00E11, .33, 1000
9.70E10, .33, 1100
*PLASTIC
2.64E8, 0.000000, 0
2.79E8, 0.007185, 0
3.31E8, 0.025556, 0
3.92E8, 0.051413, 0
4.57E8, 0.091745, 0
4.84E8, 0.115659, 0
5.16E8, 0.150734, 0
5.33E8, 0.174145, 0
5.51E8, 0.204152, 0
5.62E8, 0.226766, 0
5.69E8, 0.247764, 0
5.59E8, 0.280197, 0
2.64E8, 0.000000, 200
2.79E8, 0.007185, 200
3.31E8, 0.025556, 200
```

3.92E8, 0.051413, 200
4.57E8, 0.091745, 200
4.84E8, 0.115659, 200
5.16E8, 0.150734, 200
5.33E8, 0.174145, 200
5.51E8, 0.204152, 200
5.62E8, 0.226766, 200
5.69E8, 0.247764, 200
5.59E8, 0.280197, 200
3.51E7, 0.000000, 700
3.71E7, 0.007185, 700
4.40E7, 0.025556, 700
5.22E7, 0.051413, 700
6.08E7, 0.091745, 700
6.44E7, 0.115659, 700
6.86E7, 0.150734, 700
7.09E7, 0.174145, 700
7.33E7, 0.204152, 700
7.47E7, 0.226766, 700
7.56E7, 0.247764, 700
7.43E7, 0.280197, 700
4.38E6, 0.000000, 1000
4.63E6, 0.007185, 1000
5.50E6, 0.025556, 1000
6.51E6, 0.051413, 1000
7.58E6, 0.091745, 1000
8.04E6, 0.115659, 1000
8.56E6, 0.150734, 1000
8.85E6, 0.174145, 1000
9.15E6, 0.204152, 1000
9.33E6, 0.226766, 1000
9.44E6, 0.247764, 1000
9.28E6, 0.280197, 1000
*SPECIFIC HEAT
660
*RATE DEPENDENT
40, 5
*DENSITY
7850

```
**THE ANALYSIS STEP
*-----------------------------------DEFINITION OF BOUNDARY CONDITIONS
OUTER-R, XSYMM
BOUND1, 1,6,0.0
BOUND2, 1,6,0.0
BOUND3, 1,6,0.0
BOUND4, 1,6,0.0
BOUND5, 1,6,0.0
*NSET, NSET=ALL, ELSET=PLATE
*INITIAL CONDITION, TYPE=TEMPERATURE
PLATE, 23.
**-----------------------------------DEFINITION OF LOAD
*AMPLITUDE, NAME=BLAST, DEFINITION=TABULAR
0.0,1.0,  15E-6,1, 15.1E-6,0.0
**-----------------------------------ANALYSIS STEP BEGINS
*STEP
*DYNAMIC, EXPLICIT, ADIABATICS
,15E-6
*DLOAD, AMPLITUDE=BLAST
TOPSURF, P3, 4.04E7
*OUTPUT, FIELD, VARIABLE=ALL,OP=NEW, NUMBER INTERVAL=100
*END STEP
*STEP
*DYNAMIC, EXPLICIT, ADIABATICS
,35E-6
*DLOAD, OP=NEW
*END STEP
*STEP
*DYNAMIC, EXPLICIT, ADIABATICS
,200E-6
*DLOAD, OP=NEW
*END STEP
*STEP
*DYNAMIC, EXPLICIT, ADIABATICS
,250E-6
*DLOAD, OP=NEW
*END STEP
```

UNIFORM BLAST LOADING ON BUILT-IN PLATE USING MATERIAL PROPERTIES THAT EXCLUDE TEMPERATURE DEPENDENCY

```
*HEADING
CIRCULAR PLATE SUBJECTED TO BLAST LOADING
SI UNITS (Kg, M, S, N)
*PREPRINT, ECHO=NO, MODEL=NO
**----------------------------------------DEFINITION OF NODES
*NODE
1,      0.0000, 0.0
51,     0.0125, 0.0
151,    0.0625, 0.0
**----------------------------------------
*NGEN, NSET=EDGE1
1,    51,  1
51,  151, 1
**----------------------------------------COPY  EDGE1 FOR EACH OF THE EDGES
*NCOPY, SHIFT, OLDSET=EDGE1, CHANGE NUMBER=4000, NEWSET=EDGE2
0.0, 0.0016, 0.0
0.0, 0.0, 0.0, 0.0, 0.0, 0.0, 0.0
*NCOPY, SHIFT, OLDSET=EDGE1, CHANGE NUMBER=10000, NEWSET=EDGE3
0.0, 0.0032, 0.0
0.0, 0.0, 0.0, 0.0, 0.0, 0.0, 0.0
*NCOPY, SHIFT, OLDSET=EDGE1, CHANGE NUMBER=14000, NEWSET=EDGE4
0.0, 0.0048, 0.0
0.0, 0.0, 0.0, 0.0, 0.0, 0.0, 0.0
**
*NFILL, NSET=PLATE
EDGE1, EDGE2, 4, 1000
EDGE2, EDGE3, 6, 1000
EDGE3, EDGE4, 4, 1000
**
*NGEN, NSET=OUTER-R
4151,10151, 1000
**----------------------------------------DEFINITION OF ELEMENTS
*ELEMENT, TYPE=CAX4R, ELSET=PLATE
1, 1, 2, 1002, 1001
4001, 4001, 4002, 5002, 5001
10001, 10001, 10002, 11002, 11001
*ELGEN, ELSET=PLATE
1, 50, 1, 1, 4, 1000, 1000
4001, 150, 1, 1, 6, 1000, 1000
10001, 50, 1, 1, 4, 1000, 1000
```

```
**----------------------------------------------DEFINITION OF SURFACES
*ELSET, ELSET=TOPSURF, GENERATE
9051, 9200, 1
*SURFACE, TYPE=ELEMENT, NAME=LOAD_PLATE
TOPSURF, S3
**----------------------------------------------DEFINATION OF BUILT-IN BC
*NGEN, NSET=BOUND1
1, 51, 1
*NGEN, NSET=BOUND2
51, 4051, 1000
*NGEN, NSET=BOUND3
10051, 14051, 1000
*NGEN, NSET=BOUND4
14001, 14051, 1
*NGEN, NSET=BOUND5
1, 12001, 1000
**-------------------------------------DEFINITION OF MATERIAL PROPERTIES
*SOLID SECTION, MATERIAL=STEEL, ELSET=PLATE
*MATERIAL, NAME=STEEL
*INELASTIC HEAT FRACTION
0.9
*ELASTIC
2.10E11, .33
*PLASTIC
2.64E8, 0.000000
2.79E8, 0.007185
3.31E8, 0.025556
3.92E8, 0.051413
4.57E8, 0.091745
4.84E8, 0.115659
5.16E8, 0.150734
5.33E8, 0.174145
5.51E8, 0.204152
5.62E8, 0.226766
5.69E8, 0.247764
5.59E8, 0.280197
*SPECIFIC HEAT
660
*RATE DEPENDENT
40, 5
*DENSITY
7850
```

```
**----------------------------------------DEFINATION OF BOUNDARY CONDITIONS
*BOUNDARY
OUTER-R, XSYMM
BOUND1, 1,6,0.0
BOUND2, 1,6,0.0
BOUND3, 1,6,0.0
BOUND4, 1,6,0.0
BOUND5, 1,6,0.0
**DEFINITION OF LOAD
*AMPLITUDE, NAME=BLAST, DEFINITION=TABULAR
0.0,1.0,  15E-6,1, 15.1E-6,0.0
**----------------------------------------ANALYSIS STEPS BEGIN
*STEP
*DYNAMIC, EXPLICIT
,15E-6
*DLOAD, AMPLITUDE=BLAST
TOPSURF, P3, 4.04E7
*OUTPUT, FIELD, VARIABLE=ALL,OP=NEW, NUMBER INTERVAL=100
*END STEP
*STEP
*DYNAMIC, EXPLICIT
,35E-6
*DLOAD, OP=NEW
*END STEP
*STEP
*DYNAMIC, EXPLICIT
,200E-6
*DLOAD, OP=NEW
*END STEP
*STEP
*DYNAMIC, EXPLICIT
,250E-6
*DLOAD, OP=NEW
*END STEP
```

UNIFORM BLAST LOADING ON CLAMPED SQUARE PLATE USING MATERIAL PROPERTIES THAT INCLUDE TEMPERATURE DEPENDENCY

```
*HEADING
BLAST LOADING OF CLAMPED SQUARE PLATES
SI UNITS (kg, M, S, N)
*PREPRINT, MODEL=NO, ECHO=NO
**----------------------------------DEFINITION OF NODES
*NODE
 1,  0,0,0
 21, 0.0455, 0., 0.
 31, 0.0555, 0., 0.
 81, 0.1000, 0., 0.
*NGEN, NSET=EDGE1
 1, 21, 1
 21, 31, 1
 31, 81, 1
**
*NCOPY, SHIFT, OLDSET=EDGE1, CHANGE NUMBER=2000, NEWSET=EDGE2
 0,0.0455,0
 0,0,1, 0,0,1, 0
*NCOPY, SHIFT, OLDSET=EDGE1, CHANGE NUMBER=3000, NEWSET=EDGE3
 0,0.0555,0
 0,0,1, 0,0,1, 0
*NCOPY, SHIFT, OLDSET=EDGE1, CHANGE NUMBER=8000, NEWSET=EDGE4
 0,0.1,0
 0,0,1, 0,0,1, 0
**
*NFILL, NSET=FACE1
 EDGE1,EDGE2, 20, 100
 EDGE2,EDGE3, 10, 100
 EDGE3,EDGE4, 50, 100
** ---------------------------------- --COPING  FACE1 FOR EACH OF THE FACES
*NCOPY, SHIFT, OLDSET=FACE1, NEWSET=FACE2, CHANGE NUMBER=10000
 0,0,0.0032
 0,0,1, 0,0,1, 0
*NCOPY, SHIFT, OLDSET=FACE1, NEWSET=FACE3, CHANGE NUMBER=20000
 0,0,0.0032
 0,0,1, 0,0,1, 0
*NCOPY, SHIFT, OLDSET=FACE1, NEWSET=FACE4, CHANGE NUMBER=30000
 0,0,0.0036
 0,0,1, 0,0,1, 0
*NCOPY, SHIFT, OLDSET=FACE1, NEWSET=FACE5, CHANGE NUMBER=40000
 0,0,0.004
 0,0,1, 0,0,1, 0
*NCOPY, SHIFT, OLDSET=FACE1, NEWSET=FACE6, CHANGE NUMBER=50000
 0,0,0.0044
```

```
 0,0,1, 0,0,1, 0
*NCOPY, SHIFT, OLDSET=FACE1, NEWSET=FACE7, CHANGE NUMBER=60000
 0,0,0.0048
 0,0,1, 0,0,1, 0
*NCOPY, SHIFT, OLDSET=FACE1, NEWSET=FACE8, CHANGE NUMBER=70000
 0,0,0.0048
 0,0,1, 0,0,1, 0
*NCOPY, SHIFT, OLDSET=FACE1, NEWSET=FACE9, CHANGE NUMBER=80000
 0,0,0.008
 0,0,1, 0,0,1, 0
**------------------------------ DEFINITION OF ELEMENTS
*ELEMENT, TYPE=C3D8R, ELSET=CLAMP_BOT
 1, 1,2,102,101, 10001,10002,10102,10101
 2101, 2001,2002,2102,2101, 12001,12002,12102,12101
 3101, 3001,3002,3102,3101, 13001,13002,13102,13101
*ELGEN, ELSET=CLAMP_BOT
 1, 80,1,1, 20,100,100
 2101,80,1,1,10,100,100
 3101,30,1,1,50,100,100
**
*ELEMENT, TYPE=C3D8R, ELSET=PLATE
 10001, 20001,20002,20102,20101, 30001,30002,30102,30101
*ELGEN, ELSET=PLATE
 10001, 80,1,1, 80,100,100, 4,10000,10000
**
*ELEMENT, TYPE=C3D8R, ELSET=CLAMP_TOP
 50001, 70001,70002,70102,70101, 80001,80002,80102,80101
 52101, 72001,72002,72102,72101, 82001,82002,82102,82101
 53101, 73001,73002,73102,73101, 83001,83002,83102,83101
*ELGEN, ELSET=CLAMP_TOP
 50001,80,1,1, 20,100,100
 52101,80,1,1, 10,100,100
 53101,30,1,1, 50,100,100
**------------------------------ DEFINIION OF SECTIONS
*SOLID SECTION,ELSET=CLAMP_TOP, MATERIAL=RIGID
*SOLID SECTION,ELSET=PLATE, MATERIAL=STEEL
*SOLID SECTION,ELSET=CLAMP_BOT, MATERIAL=RIGID
**-------------------------------DEFINITION OF RIGID NODES
*NODE, NSET=NS_REFNODE
1000000, 0, 0, -0.02
2000000, 0, 0,  0.02
**-----------------------------------DEFINITION OF SURFACES
*RIGID BODY, REFNODE=1000000, ELSET=CLAMP_BOT
*ELSET, ELSET=CLAMP_BOT_FACEP5, GENERATE
 3031,3080,1
*ELSET, ELSET=CLAMP_BOT_FACEP4, GENERATE
```

```
 3130,8030,100
*SURFACE, TYPE=ELEMENT,NAME=SURF_CLAMP_BOT
 CLAMP_BOT,S2
 CLAMP_BOT_FACEP4,S4
 CLAMP_BOT_FACEP5,S5
**
*ELSET, ELSET=PLATE_BOT, GENERATE
 10001,17980,1
*SURFACE, TYPE=ELEMENT, NAME=SURF_PLATE_BOT
 PLATE_BOT, S1
**
*ELSET, ELSET=PLATE_TOP, GENERATE
 40001,47980,1
*SURFACE, TYPE=ELEMENT, NAME=SURF_PLATE_TOP
 PLATE_TOP, S2
*ELSET, ELSET=LOAD_PLATE, GENERATE
43031, 43080, 1
43131, 43180, 1
43231, 43280, 1
43331, 43380, 1
43431, 43480, 1
43531, 43580, 1
43631, 43680, 1
43731, 43780, 1
43831, 43880, 1
43931, 43980, 1
44031, 44080, 1
44131, 44180, 1
44231, 44280, 1
44331, 44380, 1
44431, 44480, 1
44531, 44580, 1
44631, 44680, 1
44731, 44780, 1
44831, 44880, 1
44931, 44980, 1
45031, 45080, 1
45131, 45180, 1
45231, 45280, 1
45331, 45380, 1
45431, 45480, 1
45531, 45580, 1
45631, 45680, 1
45731, 45780, 1
45831, 45880, 1
45931, 45980, 1
```

```
46031, 46080, 1
46131, 46180, 1
46231, 46280, 1
46331, 46380, 1
46431, 46480, 1
46531, 46580, 1
46631, 46680, 1
46731, 46780, 1
46831, 46880, 1
46931, 46980, 1
47031, 47080, 1
47131, 47180, 1
47231, 47280, 1
47331, 47380, 1
47431, 47480, 1
47531, 47580, 1
47631, 47680, 1
47731, 47780, 1
47831, 47880, 1
47931, 47980, 1
**
*RIGID BODY, REFNODE=2000000, ELSET=CLAMP_TOP
*ELSET, ELSET=CLAMP_TOP_FACEP5, GENERATE
 53031,53080,1
*ELSET, ELSET=CLAMP_TOP_FACEP4, GENERATE
 53130,58030,100
*SURFACE, TYPE=ELEMENT,NAME=SURF_CLAMP_TOP
 CLAMP_TOP,S1
 CLAMP_TOP_FACEP4,S4
 CLAMP_TOP_FACEP5,S5
**----------------------------------DEFINITION OF MATERIAL PROPERTIES
*MATERIAL, NAME=STEEL
*INELASTIC HEAT FRACTION
*ELASTIC
2.10E11, .33, 0
1.98E11, .33, 200
1.75E11, .33, 600
1.47E11, .33, 700
1.25E11, .33, 800
1.09E11, .33, 900
1.00E11, .33, 1000
9.70E10, .33, 1100
*PLASTIC
2.37E8, 0.000000, 0
2.51E8, 0.007185, 0
2.97E8, 0.025556, 0
```

3.52E8, 0.051413, 0
4.10E8, 0.091745, 0
4.35E8, 0.115659, 0
4.63E8, 0.150734, 0
4.79E8, 0.174145, 0
4.95E8, 0.204152, 0
5.04E8, 0.226766, 0
5.11E8, 0.247764, 0
5.01E8, 0.280197, 0
2.37E8, 0.000000, 200
2.51E8, 0.007185, 200
2.97E8, 0.025556, 200
3.52E8, 0.051413, 200
4.10E8, 0.091745, 200
4.35E8, 0.115659, 200
4.63E8, 0.150734, 200
4.79E8, 0.174145, 200
4.95E8, 0.204152, 200
5.04E8, 0.226766, 200
5.11E8, 0.247764, 200
5.01E8, 0.280197, 200
3.15E7, 0.000000, 700
3.33E7, 0.007185, 700
3.95E7, 0.025556, 700
4.69E7, 0.051413, 700
5.45E7, 0.091745, 700
5.78E7, 0.115659, 700
6.16E7, 0.150734, 700
6.37E7, 0.174145, 700
6.58E7, 0.204152, 700
6.71E7, 0.226766, 700
6.79E7, 0.247764, 700
6.67E7, 0.280197, 700
3.93E6, 0.000000, 1000
4.15E6, 0.007185, 1000
4.94E6, 0.025556, 1000
5.85E6, 0.051413, 1000
6.81E6, 0.091745, 1000
7.22E6, 0.115659, 1000
7.69E6, 0.150734, 1000
7.94E6, 0.174145, 1000
8.22E6, 0.204152, 1000
8.37E6, 0.226766, 1000
8.47E6, 0.247764, 1000
8.33E6, 0.280197, 1000
*SPECIFIC HEAT

```
660
*RATE DEPENDENT
40.4, 5
*DENSITY
7850
**
*MATERIAL, NAME=RIGID
*ELASTIC
200E9, 0.3
*DENSITY
7800.
**------------------------------DEFINITION OF BOUNDARY CONDITIONS
*NSET, NSET=XSYMM, GENERATE
 23081,28081,100
 33081,38081,100
 43081,48081,100
 53081,58081,100
 63081,68081,100
**------------------------------
*NSET, NSET=YSYMM, GENERATE
 28031, 28081, 1
 38031, 38081, 1
 48031, 48081, 1
 58031, 58081, 1
 68031, 68081, 1
**-----------------------------ALL SYMMETRIC BC CREATED
*BOUNDARY, OP=NEW, TYPE=DISPLACEMENT
 XSYMM,  1,1, 0.0
 YSYMM,  2,2, 0.0
 1000000, 1,6, 0.0
 2000000, 1,2, 0.0
 2000000, 4,6, 0.0
**
*NSET, NSET=NS_ALL_PLATE, ELSET=PLATE
*INITIAL CONDITION, TYPE=TEMPERATURE
 NS_ALL_PLATE, 23.
**---------------------------------DEFINITION OF LOAD
*AMPLITUDE, NAME=BLAST, DEFINITION=TABULAR
0.0,1.0, 15E-6,1, 15.1E-6,0.0
**
**----------------------------THE ANALYSIS STEPS BEGIN
*STEP
*DYNAMIC, EXPLICIT, ADIABATICS
,0.005E-6
*CONTACT PAIR, INTERACTION=SMOOTH
 SURF_PLATE_TOP,SURF_CLAMP_TOP
```

```
 SURF_PLATE_BOT,SURF_CLAMP_BOT
*SURFACE INTERACTION, NAME=SMOOTH
*FRICTION
 0.25
*CLOAD
 2000000,3,-20E6
*OUTPUT, FIELD, VARIABLE=ALL, OP=NEW, NUMBER INTERVALS=2
*END STEP
**-----------------------------------------------
*STEP
*DYNAMIC, EXPLICIT, ADIABATICS
,15E-6
*DLOAD, AMPLITUDE=BLAST
 LOAD_PLATE, P2,  7.66E7
*OUTPUT, FIELD, VARIABLE=ALL, OP=NEW, NUMBER INTERVALS=100
*END STEP
**-----------------------------------------------
*STEP
*DYNAMIC, EXPLICIT, ADIABATICS
,200E-6
*DLOAD, OP=NEW
*END STEP
**-----------------------------------------------
*STEP
*DYNAMIC, EXPLICIT, ADIABATICS
,335E-6
*DLOAD, OP=NEW
*END STEP
**END
END OF ANALYSIS
```

UNIFORM BLAST LOADING ON CLAMPED SQUARE PLATE USING MATERIAL PROPERTIES THAT EXCLUDE TEMPERATURE DEPENDENCY

```
*HEADING
BLAST LOADING OF CLAMPED SQUARE PLATES
SI UNITS (kg, M, S, N)
*PREPRINT, MODEL=NO, ECHO=NO
**----------------------------------DEFINIION OF NODES
*NODE
 1,  0,0,0
 21, 0.0455, 0., 0.
 31, 0.0555, 0., 0.
 81, 0.1000, 0., 0.
*NGEN, NSET=EDGE1
 1,  21, 1
 21, 31, 1
 31, 81, 1
**
*NCOPY, SHIFT, OLDSET=EDGE1, CHANGE NUMBER=2000, NEWSET=EDGE2
 0,0.0455,0
 0,0,1, 0,0,1, 0
*NCOPY, SHIFT, OLDSET=EDGE1, CHANGE NUMBER=3000, NEWSET=EDGE3
 0,0.0555,0
 0,0,1, 0,0,1, 0
*NCOPY, SHIFT, OLDSET=EDGE1, CHANGE NUMBER=8000, NEWSET=EDGE4
 0,0.1,0
 0,0,1, 0,0,1, 0
**
*NFILL, NSET=FACE1
 EDGE1,EDGE2, 20, 100
 EDGE2,EDGE3, 10, 100
 EDGE3,EDGE4, 50, 100
** ---------------------------------- COPING FACE1 FOR THE OTHER FACES
*NCOPY, SHIFT, OLDSET=FACE1, NEWSET=FACE2, CHANGE NUMBER=10000
 0,0,0.0032
 0,0,1, 0,0,1, 0
*NCOPY, SHIFT, OLDSET=FACE1, NEWSET=FACE3, CHANGE NUMBER=20000
 0,0,0.0032
 0,0,1, 0,0,1, 0
*NCOPY, SHIFT, OLDSET=FACE1, NEWSET=FACE4, CHANGE NUMBER=30000
 0,0,0.0036
 0,0,1, 0,0,1, 0
*NCOPY, SHIFT, OLDSET=FACE1, NEWSET=FACE5, CHANGE NUMBER=40000
 0,0,0.004
 0,0,1, 0,0,1, 0
*NCOPY, SHIFT, OLDSET=FACE1, NEWSET=FACE6, CHANGE NUMBER=50000
 0,0,0.0044
```

```
 0,0,1, 0,0,1, 0
*NCOPY, SHIFT, OLDSET=FACE1, NEWSET=FACE7, CHANGE NUMBER=60000
 0,0,0.0048
 0,0,1, 0,0,1, 0
*NCOPY, SHIFT, OLDSET=FACE1, NEWSET=FACE8, CHANGE NUMBER=70000
 0,0,0.0048
 0,0,1, 0,0,1, 0
*NCOPY, SHIFT, OLDSET=FACE1, NEWSET=FACE9, CHANGE NUMBER=80000
 0,0,0.008
 0,0,1, 0,0,1, 0
**------------------------------ DEFINITION OF ELEMENTS
*ELEMENT, TYPE=C3D8R, ELSET=CLAMP_BOT
 1, 1,2,102,101, 10001,10002,10102,10101
 2101, 2001,2002,2102,2101, 12001,12002,12102,12101
 3101, 3001,3002,3102,3101, 13001,13002,13102,13101
*ELGEN, ELSET=CLAMP_BOT
 1, 80,1,1, 20,100,100
 2101,80,1,1,10,100,100
 3101,30,1,1,50,100,100
**------------------------------
*ELEMENT, TYPE=C3D8R, ELSET=PLATE
 10001, 20001,20002,20102,20101, 30001,30002,30102,30101
*ELGEN, ELSET=PLATE
 10001, 80,1,1, 80,100,100, 4,10000,10000
**------------------------------
*ELEMENT, TYPE=C3D8R, ELSET=CLAMP_TOP
 50001, 70001,70002,70102,70101, 80001,80002,80102,80101
 52101, 72001,72002,72102,72101, 82001,82002,82102,82101
 53101, 73001,73002,73102,73101, 83001,83002,83102,83101
*ELGEN, ELSET=CLAMP_TOP
 50001,80,1,1, 20,100,100
 52101,80,1,1, 10,100,100
 53101,30,1,1, 50,100,100
**------------------------------ DEFINITION OF SECTIONS
*SOLID SECTION,ELSET=CLAMP_TOP, MATERIAL=RIGID
*SOLID SECTION,ELSET=PLATE, MATERIAL=STEEL
*SOLID SECTION,ELSET=CLAMP_BOT, MATERIAL=RIGID
**------------------------------DEFINITION OF RIGID NODES
*NODE, NSET=NS_REFNODE
1000000, 0, 0, -0.02
2000000, 0, 0,  0.02
*8------------------------------DEFINIION OF SURFACES
*RIGID BODY, REFNODE=1000000, ELSET=CLAMP_BOT
*ELSET, ELSET=CLAMP_BOT_FACEP5, GENERATE
 3031,3080,1
*ELSET, ELSET=CLAMP_BOT_FACEP4, GENERATE
```

```
 3130,8030,100
*SURFACE, TYPE=ELEMENT,NAME=SURF_CLAMP_BOT
 CLAMP_BOT,S2
 CLAMP_BOT_FACEP4,S4
 CLAMP_BOT_FACEP5,S5
**------------------------------ PLATE SURFACES
*ELSET, ELSET=PLATE_BOT, GENERATE
 10001,17980,1
*SURFACE, TYPE=ELEMENT, NAME=SURF_PLATE_BOT
 PLATE_BOT, S1
**
*ELSET, ELSET=PLATE_TOP, GENERATE
 40001,47980,1
*SURFACE, TYPE=ELEMENT, NAME=SURF_PLATE_TOP
 PLATE_TOP, S2
*ELSET, ELSET=LOAD_PLATE, GENERATE
43031, 43080, 1
43131, 43180, 1
43231, 43280, 1
43331, 43380, 1
43431, 43480, 1
43531, 43580, 1
43631, 43680, 1
43731, 43780, 1
43831, 43880, 1
43931, 43980, 1
44031, 44080, 1
44131, 44180, 1
44231, 44280, 1
44331, 44380, 1
44431, 44480, 1
44531, 44580, 1
44631, 44680, 1
44731, 44780, 1
44831, 44880, 1
44931, 44980, 1
45031, 45080, 1
45131, 45180, 1
45231, 45280, 1
45331, 45380, 1
45431, 45480, 1
45531, 45580, 1
45631, 45680, 1
45731, 45780, 1
45831, 45880, 1
45931, 45980, 1
```

```
46031, 46080, 1
46131, 46180, 1
46231, 46280, 1
46331, 46380, 1
46431, 46480, 1
46531, 46580, 1
46631, 46680, 1
46731, 46780, 1
46831, 46880, 1
46931, 46980, 1
47031, 47080, 1
47131, 47180, 1
47231, 47280, 1
47331, 47380, 1
47431, 47480, 1
47531, 47580, 1
47631, 47680, 1
47731, 47780, 1
47831, 47880, 1
47931, 47980, 1
**
*RIGID BODY, REFNODE=2000000, ELSET=CLAMP_TOP
*ELSET, ELSET=CLAMP_TOP_FACEP5, GENERATE
 53031,53080,1
*ELSET, ELSET=CLAMP_TOP_FACEP4, GENERATE
 53130,58030,100
*SURFACE, TYPE=ELEMENT,NAME=SURF_CLAMP_TOP
 CLAMP_TOP,S1
 CLAMP_TOP_FACEP4,S4
 CLAMP_TOP_FACEP5,S5
**----------------------------------DEFINITION OF MATERIL PROPERTIES
*MATERIAL, NAME=STEEL
*INELASTIC HEAT FRACTION
*ELASTIC
2.10E11
*PLASTIC
2.37E8, 0.000000
2.51E8, 0.007185
2.97E8, 0.025556
3.52E8, 0.051413
4.10E8, 0.091745
4.35E8, 0.115659
4.63E8, 0.150734
4.79E8, 0.174145
4.95E8, 0.204152
5.04E8, 0.226766
```

```
5.11E8, 0.247764
5.01E8, 0.280197
*SPECIFIC HEAT
660
*RATE DEPENDENT
40.4, 5
*DENSITY
7850
**
*MATERIAL, NAME=RIGID
*ELASTIC
200E9, 0.3
*DENSITY
7800.
**------------------------------DEFINITION OF BOUNDARY CONDITIONS
*NSET, NSET=XSYMM, GENERATE
 23081,28081,100
 33081,38081,100
 43081,48081,100
 53081,58081,100
 63081,68081,100
**------------------------------
*NSET, NSET=YSYMM, GENERATE
 28031, 28081, 1
 38031, 38081, 1
 48031, 48081, 1
 58031, 58081, 1
 68031, 68081, 1
**------------------------------
*BOUNDARY, OP=NEW, TYPE=DISPLACEMENT
 XSYMM,   1,1, 0.0
 YSYMM,   2,2, 0.0
 1000000, 1,6, 0.0
 2000000, 1,2, 0.0
 2000000, 4,6, 0.0
**------------------------------DEFINITION OF LOAD
*AMPLITUDE, NAME=BLAST, DEFINITION=TABULAR
0.0,1.0, 15E-6,1, 15.1E-6,0.0
**
**------------------------------ANALYSIS STEPS BEGIN
*STEP
*DYNAMIC, EXPLICIT, ADIABATICS
,0.005E-6
*CONTACT PAIR, INTERACTION=SMOOTH
 SURF_PLATE_TOP,SURF_CLAMP_TOP
 SURF_PLATE_BOT,SURF_CLAMP_BOT
```

```
*SURFACE INTERACTION, NAME=SMOOTH
*FRICTION
 0.25
*CLOAD
 2000000,3,-10E6
*OUTPUT, FIELD, VARIABLE=ALL, OP=NEW, NUMBER INTERVALS=2
*END STEP
**-----------------------------------------------
*STEP
*DYNAMIC, EXPLICIT
,15E-6
*DLOAD, AMPLITUDE=BLAST
 LOAD_PLATE, P2, 7.66E7
*OUTPUT, FIELD, VARIABLE=ALL, OP=NEW, NUMBER INTERVALS=100
*END STEP
**-----------------------------------------------
*STEP
*DYNAMIC, EXPLICIT
,100E-6
*DLOAD, OP=NEW
*END STEP
**-----------------------------------------------
*STEP
*DYNAMIC, EXPLICIT
,235E-6
*DLOAD, OP=NEW
*END STEP
**END
```

UNIFORM BLAST LOADING ON BUILT-IN PLATE USING MATERIAL PROPERTIES THAT INCLUDE TEMPERATURE DEPENDENCY

```
*HEADING
BLAST LOADING OF SQUARE PLATES
SI UNITS (kg, M, S, N)
*PREPRINT, MODEL=NO, ECHO=NO
**----------------------------------DEFINITION OF NODES
*NODE
 1,  0,0,0
 21, 0.0555, 0., 0.
 41, 0.1000, 0., 0.
*NGEN, NSET=EDGE1
 1, 21, 1
 21, 41, 1
**
*NCOPY, SHIFT, OLDSET=EDGE1, CHANGE NUMBER=2000, NEWSET=EDGE2
 0,0.0555,0
 0,0,1, 0,0,1, 0
*NCOPY, SHIFT, OLDSET=EDGE1, CHANGE NUMBER=4000, NEWSET=EDGE3
 0,0.1,0
 0,0,1, 0,0,1, 0
**
*NFILL, NSET=FACE1
 EDGE1,EDGE2, 20, 100
 EDGE2,EDGE3, 20, 100
** ---------------------------------- COPYING FACE1 FOR EACH OF THE FACE1
*NCOPY, SHIFT, OLDSET=FACE1, NEWSET=FACE2, CHANGE NUMBER=10000
 0,0,0.02
 0,0,1, 0,0,1, 0
*NCOPY, SHIFT, OLDSET=FACE1, NEWSET=FACE3, CHANGE NUMBER=20000
 0,0,0.0204
 0,0,1, 0,0,1, 0
*NCOPY, SHIFT, OLDSET=FACE1, NEWSET=FACE4, CHANGE NUMBER=30000
 0,0,0.0208
 0,0,1, 0,0,1, 0
*NCOPY, SHIFT, OLDSET=FACE1, NEWSET=FACE5, CHANGE NUMBER=40000
 0,0,0.0212
 0,0,1, 0,0,1, 0
*NCOPY, SHIFT, OLDSET=FACE1, NEWSET=FACE6, CHANGE NUMBER=50000
 0,0,0.0216
 0,0,1, 0,0,1, 0
*NCOPY, SHIFT, OLDSET=FACE1, NEWSET=FACE7, CHANGE NUMBER=60000
 0,0,0.0416
 0,0,1, 0,0,1, 0
```

```
**--------------------------------DEFINITION OF ELEMENTS
*ELEMENT, TYPE=C3D8R, ELSET=CLAMP_BOT
 1, 1,2,102,101, 10001,10002,10102,10101
 2101, 2001,2002,2102,2101, 12001,12002,12102,12101
*ELGEN, ELSET=CLAMP_BOT
 1, 40,1,1, 20,100,100
 2101,20,1,1,20,100,100
**------------------------------
*ELEMENT, TYPE=C3D8R, ELSET=PLATE
 10001, 10001,10002,10102,10101, 20001,20002,20102,20101
*ELGEN, ELSET=PLATE
 10001, 40,1,1, 40,100,100, 4,10000,10000
**------------------------------
*ELEMENT, TYPE=C3D8R, ELSET=CLAMP_TOP
 50001, 50001,50002,50102,50101, 60001,60002,60102,60101
 52101, 52001,52002,52102,52101, 62001,62002,62102,62101
*ELGEN, ELSET=CLAMP_TOP
 50001,40,1,1, 20,100,100
 52101,20,1,1, 20,100,100
**--------------------------------DEFINITION OF SECTIONS
*SOLID SECTION,ELSET=CLAMP_TOP, MATERIAL=STEEL
*SOLID SECTION,ELSET=PLATE, MATERIAL=STEEL
*SOLID SECTION,ELSET=CLAMP_BOT, MATERIAL=STEEL
**------------------------------
*ELSET, ELSET=PLATE_BOT, GENERATE
 10001,13940,1
*ELSET, ELSET=LOAD_PLATE, GENERATE
42021, 42040, 1
42121, 42140, 1
42221, 42240, 1
42321, 42340, 1
42421, 42440, 1
42521, 42540, 1
42621, 42640, 1
42721, 42740, 1
42821, 42840, 1
42921, 42940, 1
43021, 43040, 1
43121, 43140, 1
43221, 43240, 1
43321, 43340, 1
43421, 43440, 1
43521, 43540, 1
43621, 43640, 1
43721, 43740, 1
43821, 43840, 1
```

```
43921, 43940, 1
**----------------------------------DEFINITION OF MATERIAL PROPERTIES
*MATERIAL, NAME=STEEL
*INELASTIC HEAT FRACTION
*ELASTIC
2.10E11, .33, 0
1.98E11, .33, 200
1.75E11, .33, 600
1.47E11, .33, 700
1.25E11, .33, 800
1.09E11, .33, 900
1.00E11, .33, 1000
9.70E10, .33, 1100
*PLASTIC
2.37E8, 0.000000, 0
2.51E8, 0.007185, 0
2.97E8, 0.025556, 0
3.52E8, 0.051413, 0
4.10E8, 0.091745, 0
4.35E8, 0.115659, 0
4.63E8, 0.150734, 0
4.79E8, 0.174145, 0
4.95E8, 0.204152, 0
5.04E8, 0.226766, 0
5.11E8, 0.247764, 0
5.01E8, 0.280197, 0
2.37E8, 0.000000, 200
2.51E8, 0.007185, 200
2.97E8, 0.025556, 200
3.52E8, 0.051413, 200
4.10E8, 0.091745, 200
4.35E8, 0.115659, 200
4.35E8, 0.150734, 200
4.63E8, 0.174145, 200
4.79E8, 0.204152, 200
5.04E8, 0.226766, 200
5.11E8, 0.247764, 200
5.01E8, 0.280197, 200
4.19E6, 0.000000, 700
4.43E6, 0.007185, 700
5.26E6, 0.025556, 700
6.23E6, 0.051413, 700
7.25E6, 0.091745, 700
7.69E6, 0.115659, 700
8.19E6, 0.150734, 700
8.47E6, 0.174145, 700
```

```
8.75E6, 0.204152, 700
8.92E6, 0.226766, 700
9.03E6, 0.247764, 700
8.87E6, 0.280197, 700
6.48E4, 0.000000, 1000
6.85E4, 0.007185, 1000
8.14E4, 0.025556, 1000
9.63E4, 0.051413, 1000
11.2E4, 0.091745, 1000
11.9E4, 0.115659, 1000
12.7E4, 0.150734, 1000
13.1E4, 0.174145, 1000
13.5E4, 0.204152, 1000
13.8E4, 0.226766, 1000
13.9E4, 0.247764, 1000
13.7E4, 0.280197, 1000
*SPECIFIC HEAT
660
*RATE DEPENDENT
40.4, 5
*DENSITY
7850
**----------------------------------DEFINITION OF BOUNDARY NODES
*NSET, NSET=XSYMM, GENERATE
 12041,14041,100
 22041,24041,100
 32041,34041,100
 42041,44041,100
 52041,54041,100
**-----------------------------
*NSET, NSET=YSYMM, GENERATE
 14021, 14041, 1
 24021, 24041, 1
 34021, 34041, 1
 44021, 44041, 1
 54021, 54041, 1
**-----------------------------
*NSET, NSET=BOUND1, GENERATE
1,    41,    1
10001, 10041, 1
20001, 20041, 1
30001, 30041, 1
40001, 40041, 1
50001, 50041, 1
60001, 60041, 1
*NSET, NSET=BOUND2, GENERATE
```

```
41,   2041,  100
10041, 12041, 100
20041, 22041, 100
30041, 32041, 100
40041, 42041, 100
50041, 52041, 100
60041, 62041, 100
*NSET, NSET=BOUND3, GENERATE
4001,  4021,  1
14001, 14021, 1
24001, 24021, 1
34001, 34021, 1
44001, 44021, 1
54001, 54021, 1
64001, 64021, 1
*NSET, NSET=BOUND4, GENERATE
1,          4001,  100
10001, 14001, 100
20001, 24001, 100
30001, 34001, 100
40001, 44001, 100
50001, 54001, 100
60001, 64001, 100
**------------------------------DEFINITION OF BOUNDARY CONDITIONS
*BOUNDARY, OP=NEW, TYPE=DISPLACEMENT
 XSYMM,  1, 1, 0.0
 YSYMM,  2, 2, 0.0
 BOUND1, 1, 6, 0.0
 BOUND2, 1, 6, 0.0
 BOUND3, 1, 6, 0.0
 BOUND4, 1, 6, 0.0
**---------------------------
*NSET, NSET=NS_ALL_PLATE, ELSET=PLATE
*INITIAL CONDITION, TYPE=TEMPERATURE
 NS_ALL_PLATE, 23.
**------------------------------DEFINITION OF LOAD
*AMPLITUDE, NAME=BLAST, DEFINITION=TABULAR
0.0,1.0, 15E-6,1, 15.1E-6,0.0
**---------------------------- ANALYSIS STEPS BEGIN
*STEP
*DYNAMIC, EXPLICIT, ADIABATICS
,15E-6
*DLOAD, AMPLITUDE=BLAST
 LOAD_PLATE, P2, 7.66E7
*OUTPUT, FIELD, VARIABLE=ALL, OP=NEW, NUMBER INTERVALS=100
*END STEP
```

```
**----------------------------------
*STEP
*DYNAMIC, EXPLICIT, ADIABATICS
,35E-6
*DLOAD, OP=NEW
*END STEP
**----------------------------------
*STEP
*DYNAMIC, EXPLICIT, ADIABATICS
,100E-6
*DLOAD, OP=NEW
*END STEP
**END
```

UNIFORM BLAST LOADING ON BUILT-IN SQUARE PLATE USING MATERIAL PROPERTIES THAT EXCLUDE TEMPERATURE DEPENDENCY

```
*HEADING
BLAST LOADING OF BUILT-IN SQUARE PLATES
SI UNITS (kg, M, S, N)
*PREPRINT, MODEL=NO, ECHO=NO
**----------------------------------DEFINITION OF NODES
*NODE
 1,  0,0,0
 21, 0.0455, 0., 0.
 31, 0.0555, 0., 0.
 81, 0.1000, 0., 0.
*NGEN, NSET=EDGE1
 1, 21, 1
 21, 31, 1
 31, 81, 1
**
*NCOPY, SHIFT, OLDSET=EDGE1, CHANGE NUMBER=2000, NEWSET=EDGE2
 0,0.0455,0
 0,0,1, 0,0,1, 0
*NCOPY, SHIFT, OLDSET=EDGE1, CHANGE NUMBER=3000, NEWSET=EDGE3
 0,0.0555,0
 0,0,1, 0,0,1, 0
*NCOPY, SHIFT, OLDSET=EDGE1, CHANGE NUMBER=8000, NEWSET=EDGE4
 0,0.1,0
 0,0,1, 0,0,1, 0
**
*NFILL, NSET=FACE1
 EDGE1,EDGE2, 20, 100
 EDGE2,EDGE3, 10, 100
 EDGE3,EDGE4, 50, 100
** ---------------------------------- COPING FACE1 FOR EACH OF THE FACES
*NCOPY, SHIFT, OLDSET=FACE1, NEWSET=FACE2, CHANGE NUMBER=10000
 0,0,0.0032
 0,0,1, 0,0,1, 0
*NCOPY, SHIFT, OLDSET=FACE1, NEWSET=FACE3, CHANGE NUMBER=20000
 0,0,0.0036
 0,0,1, 0,0,1, 0
*NCOPY, SHIFT, OLDSET=FACE1, NEWSET=FACE4, CHANGE NUMBER=30000
 0,0,0.004
 0,0,1, 0,0,1, 0
*NCOPY, SHIFT, OLDSET=FACE1, NEWSET=FACE5, CHANGE NUMBER=40000
 0,0,0.0044
 0,0,1, 0,0,1, 0
*NCOPY, SHIFT, OLDSET=FACE1, NEWSET=FACE6, CHANGE NUMBER=50000
 0,0,0.0048
```

```
 0,0,1, 0,0,1, 0
*NCOPY, SHIFT, OLDSET=FACE1, NEWSET=FACE7, CHANGE NUMBER=60000
 0,0,0.0052
 0,0,1, 0,0,1, 0
**----------DEFINITION OF ELEMENTS
*ELEMENT, TYPE=C3D8R, ELSET=BUILT_BOT
 1, 1,2,102,101, 10001,10002,10102,10101
 2101, 2001,2002,2102,2101, 12001,12002,12102,12101
 3101, 3001,3002,3102,3101, 13001,13002,13102,13101
*ELGEN, ELSET=BUILT_BOT
 1, 80,1,1, 20,100,100
 2101,80,1,1,10,100,100
 3101,30,1,1,50,100,100
**----------
*ELEMENT, TYPE=C3D8R, ELSET=PLATE
 10001, 20001,20002,20102,20101, 30001,30002,30102,30101
*ELGEN, ELSET=PLATE
 10001, 80,1,1, 80,100,100, 4,10000,10000
**---------- DEFINITION OF SECTIONS
*SOLID SECTION,ELSET=PLATE, MATERIAL=STEEL
*SOLID SECTION,ELSET=BUILT_BOT, MATERIAL=STEEL
**
*ELSET, ELSET=BUILT_BOT_FACEP5, GENERATE
 3031,3080,1
*ELSET, ELSET=BUILT_BOT_FACEP4, GENERATE
 3130,8030,100
*SURFACE, TYPE=ELEMENT,NAME=SURF_BUILT_BOT
 BUILT_BOT,S2
 BUILT_BOT_FACEP4,S4
 BUILT_BOT_FACEP5,S5
**----------
*ELSET, ELSET=PLATE_BOT, GENERATE
 10001,17980,1
*SURFACE, TYPE=ELEMENT, NAME=SURF_PLATE_BOT
 PLATE_BOT, S1
**
*ELSET, ELSET=PLATE_TOP, GENERATE
 40001,47980,1
*SURFACE, TYPE=ELEMENT, NAME=SURF_PLATE_TOP
 PLATE_TOP, S2
**----------DEFINITION OF SURFACES
*ELSET, ELSET=LOAD_PLATE, GENERATE
43031, 43080, 1
43131, 43180, 1
43231, 43280, 1
43331, 43380, 1
```

43431, 43480, 1
43531, 43580, 1
43631, 43680, 1
43731, 43780, 1
43831, 43880, 1
43931, 43980, 1
44031, 44080, 1
44131, 44180, 1
44231, 44280, 1
44331, 44380, 1
44431, 44480, 1
44531, 44580, 1
44631, 44680, 1
44731, 44780, 1
44831, 44880, 1
44931, 44980, 1
45031, 45080, 1
45131, 45180, 1
45231, 45280, 1
45331, 45380, 1
45431, 45480, 1
45531, 45580, 1
45631, 45680, 1
45731, 45780, 1
45831, 45880, 1
45931, 45980, 1
46031, 46080, 1
46131, 46180, 1
46231, 46280, 1
46331, 46380, 1
46431, 46480, 1
46531, 46580, 1
46631, 46680, 1
46731, 46780, 1
46831, 46880, 1
46931, 46980, 1
47031, 47080, 1
47131, 47180, 1
47231, 47280, 1
47331, 47380, 1
47431, 47480, 1
47531, 47580, 1
47631, 47680, 1
47731, 47780, 1
47831, 47880, 1
47931, 47980, 1

```
**----------------------------------DEFINITION OF MATERIAL PROPERTIES
*MATERIAL, NAME=STEEL
*INELASTIC HEAT FRACTION
*ELASTIC
2.10E11, .33
*PLASTIC
2.37E8, 0.000000
2.51E8, 0.007185
2.97E8, 0.025556
3.52E8, 0.051413
4.10E8, 0.091745
4.35E8, 0.115659
4.63E8, 0.150734
4.79E8, 0.174145
4.95E8, 0.204152
5.04E8, 0.226766
5.11E8, 0.247764
5.01E8, 0.280197
*SPECIFIC HEAT
660
*RATE DEPENDENT
40.4, 5
*DENSITY
7850
**--------------------------------DEFINITION OF BOUNDARY CONDITIONS
*NSET, NSET=XSYMM, GENERATE
 23081,28081,100
 33081,38081,100
 43081,48081,100
 53081,58081,100
 63081,68081,100
**----------------------------
*NSET, NSET=YSYMM, GENERATE
 28031, 28081, 1
 38031, 38081, 1
 48031, 48081, 1
 58031, 58081, 1
 68031, 68081, 1
**-------------------------
*NSET, NSET=BOUND1, GENERATE
1,    81,   1
10001, 10081, 1
20001, 20081, 1
30001, 30081, 1
40001, 40081, 1
50001, 50081, 1
```

```
60001, 60081, 1
*NSET, NSET=BOUND2, GENERATE
1,    8001,  100
10001, 18001, 100
20001, 28001, 100
30001, 38001, 100
40001, 48001, 100
50001, 58001, 100
60001, 68001, 100
**-----------------------------
 *BOUNDARY, OP=NEW, TYPE=DISPLACEMENT
 XSYMM,   1,1, 0.0
 YSYMM,   2,2, 0.0
 BOUND1, 1, 6, 0.0
 BOUND2, 1, 6, 0.0
**------------------------------DEFINITION OF LOAD
*AMPLITUDE, NAME=BLAST, DEFINITION=TABULAR
0.0,1.0, 15E-6,1, 15.1E-6,0.0
**---------------------------ANALYSIS STEPS BEGIN
*STEP
*DYNAMIC, EXPLICIT
,0.005E-6
*CONTACT PAIR, INTERACTION=SMOOTH
 SURF_PLATE_BOT,SURF_BUILT_BOT
*SURFACE INTERACTION, NAME=SMOOTH
*FRICTION
 0.9
*OUTPUT, FIELD, VARIABLE=ALL, OP=NEW, NUMBER INTERVALS=2
*END STEP
**----------------------------THE ANALYSIS STEP BEGINS HERE
*STEP
*DYNAMIC, EXPLICIT
,15E-6
*DLOAD, AMPLITUDE=BLAST
 LOAD_PLATE, P2, 7.66E7
*OUTPUT, FIELD, VARIABLE=ALL, OP=NEW, NUMBER INTERVALS=100
*END STEP
**---------------------------------------------
*STEP
*DYNAMIC, EXPLICIT
,200E-6
*DLOAD, OP=NEW
*END STEP
**---------------------------------------------
*STEP
*DYNAMIC, EXPLICIT
```

```
,235E-6
*DLOAD, OP=NEW
*END STEP
**END
**END OF ANALYSIS
```

UNIFORM BLAST LOADING ON CLAMPED RECTANGULAR BEAM USING MATERIAL PROPERTIES THAT INCLUDE TEMPERATURE DEPENDENCY

```
*HEADING
BLAST LOADING OF CLAMPED RECTANGULAR BEAMS
SI UNITS (Kg, M, S, N)
*PREPRINT, MODEL=NO, ECHO=NO
**----------------------------------DEFINITION OF NODES
*NODE
 1,  0,0,0
 16, 0.0254, 0., 0.
 31, 0.0508, 0., 0.
 81, 0.1524, 0., 0.
*NGEN, NSET=EDGE1
 1,  16, 1
 16, 31, 1
 31, 81, 1
**
*NCOPY, SHIFT, OLDSET=EDGE1, CHANGE NUMBER=2000, NEWSET=EDGE2
 0, 0.0127, 0
 0, 0, 1, 0, 0,1, 0
*NFILL, NSET=FACE1
 EDGE1,EDGE2, 20, 100
** ---------------------------------------- FACE1 FOR EACH OF THE FACES
*NCOPY, SHIFT, OLDSET=FACE1, NEWSET=FACE2, CHANGE NUMBER=10000
 0,0,0.0032
 0,0,1, 0,0,1, 0
*NCOPY, SHIFT, OLDSET=FACE1, NEWSET=FACE3, CHANGE NUMBER=20000
 0,0,0.0032
 0,0,1, 0,0,1, 0
*NCOPY, SHIFT, OLDSET=FACE1, NEWSET=FACE4, CHANGE NUMBER=30000
 0,0,0.0041525
 0,0,1, 0,0,1, 0
*NCOPY, SHIFT, OLDSET=FACE1, NEWSET=FACE5, CHANGE NUMBER=40000
 0,0,0.005105
 0,0,1, 0,0,1, 0
*NCOPY, SHIFT, OLDSET=FACE1, NEWSET=FACE6, CHANGE NUMBER=50000
 0,0,0.0060575
 0,0,1, 0,0,1, 0
*NCOPY, SHIFT, OLDSET=FACE1, NEWSET=FACE7, CHANGE NUMBER=60000
 0,0,0.00701
 0,0,1, 0,0,1, 0
*NCOPY, SHIFT, OLDSET=FACE1, NEWSET=FACE8, CHANGE NUMBER=70000
 0,0,0.0079625
 0,0,1, 0,0,1, 0
*NCOPY, SHIFT, OLDSET=FACE1, NEWSET=FACE9, CHANGE NUMBER=80000
 0,0,0.008915
```

```
 0,0,1, 0,0,1, 0
*NCOPY, SHIFT, OLDSET=FACE1, NEWSET=FACE10, CHANGE
NUMBER=90000
 0,0,0.0098675
 0,0,1, 0,0,1, 0
*NCOPY, SHIFT, OLDSET=FACE1, NEWSET=FACE11, CHANGE
NUMBER=100000
 0,0,0.01082
 0,0,1, 0,0,1, 0
*NCOPY, SHIFT, OLDSET=FACE1, NEWSET=FACE12, CHANGE
NUMBER=110000
 0,0,0.0117725
 0,0,1, 0,0,1, 0
*NCOPY, SHIFT, OLDSET=FACE1, NEWSET=FACE13, CHANGE
NUMBER=120000
 0,0,0.012725
 0,0,1, 0,0,1, 0
*NCOPY, SHIFT, OLDSET=FACE1, NEWSET=FACE14, CHANGE
NUMBER=130000
 0,0,0.012725
 0,0,1, 0,0,1, 0
*NCOPY, SHIFT, OLDSET=FACE1, NEWSET=FACE15, CHANGE
NUMBER=140000
 0,0,0.015925
 0,0,1, 0,0,1, 0
**----------------------------------------DEFINITION OF ELEMENTS
*ELEMENT, TYPE=C3D8R, ELSET=CLAMP_BOT
 1, 1,2,102,101, 10001,10002,10102,10101
*ELGEN, ELSET=CLAMP_BOT
 1, 30,1,1, 20,100,100
**
*ELEMENT, TYPE=C3D8R, ELSET=BEAM
 10001, 20001,20002,20102,20101, 30001,30002,30102,30101
*ELGEN, ELSET=BEAM
 10001, 80,1,1, 20,100,100, 10,10000,10000
**
*ELEMENT, TYPE=C3D8R, ELSET=CLAMP_TOP
 110001, 130001,130002,130102,130101, 140001,140002,140102,140101
*ELGEN, ELSET=CLAMP_TOP
 110001,30,1,1, 20,100,100
**---------------------------------DEFINITION OF SECTIONS
*SOLID SECTION,ELSET=CLAMP_TOP, MATERIAL=RIGID
*SOLID SECTION,ELSET=BEAM, MATERIAL=ALUMINIUM
*SOLID SECTION,ELSET=CLAMP_BOT, MATERIAL=RIGID
```

```
**----------------------------------DEFINITION OF RIGID BODY NODES
*NODE, NSET=NS_REFNODE
1000000, 0, 0, -0.05
2000000, 0, 0,  0.05
**----------------------------------DEFINITION OF SURFACES
*RIGID BODY, REFNODE=1000000, ELSET=CLAMP_BOT
*ELSET, ELSET=CLAMP_BOT_FACEP4, GENERATE
 30,1930,100
*SURFACE, TYPE=ELEMENT,NAME=SURF_CLAMP_BOT
 CLAMP_BOT,S2
 CLAMP_BOT_FACEP4,S4
**
*ELSET, ELSET=BEAM_BOT, GENERATE
 10001,11980,1
*SURFACE, TYPE=ELEMENT, NAME=SURF_BEAM_BOT
 BEAM_BOT, S1
**
*ELSET, ELSET=BEAM_TOP, GENERATE
 100001,101980,1
*SURFACE, TYPE=ELEMENT, NAME=SURF_BEAM_TOP
 BEAM_TOP, S2
**
*ELSET, ELSET=LOAD_BEAM, GENERATE
100031, 100080, 1
100131, 100180, 1
100231, 100280, 1
100331, 100380, 1
100431, 100480, 1
100531, 100580, 1
100631, 100680, 1
100731, 100780, 1
100831, 100880, 1
100931, 100980, 1
101031, 101080, 1
101131, 101180, 1
101231, 101280, 1
101331, 101380, 1
101431, 101480, 1
101531, 101580, 1
101631, 101680, 1
101731, 101780, 1
101831, 101880, 1
101931, 101980, 1
*RIGID BODY, REFNODE=2000000, ELSET=CLAMP_TOP
*ELSET, ELSET=CLAMP_TOP_FACEP4, GENERATE
```

```
 110030,111930,100
*SURFACE, TYPE=ELEMENT,NAME=SURF_CLAMP_TOP
 CLAMP_TOP,S1
 CLAMP_TOP_FACEP4,S4
**----------------------------------DEFINITION OF MATERIAL PROPERTIES
*MATERIAL, NAME=ALUMINIUM
*INELASTIC HEAT FRACTION
*ELASTIC
7.24E10, .32, 0
6.07E10, .32, 25
3.74E10, .32, 100
3.24E10, .32, 200
3.02E10, .32, 300
*PLASTIC
2.81E8, 0.000000, 0
2.83E8, 0.007150, 0
2.86E8, 0.007710, 0
2.88E8, 0.008070, 0
2.90E8, 0.008480, 0
2.93E8, 0.009030, 0
2.95E8, 0.009670, 0
2.97E8, 0.010200, 0
2.99E8, 0.010800, 0
3.00E8, 0.011300, 0
3.03E8, 0.013400, 0
3.01E8, 0.013900, 0
2.81E8, 0.000000, 25
2.83E8, 0.007150, 25
2.86E8, 0.007710, 25
2.88E8, 0.008070, 25
2.90E8, 0.008480, 25
2.93E8, 0.009030, 25
2.95E8, 0.009670, 25
2.97E8, 0.010200, 25
2.99E8, 0.010800, 25
3.00E8, 0.011300, 25
3.03E8, 0.013400, 25
3.01E8, 0.013900, 25
2.43E8, 0.000000, 100
2.45E8, 0.007150, 100
2.48E8, 0.007710, 100
2.50E8, 0.008070, 100
2.51E8, 0.008480, 100
2.54E8, 0.009030, 100
2.56E8, 0.009670, 100
2.57E8, 0.010200, 100
```

```
2.59E8, 0.010800, 100
2.60E8, 0.011300, 100
2.63E8, 0.013400, 100
2.61E8, 0.013900, 100
1.93E8, 0.000000, 200
1.95E8, 0.007150, 200
1.97E8, 0.007710, 200
1.98E8, 0.008070, 200
2.00E8, 0.008480, 200
2.02E8, 0.009030, 200
2.03E8, 0.009670, 200
2.04E8, 0.010200, 200
2.06E8, 0.010800, 200
2.07E8, 0.011300, 200
2.09E8, 0.013400, 200
2.07E8, 0.013900, 200
2.65E7, 0.000000, 300
2.66E7, 0.007150, 300
2.69E7, 0.007710, 300
2.71E7, 0.008070, 300
2.73E7, 0.008480, 300
2.76E7, 0.009030, 300
2.78E7, 0.009670, 300
2.80E7, 0.010200, 300
2.82E7, 0.010800, 300
2.82E7, 0.011300, 300
2.85E7, 0.013400, 300
2.83E7, 0.013900, 300
*SPECIFIC HEAT
937.4
*RATE DEPENDENT
6500, 4
*DENSITY
2686
**
*MATERIAL, NAME=RIGID
*ELASTIC
200E9, 0.3
*DENSITY
2686.
**------------------------------DEFINITION OF BOUNDARY CONDITIONS
*NSET, NSET=XSYMM, GENERATE
 20081, 22081, 100
 30081, 32081, 100
 40081, 42081, 100
 50081, 52081, 100
```

```
 60081, 62081, 100
 70081, 72081, 100
 80081, 82081, 100
 90081, 92081, 100
 100081,102081, 100
 110081,112081, 100
 120081,123081, 100
**
*NSET, NSET=YSYMM, GENERATE
 22001,   22081,  1
 32001,   32081,  1
 42001,   42081,  1
 52001,   52081,  1
 62001,   62081,  1
 72001,   72081,  1
 82001,   82081,  1
 92001,   92081,  1
 102001, 102081, 1
 112001, 112081, 1
 122001, 122081, 1
*NSET, NSET=B1, GENERATE
20001,   20031, 1
30001,   30031, 1
40001,   40031, 1
50001,   50031, 1
60001,   60031, 1
70001,   70031, 1
80001,   80031, 1
90001,   90031, 1
100001, 100031,1
110001, 110031,1
120001, 120031,1
*NSET, NSET=B2, GENERATE
20001,   22001, 100
30001,   32001, 100
40001,   42001, 100
50001,   52001, 100
60001,   62001, 100
70001,   72001, 100
80001,   82001, 100
90001,   92001, 100
100001, 102001, 100
110001, 112001, 100
120001, 122001, 100
*NSET, NSET=B3, GENERATE
22001,  22031,  1
```

```
32001,  32031,  1
42001,   42031,  1
52001,   52031,  1
62001,   62031,  1
72001,   72031,  1
82001,   82031,  1
92001,   92031,  1
102001,  102031, 1
112001,  112031, 1
122001,  122031, 1
*NSET, NSET=B4, GENERATE
120030, 122030, 100
**
*BOUNDARY, OP=NEW, TYPE=DISPLACEMENT
 XSYMM,   1,1, 0.0
 YSYMM,   2,2, 0.0
 B1, 1,6, 0.0
 B2, 1,6, 0.0
 B3, 1,6, 0.0
 B4, 1,6, 0.0
 1000000, 1,6, 0.0
 2000000, 1,2, 0.0
 2000000, 4,6, 0.0
**
*NSET, NSET=NS_ALL_BEAM, ELSET=BEAM
*INITIAL CONDITION, TYPE=TEMPERATURE
 NS_ALL_BEAM, 0.
**----------------------------------DEFINITION OF LOAD
*AMPLITUDE, NAME=BLAST, DEFINITION=TABULAR
0.0,1.0, 30E-6,1, 30.1E-6,0.0
**---------------------------ANALYSIS STEPS BEGIN
*STEP
*DYNAMIC, EXPLICIT, ADIABATICS
,0.005E-6
*CONTACT PAIR, INTERACTION=SMOOTH
 SURF_BEAM_TOP,SURF_CLAMP_TOP
 SURF_BEAM_BOT,SURF_CLAMP_BOT
*SURFACE INTERACTION, NAME=SMOOTH
*FRICTION
 0.35
*CLOAD
 2000000,3,-1E5
*OUTPUT, FIELD, VARIABLE=ALL, OP=NEW, NUMBER INTERVALS=2
*END STEP
```

```
**
*STEP
*DYNAMIC, EXPLICIT, ADIABATICS
,30E-6
*DLOAD, AMPLITUDE=BLAST
 LOAD_BEAM, P2, 5.92E7
*OUTPUT, FIELD, VARIABLE=ALL, OP=NEW, NUMBER INTERVALS=100
*END STEP
**
*STEP
*DYNAMIC, EXPLICIT, ADIABATICS
,470E-6
*DLOAD, OP=NEW
*END STEP
**
*STEP
*DYNAMIC, EXPLICIT, ADIABATICS
,350E-6
*DLOAD, OP=NEW
*END STEP
**END
**END OF STEP
```

UNIFORM BLAST LOADING ON CLAMPED RECTANGULAR BEAM USING MATERIAL PROPERTIES THAT EXCLUDE TEMPERATURE DEPENDENCY

```
*HEADING
BLAST LOADING OF CLAMPED RECTANGULAR BEAMS
SI UNITS (Kg, M, S, N)
*PREPRINT, MODEL=NO, ECHO=NO
**----------------------------------DEFINITION OF NODES
*NODE
 1,  0,0,0
 16, 0.0254, 0., 0.
 31, 0.0508, 0., 0.
 81, 0.1524, 0., 0.
*NGEN, NSET=EDGE1
 1,  16, 1
 16, 31, 1
 31, 81, 1
**
*NCOPY, SHIFT, OLDSET=EDGE1, CHANGE NUMBER=2000, NEWSET=EDGE2
 0, 0.0127, 0
 0, 0, 1, 0, 0,1, 0
*NFILL, NSET=FACE1
 EDGE1,EDGE2, 20, 100
** ---------------------------------------- FACE1 FOR EACH OF THE FACES
*NCOPY, SHIFT, OLDSET=FACE1, NEWSET=FACE2, CHANGE NUMBER=10000
 0,0,0.0032
 0,0,1, 0,0,1, 0
*NCOPY, SHIFT, OLDSET=FACE1, NEWSET=FACE3, CHANGE NUMBER=20000
 0,0,0.0032
 0,0,1, 0,0,1, 0
*NCOPY, SHIFT, OLDSET=FACE1, NEWSET=FACE4, CHANGE NUMBER=30000
 0,0,0.0041525
 0,0,1, 0,0,1, 0
*NCOPY, SHIFT, OLDSET=FACE1, NEWSET=FACE5, CHANGE NUMBER=40000
 0,0,0.005105
 0,0,1, 0,0,1, 0
*NCOPY, SHIFT, OLDSET=FACE1, NEWSET=FACE6, CHANGE NUMBER=50000
 0,0,0.0060575
 0,0,1, 0,0,1, 0
*NCOPY, SHIFT, OLDSET=FACE1, NEWSET=FACE7, CHANGE NUMBER=60000
 0,0,0.00701
 0,0,1, 0,0,1, 0
*NCOPY, SHIFT, OLDSET=FACE1, NEWSET=FACE8, CHANGE NUMBER=70000
 0,0,0.0079625
 0,0,1, 0,0,1, 0
*NCOPY, SHIFT, OLDSET=FACE1, NEWSET=FACE9, CHANGE NUMBER=80000
 0,0,0.008915
```

```
 0,0,1, 0,0,1, 0
*NCOPY, SHIFT, OLDSET=FACE1, NEWSET=FACE10, CHANGE
NUMBER=90000
 0,0,0.0098675
 0,0,1, 0,0,1, 0
*NCOPY, SHIFT, OLDSET=FACE1, NEWSET=FACE11, CHANGE
NUMBER=100000
 0,0,0.01082
 0,0,1, 0,0,1, 0
*NCOPY, SHIFT, OLDSET=FACE1, NEWSET=FACE12, CHANGE
NUMBER=110000
 0,0,0.0117725
 0,0,1, 0,0,1, 0
*NCOPY, SHIFT, OLDSET=FACE1, NEWSET=FACE13, CHANGE
NUMBER=120000
 0,0,0.012725
 0,0,1, 0,0,1, 0
*NCOPY, SHIFT, OLDSET=FACE1, NEWSET=FACE14, CHANGE
NUMBER=130000
 0,0,0.012725
 0,0,1, 0,0,1, 0
*NCOPY, SHIFT, OLDSET=FACE1, NEWSET=FACE15, CHANGE
NUMBER=140000
 0,0,0.015925
 0,0,1, 0,0,1, 0
**----------------------------------------DEFINITION OF ELEMENTS
*ELEMENT, TYPE=C3D8R, ELSET=CLAMP_BOT
 1, 1,2,102,101, 10001,10002,10102,10101
*ELGEN, ELSET=CLAMP_BOT
 1, 30,1,1, 20,100,100
**
*ELEMENT, TYPE=C3D8R, ELSET=BEAM
 10001, 20001,20002,20102,20101, 30001,30002,30102,30101
*ELGEN, ELSET=BEAM
 10001, 80,1,1, 20,100,100, 10,10000,10000
**
*ELEMENT, TYPE=C3D8R, ELSET=CLAMP_TOP
 110001, 130001,130002,130102,130101, 140001,140002,140102,140101
*ELGEN, ELSET=CLAMP_TOP
 110001,30,1,1, 20,100,100
**---------------------------------DEFINITION OF SECTIONS
*SOLID SECTION,ELSET=CLAMP_TOP, MATERIAL=RIGID
*SOLID SECTION,ELSET=BEAM, MATERIAL=ALUMINIUM
*SOLID SECTION,ELSET=CLAMP_BOT, MATERIAL=RIGID
```

```
**----------------------------------DEFINITION OF RIGID BODY NODES
*NODE, NSET=NS_REFNODE
1000000, 0, 0, -0.05
2000000, 0, 0,  0.05
**----------------------------------DEFINITION OF SURFACES
*RIGID BODY, REFNODE=1000000, ELSET=CLAMP_BOT
*ELSET, ELSET=CLAMP_BOT_FACEP4, GENERATE
 30,1930,100
*SURFACE, TYPE=ELEMENT,NAME=SURF_CLAMP_BOT
 CLAMP_BOT,S2
 CLAMP_BOT_FACEP4,S4
**
*ELSET, ELSET=BEAM_BOT, GENERATE
 10001,11980,1
*SURFACE, TYPE=ELEMENT, NAME=SURF_BEAM_BOT
 BEAM_BOT, S1
**
*ELSET, ELSET=BEAM_TOP, GENERATE
 100001,101980,1
*SURFACE, TYPE=ELEMENT, NAME=SURF_BEAM_TOP
 BEAM_TOP, S2
**
*ELSET, ELSET=LOAD_BEAM, GENERATE
100031, 100080, 1
100131, 100180, 1
100231, 100280, 1
100331, 100380, 1
100431, 100480, 1
100531, 100580, 1
100631, 100680, 1
100731, 100780, 1
100831, 100880, 1
100931, 100980, 1
101031, 101080, 1
101131, 101180, 1
101231, 101280, 1
101331, 101380, 1
101431, 101480, 1
101531, 101580, 1
101631, 101680, 1
101731, 101780, 1
101831, 101880, 1
101931, 101980, 1
*RIGID BODY, REFNODE=2000000, ELSET=CLAMP_TOP
*ELSET, ELSET=CLAMP_TOP_FACEP4, GENERATE
```

```
 110030,111930,100
*SURFACE, TYPE=ELEMENT,NAME=SURF_CLAMP_TOP
 CLAMP_TOP,S1
 CLAMP_TOP_FACEP4,S4
**----------------------------------DEFINITION OF MATERIAL PROPERTIES
*MATERIAL, NAME=ALUMINIUM
*INELASTIC HEAT FRACTION
*ELASTIC
7.24E10, .32
*PLASTIC
2.81E8, 0.000000
2.83E8, 0.007150
2.86E8, 0.007710
2.88E8, 0.008070
2.90E8, 0.008480
2.93E8, 0.009030
2.95E8, 0.009670
2.97E8, 0.010200
2.99E8, 0.010800
3.00E8, 0.011300
3.03E8, 0.013400
3.01E8, 0.013900
*RATE DEPENDENT
6500, 4
*DENSITY
2686
**
*MATERIAL, NAME=RIGID
*ELASTIC
200E9, 0.3
*DENSITY
2686.
**-------------------------------DEFINITION OF BOUNDARY CONDITIONS
*NSET, NSET=XSYMM, GENERATE
 20081,   22081, 100
 30081,   32081, 100
 40081,   42081, 100
 50081,   52081, 100
 60081,   62081, 100
 70081,   72081, 100
 80081,   82081, 100
 90081,   92081, 100
 100081,102081, 100
 110081,112081, 100
 120081,123081, 100
**
```

```
*NSET, NSET=YSYMM, GENERATE
 22001,   22081,  1
 32001,   32081,  1
 42001,   42081,  1
 52001,   52081,  1
 62001,   62081,  1
 72001,   72081,  1
 82001,   82081,  1
 92001,   92081,  1
 102001, 102081, 1
 112001, 112081, 1
 122001, 122081, 1
*NSET, NSET=B1, GENERATE
20001,   20031, 1
30001,   30031, 1
40001,   40031, 1
50001,   50031, 1
60001,   60031, 1
70001,   70031, 1
80001,   80031, 1
90001,   90031, 1
100001, 100031,1
110001, 110031,1
120001, 120031,1
*NSET, NSET=B2, GENERATE
20001,   22001, 100
30001,   32001, 100
40001,   42001, 100
50001,   52001, 100
60001,   62001, 100
70001,   72001, 100
80001,   82001, 100
90001,   92001, 100
100001, 102001, 100
110001, 112001, 100
120001, 122001, 100
*NSET, NSET=B3, GENERATE
22001,  22031,  1
32001,  32031,  1
42001,   42031,  1
52001,   52031,  1
62001,   62031,  1
72001,   72031,  1
82001,   82031,  1
92001,   92031,  1
102001,  102031, 1
```

```
112001, 112031, 1
122001, 122031, 1
*NSET, NSET=B4, GENERATE
120030, 122030, 100
**
*BOUNDARY, OP=NEW, TYPE=DISPLACEMENT
 XSYMM,  1,1, 0.0
 YSYMM,  2,2, 0.0
 B1, 1,6, 0.0
 B2, 1,6, 0.0
 B3, 1,6, 0.0
 B4, 1,6, 0.0
 1000000, 1,6, 0.0
 2000000, 1,2, 0.0
 2000000, 4,6, 0.0
**----------------------------------DEFINITION OF LOAD
*AMPLITUDE, NAME=BLAST, DEFINITION=TABULAR
0.0,1.0, 30E-6,1, 30.1E-6,0.0
**----------------------------ANALYSIS STEPS BEGIN
*STEP
*DYNAMIC, EXPLICIT, ADIABATICS
,0.005E-6
*CONTACT PAIR, INTERACTION=SMOOTH
 SURF_BEAM_TOP,SURF_CLAMP_TOP
 SURF_BEAM_BOT,SURF_CLAMP_BOT
*SURFACE INTERACTION, NAME=SMOOTH
*FRICTION
 0.35
*CLOAD
 2000000,3,-1E5
*OUTPUT, FIELD, VARIABLE=ALL, OP=NEW, NUMBER INTERVALS=2
*END STEP
**
*STEP
*DYNAMIC, EXPLICIT, ADIABATICS
,30E-6
*DLOAD, AMPLITUDE=BLAST
 LOAD_BEAM, P2, 5.92E7
*OUTPUT, FIELD, VARIABLE=ALL, OP=NEW, NUMBER INTERVALS=100
*END STEP
**
*STEP
*DYNAMIC, EXPLICIT, ADIABATICS
,470E-6
*DLOAD, OP=NEW
*END STEP
```

```
**
*STEP
*DYNAMIC, EXPLICIT, ADIABATICS
,350E-6
*DLOAD, OP=NEW
*END STEP
**END
**END OF STEP
```

UNIFORM BLAST LOADING ON BUILT-IN RECTANGULAR BEAM USING MATERIAL PROPERTIES THAT INCLUDE TEMPERATURE DEPENDENCY

```
*HEADING
BLAST LOADING OF CLAMPED RECTANGULAR BEAMS
SI UNITS (Kg, M, S, N)
*PREPRINT, MODEL=NO, ECHO=NO
**----------------------------------DEFINITION OF NODES
*NODE
 1,  0,0,0
 16, 0.0254, 0., 0.
 31, 0.0508, 0., 0.
 81, 0.1524, 0., 0.
*NGEN, NSET=EDGE1
 1,  16, 1
 16, 31, 1
 31, 81, 1
**
*NCOPY, SHIFT, OLDSET=EDGE1, CHANGE NUMBER=2000, NEWSET=EDGE2
 0, 0.0127, 0
 0, 0, 1, 0, 0,1, 0
*NFILL, NSET=FACE1
 EDGE1,EDGE2, 20, 100
** ---------------------------------------COPING FACE1 FOR EACH OF THE FACES
*NCOPY, SHIFT, OLDSET=FACE1, NEWSET=FACE2, CHANGE NUMBER=10000
 0,0,0.0032
 0,0,1, 0,0,1, 0
*NCOPY, SHIFT, OLDSET=FACE1, NEWSET=FACE3, CHANGE NUMBER=20000
 0,0,0.0032
 0,0,1, 0,0,1, 0
*NCOPY, SHIFT, OLDSET=FACE1, NEWSET=FACE4, CHANGE NUMBER=30000
 0,0,0.0041525
 0,0,1, 0,0,1, 0
*NCOPY, SHIFT, OLDSET=FACE1, NEWSET=FACE5, CHANGE NUMBER=40000
 0,0,0.005105
 0,0,1, 0,0,1, 0
*NCOPY, SHIFT, OLDSET=FACE1, NEWSET=FACE6, CHANGE NUMBER=50000
 0,0,0.0060575
 0,0,1, 0,0,1, 0
*NCOPY, SHIFT, OLDSET=FACE1, NEWSET=FACE7, CHANGE NUMBER=60000
 0,0,0.00701
 0,0,1, 0,0,1, 0
*NCOPY, SHIFT, OLDSET=FACE1, NEWSET=FACE8, CHANGE NUMBER=70000
 0,0,0.0079625
 0,0,1, 0,0,1, 0
*NCOPY, SHIFT, OLDSET=FACE1, NEWSET=FACE9, CHANGE NUMBER=80000
 0,0,0.008915
```

```
 0,0,1, 0,0,1, 0
*NCOPY, SHIFT, OLDSET=FACE1, NEWSET=FACE10, CHANGE
NUMBER=90000
 0,0,0.0098675
 0,0,1, 0,0,1, 0
*NCOPY, SHIFT, OLDSET=FACE1, NEWSET=FACE11, CHANGE
NUMBER=100000
 0,0,0.01082
 0,0,1, 0,0,1, 0
*NCOPY, SHIFT, OLDSET=FACE1, NEWSET=FACE12, CHANGE
NUMBER=110000
 0,0,0.0117725
 0,0,1, 0,0,1, 0
*NCOPY, SHIFT, OLDSET=FACE1, NEWSET=FACE13, CHANGE
NUMBER=120000
 0,0,0.012725
 0,0,1, 0,0,1, 0
**----------------------------------------DEFINITION OF ELEMENTS
*ELEMENT, TYPE=C3D8R, ELSET=CLAMP_BOT
 1, 1,2,102,101, 10001,10002,10102,10101
*ELGEN, ELSET=CLAMP_BOT
 1, 30,1,1, 20,100,100
**---------------------------
*ELEMENT, TYPE=C3D8R, ELSET=BEAM
 10001, 20001,20002,20102,20101, 30001,30002,30102,30101
*ELGEN, ELSET=BEAM
 10001, 80,1,1, 20,100,100, 10,10000,10000
**---------------------------------DEINITION OF SECTIION
*SOLID SECTION,ELSET=BEAM, MATERIAL=ALUMINIUM
*SOLID SECTION,ELSET=CLAMP_BOT, MATERIAL=RIGID
**---------------------------------DEFINITION OF RIGID BODY NODE
*NODE, NSET=NS_REFNODE
1000000, 0, 0, -0.05
**---------------------------------DEFINITION OF SURFACES
*RIGID BODY, REFNODE=1000000, ELSET=CLAMP_BOT
*ELSET, ELSET=CLAMP_BOT_FACEP4, GENERATE
 30,1930,100
*SURFACE, TYPE=ELEMENT,NAME=SURF_CLAMP_BOT
 CLAMP_BOT,S2
 CLAMP_BOT_FACEP4,S4
**
*ELSET, ELSET=BEAM_BOT, GENERATE
 10001,11980,1
*SURFACE, TYPE=ELEMENT, NAME=SURF_BEAM_BOT
 BEAM_BOT, S1
**
```

```
*ELSET, ELSET=BEAM_TOP, GENERATE
 100001,101980,1
*SURFACE, TYPE=ELEMENT, NAME=SURF_BEAM_TOP
 BEAM_TOP, S2
**
*ELSET, ELSET=LOAD_BEAM, GENERATE
100031, 100080, 1
100131, 100180, 1
100231, 100280, 1
100331, 100380, 1
100431, 100480, 1
100531, 100580, 1
100631, 100680, 1
100731, 100780, 1
100831, 100880, 1
100931, 100980, 1
101031, 101080, 1
101131, 101180, 1
101231, 101280, 1
101331, 101380, 1
101431, 101480, 1
101531, 101580, 1
101631, 101680, 1
101731, 101780, 1
101831, 101880, 1
101931, 101980, 1
**----------------------------------DEFINITION OF MATERIAL PROPERTIES
*MATERIAL, NAME=ALUMINIUM
*INELASTIC HEAT FRACTION
*ELASTIC
7.24E10, .32, 0
6.07E10, .32, 25
3.74E10, .32, 100
3.24E10, .32, 200
3.02E10, .32, 300
*PLASTIC
2.81E8, 0.000000, 0
2.83E8, 0.007150, 0
2.86E8, 0.007710, 0
2.88E8, 0.008070, 0
2.90E8, 0.008480, 0
2.93E8, 0.009030, 0
2.95E8, 0.009670, 0
2.97E8, 0.010200, 0
2.99E8, 0.010800, 0
3.00E8, 0.011300, 0
```

3.03E8, 0.013400, 0
3.01E8, 0.013900, 0
2.81E8, 0.000000, 25
2.83E8, 0.007150, 25
2.86E8, 0.007710, 25
2.88E8, 0.008070, 25
2.90E8, 0.008480, 25
2.93E8, 0.009030, 25
2.95E8, 0.009670, 25
2.97E8, 0.010200, 25
2.99E8, 0.010800, 25
3.00E8, 0.011300, 25
3.03E8, 0.013400, 25
3.01E8, 0.013900, 25
2.43E8, 0.000000, 100
2.45E8, 0.007150, 100
2.48E8, 0.007710, 100
2.50E8, 0.008070, 100
2.51E8, 0.008480, 100
2.54E8, 0.009030, 100
2.56E8, 0.009670, 100
2.57E8, 0.010200, 100
2.59E8, 0.010800, 100
2.60E8, 0.011300, 100
2.63E8, 0.013400, 100
2.61E8, 0.013900, 100
1.93E8, 0.000000, 200
1.95E8, 0.007150, 200
1.97E8, 0.007710, 200
1.98E8, 0.008070, 200
2.00E8, 0.008480, 200
2.02E8, 0.009030, 200
2.03E8, 0.009670, 200
2.04E8, 0.010200, 200
2.06E8, 0.010800, 200
2.07E8, 0.011300, 200
2.09E8, 0.013400, 200
2.07E8, 0.013900, 200
2.65E7, 0.000000, 300
2.66E7, 0.007150, 300
2.69E7, 0.007710, 300
2.71E7, 0.008070, 300
2.73E7, 0.008480, 300
2.76E7, 0.009030, 300
2.78E7, 0.009670, 300
2.80E7, 0.010200, 300

```
2.82E7, 0.010800, 300
2.82E7, 0.011300, 300
2.85E7, 0.013400, 300
2.83E7, 0.013900, 300
*SPECIFIC HEAT
937.4
*RATE DEPENDENT
6500, 4
*DENSITY
2686
**
*MATERIAL, NAME=RIGID
*ELASTIC
200E9, 0.3
*DENSITY
7800.
**----------------------------------DEFINITION OF BOUNDARY CONDITIONS
*NSET, NSET=XSYMM, GENERATE
 20081,   22081, 100
 30081,   32081, 100
 40081,   42081, 100
 50081,   52081, 100
 60081,   62081, 100
 70081,   72081, 100
 80081,   82081, 100
 90081,   92081, 100
 100081,102081, 100
 110081,112081, 100
 120081,123081, 100
**
*NSET, NSET=YSYMM, GENERATE
 22001,   22081,  1
 32001,   32081,  1
 42001,   42081,  1
 52001,   52081,  1
 62001,   62081,  1
 72001,   72081,  1
 82001,   82081,  1
 92001,   92081,  1
 102001, 102081, 1
 112001, 112081, 1
 122001, 122081, 1
*NSET, NSET=B1, GENERATE
20001,   20031, 1
30001,   30031, 1
40001,   40031, 1
```

```
50001,   50031, 1
60001,   60031, 1
70001,   70031, 1
80001,   80031, 1
90001,   90031, 1
100001, 100031,1
110001, 110031,1
120001, 120031,1
*NSET, NSET=B2, GENERATE
20001,    22001, 100
30001,    32001, 100
40001,    42001, 100
50001,    52001, 100
60001,    62001, 100
70001,    72001, 100
80001,    82001, 100
90001,    92001, 100
100001, 102001, 100
110001, 112001, 100
120001, 122001, 100
*NSET, NSET=B3, GENERATE
22001,    22031,  1
32001,    32031,  1
42001,    42031,  1
52001,    52031,  1
62001,    62031,  1
72001,    72031,  1
82001,    82031,  1
92001,    92031,  1
102001,  102031, 1
112001,  112031, 1
122001,  122031, 1
*NSET, NSET=B4, GENERATE
120030, 122030, 100
**--------------------------DEFINITION OF BOUNDARY CONDITIONS
*BOUNDARY, OP=NEW, TYPE=DISPLACEMENT
 XSYMM,   1,1, 0.0
 YSYMM,   2,2, 0.0
 B1, 1,6, 0.0
 B2, 1,6, 0.0
 B3, 1,6, 0.0
 B4, 1,6, 0.0
 1000000, 1,6, 0.0
```

```
**
*NSET, NSET=NS_ALL_BEAM, ELSET=BEAM
*INITIAL CONDITION, TYPE=TEMPERATURE
 NS_ALL_BEAM, 0.
**------------------------------DEFINITION OF LOAD
*AMPLITUDE, NAME=BLAST, DEFINITION=TABULAR
0.0,1.0, 30E-6,1, 30.1E-6,0.0
**------------------------------ANALYSIS STEPS BEGIN
*STEP
*DYNAMIC, EXPLICIT, ADIABATICS
,0.005E-6
*CONTACT PAIR, INTERACTION=SMOOTH
 SURF_BEAM_BOT,SURF_CLAMP_BOT
*SURFACE INTERACTION, NAME=SMOOTH
*FRICTION
 1.0
*OUTPUT, FIELD, VARIABLE=ALL, OP=NEW, NUMBER INTERVALS=2
*END STEP
**
*STEP
*DYNAMIC, EXPLICIT, ADIABATICS
,30E-6
*DLOAD, AMPLITUDE=BLAST
 LOAD_BEAM, P2, 5.92E7
*OUTPUT, FIELD, VARIABLE=ALL, OP=NEW, NUMBER INTERVALS=100
*END STEP
**
*STEP
*DYNAMIC, EXPLICIT, ADIABATICS
,470E-6
*DLOAD, OP=NEW
*END STEP
**
*STEP
*DYNAMIC, EXPLICIT, ADIABATICS
,350E-6
*DLOAD, OP=NEW
*END STEP
**END
**END OF ANALYSIS
```

UNIFORM BLAST LOADING ON BUILT-IN RECTANGULAR BEAM USING MATERIAL PROPERTIES THAT EXCLUDE TEMPERATURE DEPENDENCY

```
*HEADING
BLAST LOADING OF CLAMPED RECTANGULAR BEAMS
SI UNITS (Kg, M, S, N)
*PREPRINT, MODEL=NO, ECHO=NO
**----------------------------------DEFINITION OF NODES
*NODE
 1,  0,0,0
 16, 0.0254, 0., 0.
 31, 0.0508, 0., 0.
 81, 0.1524, 0., 0.
*NGEN, NSET=EDGE1
 1,  16, 1
 16, 31, 1
 31, 81, 1
**
*NCOPY, SHIFT, OLDSET=EDGE1, CHANGE NUMBER=2000, NEWSET=EDGE2
 0, 0.0127, 0
 0, 0, 1, 0, 0,1, 0
*NFILL, NSET=FACE1
 EDGE1,EDGE2, 20, 100
** ---------------------------------------COPING FACE1 FOR EACH OF THE FACES
*NCOPY, SHIFT, OLDSET=FACE1, NEWSET=FACE2, CHANGE NUMBER=10000
 0,0,0.0032
 0,0,1, 0,0,1, 0
*NCOPY, SHIFT, OLDSET=FACE1, NEWSET=FACE3, CHANGE NUMBER=20000
 0,0,0.0032
 0,0,1, 0,0,1, 0
*NCOPY, SHIFT, OLDSET=FACE1, NEWSET=FACE4, CHANGE NUMBER=30000
 0,0,0.0041525
 0,0,1, 0,0,1, 0
*NCOPY, SHIFT, OLDSET=FACE1, NEWSET=FACE5, CHANGE NUMBER=40000
 0,0,0.005105
 0,0,1, 0,0,1, 0
*NCOPY, SHIFT, OLDSET=FACE1, NEWSET=FACE6, CHANGE NUMBER=50000
 0,0,0.0060575
 0,0,1, 0,0,1, 0
*NCOPY, SHIFT, OLDSET=FACE1, NEWSET=FACE7, CHANGE NUMBER=60000
 0,0,0.00701
 0,0,1, 0,0,1, 0
*NCOPY, SHIFT, OLDSET=FACE1, NEWSET=FACE8, CHANGE NUMBER=70000
 0,0,0.0079625
 0,0,1, 0,0,1, 0
*NCOPY, SHIFT, OLDSET=FACE1, NEWSET=FACE9, CHANGE NUMBER=80000
 0,0,0.008915
```

```
 0,0,1, 0,0,1, 0
*NCOPY, SHIFT, OLDSET=FACE1, NEWSET=FACE10, CHANGE
NUMBER=90000
 0,0,0.0098675
 0,0,1, 0,0,1, 0
*NCOPY, SHIFT, OLDSET=FACE1, NEWSET=FACE11, CHANGE
NUMBER=100000
 0,0,0.01082
 0,0,1, 0,0,1, 0
*NCOPY, SHIFT, OLDSET=FACE1, NEWSET=FACE12, CHANGE
NUMBER=110000
 0,0,0.0117725
 0,0,1, 0,0,1, 0
*NCOPY, SHIFT, OLDSET=FACE1, NEWSET=FACE13, CHANGE
NUMBER=120000
 0,0,0.012725
 0,0,1, 0,0,1, 0
**----------------------------------------DEFINITION OF ELEMENTS
*ELEMENT, TYPE=C3D8R, ELSET=CLAMP_BOT
 1, 1,2,102,101, 10001,10002,10102,10101
*ELGEN, ELSET=CLAMP_BOT
 1, 30,1,1, 20,100,100
**-----------------------------
*ELEMENT, TYPE=C3D8R, ELSET=BEAM
 10001, 20001,20002,20102,20101, 30001,30002,30102,30101
*ELGEN, ELSET=BEAM
 10001, 80,1,1, 20,100,100, 10,10000,10000
**---------------------------------DEINITION OF SECTIION
*SOLID SECTION,ELSET=BEAM, MATERIAL=ALUMINIUM
*SOLID SECTION,ELSET=CLAMP_BOT, MATERIAL=RIGID
**---------------------------------DEFINITION OF RIGID BODY NODE
*NODE, NSET=NS_REFNODE
1000000, 0, 0, -0.05
**-----------------------------------DEFINITION OF SURFACES
*RIGID BODY, REFNODE=1000000, ELSET=CLAMP_BOT
*ELSET, ELSET=CLAMP_BOT_FACEP4, GENERATE
 30,1930,100
*SURFACE, TYPE=ELEMENT,NAME=SURF_CLAMP_BOT
 CLAMP_BOT,S2
 CLAMP_BOT_FACEP4,S4
**
*ELSET, ELSET=BEAM_BOT, GENERATE
 10001,11980,1
*SURFACE, TYPE=ELEMENT, NAME=SURF_BEAM_BOT
 BEAM_BOT, S1
**
```

```
*ELSET, ELSET=BEAM_TOP, GENERATE
 100001,101980,1
*SURFACE, TYPE=ELEMENT, NAME=SURF_BEAM_TOP
 BEAM_TOP, S2
**
*ELSET, ELSET=LOAD_BEAM, GENERATE
100031, 100080, 1
100131, 100180, 1
100231, 100280, 1
100331, 100380, 1
100431, 100480, 1
100531, 100580, 1
100631, 100680, 1
100731, 100780, 1
100831, 100880, 1
100931, 100980, 1
101031, 101080, 1
101131, 101180, 1
101231, 101280, 1
101331, 101380, 1
101431, 101480, 1
101531, 101580, 1
101631, 101680, 1
101731, 101780, 1
101831, 101880, 1
101931, 101980, 1
**----------------------------------DEFINITION OF MATERIAL PROPERTIES
*MATERIAL, NAME=ALUMINIUM
*INELASTIC HEAT FRACTION
*ELASTIC
7.24E10, .32
*PLASTIC
2.81E8, 0.000000
2.83E8, 0.007150
2.86E8, 0.007710
2.88E8, 0.008070
2.90E8, 0.008480
2.93E8, 0.009030
2.95E8, 0.009670
2.97E8, 0.010200
2.99E8, 0.010800
3.00E8, 0.011300
3.03E8, 0.013400
3.01E8, 0.013900
*RATE DEPENDENT
6500, 4
```

```
*DENSITY
2686
**
*MATERIAL, NAME=RIGID
*ELASTIC
200E9, 0.3
*DENSITY
7800.
**----------------------------------DEFINITION OF BOUNDARY CONDITIONS
*NSET, NSET=XSYMM, GENERATE
 20081,   22081, 100
 30081,   32081, 100
 40081,   42081, 100
 50081,   52081, 100
 60081,   62081, 100
 70081,   72081, 100
 80081,   82081, 100
 90081,   92081, 100
 100081,102081, 100
 110081,112081, 100
 120081,123081, 100
**
*NSET, NSET=YSYMM, GENERATE
 22001,   22081,  1
 32001,   32081,  1
 42001,   42081,  1
 52001,   52081,  1
 62001,   62081,  1
 72001,   72081,  1
 82001,   82081,  1
 92001,   92081,  1
 102001, 102081, 1
 112001, 112081, 1
 122001, 122081, 1
*NSET, NSET=B1, GENERATE
20001,   20031, 1
30001,   30031, 1
40001,   40031, 1
50001,   50031, 1
60001,   60031, 1
70001,   70031, 1
80001,   80031, 1
90001,   90031, 1
100001, 100031,1
110001, 110031,1
120001, 120031,1
```

```
 1.0
*OUTPUT, FIELD, VARIABLE=ALL, OP=NEW, NUMBER INTERVALS=2
*END STEP
**
*STEP
*DYNAMIC, EXPLICIT, ADIABATICS
,30E-6
*DLOAD, AMPLITUDE=BLAST
 LOAD_BEAM, P2, 5.92E7
*OUTPUT, FIELD, VARIABLE=ALL, OP=NEW, NUMBER INTERVALS=100
*END STEP
**
*STEP
*DYNAMIC, EXPLICIT, ADIABATICS
,470E-6
*DLOAD, OP=NEW
*END STEP
**
*STEP
*DYNAMIC, EXPLICIT, ADIABATICS
,350E-6
*DLOAD, OP=NEW
*END STEP
**END
**END OF ANALYSIS
```

UNIFORM BLAST LOADING ON CLAMPED T-BEAM USING MATERIAL PROPERTIES THAT INCLUDE TEMPERATURE DEPENDENCY

```
*HEADING
BLAST LOADING OF T-BEAMS
SI UNITS (kg, M, S, N)
*PREPRINT, MODEL=NO, ECHO=NO
**----------------------------------DEFINITION OF NODES
*NODE
 1, 0,      0, 0
 21, 0.0016, 0., 0.
 51, 0.00525, 0., 0.
*NGEN, NSET=EDGE1
 1, 21, 1
 21, 51, 1
**
*NCOPY, SHIFT, OLDSET=EDGE1, CHANGE NUMBER=2000, NEWSET=EDGE2
 0, 0.05, 0
 0, 0,1, 0, 0, 1, 0
*NCOPY, SHIFT, OLDSET=EDGE1, CHANGE NUMBER=9000, NEWSET=EDGE3
 0,0.15,0
 0,0,1, 0,0,1, 0
**
*NFILL, NSET=FACE1
 EDGE1,EDGE2, 20, 100
 EDGE2,EDGE3, 70, 100
** ---------------------------------------COPING FACE1 FOR EACH OF THE FACES
*NCOPY, SHIFT, OLDSET=FACE1, NEWSET=FACE2, CHANGE NUMBER=10000
 0,0,0.0001
 0,0,1, 0,0,1, 0
*NCOPY, SHIFT, OLDSET=FACE1, NEWSET=FACE3, CHANGE NUMBER=20000
 0,0,0.0001
 0,0,1, 0,0,1, 0
*NCOPY, SHIFT, OLDSET=FACE1, NEWSET=FACE4, CHANGE NUMBER=30000
 0,0,0.00122
 0,0,1, 0,0,1, 0
*NCOPY, SHIFT, OLDSET=FACE1, NEWSET=FACE5, CHANGE NUMBER=40000
 0,0,0.00234
 0,0,1, 0,0,1, 0
*NCOPY, SHIFT, OLDSET=FACE1, NEWSET=FACE6, CHANGE NUMBER=50000
 0,0,0.00346
 0,0,1, 0,0,1, 0
*NCOPY, SHIFT, OLDSET=FACE1, NEWSET=FACE7, CHANGE NUMBER=60000
 0,0,0.00458
 0,0,1, 0,0,1, 0
*NCOPY, SHIFT, OLDSET=FACE1, NEWSET=FACE8, CHANGE NUMBER=70000
 0,0,0.0057
```

```
 0,0,1, 0,0,1, 0
*NCOPY, SHIFT, OLDSET=FACE1, NEWSET=FACE9, CHANGE NUMBER=80000
 0,0,0.00682
 0,0,1, 0,0,1, 0
*NCOPY, SHIFT, OLDSET=FACE1, NEWSET=FACE10, CHANGE
NUMBER=90000
 0,0,0.00794
 0,0,1, 0,0,1, 0
*NCOPY, SHIFT, OLDSET=FACE1, NEWSET=FACE11, CHANGE
NUMBER=100000
 0,0,0.00906
 0,0,1, 0,0,1, 0
*NCOPY, SHIFT, OLDSET=FACE1, NEWSET=FACE12, CHANGE
NUMBER=110000
 0,0,0.01018
 0,0,1, 0,0,1, 0
*NCOPY, SHIFT, OLDSET=FACE1, NEWSET=FACE13, CHANGE
NUMBER=120000
 0,0,0.0113
 0,0,1, 0,0,1, 0
*NCOPY, SHIFT, OLDSET=FACE1, NEWSET=FACE14, CHANGE
NUMBER=130000
 0,0,0.0113
 0,0,1, 0,0,1, 0
*NCOPY, SHIFT, OLDSET=FACE1, NEWSET=FACE15, CHANGE
NUMBER=140000
 0,0,0.0114
 0,0,1, 0,0,1, 0
**---------------------------- DEFINITION OF ELEMENTS
*ELEMENT, TYPE=C3D8R, ELSET=CLAMP_BOT
 1, 1, 2, 102, 101, 10001, 10002, 10102, 10101
*ELGEN, ELSET=CLAMP_BOT
 1, 20, 1, 1, 20, 100, 100
**
*ELEMENT, TYPE=C3D8R, ELSET=TBEAM
 10001, 20001, 20002, 20102, 20101, 30001, 30002, 30102, 30101
 80001, 90001, 90002, 90102, 90101, 100001, 100002, 100102, 100101
*ELGEN, ELSET=TBEAM
 10001, 20, 1, 1, 90, 100, 100, 7, 10000, 10000
 80001, 50, 1, 1, 90, 100, 100, 3, 10000, 10000
**----------------------------DEFINITION OF SURFACES
*ELEMENT, TYPE=C3D8R, ELSET=CLAMP_TOP
 110001, 130001, 130002, 130102, 130101, 140001, 140002, 140102, 140101
*ELGEN, ELSET=CLAMP_TOP
 110001,50,1,1, 20,100,100
```

```
**---------------------------------- DEFINITION OF SECTIONS
*SOLID SECTION, ELSET=CLAMP_TOP,  MATERIAL=RIGID
*SOLID SECTION, ELSET=TBEAM, MATERIAL=ALUMINIUM
*SOLID SECTION,ELSET=CLAMP_BOT, MATERIAL=RIGID
**----------------------------------DEFINITION OF RIGID BODY NODES
*NODE, NSET=NS_REFNODE
1000000, 0, 0, -0.05
2000000, 0, 0,  0.05
**----------------------------------DEFINITION OF SURFACES
*RIGID BODY, REFNODE=1000000, ELSET=CLAMP_BOT
*SURFACE, TYPE=ELEMENT,NAME=SURF_CLAMP_BOT
 CLAMP_BOT,S2
**
*ELSET, ELSET=TBEAM_BOT, GENERATE
 10001,18920,1
*SURFACE, TYPE=ELEMENT, NAME=SURF_TBEAM_BOT
 TBEAM_BOT, S1
**
*ELSET, ELSET=TBEAM_TOP, GENERATE
 100001,108950,1
*SURFACE, TYPE=ELEMENT, NAME=SURF_TBEAM_TOP
 TBEAM_TOP, S2
*RIGID BODY, REFNODE=2000000, ELSET=CLAMP_TOP
*SURFACE, TYPE=ELEMENT,NAME=SURF_CLAMP_TOP
 CLAMP_TOP,S1
*ELSET, ELSET=LOAD_TBEAM, GENERATE
102001, 102050, 1
102101, 102150, 1
102201, 102250, 1
102301, 102350, 1
102401, 102450, 1
102501, 102550, 1
102601, 102650, 1
102701, 102750, 1
102801, 102850, 1
102901, 102950, 1
103001, 103050, 1
103101, 103150, 1
103201, 103250, 1
103301, 103350, 1
103401, 103450, 1
103501, 103550, 1
103601, 103650, 1
103701, 103750, 1
103801, 103850, 1
103901, 103950, 1
```

104001, 104050, 1
104101, 104150, 1
104201, 104250, 1
104301, 104350, 1
104401, 104450, 1
104501, 104550, 1
104601, 104650, 1
104701, 104750, 1
104801, 104850, 1
104901, 104950, 1
105001, 105050, 1
105101, 105150, 1
105201, 105250, 1
105301, 105350, 1
105401, 105450, 1
105501, 105550, 1
105601, 105650, 1
105701, 105750, 1
105801, 105850, 1
105901, 105950, 1
106001, 106050, 1
106101, 106150, 1
106201, 106250, 1
106301, 106350, 1
106401, 106450, 1
106501, 106550, 1
106601, 106650, 1
106701, 106750, 1
106801, 106850, 1
106901, 106950, 1
107001, 107050, 1
107101, 107150, 1
107201, 107250, 1
107301, 107350, 1
107401, 107450, 1
107501, 107550, 1
107601, 107650, 1
107701, 107750, 1
107801, 107850, 1
107901, 107950, 1
108001, 108050, 1
108101, 108150, 1
108201, 108250, 1
108301, 108350, 1
108401, 108450, 1
108501, 108550, 1

```
108601, 108650, 1
108701, 108750, 1
108801, 108850, 1
108901, 108950, 1
**----------DEFINITION OF MATERIAL PROPERTIES
*MATERIAL, NAME=ALUMINIUM
*INELASTIC HEAT FRACTION
*ELASTIC
7.24E10, .32, 0
6.07E10, .32, 25
3.74E10, .32, 100
3.24E10, .32, 200
3.02E10, .32, 300
*PLASTIC
2.81E8, 0.000000, 0
2.83E8, 0.007150, 0
2.86E8, 0.007710, 0
2.88E8, 0.008070, 0
2.90E8, 0.008480, 0
2.93E8, 0.009030, 0
2.95E8, 0.009670, 0
2.97E8, 0.010200, 0
2.99E8, 0.010800, 0
3.00E8, 0.011300, 0
3.03E8, 0.013400, 0
3.01E8, 0.013900, 0
2.81E8, 0.000000, 25
2.83E8, 0.007150, 25
2.86E8, 0.007710, 25
2.88E8, 0.008070, 25
2.90E8, 0.008480, 25
2.93E8, 0.009030, 25
2.95E8, 0.009670, 25
2.97E8, 0.010200, 25
2.99E8, 0.010800, 25
3.00E8, 0.011300, 25
3.03E8, 0.013400, 25
3.01E8, 0.013900, 25
2.43E8, 0.000000, 100
2.45E8, 0.007150, 100
2.48E8, 0.007710, 100
2.50E8, 0.008070, 100
2.51E8, 0.008480, 100
2.54E8, 0.009030, 100
2.56E8, 0.009670, 100
2.57E8, 0.010200, 100
```

```
2.59E8, 0.010800, 100
2.60E8, 0.011300, 100
2.63E8, 0.013400, 100
2.61E8, 0.013900, 100
1.93E8, 0.000000, 200
1.95E8, 0.007150, 200
1.97E8, 0.007710, 200
1.98E8, 0.008070, 200
2.00E8, 0.008480, 200
2.02E8, 0.009030, 200
2.03E8, 0.009670, 200
2.04E8, 0.010200, 200
2.06E8, 0.010800, 200
2.07E8, 0.011300, 200
2.09E8, 0.013400, 200
2.07E8, 0.013900, 200
2.65E7, 0.000000, 300
2.66E7, 0.007150, 300
2.69E7, 0.007710, 300
2.71E7, 0.008070, 300
2.73E7, 0.008480, 300
2.76E7, 0.009030, 300
2.78E7, 0.009670, 300
2.80E7, 0.010200, 300
2.82E7, 0.010800, 300
2.82E7, 0.011300, 300
2.85E7, 0.013400, 300
2.83E7, 0.013900, 300
*SPECIFIC HEAT
937.4
*RATE DEPENDENT
6500, 4
*DENSITY
2686
*MATERIAL, NAME=RIGID
*ELASTIC
200E9, 0.3
*DENSITY
7800.
**------------------------------DEFINITION OF BOUNDARY CONDITIONS
*NSET, NSET=XSYMM, GENERATE
 22101,  29001,  100
 32101,  39001,  100
 42101,  49001,  100
 52101,  59001,  100
 62101,  69001,  100
```

```
 72101,  79001,  100
 82101,  89001,  100
 92101,  99001,  100
 102101, 109001, 100
 112101, 119001, 100
 122101, 129001, 100
**
**----------------------------
**
*NSET, NSET=YSYMM, GENERATE
 29001,  29051,  1
 39001,  39051,  1
 49001,  49051,  1
 59001,  59051,  1
 69001,  69051,  1
 79001,  79051,  1
 89001,  89051,  1
 99001,  99051,  1
 109001, 109051, 1
 119001, 119051, 1
 129001, 129051, 1
**
*BOUNDARY, OP=NEW, TYPE=DISPLACEMENT
 XSYMM,  1,1, 0.0
 YSYMM,  2,2, 0.0
 1000000, 1,6, 0.0
 2000000, 1,2, 0.0
 2000000, 4,6, 0.0
**
*NSET, NSET=NS_ALL_TBEAM, ELSET=TBEAM
*INITIAL CONDITION, TYPE=TEMPERATURE
 NS_ALL_TBEAM, 0.
**----------------------------DEFINITION OF LOAD
*AMPLITUDE, NAME=BLAST, DEFINITION=TABULAR
0.0,1.0, 15E-6,1, 15.1E-6,0.0
**---------------------------- ANALYSIS STEPS BEGIN
**
*STEP
*DYNAMIC, EXPLICIT, ADIABATICS
,0.005E-6
*CONTACT PAIR, INTERACTION=SMOOTH
 SURF_TBEAM_TOP,SURF_CLAMP_TOP
 SURF_TBEAM_BOT,SURF_CLAMP_BOT
*SURFACE INTERACTION, NAME=SMOOTH
*FRICTION
 0.35
```

```
*CLOAD
 2000000,3,-1E4
*OUTPUT, FIELD, VARIABLE=ALL, OP=NEW, NUMBER INTERVALS=2
*END STEP
**
*STEP
*DYNAMIC, EXPLICIT, ADIABATICS
,15E-6
*DLOAD, AMPLITUDE=BLAST
 LOAD_TBEAM, P2, 3.59E7
*OUTPUT, FIELD, VARIABLE=ALL, OP=NEW, NUMBER INTERVALS=100
*END STEP
**
*STEP
*DYNAMIC, EXPLICIT, ADIABATICS
,235E-6
*DLOAD, OP=NEW
*END STEP
**
*STEP
*DYNAMIC, EXPLICIT, ADIABATICS
,400E-6
*DLOAD, OP=NEW
*END STEP
**END
**END OF ANALYSIS
```

UNIFORM BLAST LOADING ON CLAMPED T-BEAM USING MATERIAL PROPERTIES THAT EXCLUDE TEMPERATURE DEPENDENCY

```
*HEADING
BLAST LOADING OF T-BEAMS
SI UNITS (kg, M, S, N)
*PREPRINT, MODEL=NO, ECHO=NO
**----------------------------------DEFINITION OF NODES
*NODE
 1, 0,      0, 0
 21, 0.0016, 0., 0.
 51, 0.00525, 0., 0.
*NGEN, NSET=EDGE1
 1, 21, 1
 21, 51, 1
**
*NCOPY, SHIFT, OLDSET=EDGE1, CHANGE NUMBER=2000, NEWSET=EDGE2
 0, 0.05, 0
 0, 0,1, 0, 0, 1, 0
*NCOPY, SHIFT, OLDSET=EDGE1, CHANGE NUMBER=9000, NEWSET=EDGE3
 0,0.15,0
 0,0,1, 0,0,1, 0
**
*NFILL, NSET=FACE1
 EDGE1,EDGE2, 20, 100
 EDGE2,EDGE3, 70, 100
** ---------------------------------------COPING FACE1 FOR EACH OF THE FACES
*NCOPY, SHIFT, OLDSET=FACE1, NEWSET=FACE2, CHANGE NUMBER=10000
 0,0,0.0001
 0,0,1, 0,0,1, 0
*NCOPY, SHIFT, OLDSET=FACE1, NEWSET=FACE3, CHANGE NUMBER=20000
 0,0,0.0001
 0,0,1, 0,0,1, 0
*NCOPY, SHIFT, OLDSET=FACE1, NEWSET=FACE4, CHANGE NUMBER=30000
 0,0,0.00122
 0,0,1, 0,0,1, 0
*NCOPY, SHIFT, OLDSET=FACE1, NEWSET=FACE5, CHANGE NUMBER=40000
 0,0,0.00234
 0,0,1, 0,0,1, 0
*NCOPY, SHIFT, OLDSET=FACE1, NEWSET=FACE6, CHANGE NUMBER=50000
 0,0,0.00346
 0,0,1, 0,0,1, 0
*NCOPY, SHIFT, OLDSET=FACE1, NEWSET=FACE7, CHANGE NUMBER=60000
 0,0,0.00458
 0,0,1, 0,0,1, 0
*NCOPY, SHIFT, OLDSET=FACE1, NEWSET=FACE8, CHANGE NUMBER=70000
 0,0,0.0057
```

```
 0,0,1, 0,0,1, 0
*NCOPY, SHIFT, OLDSET=FACE1, NEWSET=FACE9, CHANGE NUMBER=80000
 0,0,0.00682
 0,0,1, 0,0,1, 0
*NCOPY, SHIFT, OLDSET=FACE1, NEWSET=FACE10, CHANGE
NUMBER=90000
 0,0,0.00794
 0,0,1, 0,0,1, 0
*NCOPY, SHIFT, OLDSET=FACE1, NEWSET=FACE11, CHANGE
NUMBER=100000
 0,0,0.00906
 0,0,1, 0,0,1, 0
*NCOPY, SHIFT, OLDSET=FACE1, NEWSET=FACE12, CHANGE
NUMBER=110000
 0,0,0.01018
 0,0,1, 0,0,1, 0
*NCOPY, SHIFT, OLDSET=FACE1, NEWSET=FACE13, CHANGE
NUMBER=120000
 0,0,0.0113
 0,0,1, 0,0,1, 0
*NCOPY, SHIFT, OLDSET=FACE1, NEWSET=FACE14, CHANGE
NUMBER=130000
 0,0,0.0113
 0,0,1, 0,0,1, 0
*NCOPY, SHIFT, OLDSET=FACE1, NEWSET=FACE15, CHANGE
NUMBER=140000
 0,0,0.0114
 0,0,1, 0,0,1, 0
**------------------------------ DEFINITION OF ELEMENTS
*ELEMENT, TYPE=C3D8R, ELSET=CLAMP_BOT
 1, 1, 2, 102, 101, 10001, 10002, 10102, 10101
*ELGEN, ELSET=CLAMP_BOT
 1, 20, 1, 1, 20, 100, 100
**
*ELEMENT, TYPE=C3D8R, ELSET=TBEAM
 10001, 20001, 20002, 20102, 20101, 30001, 30002, 30102, 30101
 80001, 90001, 90002, 90102, 90101, 100001, 100002, 100102, 100101
*ELGEN, ELSET=TBEAM
 10001, 20, 1, 1, 90, 100, 100, 7, 10000, 10000
 80001, 50, 1, 1, 90, 100, 100, 3, 10000, 10000
**------------------------------DEFINITION OF SURFACES
*ELEMENT, TYPE=C3D8R, ELSET=CLAMP_TOP
 110001, 130001, 130002, 130102, 130101, 140001, 140002, 140102, 140101
*ELGEN, ELSET=CLAMP_TOP
 110001,50,1,1, 20,100,100
```

```
**---------------------------------- DEFINITION OF SECTIONS
*SOLID SECTION, ELSET=CLAMP_TOP,  MATERIAL=RIGID
*SOLID SECTION, ELSET=TBEAM, MATERIAL=ALUMINIUM
*SOLID SECTION,ELSET=CLAMP_BOT, MATERIAL=RIGID
**----------------------------------DEFINITION OF RIGID BODY NODES
*NODE, NSET=NS_REFNODE
1000000, 0, 0, -0.05
2000000, 0, 0,  0.05
**----------------------------------DEFINITION OF SURFACES
*RIGID BODY, REFNODE=1000000, ELSET=CLAMP_BOT
*SURFACE, TYPE=ELEMENT,NAME=SURF_CLAMP_BOT
 CLAMP_BOT,S2
**
*ELSET, ELSET=TBEAM_BOT, GENERATE
 10001,18920,1
*SURFACE, TYPE=ELEMENT, NAME=SURF_TBEAM_BOT
 TBEAM_BOT, S1
**
*ELSET, ELSET=TBEAM_TOP, GENERATE
 100001,108950,1
*SURFACE, TYPE=ELEMENT, NAME=SURF_TBEAM_TOP
 TBEAM_TOP, S2
*RIGID BODY, REFNODE=2000000, ELSET=CLAMP_TOP
*SURFACE, TYPE=ELEMENT,NAME=SURF_CLAMP_TOP
 CLAMP_TOP,S1
*ELSET, ELSET=LOAD_TBEAM, GENERATE
102001, 102050, 1
102101, 102150, 1
102201, 102250, 1
102301, 102350, 1
102401, 102450, 1
102501, 102550, 1
102601, 102650, 1
102701, 102750, 1
102801, 102850, 1
102901, 102950, 1
103001, 103050, 1
103101, 103150, 1
103201, 103250, 1
103301, 103350, 1
103401, 103450, 1
103501, 103550, 1
103601, 103650, 1
103701, 103750, 1
103801, 103850, 1
103901, 103950, 1
```

104001, 104050, 1
104101, 104150, 1
104201, 104250, 1
104301, 104350, 1
104401, 104450, 1
104501, 104550, 1
104601, 104650, 1
104701, 104750, 1
104801, 104850, 1
104901, 104950, 1
105001, 105050, 1
105101, 105150, 1
105201, 105250, 1
105301, 105350, 1
105401, 105450, 1
105501, 105550, 1
105601, 105650, 1
105701, 105750, 1
105801, 105850, 1
105901, 105950, 1
106001, 106050, 1
106101, 106150, 1
106201, 106250, 1
106301, 106350, 1
106401, 106450, 1
106501, 106550, 1
106601, 106650, 1
106701, 106750, 1
106801, 106850, 1
106901, 106950, 1
107001, 107050, 1
107101, 107150, 1
107201, 107250, 1
107301, 107350, 1
107401, 107450, 1
107501, 107550, 1
107601, 107650, 1
107701, 107750, 1
107801, 107850, 1
107901, 107950, 1
108001, 108050, 1
108101, 108150, 1
108201, 108250, 1
108301, 108350, 1
108401, 108450, 1
108501, 108550, 1

```
108601, 108650, 1
108701, 108750, 1
108801, 108850, 1
108901, 108950, 1
**----------------------------------DEFINITION OF MATERIAL PROPERTIES
*MATERIAL, NAME=ALUMINIUM
*INELASTIC HEAT FRACTION
*ELASTIC
7.24E10, .32
*PLASTIC
2.81E8, 0.000000
2.83E8, 0.007150
2.86E8, 0.007710
2.88E8, 0.008070
2.90E8, 0.008480
2.93E8, 0.009030
2.95E8, 0.009670
2.97E8, 0.010200
2.99E8, 0.010800
3.00E8, 0.011300
3.03E8, 0.013400
3.01E8, 0.013900
*RATE DEPENDENT
6500, 4
*DENSITY
2686
*MATERIAL, NAME=RIGID
*ELASTIC
200E9, 0.3
*DENSITY
7800.
**-----------------------------DEFINITION OF BOUNDARY CONDITIONS
*NSET, NSET=XSYMM, GENERATE
 22101,  29001,  100
 32101,  39001,  100
 42101,  49001,  100
 52101,  59001,  100
 62101,  69001,  100
 72101,  79001,  100
 82101,  89001,  100
 92101,  99001,  100
 102101, 109001, 100
 112101, 119001, 100
 122101, 129001, 100
```

```
**-----------------------------
*NSET, NSET=YSYMM, GENERATE
 29001,  29051,  1
 39001,  39051,  1
 49001,  49051,  1
 59001,  59051,  1
 69001,  69051,  1
 79001,  79051,  1
 89001,  89051,  1
 99001,  99051,  1
 109001, 109051, 1
 119001, 119051, 1
 129001, 129051, 1
**
*BOUNDARY, OP=NEW, TYPE=DISPLACEMENT
 XSYMM,  1,1, 0.0
 YSYMM,  2,2, 0.0
 1000000, 1,6, 0.0
 2000000, 1,2, 0.0
 2000000, 4,6, 0.0
**----------------------------DEFINITION OF LOAD
*AMPLITUDE, NAME=BLAST, DEFINITION=TABULAR
0.0,1.0, 15E-6,1, 15.1E-6,0.0
**---------------------------- ANALYSIS STEPS BEGIN
**
*STEP
*DYNAMIC, EXPLICIT, ADIABATICS
,0.005E-6
*CONTACT PAIR, INTERACTION=SMOOTH
 SURF_TBEAM_TOP,SURF_CLAMP_TOP
 SURF_TBEAM_BOT,SURF_CLAMP_BOT
*SURFACE INTERACTION, NAME=SMOOTH
*FRICTION
 0.35
*CLOAD
 2000000,3,-1E4
*OUTPUT, FIELD, VARIABLE=ALL, OP=NEW, NUMBER INTERVALS=2
*END STEP
**
*STEP
*DYNAMIC, EXPLICIT, ADIABATICS
,15E-6
*DLOAD, AMPLITUDE=BLAST
 LOAD_TBEAM, P2, 3.59E7
*OUTPUT, FIELD, VARIABLE=ALL, OP=NEW, NUMBER INTERVALS=100
*END STEP
```

```
**
*STEP
*DYNAMIC, EXPLICIT, ADIABATICS
,235E-6
*DLOAD, OP=NEW
*END STEP
**
*STEP
*DYNAMIC, EXPLICIT, ADIABATICS
,400E-6
*DLOAD, OP=NEW
*END STEP
**END
**END OF ANALYSIS
```

UNIFORM BLAST LOADING ON CLAMPED T-BEAM USING MATERIAL PROPERTIES THAT EXCLUDE TEMPERATURE DEPENDENCY

```
*HEADING
BLAST LOADING OF T-BEAMS
SI UNITS (kg, M, S, N)
*PREPRINT, MODEL=NO, ECHO=NO
**----------------------------------DEFINITION OF NODES
*NODE
 1, 0,      0, 0
 21, 0.0016, 0., 0.
 51, 0.00525, 0., 0.
*NGEN, NSET=EDGE1
 1, 21, 1
 21, 51, 1
**
*NCOPY, SHIFT, OLDSET=EDGE1, CHANGE NUMBER=2000, NEWSET=EDGE2
 0, 0.05, 0
 0, 0,1, 0, 0, 1, 0
*NCOPY, SHIFT, OLDSET=EDGE1, CHANGE NUMBER=9000, NEWSET=EDGE3
 0,0.15,0
 0,0,1, 0,0,1, 0
**
*NFILL, NSET=FACE1
 EDGE1,EDGE2, 20, 100
 EDGE2,EDGE3, 70, 100
** ---------------------------------------COPING FACE1 FOR EACH OF THE FACES
*NCOPY, SHIFT, OLDSET=FACE1, NEWSET=FACE2, CHANGE NUMBER=10000
 0,0,0.0001
 0,0,1, 0,0,1, 0
*NCOPY, SHIFT, OLDSET=FACE1, NEWSET=FACE3, CHANGE NUMBER=20000
 0,0,0.0001
 0,0,1, 0,0,1, 0
*NCOPY, SHIFT, OLDSET=FACE1, NEWSET=FACE4, CHANGE NUMBER=30000
 0,0,0.00122
 0,0,1, 0,0,1, 0
*NCOPY, SHIFT, OLDSET=FACE1, NEWSET=FACE5, CHANGE NUMBER=40000
 0,0,0.00234
 0,0,1, 0,0,1, 0
*NCOPY, SHIFT, OLDSET=FACE1, NEWSET=FACE6, CHANGE NUMBER=50000
 0,0,0.00346
 0,0,1, 0,0,1, 0
*NCOPY, SHIFT, OLDSET=FACE1, NEWSET=FACE7, CHANGE NUMBER=60000
 0,0,0.00458
 0,0,1, 0,0,1, 0
*NCOPY, SHIFT, OLDSET=FACE1, NEWSET=FACE8, CHANGE NUMBER=70000
 0,0,0.0057
```

```
 0,0,1, 0,0,1, 0
*NCOPY, SHIFT, OLDSET=FACE1, NEWSET=FACE9, CHANGE NUMBER=80000
 0,0,0.00682
 0,0,1, 0,0,1, 0
*NCOPY, SHIFT, OLDSET=FACE1, NEWSET=FACE10, CHANGE
NUMBER=90000
 0,0,0.00794
 0,0,1, 0,0,1, 0
*NCOPY, SHIFT, OLDSET=FACE1, NEWSET=FACE11, CHANGE
NUMBER=100000
 0,0,0.00906
 0,0,1, 0,0,1, 0
*NCOPY, SHIFT, OLDSET=FACE1, NEWSET=FACE12, CHANGE
NUMBER=110000
 0,0,0.01018
 0,0,1, 0,0,1, 0
*NCOPY, SHIFT, OLDSET=FACE1, NEWSET=FACE13, CHANGE
NUMBER=120000
 0,0,0.0113
 0,0,1, 0,0,1, 0
*NCOPY, SHIFT, OLDSET=FACE1, NEWSET=FACE14, CHANGE
NUMBER=130000
 0,0,0.0113
 0,0,1, 0,0,1, 0
*NCOPY, SHIFT, OLDSET=FACE1, NEWSET=FACE15, CHANGE
NUMBER=140000
 0,0,0.0114
 0,0,1, 0,0,1, 0
**------------------------------ DEFINITION OF ELEMENTS
*ELEMENT, TYPE=C3D8R, ELSET=CLAMP_BOT
 1, 1, 2, 102, 101, 10001, 10002, 10102, 10101
*ELGEN, ELSET=CLAMP_BOT
 1, 20, 1, 1, 20, 100, 100
**
*ELEMENT, TYPE=C3D8R, ELSET=TBEAM
 10001, 20001, 20002, 20102, 20101, 30001, 30002, 30102, 30101
 80001, 90001, 90002, 90102, 90101, 100001, 100002, 100102, 100101
*ELGEN, ELSET=TBEAM
 10001, 20, 1, 1, 90, 100, 100, 7, 10000, 10000
 80001, 50, 1, 1, 90, 100, 100, 3, 10000, 10000
**------------------------------DEFINITION OF SURFACES
*ELEMENT, TYPE=C3D8R, ELSET=CLAMP_TOP
 110001, 130001, 130002, 130102, 130101, 140001, 140002, 140102, 140101
*ELGEN, ELSET=CLAMP_TOP
 110001,50,1,1, 20,100,100
```

```
**---------------------------------- DEFINITION OF SECTIONS
*SOLID SECTION, ELSET=CLAMP_TOP,  MATERIAL=RIGID
*SOLID SECTION, ELSET=TBEAM, MATERIAL=ALUMINIUM
*SOLID SECTION,ELSET=CLAMP_BOT, MATERIAL=RIGID
**----------------------------------DEFINITION OF RIGID BODY NODES
*NODE, NSET=NS_REFNODE
1000000, 0, 0, -0.05
2000000, 0, 0,  0.05
**----------------------------------DEFINITION OF SURFACES
*RIGID BODY, REFNODE=1000000, ELSET=CLAMP_BOT
*SURFACE, TYPE=ELEMENT,NAME=SURF_CLAMP_BOT
 CLAMP_BOT,S2
**
*ELSET, ELSET=TBEAM_BOT, GENERATE
 10001,18920,1
*SURFACE, TYPE=ELEMENT, NAME=SURF_TBEAM_BOT
 TBEAM_BOT, S1
**
*ELSET, ELSET=TBEAM_TOP, GENERATE
 100001,108950,1
*SURFACE, TYPE=ELEMENT, NAME=SURF_TBEAM_TOP
 TBEAM_TOP, S2
*RIGID BODY, REFNODE=2000000, ELSET=CLAMP_TOP
*SURFACE, TYPE=ELEMENT,NAME=SURF_CLAMP_TOP
 CLAMP_TOP,S1
*ELSET, ELSET=LOAD_TBEAM, GENERATE
102001, 102050, 1
102101, 102150, 1
102201, 102250, 1
102301, 102350, 1
102401, 102450, 1
102501, 102550, 1
102601, 102650, 1
102701, 102750, 1
102801, 102850, 1
102901, 102950, 1
103001, 103050, 1
103101, 103150, 1
103201, 103250, 1
103301, 103350, 1
103401, 103450, 1
103501, 103550, 1
103601, 103650, 1
103701, 103750, 1
103801, 103850, 1
103901, 103950, 1
```

104001, 104050, 1
104101, 104150, 1
104201, 104250, 1
104301, 104350, 1
104401, 104450, 1
104501, 104550, 1
104601, 104650, 1
104701, 104750, 1
104801, 104850, 1
104901, 104950, 1
105001, 105050, 1
105101, 105150, 1
105201, 105250, 1
105301, 105350, 1
105401, 105450, 1
105501, 105550, 1
105601, 105650, 1
105701, 105750, 1
105801, 105850, 1
105901, 105950, 1
106001, 106050, 1
106101, 106150, 1
106201, 106250, 1
106301, 106350, 1
106401, 106450, 1
106501, 106550, 1
106601, 106650, 1
106701, 106750, 1
106801, 106850, 1
106901, 106950, 1
107001, 107050, 1
107101, 107150, 1
107201, 107250, 1
107301, 107350, 1
107401, 107450, 1
107501, 107550, 1
107601, 107650, 1
107701, 107750, 1
107801, 107850, 1
107901, 107950, 1
108001, 108050, 1
108101, 108150, 1
108201, 108250, 1
108301, 108350, 1
108401, 108450, 1
108501, 108550, 1

```
108601, 108650, 1
108701, 108750, 1
108801, 108850, 1
108901, 108950, 1
**---------------------------------DEFINITION OF MATERIAL PROPERTIES
*MATERIAL, NAME=ALUMINIUM
*INELASTIC HEAT FRACTION
*ELASTIC
7.24E10, .32
*PLASTIC
2.81E8, 0.000000
2.83E8, 0.007150
2.86E8, 0.007710
2.88E8, 0.008070
2.90E8, 0.008480
2.93E8, 0.009030
2.95E8, 0.009670
2.97E8, 0.010200
2.99E8, 0.010800
3.00E8, 0.011300
3.03E8, 0.013400
3.01E8, 0.013900
*RATE DEPENDENT
6500, 4
*DENSITY
2686
*MATERIAL, NAME=RIGID
*ELASTIC
200E9, 0.3
*DENSITY
7800.
**-----------------------------DEFINITION OF BOUNDARY CONDITIONS
*NSET, NSET=XSYMM, GENERATE
 22101,  29001,  100
 32101,  39001,  100
 42101,  49001,  100
 52101,  59001,  100
 62101,  69001,  100
 72101,   79001,   100
 82101,   89001,   100
 92101,   99001,   100
 102101, 109001, 100
 112101, 119001, 100
 122101, 129001, 100
```

```
**-----------------------------
*NSET, NSET=YSYMM, GENERATE
 29001,  29051,  1
 39001,  39051,  1
 49001,  49051,  1
 59001,  59051,  1
 69001,  69051,  1
 79001,  79051,  1
 89001,  89051,  1
 99001,  99051,  1
 109001, 109051, 1
 119001, 119051, 1
 129001, 129051, 1
**
*BOUNDARY, OP=NEW, TYPE=DISPLACEMENT
 XSYMM,  1,1, 0.0
 YSYMM,  2,2, 0.0
 1000000, 1,6, 0.0
 2000000, 1,2, 0.0
 2000000, 4,6, 0.0
**-----------------------------DEFINITION OF LOAD
*AMPLITUDE, NAME=BLAST, DEFINITION=TABULAR
0.0,1.0, 15E-6,1, 15.1E-6,0.0
**---------------------------- ANALYSIS STEPS BEGIN
**
*STEP
*DYNAMIC, EXPLICIT, ADIABATICS
,0.005E-6
*CONTACT PAIR, INTERACTION=SMOOTH
 SURF_TBEAM_TOP,SURF_CLAMP_TOP
 SURF_TBEAM_BOT,SURF_CLAMP_BOT
*SURFACE INTERACTION, NAME=SMOOTH
*FRICTION
 0.35
*CLOAD
 2000000,3,-1E4
*OUTPUT, FIELD, VARIABLE=ALL, OP=NEW, NUMBER INTERVALS=2
*END STEP
**
*STEP
*DYNAMIC, EXPLICIT, ADIABATICS
,15E-6
*DLOAD, AMPLITUDE=BLAST
 LOAD_TBEAM, P2, 3.59E7
*OUTPUT, FIELD, VARIABLE=ALL, OP=NEW, NUMBER INTERVALS=100
*END STEP
```

```
**
*STEP
*DYNAMIC, EXPLICIT, ADIABATICS
,235E-6
*DLOAD, OP=NEW
*END STEP
**
*STEP
*DYNAMIC, EXPLICIT, ADIABATICS
,400E-6
*DLOAD, OP=NEW
*END STEP
**END
**END OF ANALYSIS
```

UNIFORM BLAST LOADING ON BUILT-IN T-BEAM USING MATERIAL PROPERTIES THAT INCLUDE TEMPERATURE DEPENDENCY

```
*HEADING
BLAST LOADING OF T-BEAMS
SI UNITS (Kg, M, S, N)
*PREPRINT, MODEL=NO, ECHO=NO
**----------------------------------DEFINITION OF NODES
*NODE
 1, 0,      0, 0
 21, 0.0016, 0., 0.
 51, 0.00525, 0., 0.
*NGEN, NSET=EDGE1
 1, 21, 1
 21, 51, 1
**
*NCOPY, SHIFT, OLDSET=EDGE1, CHANGE NUMBER=2000, NEWSET=EDGE2
 0, 0.05, 0
 0, 0,1, 0, 0, 1, 0
*NCOPY, SHIFT, OLDSET=EDGE1, CHANGE NUMBER=9000, NEWSET=EDGE3
 0,0.15,0
 0,0,1, 0,0,1, 0
**
*NFILL, NSET=FACE1
 EDGE1,EDGE2, 20, 100
 EDGE2,EDGE3, 70, 100
** ---------------------------------------COPING FACE1 FOR EACH OF THE FACES
*NCOPY, SHIFT, OLDSET=FACE1, NEWSET=FACE2, CHANGE NUMBER=10000
 0,0,0.0001
 0,0,1, 0,0,1, 0
*NCOPY, SHIFT, OLDSET=FACE1, NEWSET=FACE3, CHANGE NUMBER=20000
 0,0,0.0001
 0,0,1, 0,0,1, 0
*NCOPY, SHIFT, OLDSET=FACE1, NEWSET=FACE4, CHANGE NUMBER=30000
 0,0,0.00122
 0,0,1, 0,0,1, 0
*NCOPY, SHIFT, OLDSET=FACE1, NEWSET=FACE5, CHANGE NUMBER=40000
 0,0,0.00234
 0,0,1, 0,0,1, 0
*NCOPY, SHIFT, OLDSET=FACE1, NEWSET=FACE6, CHANGE NUMBER=50000
 0,0,0.00346
 0,0,1, 0,0,1, 0
*NCOPY, SHIFT, OLDSET=FACE1, NEWSET=FACE7, CHANGE NUMBER=60000
 0,0,0.00458
 0,0,1, 0,0,1, 0
*NCOPY, SHIFT, OLDSET=FACE1, NEWSET=FACE8, CHANGE NUMBER=70000
 0,0,0.0057
```

```
 0,0,1, 0,0,1, 0
*NCOPY, SHIFT, OLDSET=FACE1, NEWSET=FACE9, CHANGE NUMBER=80000
 0,0,0.00682
 0,0,1, 0,0,1, 0
*NCOPY, SHIFT, OLDSET=FACE1, NEWSET=FACE10, CHANGE
NUMBER=90000
 0,0,0.00794
 0,0,1, 0,0,1, 0
*NCOPY, SHIFT, OLDSET=FACE1, NEWSET=FACE11, CHANGE
NUMBER=100000
 0,0,0.00906
 0,0,1, 0,0,1, 0
*NCOPY, SHIFT, OLDSET=FACE1, NEWSET=FACE12, CHANGE
NUMBER=110000
 0,0,0.01018
 0,0,1, 0,0,1, 0
*NCOPY, SHIFT, OLDSET=FACE1, NEWSET=FACE13, CHANGE
NUMBER=120000
 0,0,0.0113
 0,0,1, 0,0,1, 0
**--------------------------------DEFINITION OF ELEMENTS
*ELEMENT, TYPE=C3D8R, ELSET=CLAMP_BOT
 1, 1, 2, 102, 101, 10001, 10002, 10102, 10101
*ELGEN, ELSET=CLAMP_BOT
 1, 20, 1, 1, 20, 100, 100
**------------------------------
*ELEMENT, TYPE=C3D8R, ELSET=TBEAM
 10001, 20001, 20002, 20102, 20101, 30001, 30002, 30102, 30101
 80001, 90001, 90002, 90102, 90101, 100001, 100002, 100102, 100101
*ELGEN, ELSET=TBEAM
 10001, 20, 1, 1, 90, 100, 100, 7, 10000, 10000
 80001, 50, 1, 1, 90, 100, 100, 3, 10000, 10000
**------------------------------------ DEFINITION OF SECTIONS
*SOLID SECTION, ELSET=TBEAM, MATERIAL=ALUMINIUM
*SOLID SECTION,ELSET=CLAMP_BOT, MATERIAL=RIGID
**------------------------------------DEFINITION OF RIGID NODE
*NODE, NSET=NS_REFNODE
1000000, 0, 0, -0.05
**------------------------------------DEFINITION OF SURFACES
*RIGID BODY, REFNODE=1000000, ELSET=CLAMP_BOT
*SURFACE, TYPE=ELEMENT,NAME=SURF_CLAMP_BOT
 CLAMP_BOT,S2
**-----------------------------------
*ELSET, ELSET=TBEAM_BOT, GENERATE
 10001,18920,1
*SURFACE, TYPE=ELEMENT, NAME=SURF_TBEAM_BOT
```

```
 TBEAM_BOT, S1
**
*ELSET, ELSET=TBEAM_TOP, GENERATE
 100001,108950,1
*SURFACE, TYPE=ELEMENT, NAME=SURF_TBEAM_TOP
 TBEAM_TOP, S2
*ELSET, ELSET=LOAD_TBEAM, GENERATE
102001, 102050, 1
102101, 102150, 1
102201, 102250, 1
102301, 102350, 1
102401, 102450, 1
102501, 102550, 1
102601, 102650, 1
102701, 102750, 1
102801, 102850, 1
102901, 102950, 1
103001, 103050, 1
103101, 103150, 1
103201, 103250, 1
103301, 103350, 1
103401, 103450, 1
103501, 103550, 1
103601, 103650, 1
103701, 103750, 1
103801, 103850, 1
103901, 103950, 1
104001, 104050, 1
104101, 104150, 1
104201, 104250, 1
104301, 104350, 1
104401, 104450, 1
104501, 104550, 1
104601, 104650, 1
104701, 104750, 1
104801, 104850, 1
104901, 104950, 1
105001, 105050, 1
105101, 105150, 1
105201, 105250, 1
105301, 105350, 1
105401, 105450, 1
105501, 105550, 1
105601, 105650, 1
105701, 105750, 1
105801, 105850, 1
```

105901, 105950, 1
106001, 106050, 1
106101, 106150, 1
106201, 106250, 1
106301, 106350, 1
106401, 106450, 1
106501, 106550, 1
106601, 106650, 1
106701, 106750, 1
106801, 106850, 1
106901, 106950, 1
107001, 107050, 1
107101, 107150, 1
107201, 107250, 1
107301, 107350, 1
107401, 107450, 1
107501, 107550, 1
107601, 107650, 1
107701, 107750, 1
107801, 107850, 1
107901, 107950, 1
108001, 108050, 1
108101, 108150, 1
108201, 108250, 1
108301, 108350, 1
108401, 108450, 1
108501, 108550, 1
108601, 108650, 1
108701, 108750, 1
108801, 108850, 1
108901, 108950, 1
**----------DEFINITION OF MATERIAL PROPERTIES
*MATERIAL, NAME=ALUMINIUM
*INELASTIC HEAT FRACTION
*ELASTIC
7.24E10, .32, 0
6.07E10, .32, 25
3.74E10, .32, 100
3.24E10, .32, 200
3.02E10, .32, 300
*PLASTIC
2.81E8, 0.000000, 0
2.83E8, 0.007150, 0
2.86E8, 0.007710, 0
2.88E8, 0.008070, 0
2.90E8, 0.008480, 0

2.93E8, 0.009030, 0
2.95E8, 0.009670, 0
2.97E8, 0.010200, 0
2.99E8, 0.010800, 0
3.00E8, 0.011300, 0
3.03E8, 0.013400, 0
3.01E8, 0.013900, 0
2.81E8, 0.000000, 25
2.83E8, 0.007150, 25
2.86E8, 0.007710, 25
2.88E8, 0.008070, 25
2.90E8, 0.008480, 25
2.93E8, 0.009030, 25
2.95E8, 0.009670, 25
2.97E8, 0.010200, 25
2.99E8, 0.010800, 25
3.00E8, 0.011300, 25
3.03E8, 0.013400, 25
3.01E8, 0.013900, 25
2.43E8, 0.000000, 100
2.45E8, 0.007150, 100
2.48E8, 0.007710, 100
2.50E8, 0.008070, 100
2.51E8, 0.008480, 100
2.54E8, 0.009030, 100
2.56E8, 0.009670, 100
2.57E8, 0.010200, 100
2.59E8, 0.010800, 100
2.60E8, 0.011300, 100
2.63E8, 0.013400, 100
2.61E8, 0.013900, 100
1.93E8, 0.000000, 200
1.95E8, 0.007150, 200
1.97E8, 0.007710, 200
1.98E8, 0.008070, 200
2.00E8, 0.008480, 200
2.02E8, 0.009030, 200
2.03E8, 0.009670, 200
2.04E8, 0.010200, 200
2.06E8, 0.010800, 200
2.07E8, 0.011300, 200
2.09E8, 0.013400, 200
2.07E8, 0.013900, 200
2.65E7, 0.000000, 300
2.66E7, 0.007150, 300
2.69E7, 0.007710, 300

```
2.71E7, 0.008070, 300
2.73E7, 0.008480, 300
2.76E7, 0.009030, 300
2.78E7, 0.009670, 300
2.80E7, 0.010200, 300
2.82E7, 0.010800, 300
2.82E7, 0.011300, 300
2.85E7, 0.013400, 300
2.83E7, 0.013900, 300
*SPECIFIC HEAT
937.4
*RATE DEPENDENT
6500, 4
*DENSITY
2686
**
*MATERIAL, NAME=RIGID
*ELASTIC
200E9, 0.3
*DENSITY
7800.
**
*NSET, NSET=BOUND1, GENERATE
 1,    2001,   100
 10001,  12001,   100
 20001,  22001,   100
 30001,  32001,   100
 40001,  42001,   100
 50001,  52001,   100
 60001,  62001,   100
 70001,  72001,   100
 80001,  82001,   100
 90001,  92001,   100
 100001,102001,  100
 110001,112001,  100
 120001,122001,  100
**
*NSET, NSET=BOUND2, GENERATE
 21,    2021,   100
 10021,  12021,  100
 20021,  22021,  100
 30021,  32021,  100
 40021,  42021,  100
 50021,  52021,  100
 60021,  62021,  100
 70021,  72021,  100
```

```
 80021,  82021,  100
 90051,  92051,  100
 100051, 102051, 100
 110051, 112051, 100
 120051, 122051, 100
*NSET, NSET=BOUND3, GENERATE
120021, 129021
*NSET, NSET=XSYMM, GENERATE
 22101,  29001,  100
 32101,  39001,  100
 42101,  49001,  100
 52101,  59001,  100
 62101,  69001,  100
 72101,  79001,  100
 82101,  89001,  100
 92101,  99001,  100
 102101, 109001, 100
 112101, 119001, 100
 122101, 129001, 100
**
*NSET, NSET=YSYMM, GENERATE
 29001,  29051,  1
 39001,  39051,  1
 49001,  49051,  1
 59001,  59051,  1
 69001,  69051,  1
 79001,  79051,  1
 89001,  89051,  1
 99001,  99051,  1
 109001, 109051, 1
 119001, 119051, 1
 129001, 129051, 1
**----------------------------------DEFINITION OF BOUNDARY CONDITIONS
*BOUNDARY, OP=NEW, TYPE=DISPLACEMENT
 XSYMM,   1,1, 0.0
 YSYMM,   2,2, 0.0
 1000000, 1,6, 0.0
 BOUND1, ENCASTRE
 BOUND2, ENCASTRE
 BOUND3, ENCASTRE
**
*NSET, NSET=NS_ALL_TBEAM, ELSET=TBEAM
*INITIAL CONDITION, TYPE=TEMPERATURE
 NS_ALL_TBEAM, 0.
```

```
**--------------------------------DEFINITION OF LOAD
*AMPLITUDE, NAME=BLAST, DEFINITION=TABULAR
0.0,1.0, 15E-6,1, 15.1E-6,0.0
**-----------------------------ANALYSIS STEPS BEGIN
*STEP
*DYNAMIC, EXPLICIT, ADIABATICS
,0.005E-6
*CONTACT PAIR, INTERACTION=SMOOTH
 SURF_TBEAM_BOT,SURF_CLAMP_BOT
*SURFACE INTERACTION, NAME=SMOOTH
*FRICTION
 1.0
*OUTPUT, FIELD, VARIABLE=ALL, OP=NEW, NUMBER INTERVALS=2
*END STEP
**
*STEP
*DYNAMIC, EXPLICIT, ADIABATICS
,15E-6
*DLOAD, AMPLITUDE=BLAST
 LOAD_TBEAM, P2, 3.59E7
*OUTPUT, FIELD, VARIABLE=ALL, OP=NEW, NUMBER INTERVALS=100
*END STEP
**
*STEP
*DYNAMIC, EXPLICIT, ADIABATICS
,235E-6
*DLOAD, OP=NEW
*END STEP
**
*STEP
*DYNAMIC, EXPLICIT, ADIABATICS
,400E-6
*DLOAD, OP=NEW
*END STEP
**END
**END OF ANALYSIS
```

UNIFORM BLAST LOADING ON BUILT-IN T-BEAM USING MATERIAL PROPERTIES THAT EXCLUDE TEMPERATURE DEPENDENCY

```
*HEADING
BLAST LOADING OF T-BEAMS
SI UNITS (Kg, M, S, N)
*PREPRINT, MODEL=NO, ECHO=NO
**----------------------------------DEFINITION OF NODES
*NODE
 1, 0,      0, 0
 21, 0.0016, 0., 0.
 51, 0.00525, 0., 0.
*NGEN, NSET=EDGE1
 1, 21, 1
 21, 51, 1
**
*NCOPY, SHIFT, OLDSET=EDGE1, CHANGE NUMBER=2000, NEWSET=EDGE2
 0, 0.05, 0
 0, 0,1, 0, 0, 1, 0
*NCOPY, SHIFT, OLDSET=EDGE1, CHANGE NUMBER=9000, NEWSET=EDGE3
 0,0.15,0
 0,0,1, 0,0,1, 0
**
*NFILL, NSET=FACE1
 EDGE1,EDGE2, 20, 100
 EDGE2,EDGE3, 70, 100
** ---------------------------------------COPING FACE1 FOR EACH OF THE FACES
*NCOPY, SHIFT, OLDSET=FACE1, NEWSET=FACE2, CHANGE NUMBER=10000
 0,0,0.0001
 0,0,1, 0,0,1, 0
*NCOPY, SHIFT, OLDSET=FACE1, NEWSET=FACE3, CHANGE NUMBER=20000
 0,0,0.0001
 0,0,1, 0,0,1, 0
*NCOPY, SHIFT, OLDSET=FACE1, NEWSET=FACE4, CHANGE NUMBER=30000
 0,0,0.00122
 0,0,1, 0,0,1, 0
*NCOPY, SHIFT, OLDSET=FACE1, NEWSET=FACE5, CHANGE NUMBER=40000
 0,0,0.00234
 0,0,1, 0,0,1, 0
*NCOPY, SHIFT, OLDSET=FACE1, NEWSET=FACE6, CHANGE NUMBER=50000
 0,0,0.00346
 0,0,1, 0,0,1, 0
*NCOPY, SHIFT, OLDSET=FACE1, NEWSET=FACE7, CHANGE NUMBER=60000
 0,0,0.00458
 0,0,1, 0,0,1, 0
*NCOPY, SHIFT, OLDSET=FACE1, NEWSET=FACE8, CHANGE NUMBER=70000
 0,0,0.0057
```

```
 0,0,1, 0,0,1, 0
*NCOPY, SHIFT, OLDSET=FACE1, NEWSET=FACE9, CHANGE NUMBER=80000
 0,0,0.00682
 0,0,1, 0,0,1, 0
*NCOPY, SHIFT, OLDSET=FACE1, NEWSET=FACE10, CHANGE
NUMBER=90000
 0,0,0.00794
 0,0,1, 0,0,1, 0
*NCOPY, SHIFT, OLDSET=FACE1, NEWSET=FACE11, CHANGE
NUMBER=100000
 0,0,0.00906
 0,0,1, 0,0,1, 0
*NCOPY, SHIFT, OLDSET=FACE1, NEWSET=FACE12, CHANGE
NUMBER=110000
 0,0,0.01018
 0,0,1, 0,0,1, 0
*NCOPY, SHIFT, OLDSET=FACE1, NEWSET=FACE13, CHANGE
NUMBER=120000
 0,0,0.0113
 0,0,1, 0,0,1, 0
**------------------------------DEFINITION OF ELEMENTS
*ELEMENT, TYPE=C3D8R, ELSET=CLAMP_BOT
 1, 1, 2, 102, 101, 10001, 10002, 10102, 10101
*ELGEN, ELSET=CLAMP_BOT
 1, 20, 1, 1, 20, 100, 100
**------------------------------
*ELEMENT, TYPE=C3D8R, ELSET=TBEAM
 10001, 20001, 20002, 20102, 20101, 30001, 30002, 30102, 30101
 80001, 90001, 90002, 90102, 90101, 100001, 100002, 100102, 100101
*ELGEN, ELSET=TBEAM
 10001, 20, 1, 1, 90, 100, 100, 7, 10000, 10000
 80001, 50, 1, 1, 90, 100, 100, 3, 10000, 10000
**------------------------------------ DEFINITION OF SECTIONS
*SOLID SECTION, ELSET=TBEAM, MATERIAL=ALUMINIUM
*SOLID SECTION,ELSET=CLAMP_BOT, MATERIAL=RIGID
**-----------------------------------DEFINITION OF RIGID NODE
*NODE, NSET=NS_REFNODE
1000000, 0, 0, -0.05
**-----------------------------------DEFINITION OF SURFACES
*RIGID BODY, REFNODE=1000000, ELSET=CLAMP_BOT
*SURFACE, TYPE=ELEMENT,NAME=SURF_CLAMP_BOT
 CLAMP_BOT,S2
**-----------------------------------
*ELSET, ELSET=TBEAM_BOT, GENERATE
 10001,18920,1
*SURFACE, TYPE=ELEMENT, NAME=SURF_TBEAM_BOT
```

```
 TBEAM_BOT, S1
**
*ELSET, ELSET=TBEAM_TOP, GENERATE
 100001,108950,1
*SURFACE, TYPE=ELEMENT, NAME=SURF_TBEAM_TOP
 TBEAM_TOP, S2
*ELSET, ELSET=LOAD_TBEAM, GENERATE
102001, 102050, 1
102101, 102150, 1
102201, 102250, 1
102301, 102350, 1
102401, 102450, 1
102501, 102550, 1
102601, 102650, 1
102701, 102750, 1
102801, 102850, 1
102901, 102950, 1
103001, 103050, 1
103101, 103150, 1
103201, 103250, 1
103301, 103350, 1
103401, 103450, 1
103501, 103550, 1
103601, 103650, 1
103701, 103750, 1
103801, 103850, 1
103901, 103950, 1
104001, 104050, 1
104101, 104150, 1
104201, 104250, 1
104301, 104350, 1
104401, 104450, 1
104501, 104550, 1
104601, 104650, 1
104701, 104750, 1
104801, 104850, 1
104901, 104950, 1
105001, 105050, 1
105101, 105150, 1
105201, 105250, 1
105301, 105350, 1
105401, 105450, 1
105501, 105550, 1
105601, 105650, 1
105701, 105750, 1
105801, 105850, 1
```

105901, 105950, 1
106001, 106050, 1
106101, 106150, 1
106201, 106250, 1
106301, 106350, 1
106401, 106450, 1
106501, 106550, 1
106601, 106650, 1
106701, 106750, 1
106801, 106850, 1
106901, 106950, 1
107001, 107050, 1
107101, 107150, 1
107201, 107250, 1
107301, 107350, 1
107401, 107450, 1
107501, 107550, 1
107601, 107650, 1
107701, 107750, 1
107801, 107850, 1
107901, 107950, 1
108001, 108050, 1
108101, 108150, 1
108201, 108250, 1
108301, 108350, 1
108401, 108450, 1
108501, 108550, 1
108601, 108650, 1
108701, 108750, 1
108801, 108850, 1
108901, 108950, 1
**----------DEFINITION OF MATERIAL PROPERTIES
*MATERIAL, NAME=ALUMINIUM
*INELASTIC HEAT FRACTION
*ELASTIC
7.24E10, .32
*PLASTIC
2.81E8, 0.000000
2.83E8, 0.007150
2.86E8, 0.007710
2.88E8, 0.008070
2.90E8, 0.008480
2.93E8, 0.009030
2.95E8, 0.009670
2.97E8, 0.010200
2.99E8, 0.010800

```
3.00E8, 0.011300
3.03E8, 0.013400
3.01E8, 0.013900
*RATE DEPENDENT
6500, 4
*DENSITY
2686
**
*MATERIAL, NAME=RIGID
*ELASTIC
200E9, 0.3
*DENSITY
7800.
**
*NSET, NSET=BOUND1, GENERATE
 1,    2001,   100
 10001,  12001,   100
 20001,  22001,   100
 30001,  32001,   100
 40001,  42001,   100
 50001,  52001,   100
 60001,  62001,   100
 70001,  72001,   100
 80001,  82001,   100
 90001,  92001,   100
 100001,102001, 100
 110001,112001, 100
 120001,122001, 100
**
*NSET, NSET=BOUND2, GENERATE
 21,    2021,   100
 10021,  12021,  100
 20021,  22021,  100
 30021,  32021,  100
 40021,  42021,  100
 50021,  52021,  100
 60021,  62021,  100
 70021,  72021,  100
 80021,   82021,   100
 90051,   92051,   100
 100051, 102051, 100
 110051, 112051, 100
 120051, 122051, 100
*NSET, NSET=BOUND3, GENERATE
120021, 129021
*NSET, NSET=XSYMM, GENERATE
```

```
 22101,  29001,  100
 32101,  39001,  100
 42101,  49001,  100
 52101,  59001,  100
 62101,  69001,  100
 72101,  79001,  100
 82101,  89001,  100
 92101,  99001,  100
 102101, 109001, 100
 112101, 119001, 100
 122101, 129001, 100
**
*NSET, NSET=YSYMM, GENERATE
 29001,  29051,  1
 39001,  39051,  1
 49001,  49051,  1
 59001,  59051,  1
 69001,  69051,  1
 79001,  79051,  1
 89001,  89051,  1
 99001,  99051,  1
 109001, 109051, 1
 119001, 119051, 1
 129001, 129051, 1
**----------------------------------DEFINITION OF BOUNDARY CONDITIONS
*BOUNDARY, OP=NEW, TYPE=DISPLACEMENT
 XSYMM,   1,1, 0.0
 YSYMM,   2,2, 0.0
 1000000, 1,6, 0.0
 BOUND1, ENCASTRE
 BOUND2, ENCASTRE
 BOUND3, ENCASTRE
**----------------------------------DEFINITION OF LOAD
*AMPLITUDE, NAME=BLAST, DEFINITION=TABULAR
0.0,1.0, 15E-6,1, 15.1E-6,0.0
**----------------------------------ANALYSIS STEPS BEGIN
*STEP
*DYNAMIC, EXPLICIT, ADIABATICS
,0.005E-6
*CONTACT PAIR, INTERACTION=SMOOTH
 SURF_TBEAM_BOT,SURF_CLAMP_BOT
*SURFACE INTERACTION, NAME=SMOOTH
*FRICTION
 1.0
*OUTPUT, FIELD, VARIABLE=ALL, OP=NEW, NUMBER INTERVALS=2
*END STEP
```

```
**
*STEP
*DYNAMIC, EXPLICIT, ADIABATICS
,15E-6
*DLOAD, AMPLITUDE=BLAST
 LOAD_TBEAM, P2, 3.59E7
*OUTPUT, FIELD, VARIABLE=ALL, OP=NEW, NUMBER INTERVALS=100
*END STEP
**
*STEP
*DYNAMIC, EXPLICIT, ADIABATICS
,235E-6
*DLOAD, OP=NEW
*END STEP
**
*STEP
*DYNAMIC, EXPLICIT, ADIABATICS
,400E-6
*DLOAD, OP=NEW
*END STEP
**END
**END OF ANALYSIS
```